2016

Studies toward the total synthesis of swerilactones A and B

BOSTON UNIVERSITY

GRADUATE SCHOOL OF ARTS AND SCIENCES

Dissertation

STUDIES TOWARD THE TOTAL SYNTHESIS OF SWERILACTONES A AND B

by

DIANE HAMANN

B.S., Lyon School of Chemistry, Physics and Electronics, Lyon, France, 2008
M.Sc., Lyon School of Chemistry, Physics and Electronics, Lyon, France, 2012

Submitted in partial fulfillment of the

requirements for the degree of

Doctor of Philosophy

2016

Approved by

First Reader

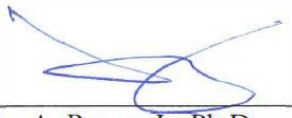

John A. Porco, Jr, Ph.D.
Professor of Chemistry

Second Reader

Aaron Beeler, Ph.D.
Associate Professor of Chemistry

DEDICATION

To my mother, Nicole, who in the face of adversity and hardship always found inner strength to emerge above the surface, stronger than ever

To mad scientist Prof. Rouzaud and his wife Gaby, for providing support and introducing me to the ethics and rigor of scientific reasoning

ACKNOWLEDGMENTS

I would first like to thank my advisor, Prof. John Porco, for his support, guidance and the high level of science he fosters in the Porco group. I learned a great deal during my Ph.D as I tackled the syntheses of two complex molecules, for which no syntheses have been published to date.

As a 'fresh', starting graduate student, I decided to join John Porco's lab because I was amazed and intrigued by the complex natural product structures, and the great people I met there convinced me to stay. I will always fondly remember the older generation of Porco lab members, and thank them for teaching me the basics of bench work to operate in the lab safely and independently. Specifically, I am in debt towards Dr. Anais Gervais, Dr. Andrew little, Dr. Stephen Scully, Dr. Dave Sloman, Dr. Suwei Dong, Dr. Qiang Zang, and Dr Huan Cong. They made the lab enjoyable and were extremely knowledgeable in all aspects of organic chemistry. I am grateful to Dr. Andy Kleinke for useful discussions on my first synthetic project regarding epidithiodiketopiperazines.

I could not have made it this far without my group of close friends/coworkers in the lab. They always provided advice and welcomed laughter. I thank Gina for being always there when I needed support on all matters of life, and for proof-reading my thesis. Adam and Vincent for providing great comical relief and rich political discussions. I am indebted to my lab mate, Dr Kiel Lazarski, for his help, advice and support, and for setting a high standard regarding scientific communication. I am also thankful to my great deskmates, Dr. Neil Lajkiewicz and Chao Qi, as I could not have asked for better, more

respectful people to share desks with. I sincerely enjoyed going through the ordeal of defending my thesis as a foreign student in the company of the talented Chao, and I will miss our discussions about Chinese culture and immigration adjustments. I am grateful to have met great minds such as Tian Qin and Wenyu Wang, and thank them for their feedback on NMR assignments. I also had the pleasure to work with great colleagues, Dr. Robert Ziegler, whose restricted food regimen and soccer watching habit I will always remember, and Dan Podgorski. Xiaowei Wu and Thomas Purgett have been gret young enthusiastic colleagues, and newly arrived Dr. Kyle Reichter and Michael have been amazing labmates. Working with talented post-docs has been a great perk, and I am indebted to Dr. Davina Fernandez-Gonzalez, Dr. Dana Winter, Dr. Pieter Bos, Dr. Alexander Grenning, Dr. Stephane Roche, Dr. Benedikt Crone, Dr. Martin Himmelbauer for their work ethic and knowledge.

I want to acknowledge my boyfriend Stephen Scully for putting up with the dire process of defending, for minutiously proof-reading my chapters, and for his unfaltering confident outlook on life. I was extremely fortunate to cross path with Dr. Marlena Konieczynska, who has been a dear friend and a partner in crime all these years, I am grateful for her presence and support and will always be. I want to thank the CIC Center (Norman Lee, Paul Ralifo), the CMD (Lauren Brown, Wil Devine, Madeline Weber, Ravi Chetree), and all the other organic labs (Schaus, Panek, Snyder, Beeler) for chemical borrowing.

Enfin, j'aimerais remercier ma mère Nicole pour son soutien et sa patience pendant ses longues années passer à 'jouer avec des tubes à essai'. Sa force de caractère et sa

résilience m’ont toujours inspiré et permis de garder la tête froide dans les moments difficiles du doctorat.

STUDIES TOWARD THE TOTAL SYNTHESIS OF SWERILACTONES A AND B

DIANE HAMANN

Boston University Graduate School of Arts and Science, 2016

Major Professor: Dr. John A. Porco, Jr., Ph.D., Professor of Chemistry

ABSTRACT

Swerilactones and related natural products were isolated from the plant *Swertia mileensis* and related species from the Gentianacea family. All members have shown moderate bioactivity in a hepatitis B virus assay. Despite their appealing framework and bioactivity, to date no syntheses of these compounds have been reported in the literature.

All members of the natural products family display a polycyclic framework, containing lactone-pyran fused bicyclic subunits, and are heavily oxygenated. En route to swerilactones A and B, featuring a complex pentacyclic (6/6/6/6) ring system, the successful syntheses of two key building blocks for studies of a biomimetic [4+2] cycloaddition have been accomplished. The challenges associated with the design of a novel synthesis of a *2H*-pyran diene are presented and ultimately relied on a Saucy-Marbet rearrangement of a propargyl vinyl ether. Reactivity studies for the *2H*-pyran have shown thermal normal demand and photoinduced, radical cation [4+2] cycloadditions are Diels-Alder modes of choice, whereas inverse demand pathways were unproductive.

Synthetic routes to obtain carboxylate and various enol ether substituted dienophilic lactones are also outlined. They relied on a unified strategy, comprised of the

rapid assembly of a β-brominated sorbate derivative *via* cross-couplings and final oxa-6π electrocyclization as an original ring closure strategy. Our attempts at coupling the *2H*-pyran intermediate with the dienophilic lactones to access the core structure of swerilactones A and B, leveraging our preliminary reactivity studies are presented in detail. In addition, alternatives strategies to assemble the core structures of swerilactones A and B are described, along with our efforts (and potential routes) toward related members of this family of natural products.

TABLE OF CONTENTS

LIST OF TABLES

LIST OF FIGURES

LIST OF SCHEMES

LIST OF ABBREVIATIONS

4Å MS ..... 4Å molecular sieves

[α] ..... specific rotation

Ac ..... acetyl

AcOH ..... acetic acid

Ac_2O ..... acetic anhydride

Alk ..... alkyl

Ar ..... aryl

aq. ..... aqueous

BINAP ..... 2,2'-bis(diphenylphosphino)-1,1'-binaphthyl

BINOL ..... 1,1'-bi-2-naphtol

$Bi(OTf)_3$ ..... bismuth triflate

$BF_3.OEt_2$ ..... boron trifluoride diethyl etherate

BHT ..... butylated hydroxytoluene

Bn ..... benzyl

BQd ..... benzoylquinidine

CAN ..... ceric(IV) ammonium nitrate

cat. ..... catalytic

CF_3SO_3H ..... triflic acid

CH_2Cl_2 ..... dichloromethane

CH_3CN ..... acetonitrile

cm^{-1} ..... wavenumber

$CpRu(MeCN)_3PF_6$..... Tris(acetonitrile)cyclopentadienylruthenium hexafluorophosphate

CSA..... camphorsulfonic acid

conc. ..... concentrated

CuCl ..... copper chloride

CuI..... copper iodide

DABCO..... 1,4-diazabicyclo[2.2.2]octane

dba..... dibenzylideneacetone

DBU ..... 1,8-diazbicyclo[5,4,0]undec-7-ene

DCE..... dichloroethane

DDQ..... 2,3-Dichloro-5,6-dicyano-1,4-benzoquinone

DFT ..... density functional theory

DMF ..... *N*,*N*-dimethylformamide

DMP ..... Dess-Martin periodinane

DMSO ..... dimethyl sulfoxide

DNA ..... deoxyribonucleic acid

EtOH ..... ethanol

EtOAc ..... ethyl acetate

Et_3N..... triethylamine

dr ..... diastereomeric ratio

EC ..... effective concentration

ee ..... enantiomeric excess

epi..... epimer

equiv ..... equivalents

Et ..... ethyl

Et_3N ..... triethylamine

FTIR ..... Fourier transform infrared spectroscopy

δ ..... chemical shift

h ..... hour(s)

H_2 ..... hydrogen

HCl ..... hydrochloric acid

HBV ..... hepatitis B virus

HIV ..... human immunodeficiency virus

HMBC ..... heteronuclear multiple bond correlation

HOMO ..... highest occupied molecular orbital

HPLC ..... high performance liquid chromatography

HRMS ..... high resolution mass spectroscopy

HSQC ..... heteronuclear single quantum coherence

Hz ..... hertz

hν ..... irradiation

I_2 ..... iodine

IBX ..... 2-idodobenzoic acid

IC ..... inhibitory concentration

*i*Pr ..... isopropyl

iPr_2NEt ..... Hunig's base

iPr_2SiCl ..... dichlorodiisopropylsilane

IR ..... infrared

$[Ir(cod)Cl]_2$ ..... bis(1,5-cyclooctadiene)diiridium(I) dichloride

J ..... coupling constant

K_2CO_3 ..... potassium carbonate

kcal ..... kilocalorie

LDA ..... Lithium diisopropylamine

L-DIPT ..... L- diisopropyl tartrate

LED ..... light-emitting diode

LiHMDS ..... lithium hexamethyldisilazide

$LiClO_4$ ..... lithium perchlorate

LiOH ..... lithium hydroxide

LUMO ..... lowest unoccupied molecular orbital

mM ..... millimolar

Me ..... methyl

MeOH ..... methanol

MeLi ..... methyl lithium

min ..... minutes

mmol ..... millimole

mp ..... melting point

Ms ..... mesyl

m/z ..... mass-to-charge ratio

NaHMDS .....sodium hexamethyldisilazide

NaOH .....sodium hydroxide

Na_2SO_4 ..... sodium sulfate

NBS.....*N*-bromosuccinimide

NHC .....*N*-heterocyclic carbene

$Ni(COD)_2$ ..... Bis(cyclooctadiene)nickel(0)

NMR ..... nuclear magnetic resonance

NOE ..... nuclear overhauser effect

$^1O_2$ ..... singlet oxygen

$^3O_2$ ..... triplet oxygen

PBu_3 ..... tributylphosphine

$Pd(OAc)_2$ ..... palladium diacetate

$Pd(PPh_3)_4$..... Tetrakis(triphenylphosphine)palladium(0)

$Pd(TFA)_2$ .....palladium(II)trilfluoroacetate

Ph .....phenyl

PhCHO.....benzaldehyde

Ph_3COOH..... trityl hydroperoxide

PhH ..... benzene

PhMe .....toluene

PIDA .....iodosobenzene diacetate

PIFA .....[bis(trifluoroacetoxy)iodo]benzene

Piv ..... pivaloyl

p-TsOH .....triphenylphosphine

PPh_3.....*p*-toluenesulfonic acid

ppm ..... parts per million

PPTS ..... pyridinium p-toluenesulfonate

Pr ..... propyl

$PtCl_2$ ..... platinum(II) chloride

PyBox.....2,6-bis[(4S)-4-phenyl-2-oxazolinyl]pyridine

R_f ..... retention factor

$[Rh(CO)_2Cl]_2$..... retention factor

rt ..... room temperature

RVC ..... reticulated vitreous carbon

SiO_2 ..... silica gel

$Sc(OTf)_3$ .....scandium triflate

TBAF ..... tetrabutylammonium fluoride

TBS ..... *tert*-butyldimethyl silyl

TEMPO 2,2,6,6-Tetramethyl-1-piperidinyloxy

Tf..... trifluoromethane sulfonate

TFA ..... trifluoroacetic acid

THF .....tetrahydrofuran

$TiCl_4$..... titanium (IV) tetrachloride

TLC ..... thin layer chromatography

TMOTf..... trimethylsilyl trifluoromethanesulfonate

μmol ..... micromolar

UV ..... ultra violet

$ZnCl_2$ ..... zinc(II) chloride

CHAPTER 1

2*H*-Pyrans: Properties, Synthesis and Use in Natural Product Synthesis

1.1 Introduction to *2H*-Pyrans: Oxa-6π Electrocyclization Equilibrium Properties

2H-Pyrans (pyrans saturated at the C_2 position) are heterocyclic compounds existing in a mixture with oxatriene *via* equilibrium through an oxa-6π electrocyclization (called dienal if R=H and dienone if R≠H, **Figure 1**). This type of electrocyclization promotes valence isomerism, since both structures are constitutional isomers interconverting through a pericyclic reaction. This process is thermo-neutral and its low activation barrier renders the rearrangement easily reversible.

Figure 1.1 *2H*-Pyran/Oxatriene Equilibrium

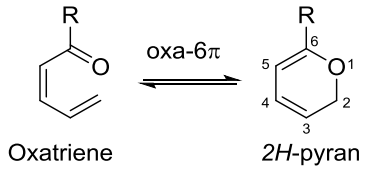

The first example of an isolated *2H*-pyran was described by Büchi and coworkers in 1957.[1] Irradiation of an ethanolic solution of *E*-β-ionone **1** with a mercury lamp promoted *E/Z* isomerization of the alkene to form *Z*-β-ionone **2** *in situ* (**Scheme 1.1**).

Scheme 1.1 Photoinduced Isomerism of *Trans*-β-ionone

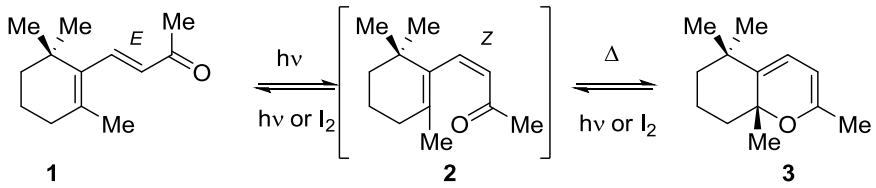

This compound further underwent oxa-6π electrocyclization to *2H*-pyran **3**, a structure which was deduced through IR analysis and successful reduction of **3**.[1] Marvell and coworkers[2] unambiguously determined the structure of *2H*-pyran **3** by ^{1}H NMR (**Scheme 1.2**). Interestingly, analysis of the ^{1}H NMR spectra indicated an additional minor compound was present, but the presumed impurity could not be separated from **3**. By increasing the temperature in the NMR sample, it was shown that the impurity's content increased as well, and upon cooling, the spectra reverted back to its original content. Repeating this experiment through several cycles yielded no decomposition. This was attributed to the equilibrium between **3** and *Z*-β-ionone **2** which is temperature dependent, shifting from a 1:4 ratio (**2:3**) at 54 ˚C to a 1:1.5 ratio (**2:3**) at 113 ˚C.

Scheme 1.2 Spectral Assignment of *2H*-pyran 3 and its valence isomer 2

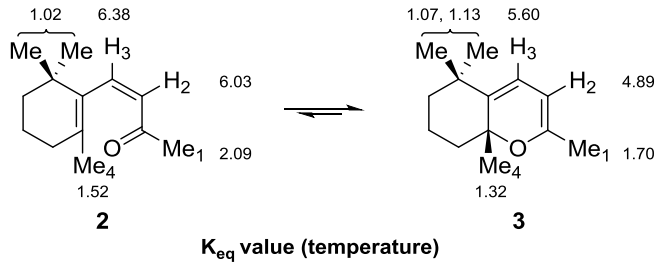

K_{eq} value (temperature)

4.6 (54 °C)

1.52 (113 °C)

Aside from this example, systematic studies regarding the valence isomerism property are few, but give general trends.[3–7] The equilibrium direction, as measured by ^{1}H NMR, depends on several factors: 1) system electronics/sterics, 2) solvent polarity, and 3) temperature. The substitution pattern of the *2H*-pyran scaffold generally has a significant influence on the valence isomerism. Steric bulk, especially with disubstitution at C_2, favors the pyran form (**Scheme 1.3**, **(A)** *vs* **(B)**, and **(C)** *vs* **(D)**). This is due to steric crowding in the dienone form, which forces the structure out of planarity, decreases the π system delocalization efficiency and destabilizes the dienone form. Electronics can have different effects, increasing the proportion of the dienone form to favor π-system conjugation ((**Scheme 1.3**, **(E)**). With electron withdrawing substituents (preferentially at the C_5 position),[8] the equilibrium shifts in favor of the corresponding *2H*-pyran valence isomer ((**Scheme 1.3**, **(F)**).[9]

Scheme 1.3 Isomerism Dependence on Steric and Electronic Factors

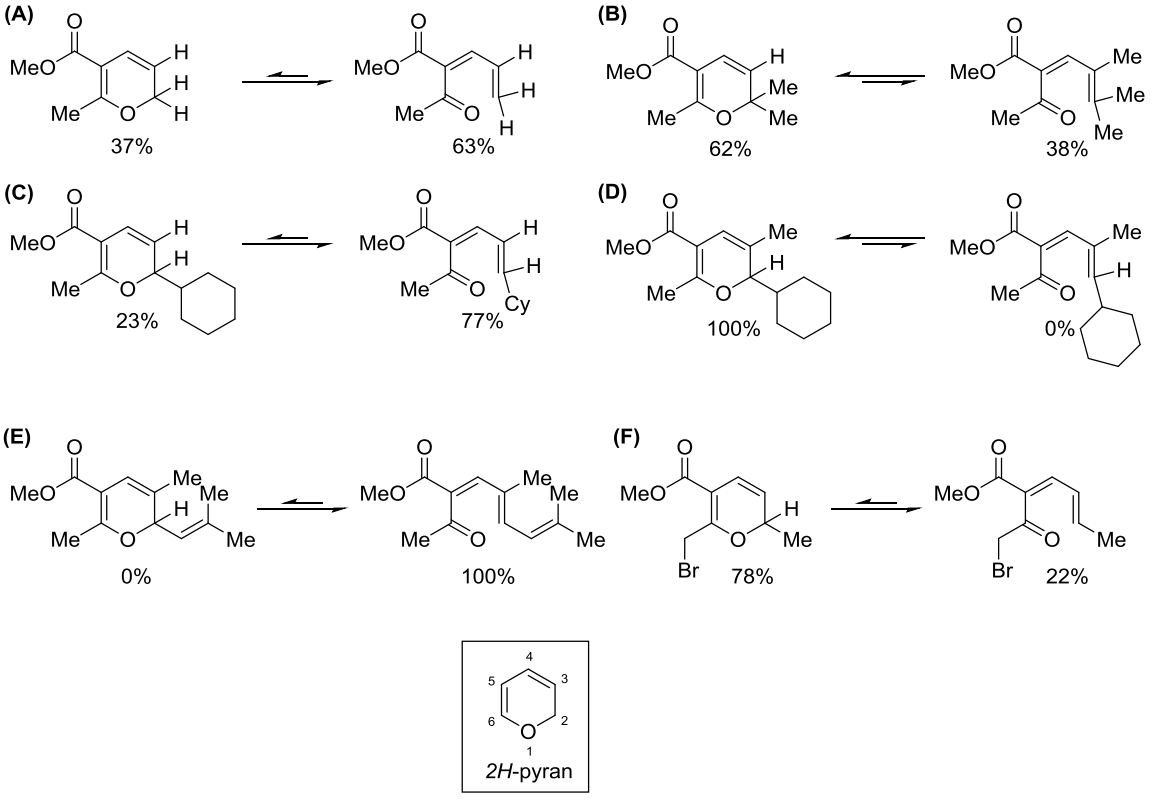

Parameters such as temperature and solvent also impact the isomerism: higher temperature typically increases the proportion of the less stable Z-β-ionone.[2] In polar aprotic solvents, the equilibrium is shifted in favor of the dienone form, potentially due to dipole minimization effects.[5]

In terms of frontier molecular orbital analysis, the valence isomerism can be seen as a dynamic 6π/ring opening equilibrium. According to the Woodward-Hoffman rules for electrocyclizations, two disrotatory modes are at play (clockwise and counter-clockwise) and are responsible for the racemic production of the pyran valence isomer (**Figure 1.2**

(A)). The pyran isomer, in return, may display a preference during retro-6π for inward or outward opening (**Figure 1.2 (B)**).

Figure 1.2 Valence Isomerism: Frontier Molecular Orbital Analysis and Experimental Controls

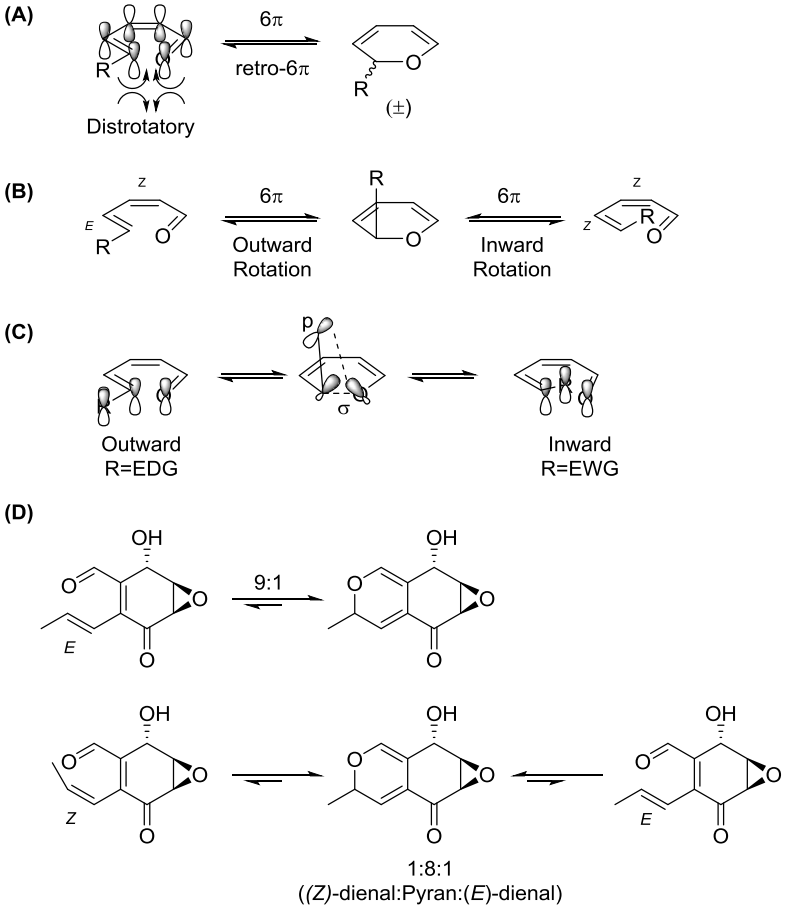

This torquoselective behavior would induce potential alkene isomerization. Similarly to the torquoselectivity observed in retro-4π,[10] electronic factors in retro-6π prevail over sterics, although their effect is less pronounced.[11] In the case of R being an electron donor (its p orbital being occupied) the transition state would be destabilized by the p_{donor}-σ orbital interaction, forcing the R group to move outward (**Figure 1.2 (C)**, left side). Alternatively, when R is an electron acceptor, the vacant p orbital would stabilize the

transition state through a favored $p_{acceptor}$-σ orbital overlap (**Figure 1.2 (C)**, right side). An interesting example showcasing this selectivity was investigated by the Porco group.[12]

Having synthesized both *E* and *Z* version of the alkenyl side chain of a dienal (**Figure 1.2 (D)**), the outcome of the valence isomerism and the isomeric distribution diverged. Starting from the stereodefined *E*-alkene, an equilibrium between the two isomers was observed, favoring the closed form (9:1 ratio of pyran:dienal). In the event where the *Z*-alkene isomer was prepared, a distribution between the three products took place: the pyran equilibrated to the *E*-and *Z*-alkene dienal in a ratio of 8:1:1 respectively. This result is indicative of a higher energy barrier associated with inward rotation of the methyl group *vs.* outward opening. Calculations supported a relative difference in activation energy ($\Delta\Delta G^{\neq}$) of 4 kcal/mol, favoring the opening to the *E* alkene.[13]

Despite the equilibrium dependence on several innate factors, the direction of the valence isomerism can be temporarily perturbed if the oxygen of the *2H*-pyran is in close proximity to another electronegative atom. Cases have been reported where chelating metals were able to shift the valence isomerism toward the ring-opened oxatriene.

Scheme 1.4 6π-Equilibrium Shift by Lewis Acid

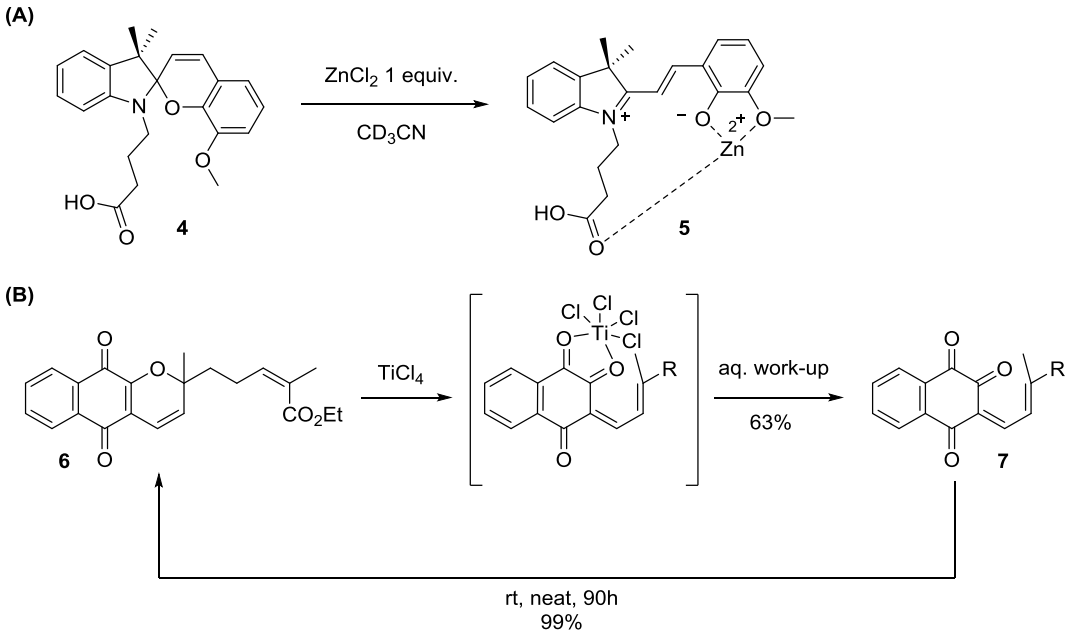

Employing equimolar equivalents of zinc(II), *2H*-pyran **4** (which normally resides in its closed form) was fully opened to chelated form **5**[14] which benefits from a long-range binding of Zn^{2+} with the carboxylic acid side chain and the electronic delocalization from the adjacent N_{sp3} (**Scheme 1.4, (A)**). Another related example was achieved by Trauner and coworkers[15] using Ti(IV) (**Scheme 1.4**, **(B)**). After acidic workup of the presumed titanium chelate of **6**, the dienone system **7** is isolated and slowly reversed back *via* 6π electrocyclization to the starting pyran structure **6.**

1.2 Synthetic Methods to access *2H*-Pyrans

2H-Pyrans, though a prevalent structure in bioactive compounds, remain a challenging target synthetically. Of note, most α-pyrans are unstable to prolonged storage at ambient

temperature, decomposing in air and with potential to self-dimerize. Multiple methods to access *2H*-pyrans depending on the substitution pattern have been developed; one would need to assess each method's limitation when synthesizing a given α-pyran structure. Due to the valence isomerism inherent to α-pyrans, most methodologies target the opened oxatriene form, which may then undergo 6π-electrocyclization to *2H*-pyrans.

1.2.1 Metal Mediated [2+2+2] Cycloisomerization of Diynes and Carbonyls

Expanding upon the large body of work targeting diyne-alkene [2+2+2] cyclizations and motivated by the access to heterocyclic framework, several groups have successfully developed formal cycloadditions of diynes and carbonyls. A general scheme and mechanism for this type of transformation is outlined in **Scheme 1.5**. First, cycloisomerization produces a metallacycle **8**, which then undergoes CO insertion to create 7-membered-metallocycle **9**. Reductive elimination affords the desired *2H*-pyran structure **10** (which may undergo valence isomerism to oxatriene **11**).

Scheme 1.5 Metal-Mediated Diyne-Carbonyls [2+2+2]

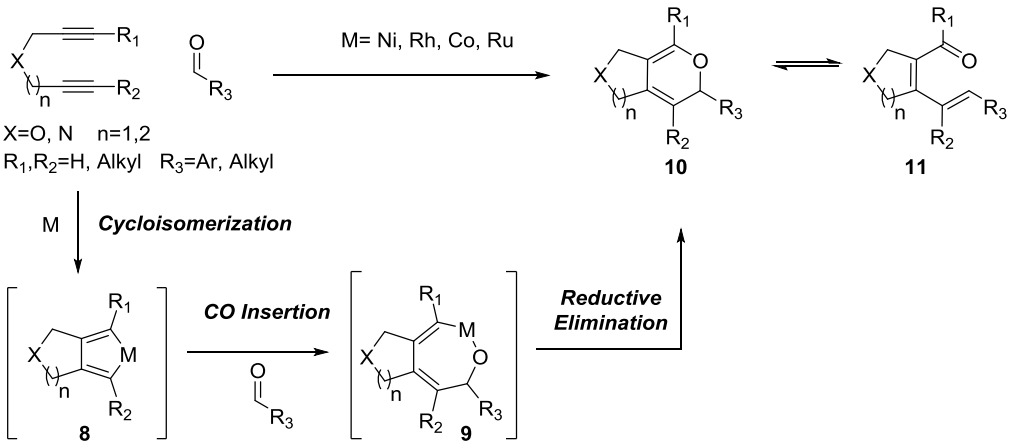

A method directly targeting *2H*-pyrans in their closed form was pioneered by the group of Tsuda in 1988.[16] Using Ni(0) as a catalyst and tertiary phosphines as ligands, the investigators were able to promote the cycloaddition of alkyl-substituted, tethered diynes with aldehydes (**Scheme 1.6**). Terminal alkynes were not well tolerated in this methodology.

Scheme 1.6 Tsuda's Ni(0)-Catalyzed Cycloaddition of Diynes and Aldehydes

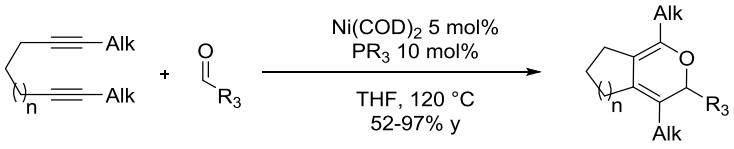

Subsequently, Vollhardt and coworkers reported a similar transformation, mediated by stoichiometric cobalt,[17] in neat acetone as a carbonyl source and a small number of terminal alkynes, expanding the scope of the reaction. In 2005, this chemistry was systematically studied by several investigators, including the Louie, Trost, Shibata, and Tanaka groups. The Louie group applied a Ni(0)/NHC catalytic system to promote cyclizations of alkyl substituted diynes with aldehydes and unactivated carbonyls (**Scheme 1.7**).[18,19]

Scheme 1.7 Louie's Ni(0)/NHC-Catalyzed Cycloaddition of Diynes and Aldehydes

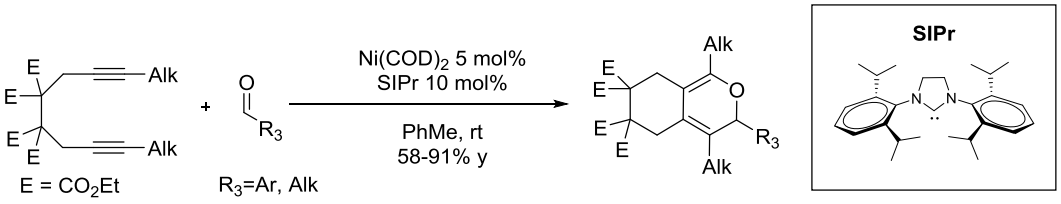

The Trost group used an alternative version, with a tethered *bis*-propargyl alcohol and cationic Ru(I) (**Scheme 1.8**).[20,21]

Scheme 1.8 Ruthenium-Catalyzed Intramolecular Cycloisomerization of Propargyl Alkynes by Trost

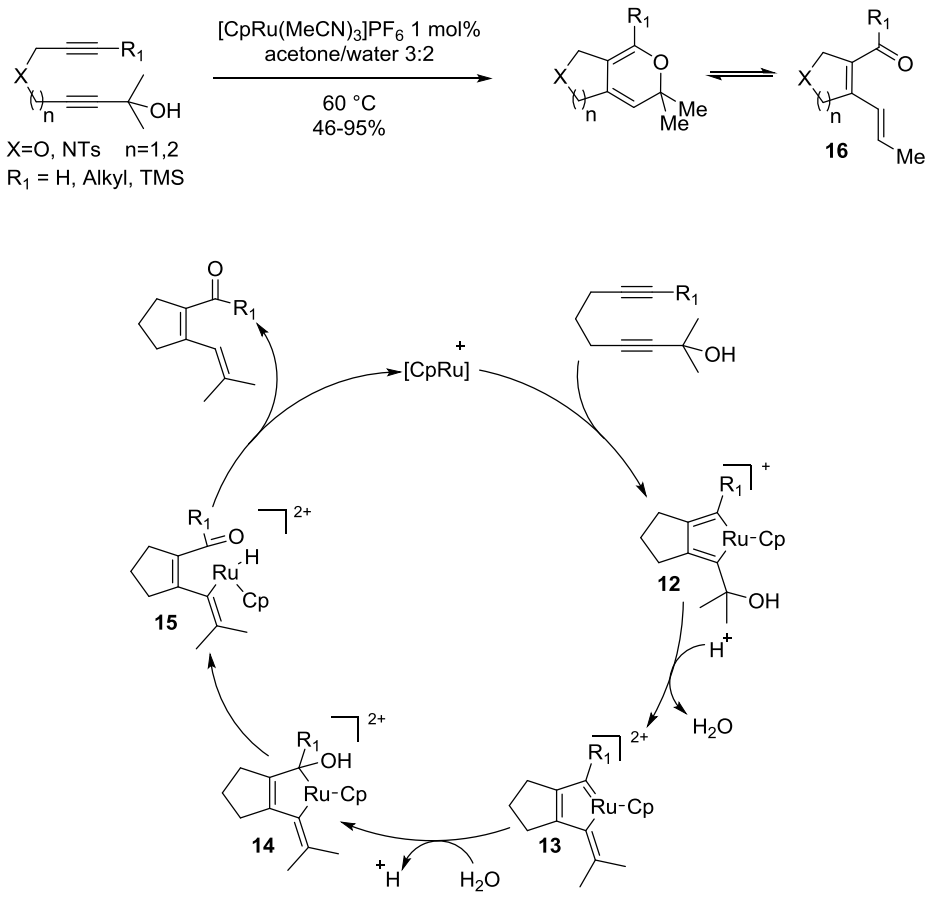

This reaction is proposed to follow a mechanism (**Scheme 1.8**) involving a cycloisomerization step of the tethered diyne to form metallacycle **12**, followed by loss of water which forms the Ru^{2+} complex **13.** Trapping by water affords complex **14** and subsequent hydride shift generates a ruthenium hydride species **15** which is poised for final reductive elimination thereby affording the oxatriene/α-pyran **16.**

More recently, the Niggeman group demonstrated a similar cycloisomerization of tethered diynol with a cooperative Ca^{2+}/CSA catalytic system.[22] The proposed mechanism does not involve formation of a metallacycle, but is based on elimination of the hydroxyl mediated by Ca^{2+}/CSA to afford the allenyl cation **17** (**Scheme 1.9**). Upon nucleophilic trapping by the neighboring alkyne (intermediate **17**) and addition of water to the resulting vinyl cation (intermediate **18**), the allenyl-enol **19** undergoes 1,5-H shift to afford the dienone structure.

Scheme 1.9 Cycloisomerization of Diynols *via* Cooperative Ca^{2+}/CSA System

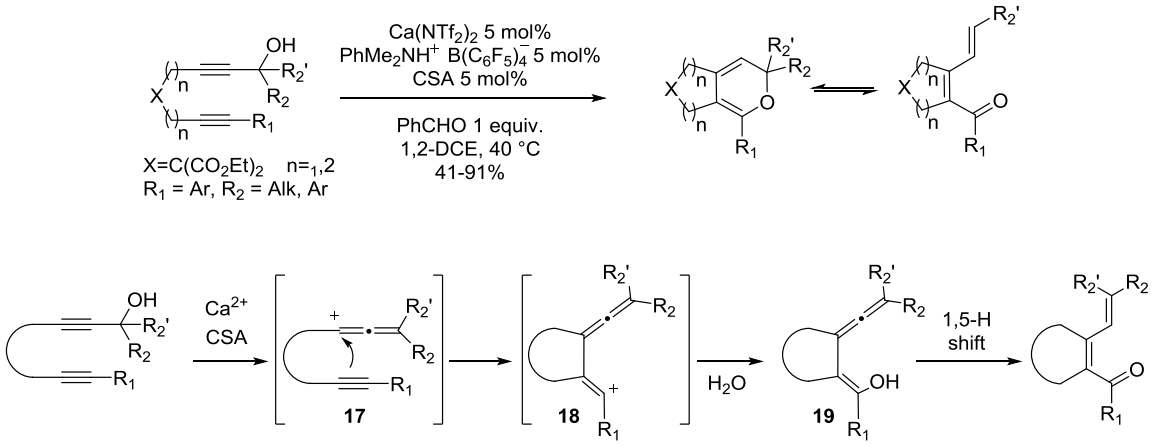

The groups of Tanaka[23,24] and Shibata[25] reported a cationic Rh(I)/BINAP system able to promote the [2+2+2] cyclization of diynes with activated and unactived ketones. A simple racemic BINAP was used as ligand by Shibata with ketoesters and diynes (**Scheme 1.10 (A)**), and a modified H_8-BINAP extended the scope to ketoesters and ketones (**Scheme 1.10 (B)**).

Scheme 1.10 Shibata's and Tanaka's Rh/BINAP Catalyzed Cyclization of Diynes and Ketoesters

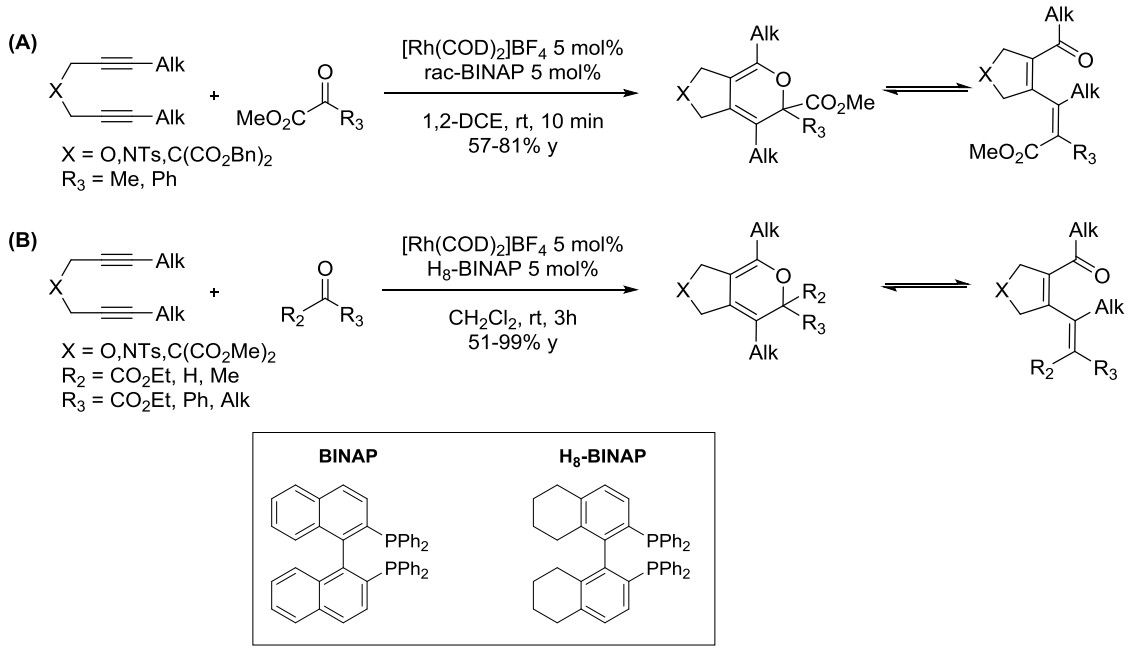

Future development for this type of methodology should be focused on increasing the scope of the reaction to access larger bicyclic systems, and better functional group tolerance as ketone or ester linked diynes are not broadly effective in this transformation.

1.2.2 2H-Pyrans via Formal [3+3] Cycloaddition

One of the most common strategies toward α-pyrans relies on a formal [3+3] cycloaddition proceeding through an overall Knoevenagel condensation of 1,3-dicarbonyls with acrylate derivatives (**Scheme 1.11**). First, an aldol reaction occurs between the enol moiety of the 1,3-dicarbonyl and the α,β-unsaturated aldehyde. Water elimination leads to an oxatriene framework, undergoing valence isomerism with its *2H*-pyran form.

Scheme 1.11 Formal [3+3] Strategy to *2H*-Pyrans

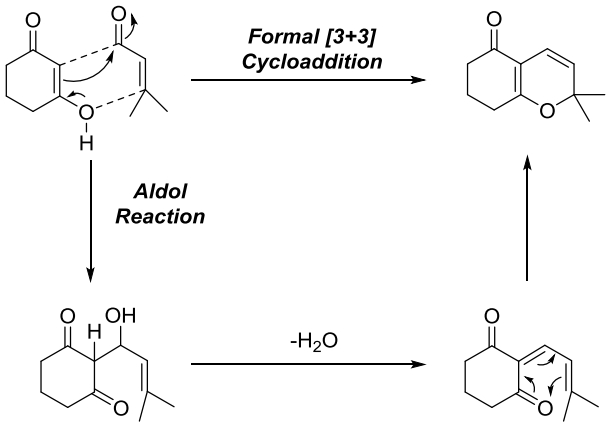

Several catalysis modes have been successfully applied to this reaction including iminium,[26–30] Lewis acid,[31,32] Brønsted acid,[33] and Lewis base catalysts.[34] Inspired by previous reports,[35–37] Hsung and coworkers have reported coupling of iminium salts derived from acrylates to pyrone derivatives (**Scheme 1.12**) which had been shown to proceed in poor yields.[38] Using a preformed piperidinium salt derived from α,β-unsaturated aldehydes (**8**) and further reaction with 4-hydroxypyrones **9**, the investigators were able to synthesize bicyclic *2H*-pyran products **10**.[26,27] This methodology was found to be efficient with cyclic unsaturated aldehydes, and was further applied to Meldrum's acid derivatives[28] and 4-hydroxycoumarins as enol nucleophiles.[29]

Scheme 1.12 Iminium-Catalyzed Cycloaddition of Pyrones with α,β-Unsaturated Aldehydes

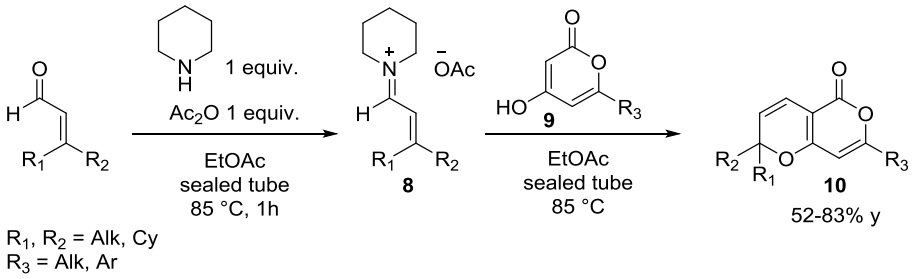

An interesting application of the latter methodology *en route* to cyclopenta[*b*]furans was developed by Mischne and coworkers.[30] An elegant one-pot process was designed (**Scheme 1.13**) wherein dimedone **11** was reacted with dienal **12** in the presence of ethylene diammonium diacetate, forming a transient pyran **13**. This intermediate, upon ring opening, slowly undergoes an *E/Z* isomerization of its polyene sidechain, giving rise to intermediate **14**. Poised for two intramolecular 4π cycloadditions, this intermediate yields the cyclopenta[*b*]furan framework **15**.

Scheme 1.13 Mischne's Cycloisomerization Cascade to Cyclopenta[*b*]furans

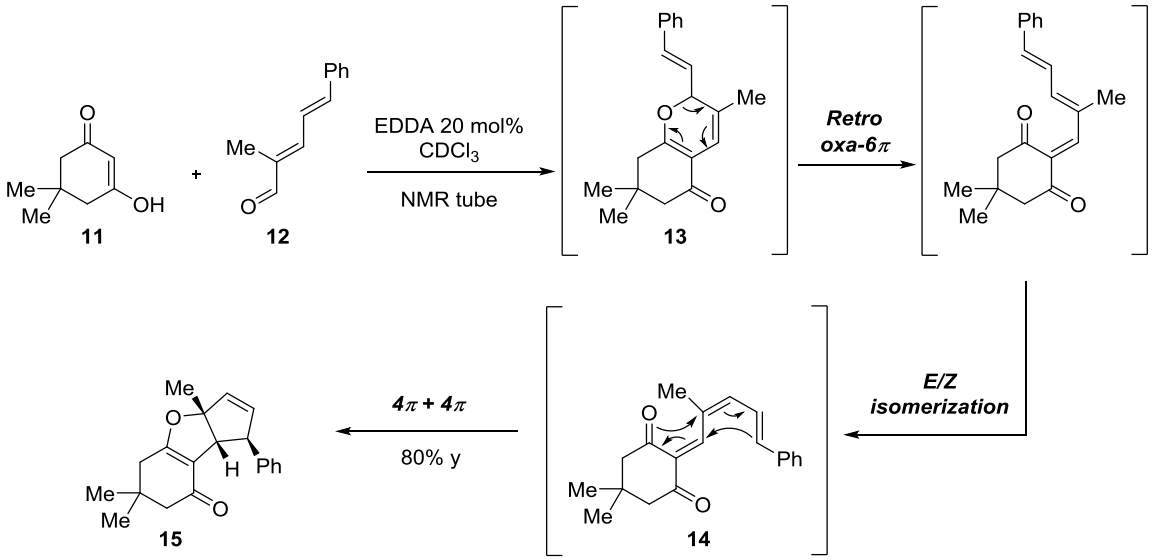

In recent publications, other catalytic systems have also been investigated. Lewis acids[32] were found to promote the reaction of 4-hydroxypyrones and cyclic 1,3-diketones with α,β-unsaturated aldehydes (**Scheme 1.14**).

Scheme 1.14 Lewis Acid Catalyzed Cycloaddition of 1,3-Dicarbonyls with α,β-Unsaturated Aldehydes

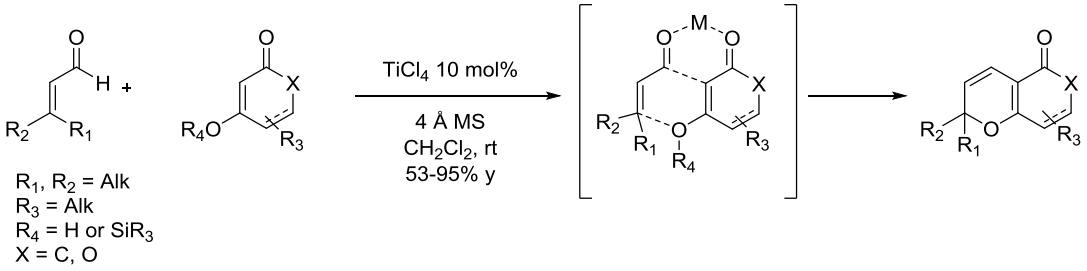

A simple phosphoric acid is also an efficient promoter at low loadings, converting coumarins and pyrones in the presence of a range of aldehydes to *2H*-pyran structures (**Scheme 1.15**).[33]

Scheme 1.15 Iminium Catalyzed Cycloaddition of Pyrones with α,β-Unsaturated Aldehydes

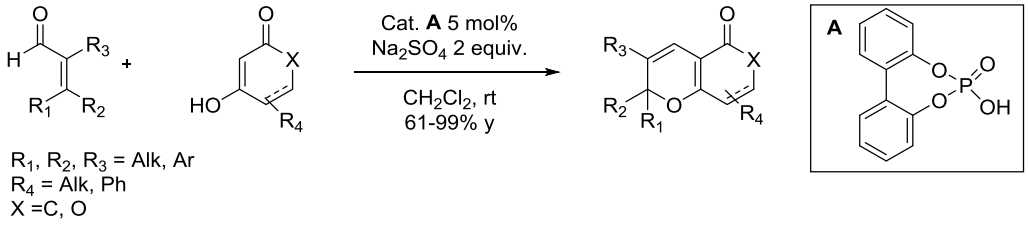

The expansion of this methodology to access acyclic 1,3-dicarbonyls remains challenging. Acyclic diketones usually display internal hydrogen-bonding, making the enol form less reactive, and tend to react in a 1,4-addition with iminiums derived from enals.[39] Only a few studies have been reported thus far with α,β-ketoesters.[9,40] Lewis base catalysis

with phosphines has so far shown more success utilizing acyclic nucleophiles, as demonstrated by the Tong group (**Scheme 1.16**), where allenic acetates were used as electrophilic partners.[34] In this instance, the formal [3+3] cycloaddition goes through a stepwise mechanism based upon phosphine addition to the allenic acetate affording a vinylogous ylide **16**, which eliminates the acetate to form the conjugated species **17**. The 1,3-diketone, through its enol form, then attacks this activated intermediate yielding the C-C linked ylide **18**. The acetic acid liberated promotes a series of proton transfers, affording the *O*-cyclized adduct **19** which affords the final *2H*-pyran **20** after elimination of phosphine.

Scheme 1.16 Phosphine-Catalyzed Cycloaddition of 1,3-Diketones with Allenic Acetates

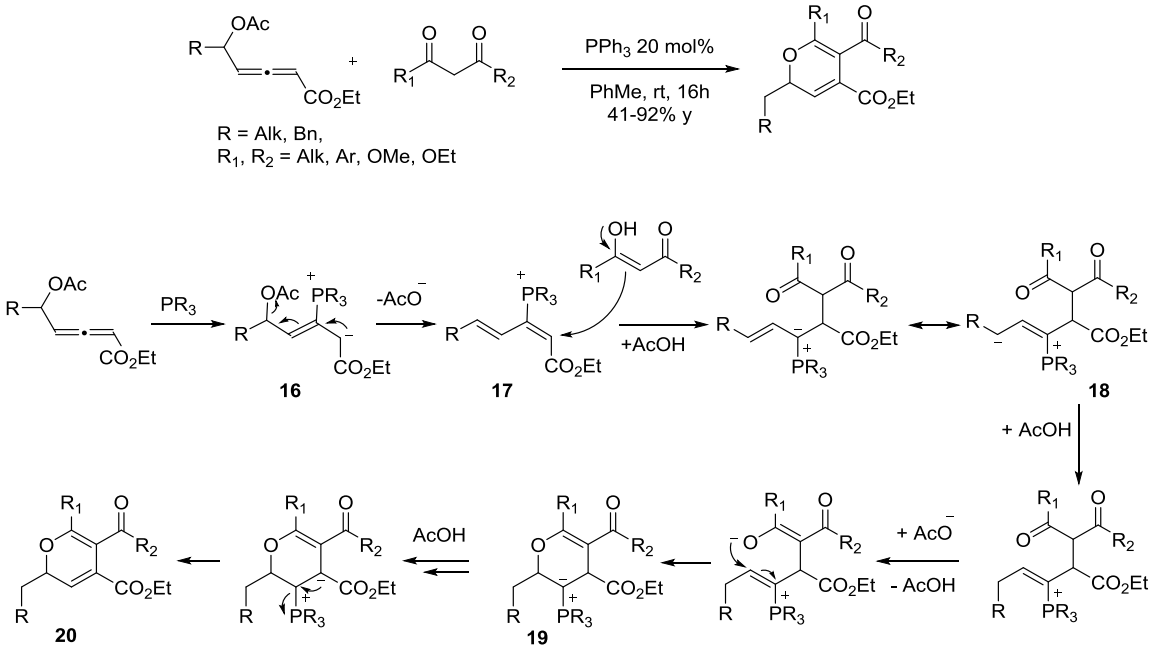

1.2.3 Claisen Rearrangement of Propargyl Vinyl Ethers

Propargyl vinyl ethers are versatile intermediates in the pursuit of heterocycle synthesis. Their use in Claisen rearrangements (known as the Saucy-Marbet reaction) represents a simple and powerful transformation toward 5 or 6-membered ring oxygen or nitrogen-containing small molecules.[41] The key formal [3,3] rearrangement has been catalyzed by a range of transition [42–44] and alkynophilic metals.[45–48]

Scheme 1.17 Propargylic Claisen Rearrangement as a Platform to Heterocycles

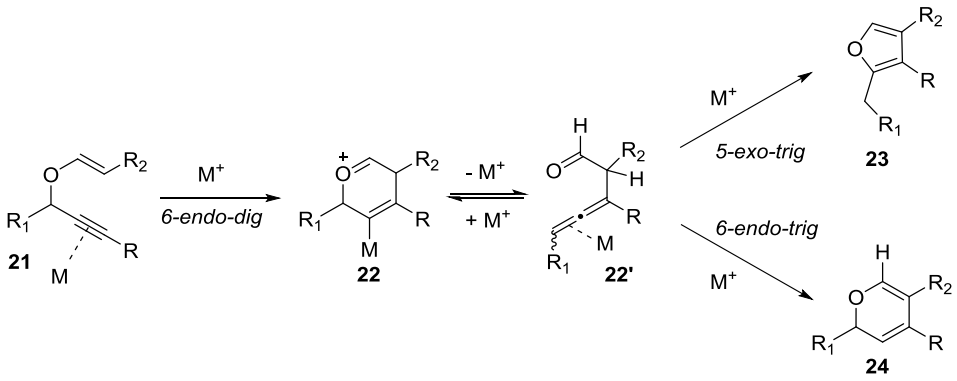

Upon metal-mediated *6-endo-dig* cyclization of **21**, six-membered-ring **22** is created and equilibrates with β-oxa allene intermediate **22'**. The latter can diverge into two pathways (**Scheme 1.17**) to form either furan **23** through a *5-exo-trig* process, or *2H*-pyran **24** *via* a *6-endo-trig* pathway. The latter pathway has been investigated by several groups. For example, the Toste group was able to trap the *6-endo* intermediate using nucleophiles such as water or appended alcohols (**Scheme 1.18**).[48]

Scheme 1.18 Nucleophilc Trapping of the *6-endo* Adduct by Toste and coworkers

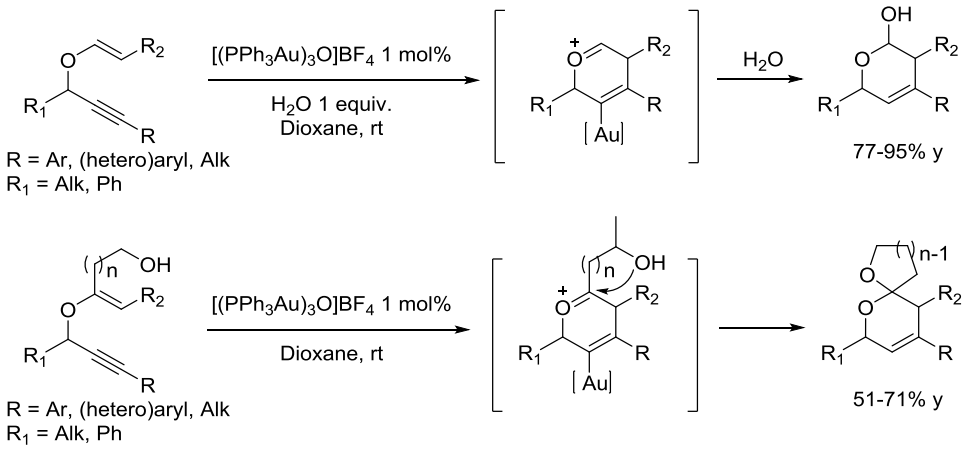

Kirsch and coworkers showed π-philic metals such as Au(I) or Ag(I)[46,47] had significant utility with substrates bearing different substitution patterns. This reaction proceeds through the use of a catalytic base to engage the allene in an isomerization sequence (**Scheme 1.19**). Ag(I) catalysis was found to be well suited for substituted vinyl ethers ($R_3 \neq H$), whereas Au(I) catalysis performed better with simpler vinyl ether substrates ($R_3 = H$, **Scheme 1.19**).

Scheme 1.19 Kirsch's One Pot Propargyl Claisen/Isomerization Sequence

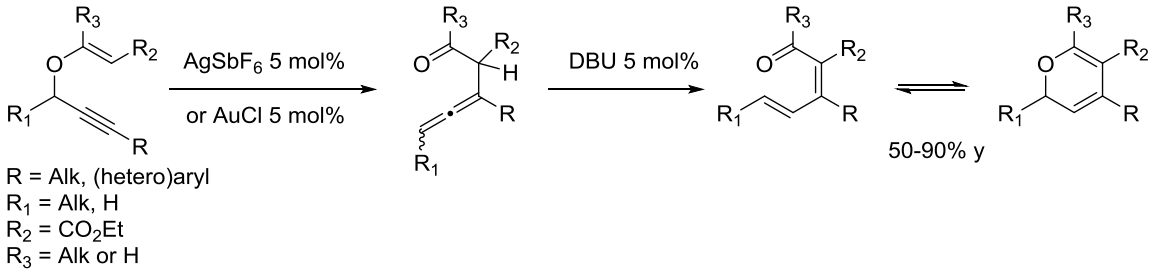

Expanding upon this methodology, Shi and coworkers[44] developed a triazole-gold catalyst/*L*-proline isomerization sequence, targeting unsubstituted vinyl ether (R_3, R_2 = H) and affording the corresponding dienals, although fast isomerization of (*E/Z*) to (*E/E*)-dienals was found to be problematic. Terminal vinyl ethers (R_3, R_2 = H) were not efficiently isomerized to dienals using gold catalysis in absence of base. To bypass this issue and perform a full and selective sequence to (*E/Z*)-dienals, the Alabugin group [42,43] screened various metals ranging from hard Lewis acids to π-philic metals. Most of them stopped the sequence at the allene stage. In contrast, [$Rh(CO)_2Cl$], promoted the desired formal [3,3]-rearrangement followed by isomerization through proto-demetallation (**Scheme 1.20**). The reaction was found to be stereoselective as the production of the (*E*,*E*)-dienal is minimized.

Scheme 1.20 Rhodium-Mediated Saucy-Marbet Rearrangement/Isomerization Cascade

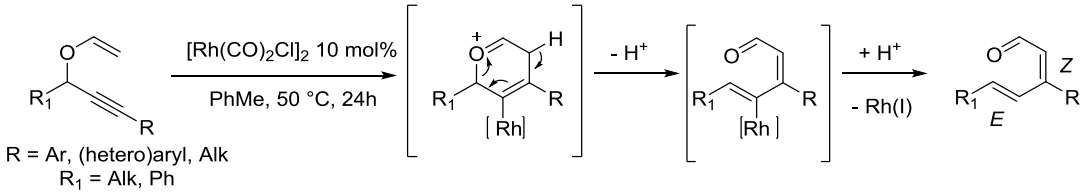

1.2.4 Other Approaches to Oxatrienes/α-Pyrans

Outside of the well-established and utilized methods targeting *2H*-pyrans or their oxatriene valence forms, additional reports have established unique ways of making oxatriene/α-pyran. The Stoltz group, during their pursuit of polycyclic pyrans[49–51] developed a method to synthesize such systems. Starting from α-iodinated hexenones or unsaturated lactones **25**, Stille coupling with β-stannylated acrylates derivatives **26** afforded dienone **27**, which then isomerized *in situ* to *2H*-pyran **28**.[51]

Scheme 1.21 Stoltz's Tandem Stille Coupling/Oxa-6π Electrocyclization

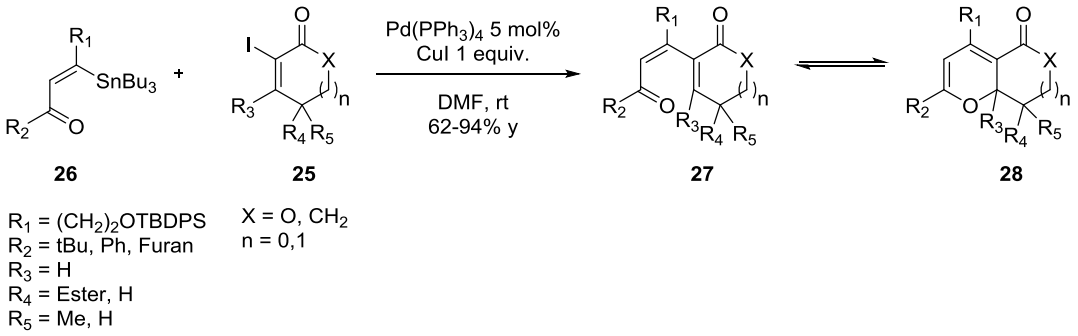

Frontier and coworkers, while studying Nazarov cyclizations of substituted dienyl diketones, serendipitously observed the formation of an α-pyran structure.[52] In the case where $R_1 \neq H$ and in the presence of DABCO, the *2H*-pyran structure **29** was formed selectively (**Scheme 1.22**) instead of the expected cyclopentenone (Nazarov) adduct **30**. A possible rationale for this selectivity arises from equilibration of *E* and *Z* isomers **31** upon addition of DABCO in order to minimize $A^{1,3}$ strain in isomer **32**. Without a deprotonation site present to drive the equilibrium to the cyclopentenone structure **33**, the tertiary amine was preferentially eliminated to afford the *Z*-isomer **31**. This species can further undergo oxa-6π electrocyclization to the pyran **29**.

Scheme 1.22 DABCO-Catalyzed Isomerization of Dienyl Diketones by Frontier and coworkers

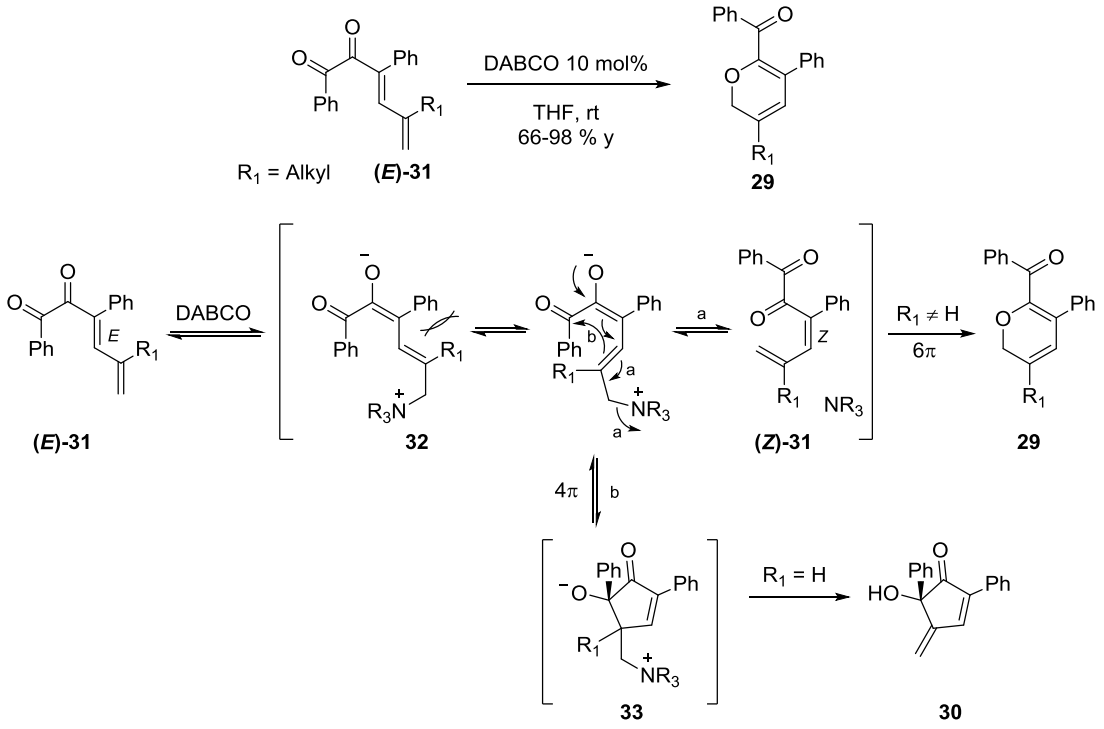

Another report also demonstrated the intermediacy of α-pyrans *en route* to cyclopentenones. Sarpong et *al.*[53] published an elegant study regarding Pt(II)-catalyzed fragmentation of epoxide-containing propargyl esters such as **34**. Upon treatment with $PtCl_2$, a mixture of cyclopentenone **35** and *2H*-pyran **36** was obtained. Resubmitting **36** to the reaction conditions afforded structure **35**, supporting the role of **36** as an intermediate *en route* to **35**. Propargyl ester (**34**), when exposed to Pt(II), underwent Rautenstrauch-type rearrangement [54,55] *via* 5-*exo*-dig ring closure and 1,2-acyl migration to afford intermediate **37**. The adjacent epoxide was then able to trap **37**, creating zwitterion **38**, which releases platinum to give rise to the *2H*-pyran framework **36**. This compound is set for the final

stage of this transformation. Compound **36** undergoes retro oxa-6π to **36'**, followed by Pt-mediated acyl shift/4π cyclization to cyclopentenone **35** *via* orthoester intermediate **39**.

Scheme 1.23 Sarpong's Pt(II) -Mediated Rearrangement of Epoxy-Propargyl Esters

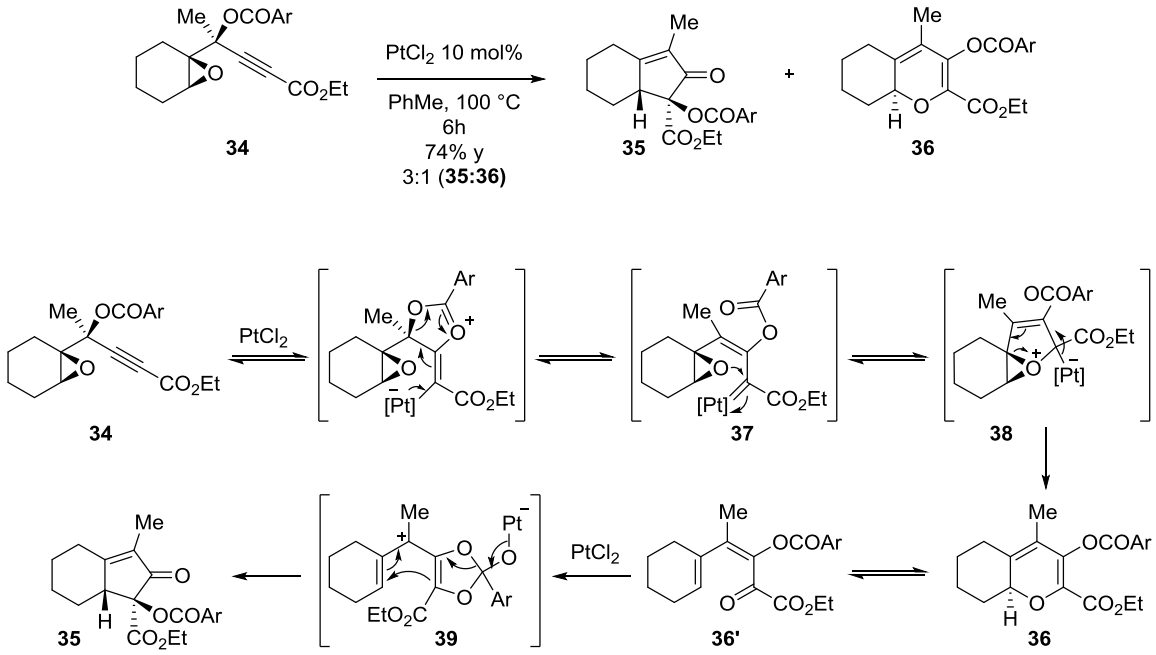

Recently, the Huang goup[56] discovered a domino [4+1]-cyclization/rearrangement to synthesize 2-methyl-*2H*-pyrans (**Scheme 1.24**). First, a tertiary phosphine-mediated formal [4+1]-cycloaddition took place between carbonate **40** and β,γ-unsaturated α-oxo ester **41**, *via* Morita-Baylis-Hillman and subsequent cyclization, affording the 2,3-dihydrofuran **42**. Second, the 5-membered ring was opened in the presence of pyrrolidine and rearranged to pyran **43**. The active intermediate in the [4+1] sequence is the dipole **44**, which was obtained following addition of the tertiary phosphine and decarboxylation of the Boc group. Intermediate **44** then reacted with the Michael acceptor portion of **41**. The created C-C linked zwitterionic species **45** was cyclized to a 2,3-dihydrofuran and

eliminated the phosphine catalyst, affording **42**. The secondary amine catalyst at this stage initiates a deprotonation/protonation sequence to oxatriene/pyran **43**.

Scheme 1.24 Huang's Domino Reaction of Carbonates and Unsaturated Ketones

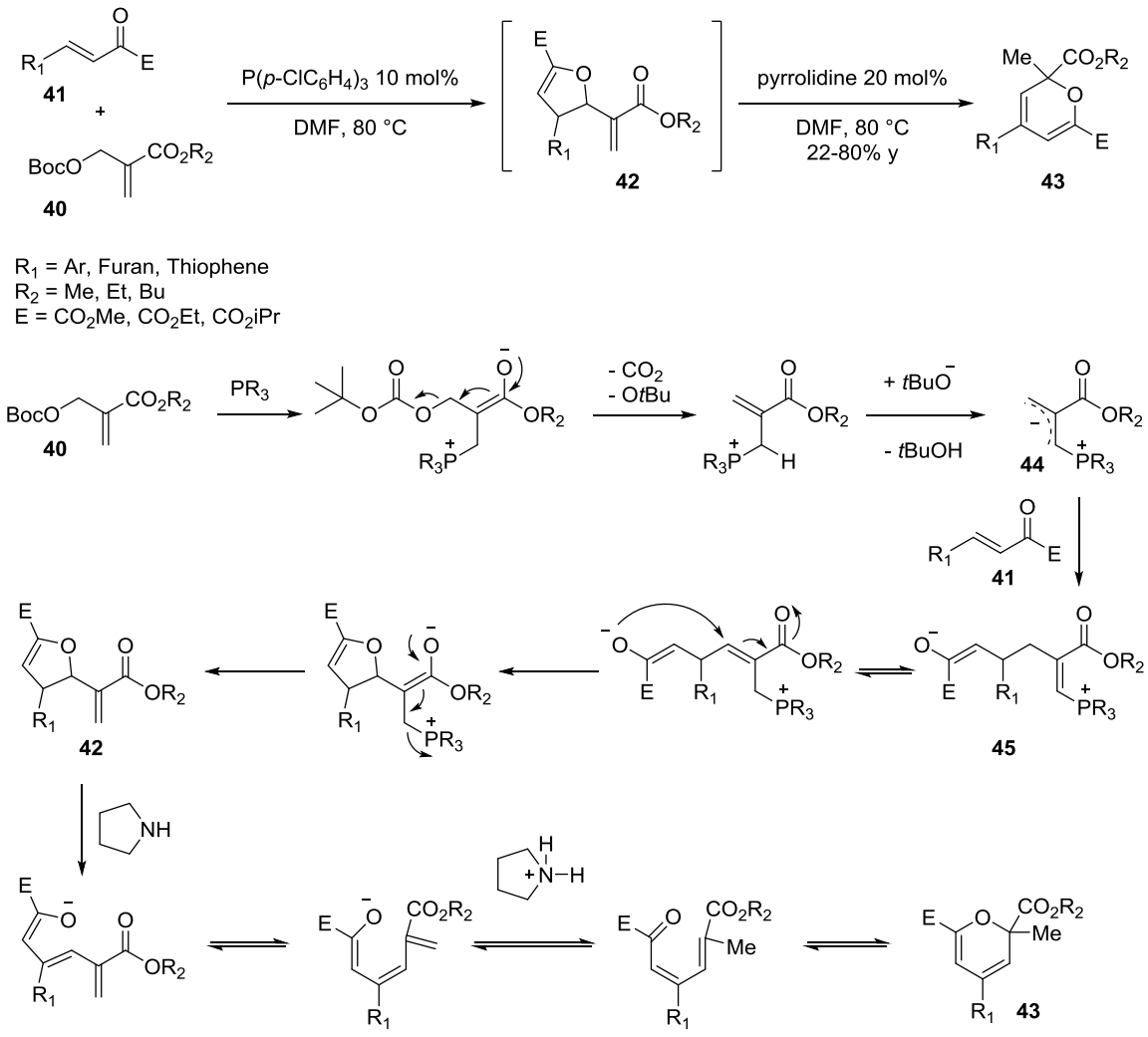

1.3 Use of *2H*-Pyrans in Biomimetic Synthesis of Natural Product

2H-Pyrans are motifs contained in a myriad of natural products (for a sample, see **Scheme 1.25**).[57] The skeleton is widely distributed in prenylated chromenes such as panduratin B (**46**),[58] daurichromenic acid (**47**), gambogic acid (**48**), and in quinone structures (tecomaquinone I (**49**)).

Scheme 1.25 *2H*-Pyran Containing Natural Products

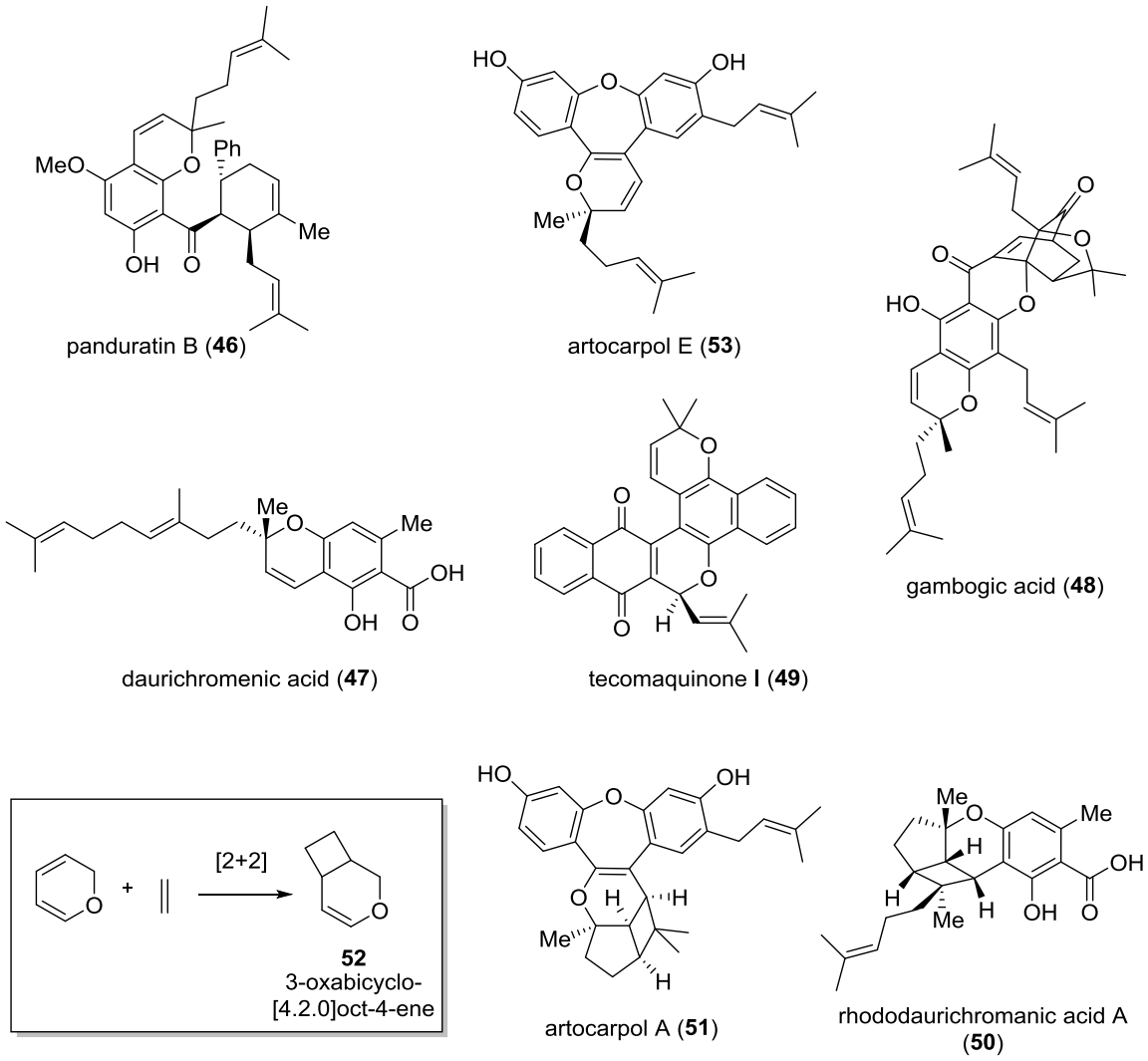

Due to their high reactivity, *2H*-pyrans have been proposed as intermediates in many biosynthetic cycloadditions. Rhododaurichromanic acid A (**50**) and artocarpol A (**51**), both displaying a 6/4 fused bicycle such as **52**, are derived from the [2+2] cycloaddition precursors daurichromenic acid (**47**)[59–61] and artocarpol E (**53**),[62,63] respectively (**Scheme 1.25**). *2H*-Pyrans are additionally thought to be intermediates in biosynthetic Diels-Alder reactions. A framework of choice in this case is a 2-oxabicyclo[2.2.2]oct-5-ene **54** (**Scheme 1.26**), which arises from a [4+2] cycloaddition between a *2H*-pyran diene and an alkene dienophile. This bridged bicyclic structure is present in natural products such as torreyanic acid (**55**),[12,13,64,65] epoxyquinol A (**56**),[12,66–70] pinnatal (**57**)[71,72] and xanthipungiolide (**58**).[73] These attractive targets have been the focus of synthetic efforts in order to demonstrate their biosynthetic origin and elucidate the role of their *2H*-pyran precursors.

Scheme 1.26 *2H*-Pyrans as Intermediates in Diels-Alder Cycloadditions Toward Natural Products

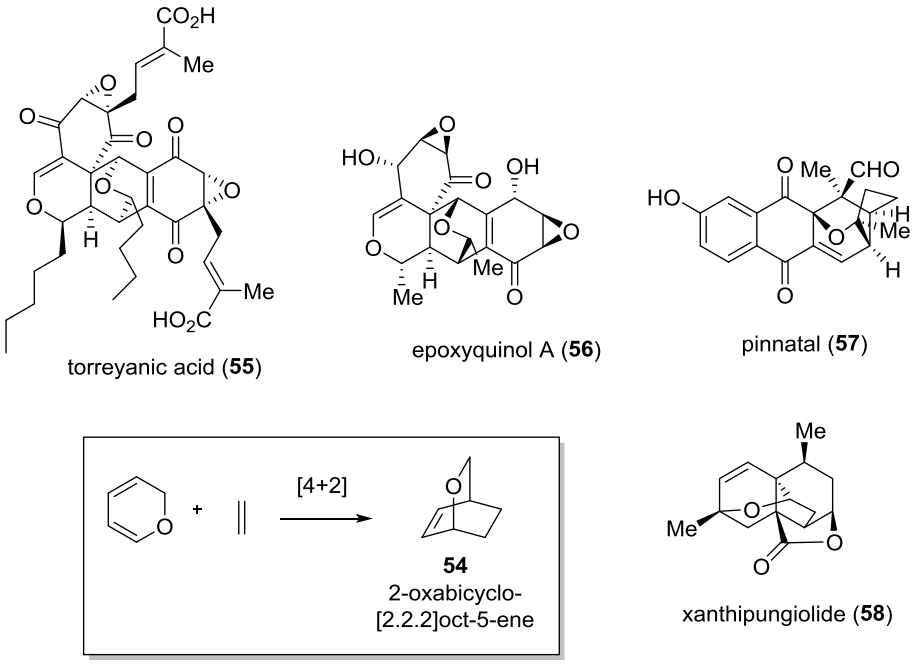

1.3.1 Biomimetic Synthesis of Torreyanic Acid, Epoxyquinol A, and Congeners

Torreyanic acid was isolated by Clardy and coworkers[64] in 1996 from the fungus species *Pestalotiopsis microspora*. The natural product demonstrated a selective cytotoxicity against several human cancer cell lines. Clardy postulated a potential biosynthesis for torreyanic acid (**55**) would rely on self-dimerization of the monomeric *2H*-pyran **59** which is in equilibrium with its dienal form **59'** through a 6π electrocyclization (**Scheme 1.27**).

Scheme 1.27 Clardy's Biosynthetic Proposal to Torreyanic Acid

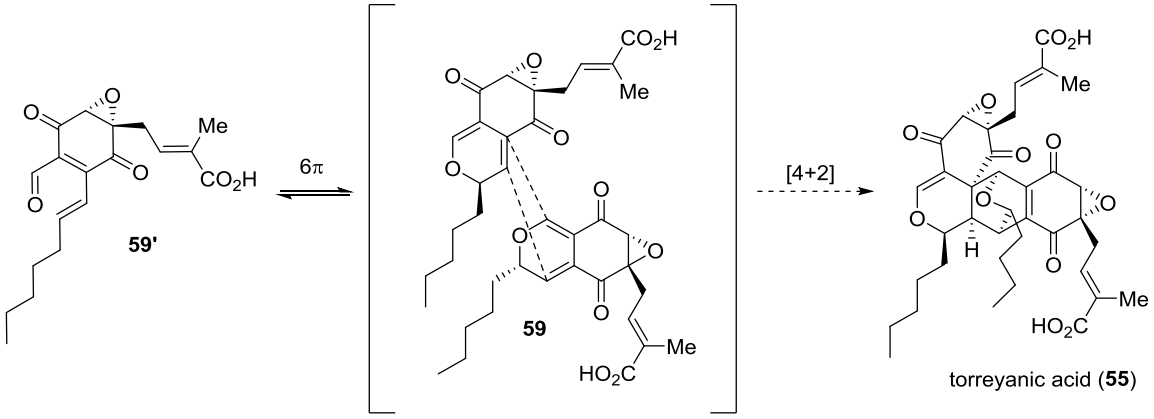

The Porco laboratory took on the challenge of proving the synthetic feasibility of this proposed biosynthesis in the early 2000's. The first racemic synthesis of torreyanic acid[65] was disclosed, followed by an enantioselective version.[13] Key to the success of this tour de force synthesis (**Scheme 1.28**) was the enantioselective elaboration of epoxyquinone **60**, which was achieved using tartrate-mediated nucleophilic epoxidation of quinone monoketal substrate **61**. This intermediate was rapidly advanced to the enantiopure epoxyquinone **62**. Oxidation with DMP enabled the formation of the desired dienal **63**, undergoing equilibrium with *syn*-pyran **64** and *anti*-pyran **64**'. In order to minimize steric interactions in the transition state, the thermodynamically favored [4+2] combination occurs by an *endo*, top approach of *anti*-pyran **64'** with *syn*-pyran **64** (similar to **Scheme 1.27**). A single dimeric compound **65** was thus obtained selectively over other dimerization pathways. Facile deprotection of the *tert*-butyl esters in the presence of TFA finally generated (+)-torreyanic acid **66**. The absolute stereochemistry of the natural compound was assigned to be identical to **66**, opposite to the one depicted in **Scheme 1.27**, (**55**).

Scheme 1.28 Porco's Biomimetic Synthesis of (+)-Torreyanic Acid

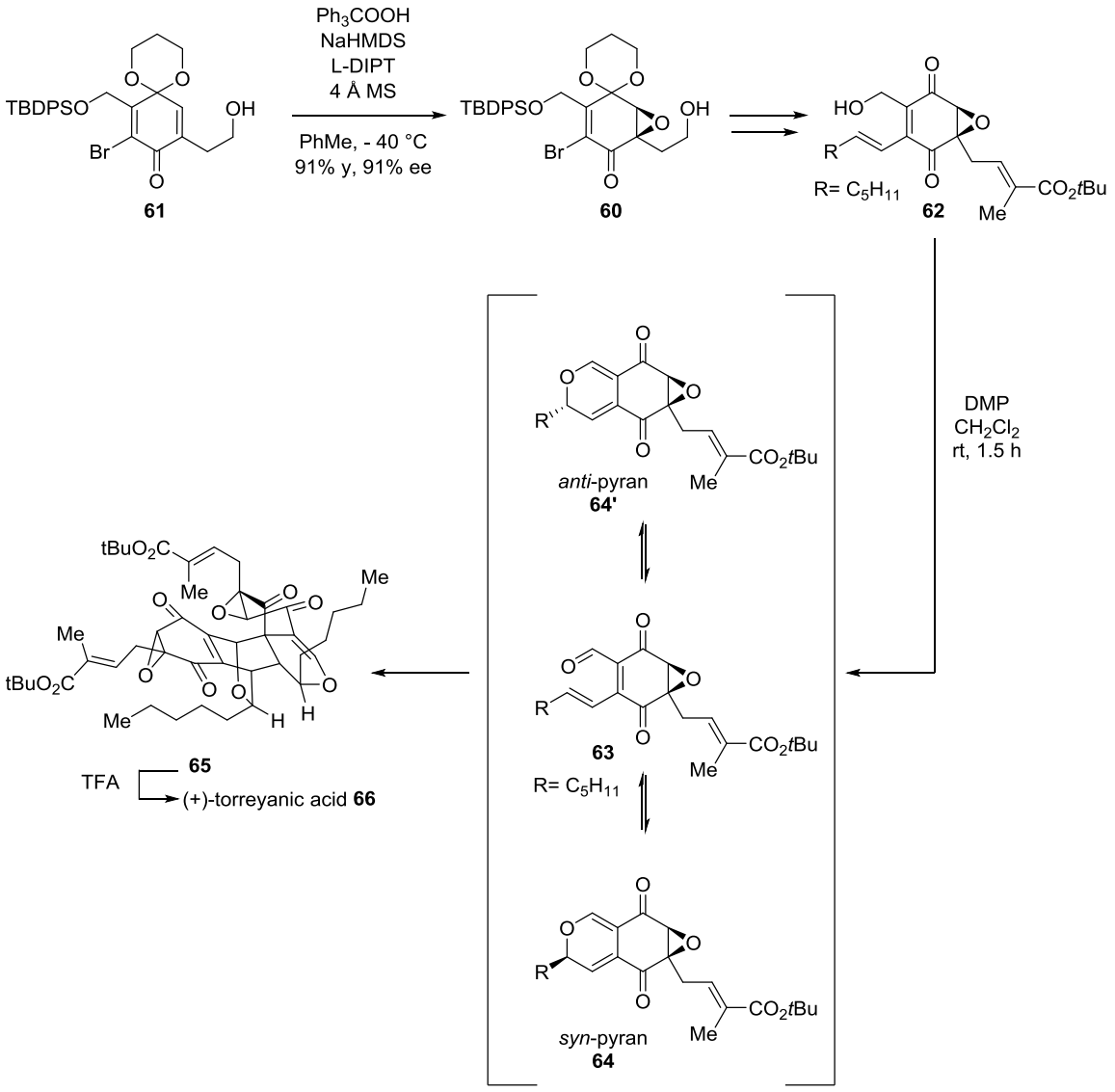

This type of dimerization was also thought to take place in the biosynthesis of the related epoxyquinols (**Scheme 1.29**).[67] Based on the co-isolation of related natural products from the same unknown soil fungus, a proposal by Hayashi and coworkers[68] outlined the potential dimerization pathways adopted by the *syn* and *anti 2H*-pyrans **67** and **67',** in

equilibrium with dienal **68**. *Syn* pyran **67** could undergo homodimerization to afford epoxyquinol B (**69**) (*endo* [4+2]) or a [4+4] cycloaddition to give epoxytwinol A (**70**). *Anti* pyran **67**' would yield epoxyquinol C (**71**) upon homodimerization (*exo* [4+2]) and could heterodimerize with *syn* **67** to generate epoxyquinol A (**56**).

Scheme 1.29 Biosynthetic Hypothesis to Epoxyquinols and Congeners

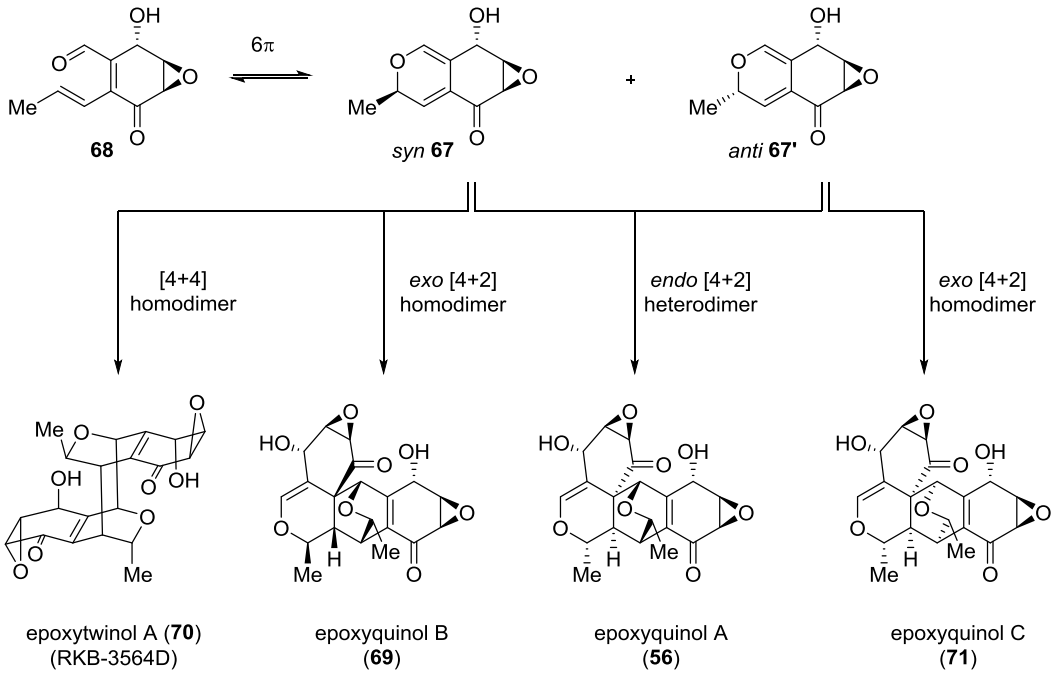

Concomitant with their isolation, the first total synthesis of epoxyquinols was reported by the Hayashi group in 2002.[68] The key epoxyquinol fragment **72**, synthesized enantioselectively according to a fairly lengthy sequence, was treated with MnO_2 to promote oxidation of the primary alcohol (**Scheme 1.30**). A 6π electrocyclization then created both *syn* and *anti*-pyrans **67** and **67'**.

Scheme 1.30 Hayashi's Synthesis of Epoxyquinols and Congeners

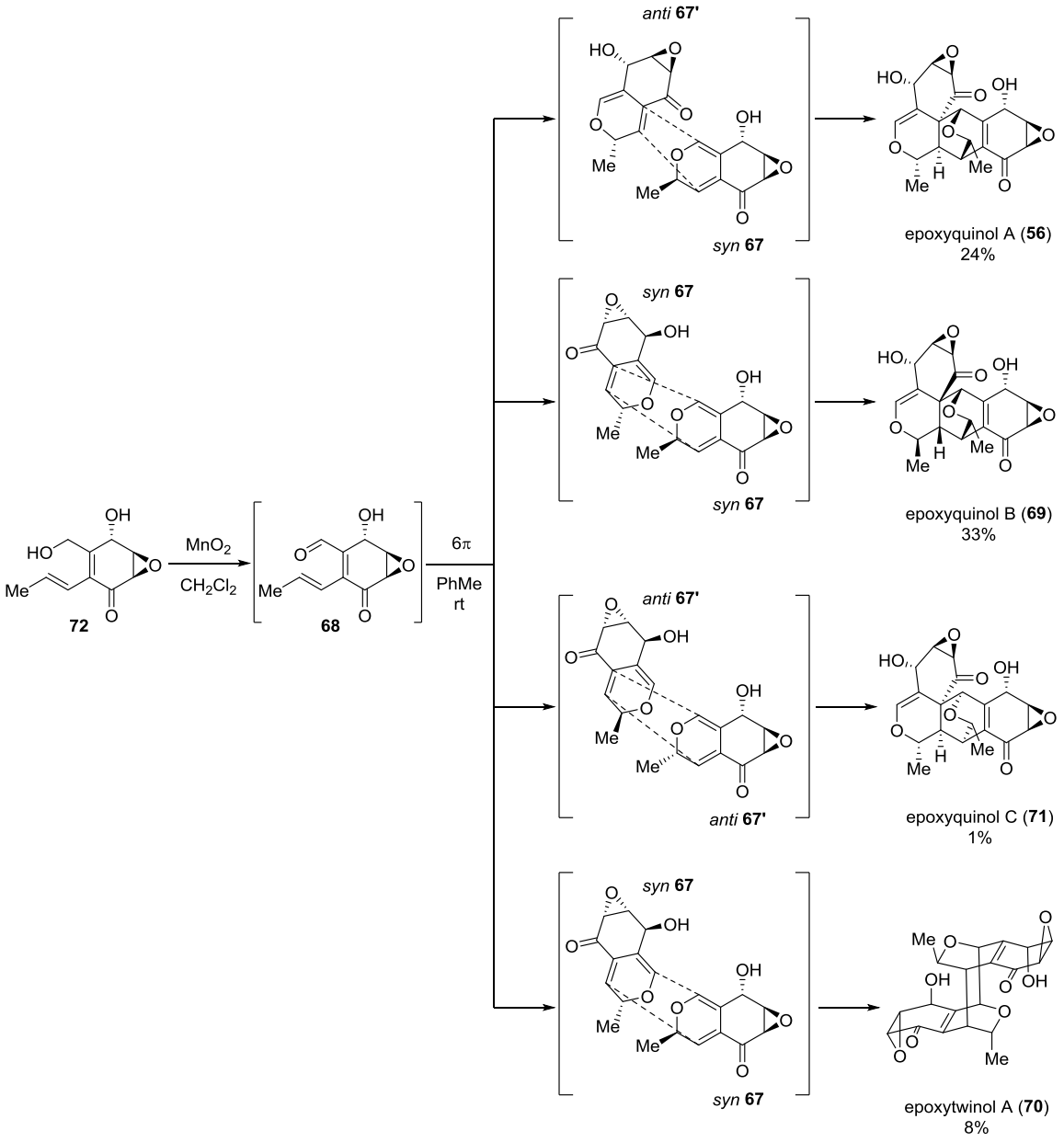

Heterodimerization yielded epoxyquinol A (**56**), and *syn* **67** homodimerization afforded epoxyquinol B (**69**) as major products. In a subsequent study,[74] a shorter, scalable route was devised to intermediate **72**, and after concentration of the crude oxidized mixture from

72 and dissolving in toluene, four compounds were isolated (**Scheme 1.30**). Arising from all the potential cyclization modes (*cf.* **Scheme 1.29**), epoxiquinols A-C, along with the [4+4] dimer epoxytwinol A were synthesized, strongly supporting the biosynthetic proposal.

The Porco group also investigated these dimerization pathways to epoxyquinols A and B[12,70] and successfully carried out a more selective synthesis of epoxytwinol A (**70**).[75] This [4+4] dimer was found to be a minor product in the oxidation/dimerization of epimers **67**/**67'** (<10% yield).[12] In order to favor [4+4] dimerization over [4+2] cycloadditions, a blocking group strategy was designed.

Scheme 1.31 Porco's Synthesis of Epoxytwinol A

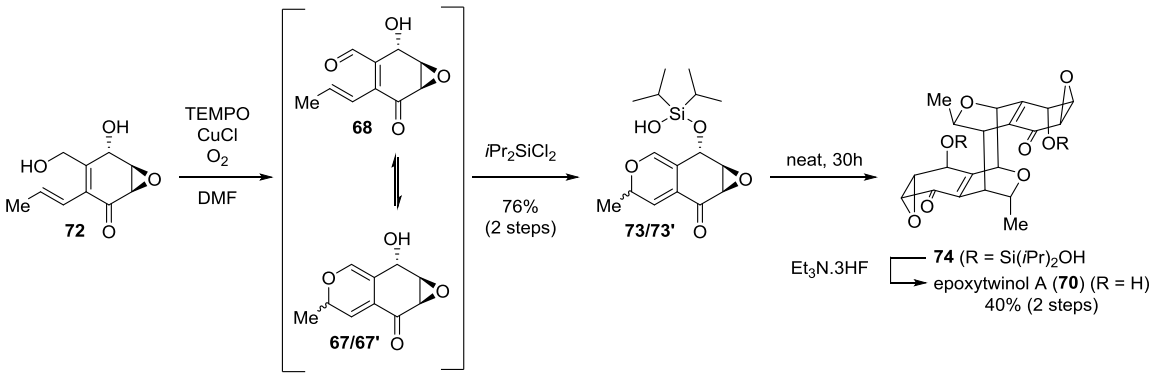

Dienal **68** was first generated using a TEMPO oxidation of **72**,[76] equilibrating to **67**/**67'** *in situ*. Dichlorodiisopropylsilane then reacted with **67**/**67'** to obtain the diisopropyl silanol diastereomeric mixture **73**/**73'**. Upon standing, the crude mixture selectively homodimerized to a *bis*-silanol protected dimer **74**, without any production of [4+2]

dimers. Ultimately, treatment with a fluoride source afforded epoxytwinol A (**70**) in an improved yield.

1.3.2 Biomimetic Synthesis of Antimalarial Naphthoquinones

Several naphthoquinone-containing compounds isolated from *Bignoniacea* tree species, among them pinnatal (**57**), have shown low single digit micromolar activity in malaria-inducing parasites.[71,77,78] Biosynthetically, a unified pathway has been suggested to proceed *via* oxa-6π/cycloadditions of naphthoquinone structures such as **75** (**Scheme 1.32**).

Scheme 1.32 Biosynthetic Proposal to Antimalarial Naphthoquinones

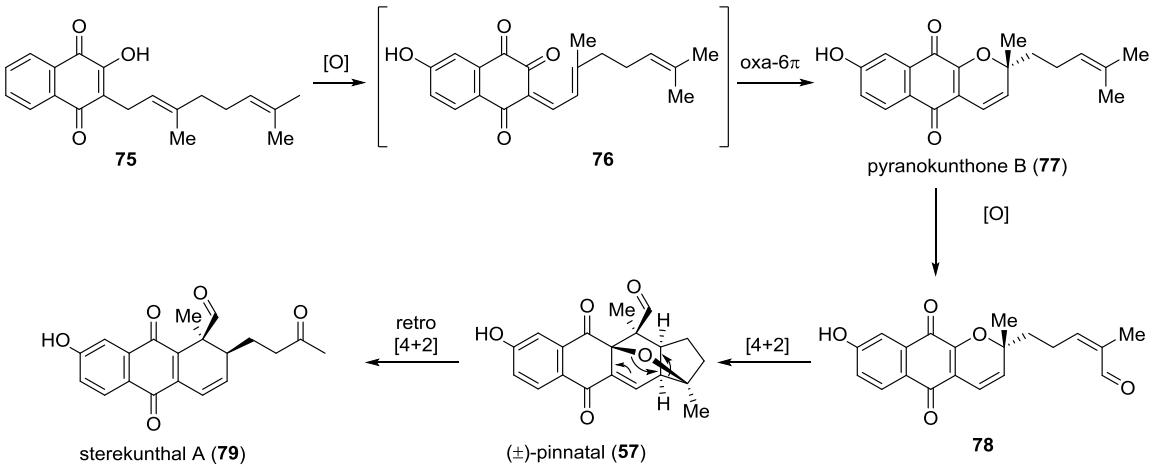

Enzymatic oxidation of **75** should produce the dienone **76** which undergoes 6π cyclization to pyranokunthone B (**77**). Further oxidation may generate the enal-containing framework **78**, suited for an intramolecular Diels-Alder cycloaddition that would produce pinnatal (**57**). This adduct could potentially undergo a retro [4+2] cycloaddition and rearrange to sterekunthal A (**79**).

Following this biomimetic proposal, Trauner and coworkers elegantly synthesized the series of aforementioned natural products in a chiral, racemic fashion (**Scheme 1.33**).[15,79] Aldehyde **80** (derived from geraniol) was condensed with naphtoquinone **81** using a modification of Hsung's iminium catalyzed [3+3] methodology (*cf. Section 1.2.2*, **Scheme 1.11**). The resulting *2H*-pyran **82,** upon protecting group manipulation, was advanced to key intermediate **78**. Facile intramolecular Diels-Alder cycloaddition then took place at room temperature, yielding chiral, racemic pinnatal (**57**). Under harsh heating, this natural product underwent retro-[4+2] cycloaddition to generate (±)-sterekunthal A (**79**), in accordance with the postulated biosynthesis (**Scheme 1.32**).

Scheme 1.33 Trauner's Biomimetic Syntheses of Antimalarial Naphtoquinones

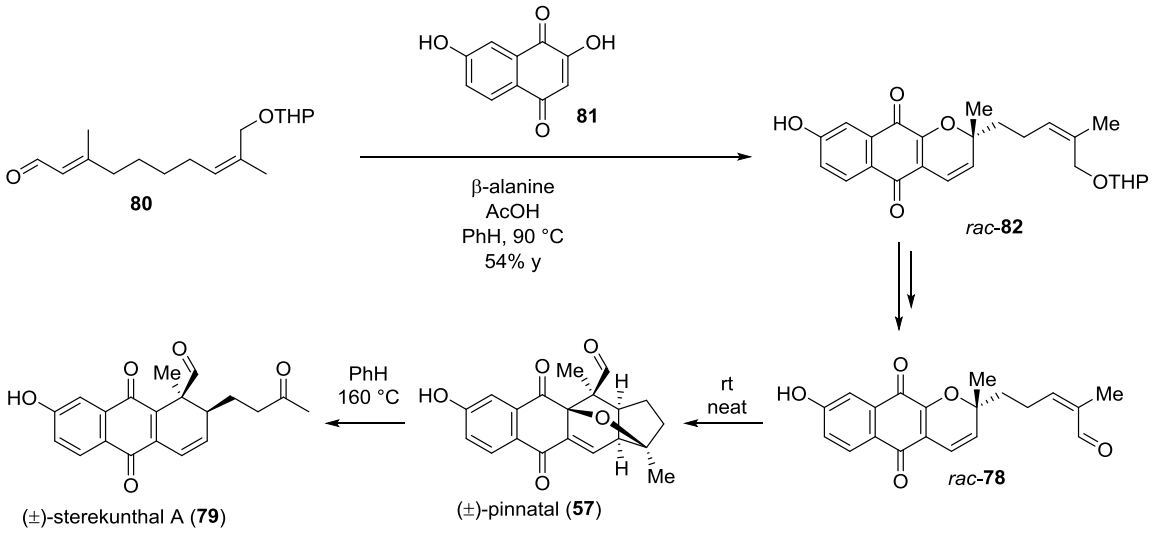

In order to obtain pinnatal and derivatives enantioselectively, Trauner hypothesized that a dynamic kinetic resolution of *rac*-**78** could be achieved *via* selective, chiral Lewis acid-catalyzed Diels-Alder cycloaddition.[15] If only one enantiomer of **78** would participate

in the intramolecular [4+2] cycloaddition (**Scheme 1.34 (A)**), the unreactive enantiomer would interconvert to *epi*-**78** *via* dienone **76**, completely driving the isomerism to the active form. This concept would require a faster pyran epimerization rate against cycloaddition to be effective. Screening a variety of chiral Lewis acids, the best result was obtained with a scandium triflate/PyBox system, affording pinnatal **57** in 40% yield and 55% ee (**Scheme 1.23(B)**). Despite the yield and enantiomeric excess suggesting only kinetic resolution took place, none of the starting *2H*-pyran **78** was recovered.

Scheme 1.34 Attempted Dynamic Kinetic Resolution to Enantioenriched Pinnatal

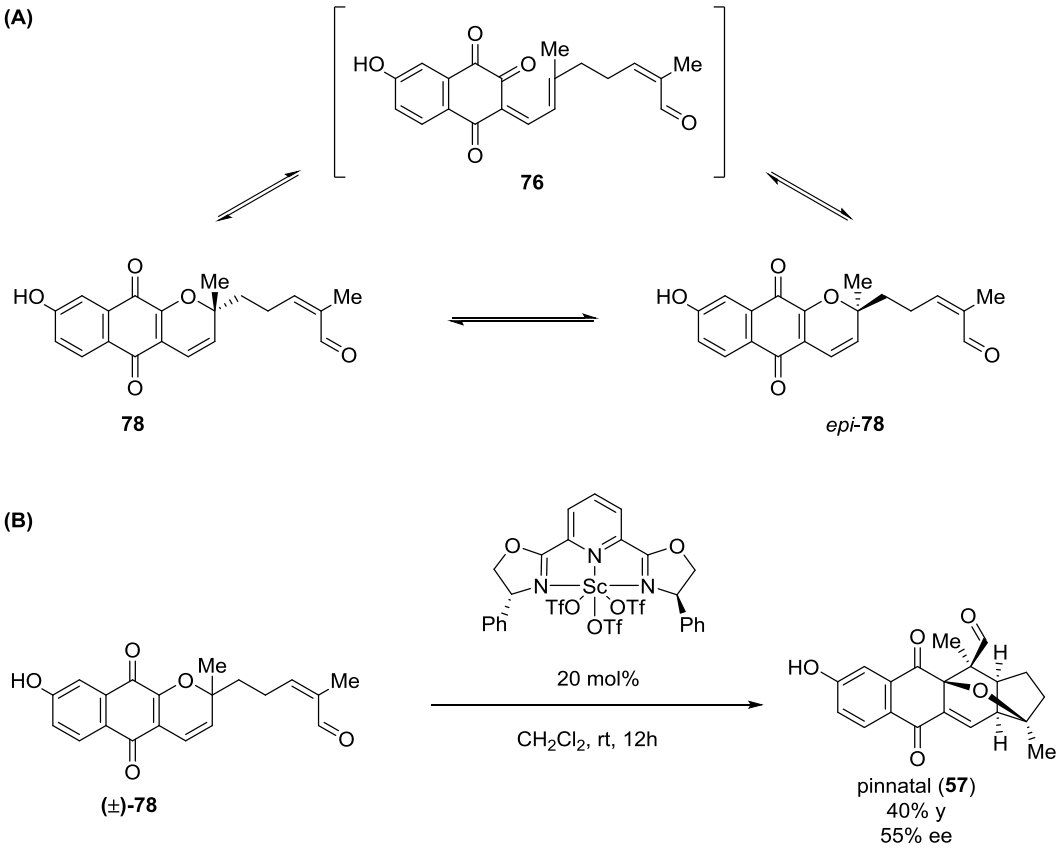

1.3.3 Biomimetic Synthesis of Artocarpols and Daurichromenic Acid Natural Products

In addition to participating in biosynthetic [4+2] cycloaddition, *2H*-pyrans are also thought to be intermediates in light-induced [2+2] cycloaddition events, forming a fused 3-oxabicyclo[4.2.0]oct-4-ene (**Scheme 1.25**). Rhododaurichromanic acid A (**50**) and B (**83**) (**Scheme 1.35**), compounds extracted from the plant *Rhododendron dauricum*,[59] have been postulated to be biosynthetically related to the potent HIV inhibitor daurichromenic acid (**47**)[80] (EC_{50} = 5.67 ng/mL). From grifolic acid (**84**), oxidation followed by oxa-6π electrocyclization may afford the *2H*-pyran moiety of daurichromenic acid (**47**). Light irradiation could trigger isomerization of the internal *E* alkene to *Z*-**47'**, and both isomers would react in an intramolecular [2+2] cycloaddition, generating rhododaurichromanic acid A (**50**) and B (**83**).

Scheme 1.35 Unified Biosynthetic Hypothesis to Chromenic Acid and Related Natural Products

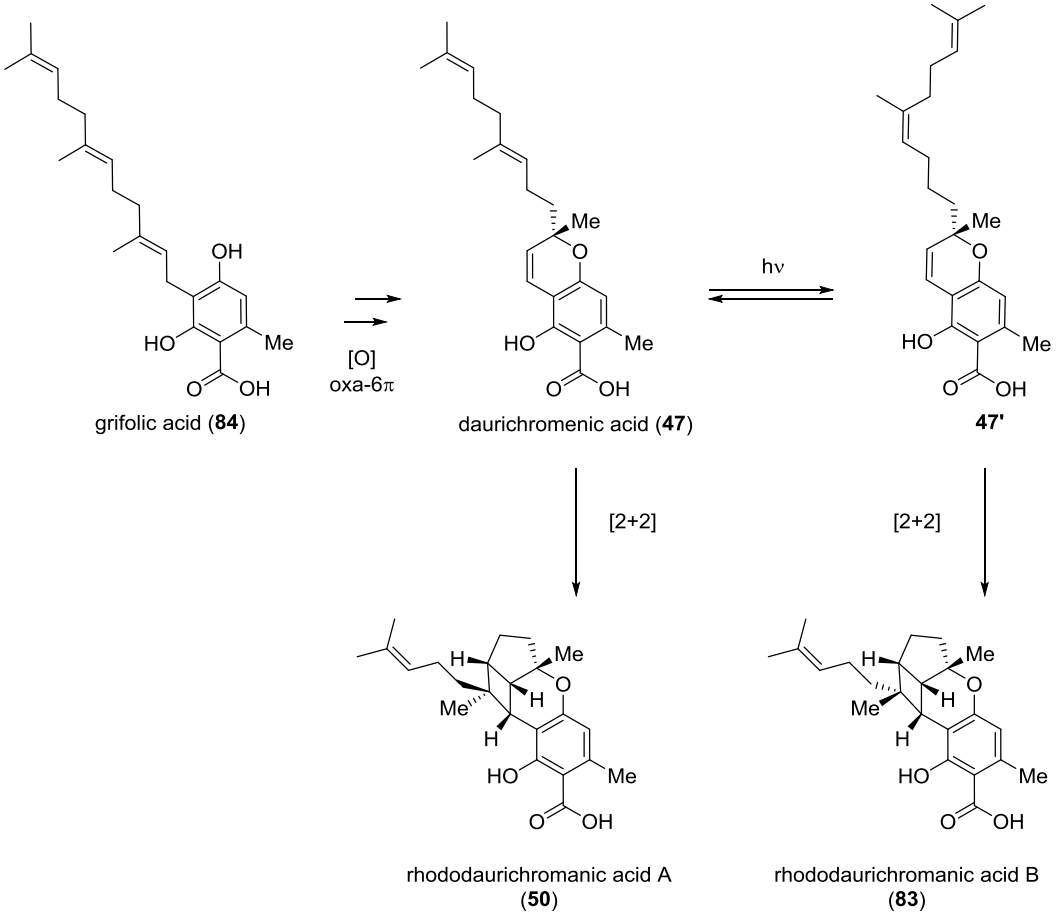

Seeking to apply their *2H*-pyran forming methodology (*cf. Section 1.2.2*) to the synthesis of complex natural products, Hsung and coworkers designed a concise biomimetic synthesis of the daurichromenic acids and their derivatives.[60] They reacted farnesol-derived α,β-unsaturated aldehyde **85** with 5-methyl-1,3-cyclohexanedione **86** in the presence of piperidine in acidic medium (**Scheme 1.36**). The resulting cyclohexanone **87** was subsequently acylated with Mander's reagent ($NCCO_2Me$) and oxidized to chromene framework **88**. Saponification at that stage failed, yielding decarboxylation.

Thus, **88** was utilized in a photochemical [2+2]-cycloaddition directly. A wavelength of 350 nm was used to induce *E/Z* isomerization and successful photogeneration of rhododaurichromanic acid A (**50**) and B (**83**) methyl esters. Final saponification of both adducts yielded the desired natural products.

Scheme 1.36 Biomimetic Synthesis of Daurichromenic Acid and Congeners by Hsung *et al*.

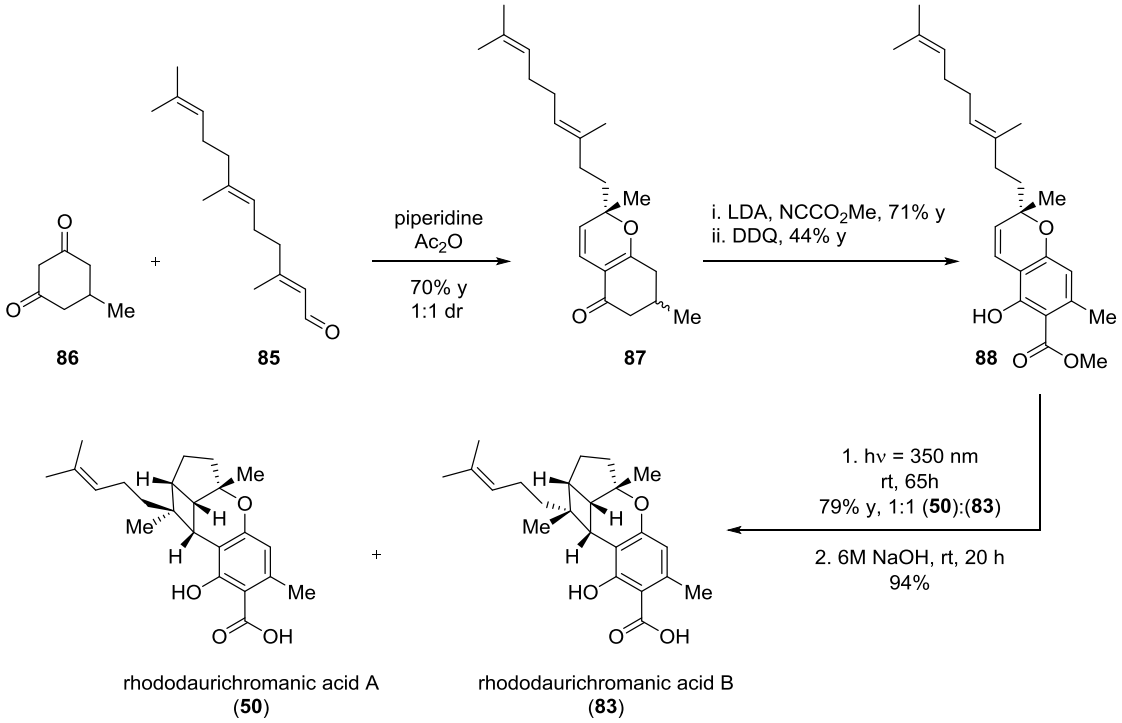

Another example of *2H*-pyrans potentially serving as intermediates in [2+2] photocycloadditions can be found in the biosynthetic proposal to artocarpol A (**51**), believed to derive from artocarpol E (**53**) (**Scheme 1.37**). These molecules were isolated from the root bark of *Artocarpus rigida*,[62,63] and display an intriguing dibenzo[*b,f*]oxepin ring system. Artocarpol A (**51**) and other family members have notable anti-inflammatory properties. Biogenetically, the core structure of artocarpols is proposed to arise from reaction of hydroxylated stilbene **89** with prenylated pyrophosphates **90** and **91**,[62] yielding

oxepine structure **92**. Following valence isomerism to artocarpol E (**53**) and [2+2]-cycloaddition, the required stereocenters for artocarpol A (**51**) could be set.

Scheme 1.37 Biosynthetic Access to Artocarpol Natural Poducts

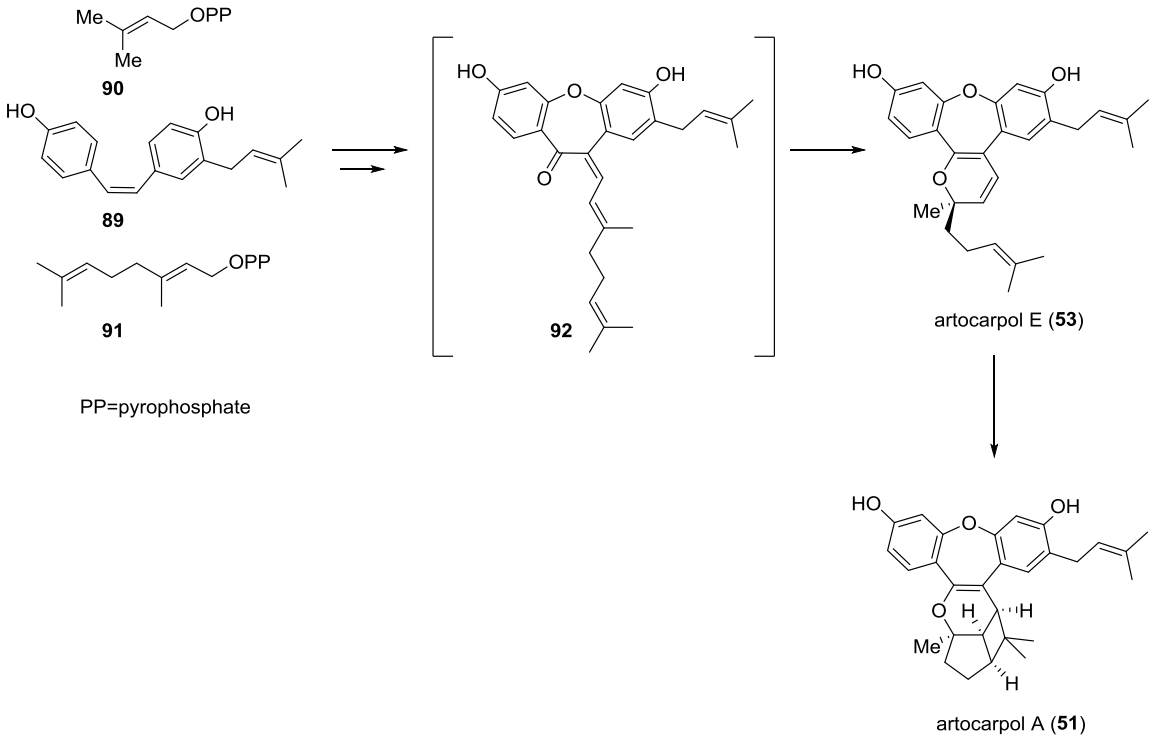

Although no synthesis of these natural products has been published so far, a study centered on producing analogues of artocarpols was reported by Wilson *et al*.[81] The key step in their investigation relied on condensation of the known oxepine **93** with an isomeric mixture of citral **94**, affording *2H*-pyran **95** in moderate yield due to formation of alkene isomers. Exposure to light in the presence of benzophenone as a sensitizer promoted [2+2]-cycloaddition to **96** in 45% yield along with retro oxa-6π ring opened products **97**. The relative stereochemistry of artocarpol analog **96** at the 6/4/5 system junction was

unambiguously assigned using 2D NMR experiments, and corresponds to the relative configuration observed in the natural product, supporting the biosynthetic proposal for artocarpols.

Scheme 1.38 Synthesis of Artocarpols Analogues by the Wilson Group

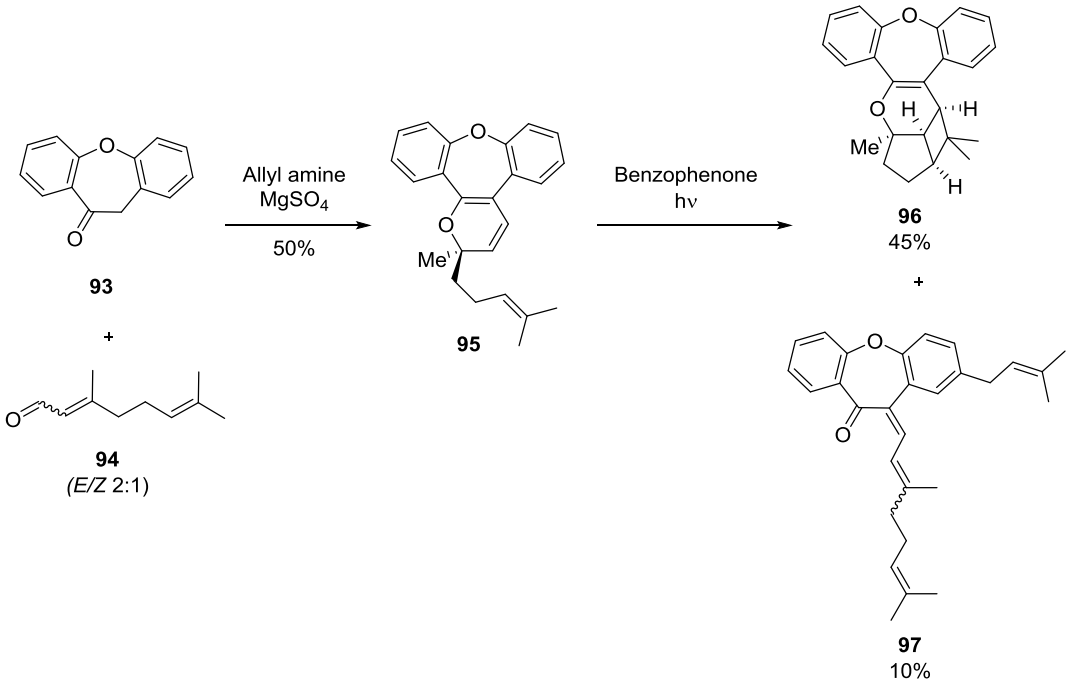

1.4 Conclusion and Summary

2H-Pyrans, despite their labile character, are ubiquitous in several classes of natural products. Several useful synthetic methods have been developed to assemble this sensitive moiety, each showing some limitations in terms of accessible substitution pattern around the heterocyclic ring. Due to their inherent reactivity, they have been postulated as biosynthetic precursors, and were further utilized as key intermediates in many biomimetic syntheses relying on cycloadditions. In these cases, preferred reactivity modes that have

been discovered include [4+2] dimerizations, intramolecular Diels-Alder annulations, and [2+2] photocycloadditions.

Future developments in this area may warrant additional investigations to expand the reaction scope and to access more complex substitutions surrounding the *2H*-pyran core. Proving their intermediacy in intermolecular Diels-Alder reaction with functionalized alkene-containing building blocks should open a new chemical space, outside of their established dimerization pathways. This crucial and overlooked aspect will be the subject of the following chapters.

CHAPTER 2

A Proposed Biomimetic Synthesis of Swerilactones A and B: Elaboration of a *2H*-Pyran and Reactivity Studies

2.1 Introduction

2.1.1 Isolation of Bioactive Molecules from Swertia mileensis

Swerilactones and related natural products were isolated in the late 2000's by Chen and coworkers[82–88] from the plant *Swertia mileensis* and several related species from the Gentianacea family. These plants have long been used in traditional Chinese medicine for treating viral hepatitis.[85] All members of the natural products family display a polycyclic framework, containing lactone-pyran fused bicyclic subunits, and are heavily oxygenated. Members showcasing a pentacyclic (6/6/6/6) ring system, including swerilactone A[82] (**Figure 2.1**, (**98**)), its C_7 epimer swerilactone B (**99**), and the more recently isolated (+)-swerileducenin A (**100**)[87] have extremely compact, cage-like structures. Their degree of complexity translates into a high number of stereocenters: seven for swerilactone A and B, eight for (+)-swerileducenin A, and two quaternary carbon centers present in each molecule. In contrast, swerilactone C (**101**) and D (**102**)[83] feature a T-shaped structure (*cf.* **Figure 2.1**, swerilactone D), with five stereocenters and one quaternary carbon center.

Other members that have been isolated from Nature have exhibited more complex polycyclic structures, such as the octacyclic swerilactones H (**103**) and I[85] (**104**) (**Figure 2.1**). The structure and relative stereochemistry for all members of the family were confirmed *via* X-ray crystallography and extensive 2D NMR studies.

Confirming their presumed therapeutic effect, all members have shown mild bioactivity in a hepatitis B virus assay.[85] Despite their appealing framework and bioactivity, to date, no synthesis of these compounds has been reported in the literature.

Figure 2.1 Representative Lactone-Containing Natural Products Isolated from the *Swertia* Genus

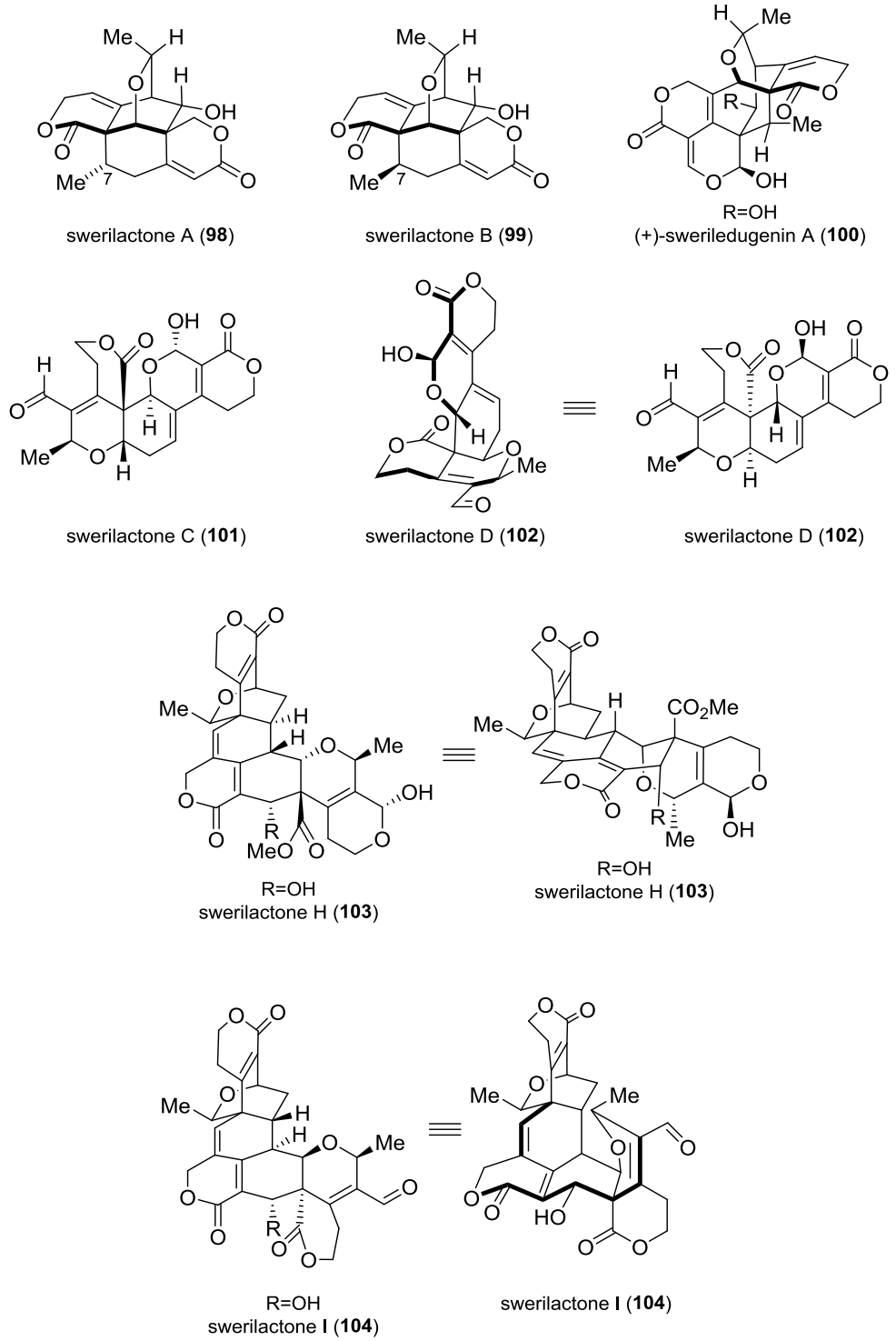

2.1.2 Proposed Biosynthesis and Bioactivity

Swerilactones are believed to be derived from secoiridoids[85] based on the presence of the δ-lactone framework (**Figure 2.2**). Iridoids, a group of monoterpenoids featuring a methylcyclopentane skeleton, are a privileged chemotype present in >1000 isolated compounds from diverse plant sources, including *Scrophulariaceae*, *Rubiaceae*, *Labiatae*, *Gentianaceae*, *Verbenaceae*, and *Oleaceae*.[4] Of note, most of the iridoids in the *Gentianaceae* family, from which the *Swertia* genus is derived, belong to the secoiridoid subclass.

Figure 2.2 General Structure and Numbering System of Iridoids and Secoiridoids

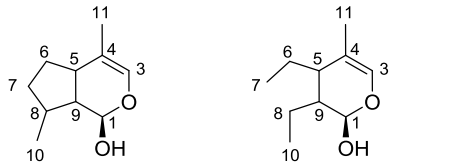

A potential biosynthetic pathway has been hypothesized for swerilactones A and B with aldol condensations as key C-C forming steps.[85] Iridotrial (**105**) is proposed to undergo a series of enzymatic transformations to arrive at intermediate **106** (**Scheme 2.1**). This compound could then diverge into two key frameworks **107** and **108** *via* differentiated hemiacetal cyclizations followed by oxidation. The α- and γ-formylated lactones **107** and **108** could potentially couple together *via* aldol reactions to generate a new cyclohexane ring-containing structure **109** (**Scheme 2.1**) *via* C_3-$C_{4'}$ and C_4-C_8' bond formations. This product would be suited to undergo subsequent aldol cyclization between C_9-C_3' yielding polycycle **110**. Upon water loss and ketone reduction at C_8, lactone **111** could form and be

reduced to core structure **112**. Additional loss of water would create a transient carbocation at C_3 that could be trapped by the adjacent alcohol at C_8, thereby affording the final bridgehead C-O bond. Similar transformations have been proposed to generate the other members of the family, relying on aldol reactions as key transformations.[85]

Scheme 2.1 Proposed Biosynthesis of Swerilactone A and B by Geng and Coworkers

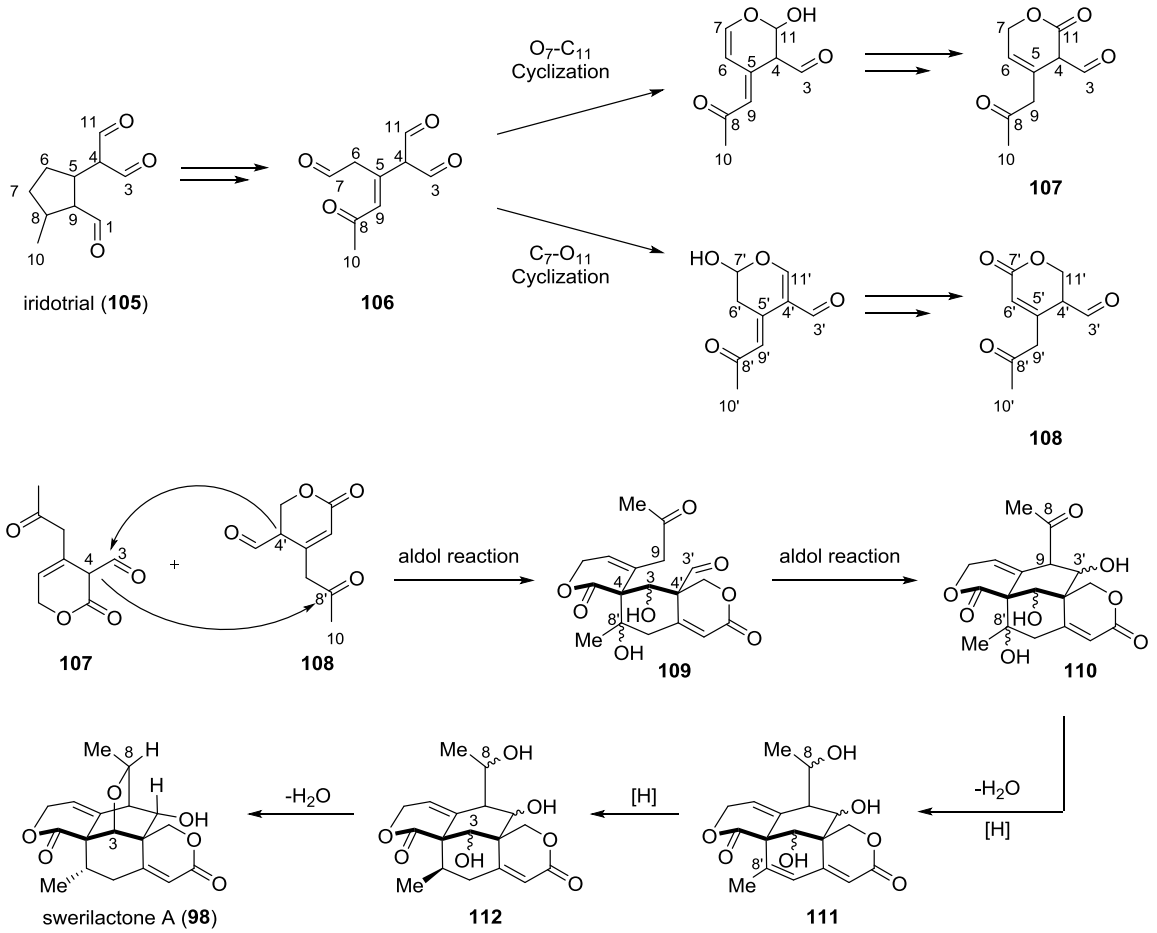

In terms of bioactivity, most members are active against one or more components of the hepatitis B virus (**Table 2.1**). Swerilactone A, C and D have weak single-digit millimolar inhibition activity against secretion of surface (HBsAg) and envelope (HBeAg)

antigens as determined by a transfected HBV cell line assay. Swerilactone E and I were found to be more potent with sub-millimolar IC_{50} values. Swerilactone H, swerileduginin and sweriyuannanlactone, on the other hand, were only active in inhibiting the HBV DNA replication mechanism but inactive against the secretion of both antigens HBeAg and HBsAg. Interestingly, modern treatments against the Hepatitis B virus are small molecules derived from nucleotides and nucleosides.[89] The current standard-of-care to treat hepatitis B is the nucleoside-based lamivudine developed by GlaxoSmithKline (*cf.* **Table 2**), which targets the virus's reverse transcriptase and displays IC_{50} values between 0.01-3 μM.[89]

Table 2.1 Anti-HBV Activities of Swerilactones and Related Natural Products

Coumpound	HBsAg IC_{50} (mM)	HBeAg IC_{50} (mM)	DNA replication IC_{50} (uM)
swerilactone A	3.66	3.58	-
swerilactone C	1.24	0.77	-
swerilactone D	2.96	1.47	-
swerilactone E	0.22	0.52	-
swerilactone H	-	-	1.53
swerilactone I	0.44	0.50	2.58
(-)-swerileduginin	-	-	26.55
sweriyunnanlactone A	-	-	60.76

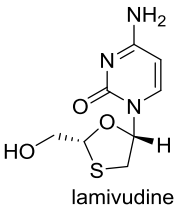

lamivudine

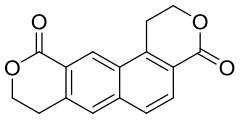

swerilactone E

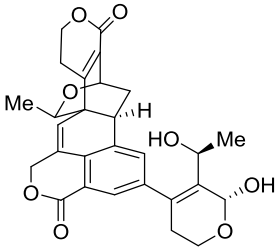

sweriyunnanlactone A

In this regard, in addition to unambiguously determine its absolute configuration, a synthesis of swerilactone A (or its core structure) could give access to a new, distinct class of small molecules active against the Hepatitis B virus, and represent a potential stepping stone toward a novel treatment.

2.2 Retrosynthetic Approaches to Swerilactones A and B

2.2.1 First Retrosynthetic Analysis

In our initial synthetic analysis, we sought to target swerilactone A and its C_7 epimer swerilactone B as a first approach to the synthesis of this family of natural products. As an alternative to their proposed biosynthesis based on successive aldol reactions (**Scheme 2.1**), we thought a viable way of assembling the core structure of swerilactone A and B would rely on a Diels-Alder cycloaddition as a key step.

Scheme 2.2 Proposed Biomimetic Access to Swerilactone A

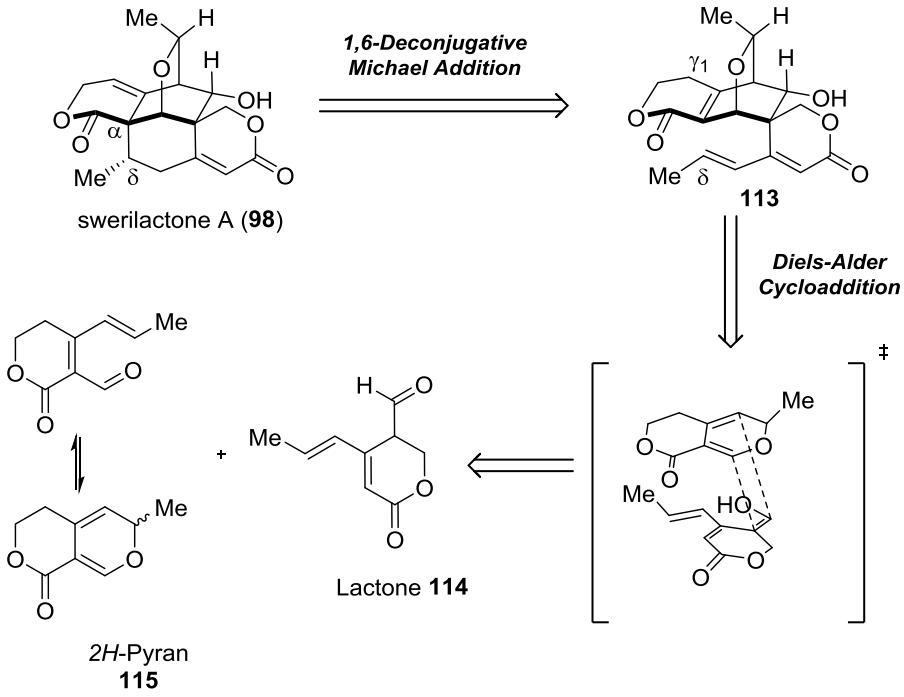

For the synthesis of swerilactone A, we hypothesized that a first disconnection could be made between the α position of the *2H*-pyran fused lactone and the δ position of the spirocyclic lactone (**Scheme 2.2**). Deprotonation at the γ_1 position of core **113** may trigger a 1,6-deconjugative Michael addition.[90,91] Intermediate **113** could potentially arise from biomimetic Diels-Alder cycloaddition of two key regioisomeric lactones: the enol tautomer of lactone **114** and a fused *2H*-pyran lactone **115**, undergoing a dynamic oxa-6π/retro-6π electrocyclization.

At the outset of our studies, it was unknown if the polarization of components **115** and **114** would allow for a normal demand or an inverse demand Diels-Alder cycloaddition. **Figure 2.3(A)** depicts the Frontier Molecular Orbital (FMO) analysis and the prevalent

HOMO-LUMO interaction associated with each mode of cycloaddition. A smaller energy gap between the HOMO of the diene and the LUMO of the dienophile is at play in a normal demand Diels-Alder. This is due to the HOMO raising effect of the electron-donating substituent on the diene and the LUMO lowering effect of the electron withdrawing group on the dienophile. In the case of inverse demand mode, the smallest energy gap is now found between the LUMO of the diene diene and the HOMO of the dienophile. This is also explained by the electron withdrawing effect of the substitutents on the diene, which lowers its LUMO, and the electron donating effect of the substituents on the dienophile, which raises its HOMO. Few examples of inverse-demand Diels-Alder reactions using enol or enolates have been reported (**Figure 2.3 (B)**);[92,93] enol ethers are more commonly employed in this cycloaddition mode, due to enhanced nucleophilicity and stability.[94]

Figure 2.3 (A) FMO Analysis for Different Diels-Alder Modes and (B) Example of Inverse Demand Reaction

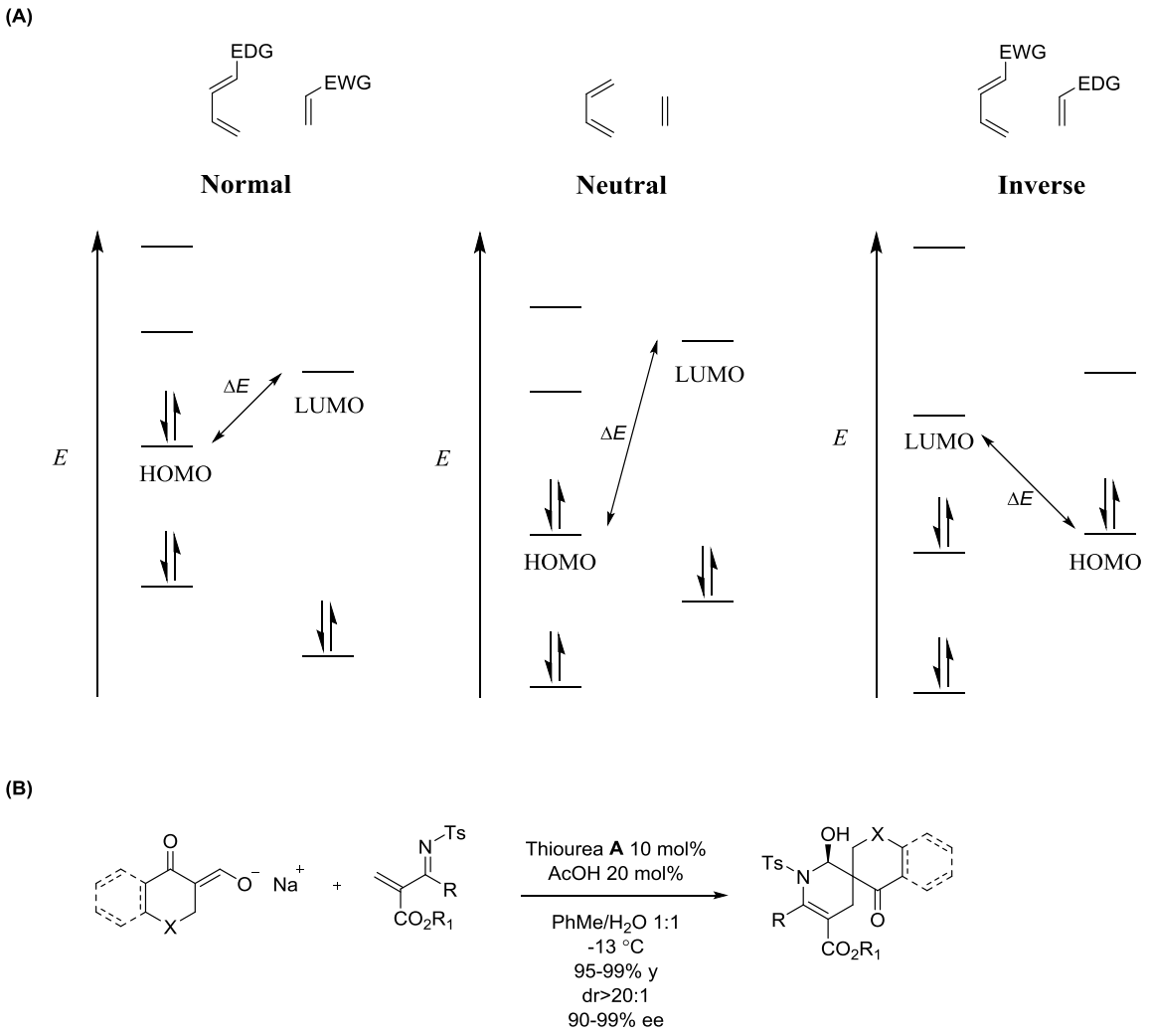

Following the FMO principles outlined in **Scheme 2.3**, we envisioned that changing the substitution from a free enol **114** to an enol ether may tune the reaction electronics. For example, by accessing the TBS- or *tert*-butyl protected enol (**114a** and **114b**), we could potentially invoke an inverse demand process. Alternatively, an acetate-substituted enol (**114c**) may enable a normal demand cycloaddition.

Figure 2.4 Potential Substitution of Enol Lactone 114

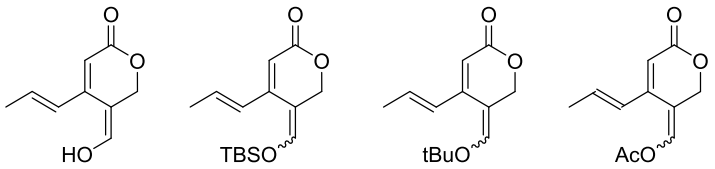

Additionally, substitution might help lock the enol ether stereochemistry to the (*E*)-enol form, which needs to be on the same side as the propenyl side chain according to our proposed Diels-Alder transition state (*cf.* **Scheme 2.2**). Since the free enol lactone **114** can adopt an (*E)* or (*Z)*- conformation, the cycloaddition event with *2H*-pyran **115** provides multiple possibilities in terms of regiochemical and stereochemical outcomes. A dienophile approach away from the pyran methyl group, a commonly observed restriction in related pyran systems (**Chapter 1, Section 1.3**), results in eight transition states, four for the *(E)*-enol (**Figure 2.5**) and four for the (*Z)*-enol **114** (not shown).

Figure 2.5 Four Possible Transition States between (*E)*-Enol 114 and Pyran 115

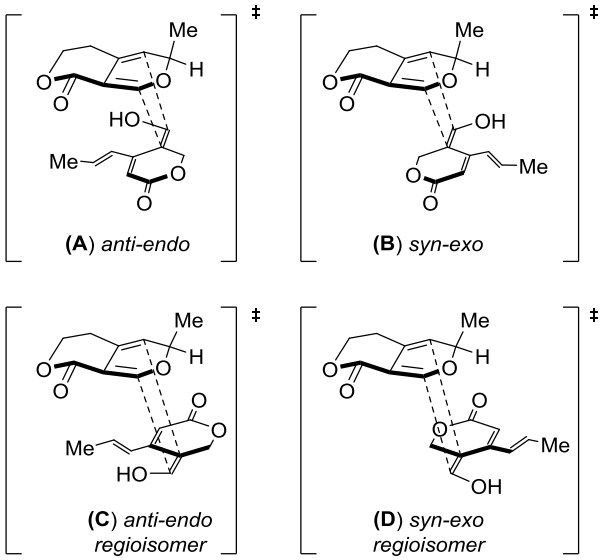

In the face of executing a complex Diels-Alder cycloaddition, we thought an alternative, stepwise reactivity mode of enol **114** could be proposed. In spite of being widely postulated as concerted transformations in Nature, [95,96] most Diels-Alder cycloadditions effected by enzymes are thought to proceed through stepwise mechanisms. For instance, macrophomate synthase (MPS) had been thought to promote a concerted [4+2] cycloaddition step[97] and its crystal structure bound to its molecular target was obtained (**Scheme 2.3**).[98] It is now known to catalyze the stepwise reaction between substituted 2-pyrone **116** and pyruvate magnesium enolate **117** to form a bicyclic adduct **118**. Using a model of the active site of MPS complexed with **117**, DFT calculations suggest an energetically favored pathway through intermediate **119** *via* a Michael/aldol cascade, with both transition states >10 kcal/mol lower in energy than the concerted Diels-Alder transition state.[99]

Scheme 2.3 Stepwise Formal Diels-Alder Cycloaddition Catalyzed by Macrophomate Synthase

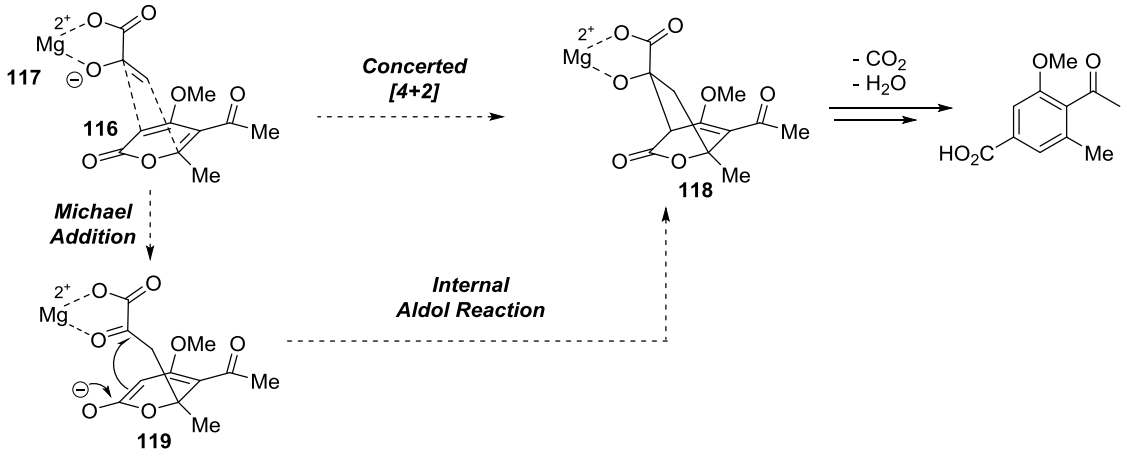

Inspired by this mechanistic interpretation, we imagined two viable stepwise pathways to assemble the core structure. Leveraging the valence isomerism of *2H*-pyran **115** in its closed form, enol lactone **114** could attack at the electrophilic position of α-pyran **115** in a Michael addition fashion (**Scheme 2.4, (A)**). The resulting extended enolate **120** may further react with the aldehyde in a vinylogous aldol reaction, thereby creating the core spirocyclic scaffold **113**. Alternatively, dienal **115'** could undergo an aldol reaction with enol lactone **114**, affording hydroxyl anion **121**, which may further cyclize to provide the same extended enolate **120** (**Scheme 2.4**, **(B)**). Aside from representing an alternative avenue to concerted [4+2] cycloaddition pathways, it would also permit investigation of asymmetric processes *e.g.* engaging the dienal valence isomer with chiral ligand/metal complexes.

Scheme 2.4 Stepwise Pathways to Swerilactone Core

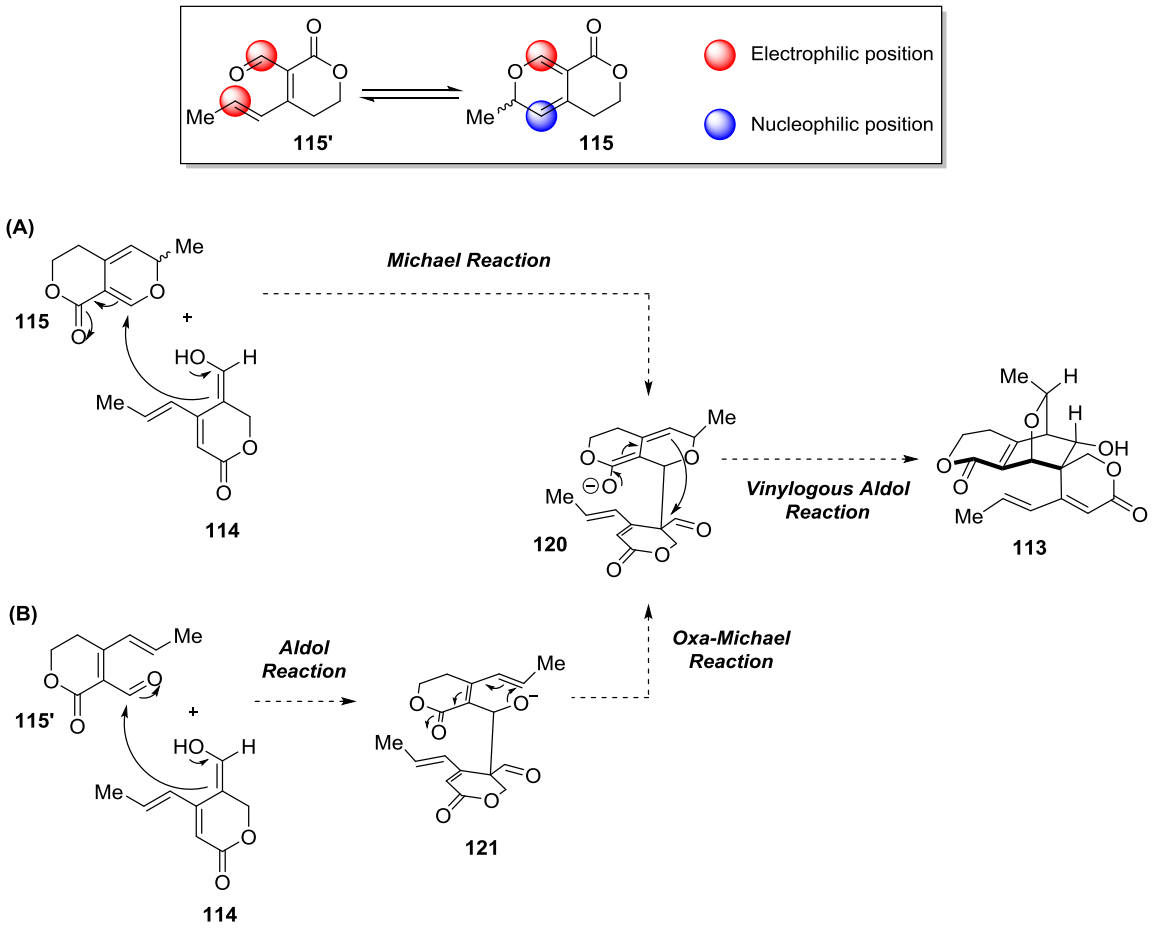

2.2.2. Revised Retrosynthetic Analysis: Ketene-Diene Diels-Alder Cycloaddition Approach

Given the large number of potential transition states for a concerted reaction pathway with *(E)*- and (*Z*)-enol **114** and the questions regarding the preferred reactivity modes adopted by pyran **115** and enol **114**, we decided to explore the possibility of a ketene as a dienophile instead of an enol. We anticipated a ketene dienophile would have the

advantage of an increased reactivity and would simplify matters in terms of regiochemical and stereochemical outcomes.

In collaboration with Prof. Richard Johnson (University of New Hampshire), DFT calculations using a model ketene dienophile were performed. Under a restricted pyran facial selectivity, and accounting for a higher reactivity of the ketene C=C bond, four transition states can presumably take place (**Figure 2.6**). Prof Johnson's preliminary DFT calculations indicated the lowest-energy transition state led to the desired regiochemical and stereochemical outcome (**Figure 2.6**, transition state *syn-endo* **(A),** $\Delta E = 0$ kcal/mol). The three other transitions states, *syn-exo* **(B)**, *anti-endo* (regioisomer **(C)**), and *syn-exo* (regioisomer **(D))** were calculated to stand respectively at 2.5, 6.3 and 7.4 kcal/mol higher in energy than the one needed for our cycloaddition (**Figure 2.6**).

Figure 2.6 Ketene-Pyran Cycloaddition: Four Possible Transition States

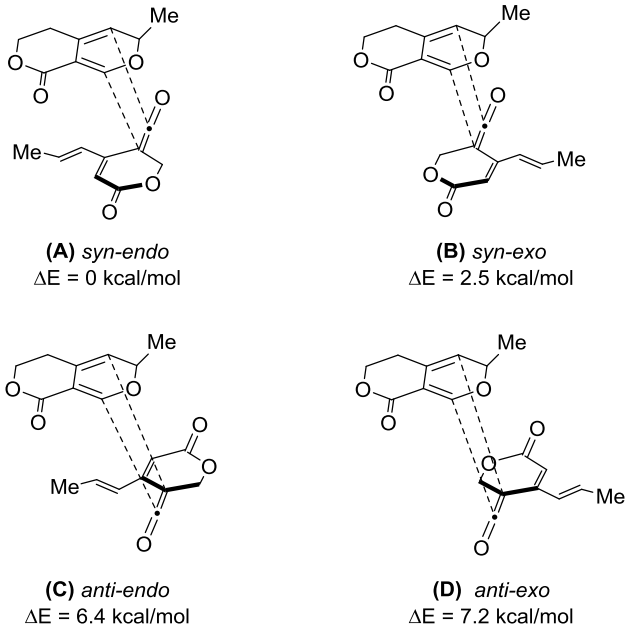

(A) *syn-endo*
ΔE = 0 kcal/mol

(B) *syn-exo*
ΔE = 2.5 kcal/mol

(C) *anti-endo*
ΔE = 6.4 kcal/mol

(D) *anti-exo*
ΔE = 7.2 kcal/mol

The lowest energy transition state **(A)** (ΔE = 0 kcal/mol**)** is depicted in **Figure 2.7**, showing the *2H*-pyran being approached from its α face (methyl group pointing upward) by the ketene in an *endo* mode.

Figure 2.7 Ketene-Pyran Lowest Energy Transition State (A) (DFT B3LYP/6-31G)**

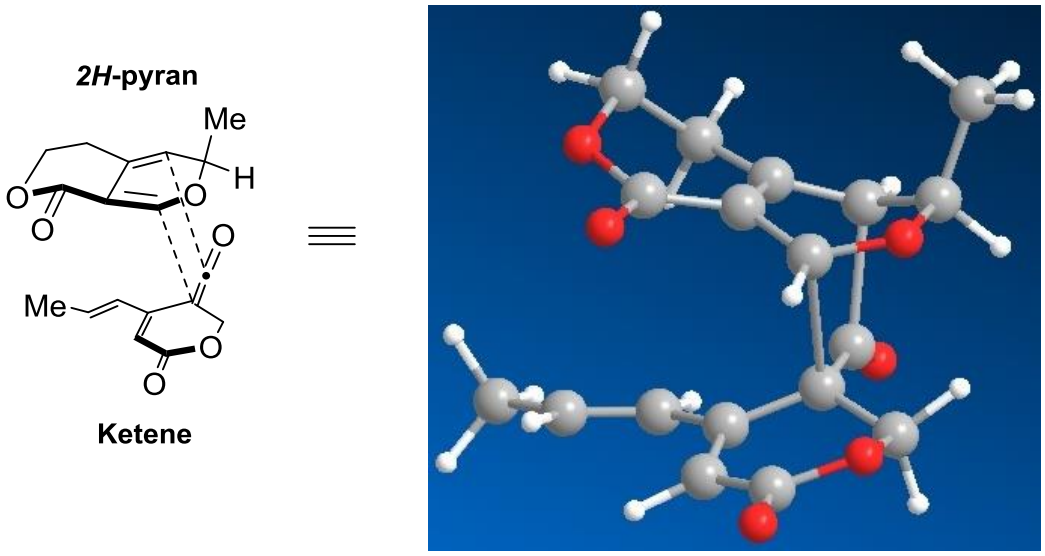

These theoretical calculations led us to revisit our retrosynthetic analysis (**Scheme 2.5**). The key [4+2] cycloaddition could take place between α-pyran **115** and a ketene derived from lactone **122**. The resulting ketone **123** would then need to be selectively reduced before or after the 1,6-deconjugative Michael addition step.

Scheme 2.5 Revised Retrosynthesis of Swerilactone A

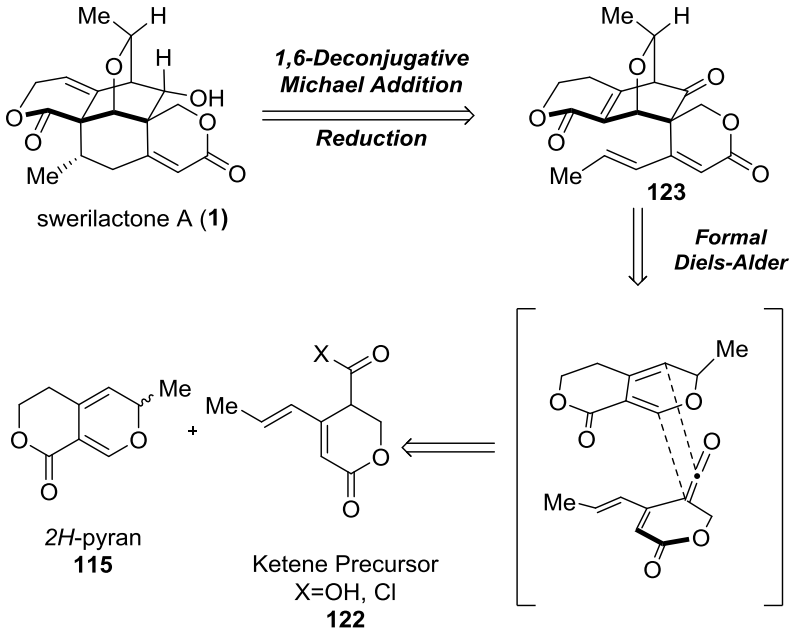

Ketenes are well-known to participate in thermal [2+2] cycloaddition rather than normal demand [4+2] with carbodienes (*cf.* **Scheme 2.6** (**A**), reaction of cyclopentadiene with diphenylketene).[100] This is due to a more favorable [π2s+π2a] overlap of the ketene π* with the HOMO of the alkene π system, inducing an orthogonal approach (**Scheme 2.6** (**B**)).

Scheme 2.6 Typical Ketene Reactivity in Thermal Diels-Alder Cycloadditions and FMO Analysis

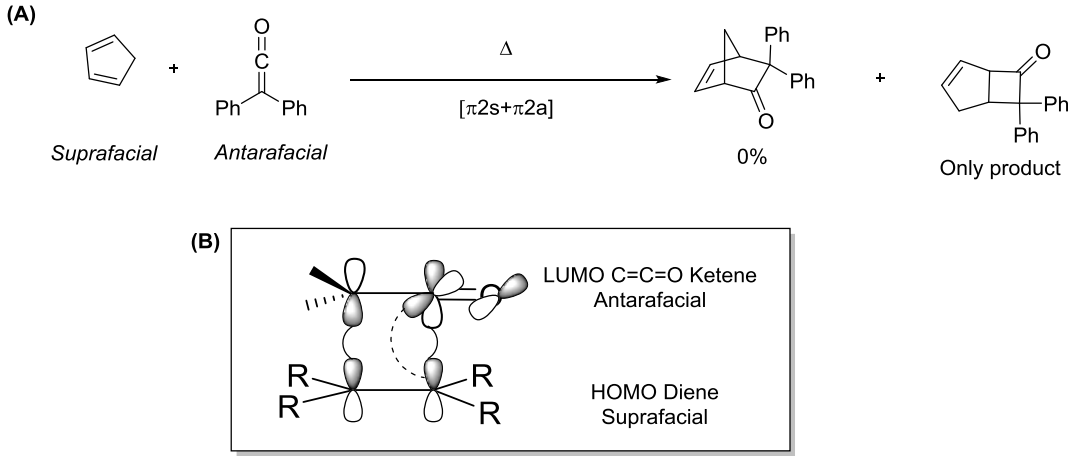

However, some literature reports have showed a preference for [4+2] cycloaddition with bulky diene partners, in which the steric hindrance prevented the ketene from adopting an antarafacial approach (**Scheme 2.7 (A)**).[101] With heterodienes, ketenes can be trapped in the presence of a chiral Lewis base, forming a ketene enolate that further reacts with the heterodiene in a stepwise manner. This strategy constitutes an inverse-demand cycloaddition[94] and yields a formal Diels-Alder heterocycloadduct enantioselectively. A number of methodologies taking advantage of this concept to create heterocycles[102] have been published using cinchona alkaloid derivatives,[103,104] NHCs[105–107] or benzotetramisoles[108,109] as Lewis bases to generate transient ketene enolates. A representative application of this strategy by Lectka and coworkers is outlined in **Scheme 2.7 (B**).[110] In this example, an acyl chloride forms a ketene upon deprotonation with Hünig's base, which is further trapped as a ketene enolate in the presence of the cinchona

alkaloid which reacts in a stepwise fashion with an *o*-quinone methide diene. The resulting cycloadduct is obtained in high enantioselectivity.

Scheme 2.7 Typical Ketene Reactivity Profile in [4+2] Cycloadditions

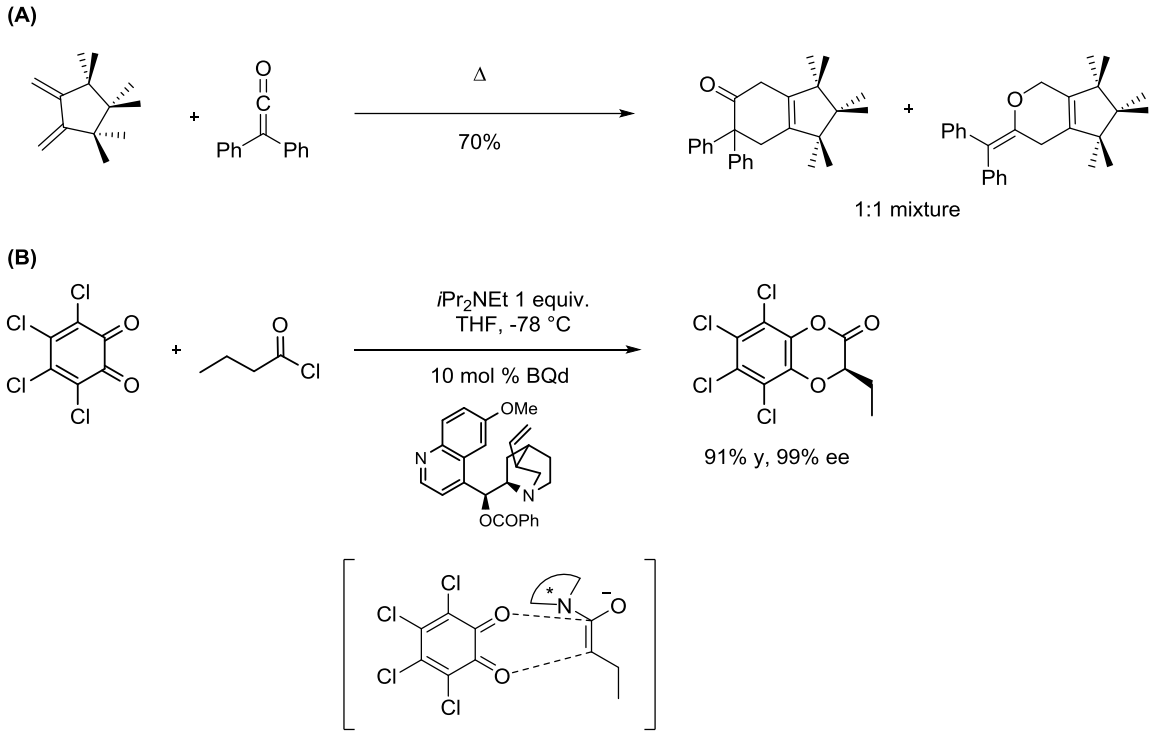

Based on these literature precedents, targeting a ketene precursor such as lactone **122** would offer some versatility. In the case where a concerted [4+2] cycloaddition did not exist, we could switch easily to a ketene enolate mechanism. The reaction in the latter case would proceed in a stepwise manner, similar to the proposal in **Scheme 2.4**. The generated ketene could be intercepted with a chiral Lewis base, yielding a reactive ammonium or azolium enolate **124** (**Scheme 2.8**). This species could converge to enolate **125** in two distinct pathways, whether directly *via* Michael addition or indirectly through hydroxyl anion **126**. Closure of **125** should generate the oxidized core for swerilactone A

123 and recycle the nucleophilic catalyst. Of note, both pathways could proceed stereoselectively.

Scheme 2.8 Potential Stepwise Pathways to an Oxidized Swerilactone Core

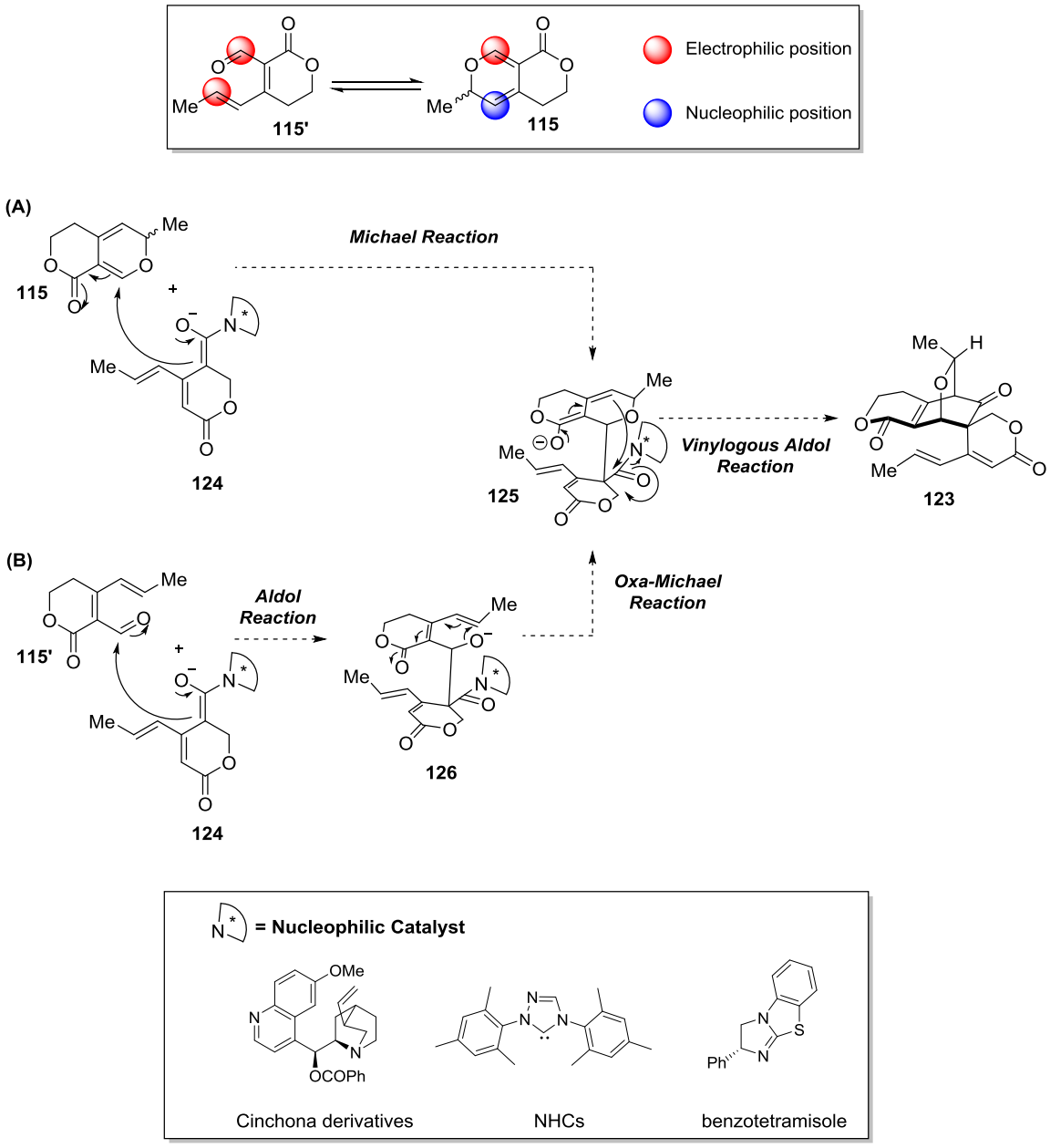

2.3. Construction of a Fused *2H*-Pyran Lactone Fragment

2.3.1 Previous Synthesis

The required first fragment according to our retrosynthetic analysis (**Section 2.2**) is the bicyclic, lactone fused *2H*-pyran **115**. At the start of our synthetic studies, a publication by Tan and coworkers[111] illustrated the successful synthesis of *2H*-pyran **115** (**Scheme 2.9**). Starting from crotonaldehyde as their source of the *trans*-propenyl moiety, they were able to synthesize enone **127** *via* an aldol reaction with ethyl acetate, followed by TBS protection and DMP oxidation (not shown). A second aldol reaction of **127** with methyl-3-hydroxypropionate **128** afforded **129** with the full carbon containing framework. Finally, protecting group removal and lactonization under heating provided lactone **130**.

Interestingly, it was demonstrated that upon treatment with DMP, lactone **130** produced the desired *2H*-pyran **115** (in a 4:1 ratio favoring the closed form **115**), along with a minor amount of lactol **131**. The presence of **131** in the reaction mixture was shown to arise from the *in situ* formation of *2H*-pyran **115**, which in contact with singlet $^1O_2$, reacted in a [4+2] cycloaddition to forms endoperoxide **132**. A Kornblum-DeLaMarre rearrangement[112] then occured in the presence of base, yielding lactol **131**.

Scheme 2.9 Tan's Synthesis of *2H*-Pyran 115 and Subsequent Cycloaddition

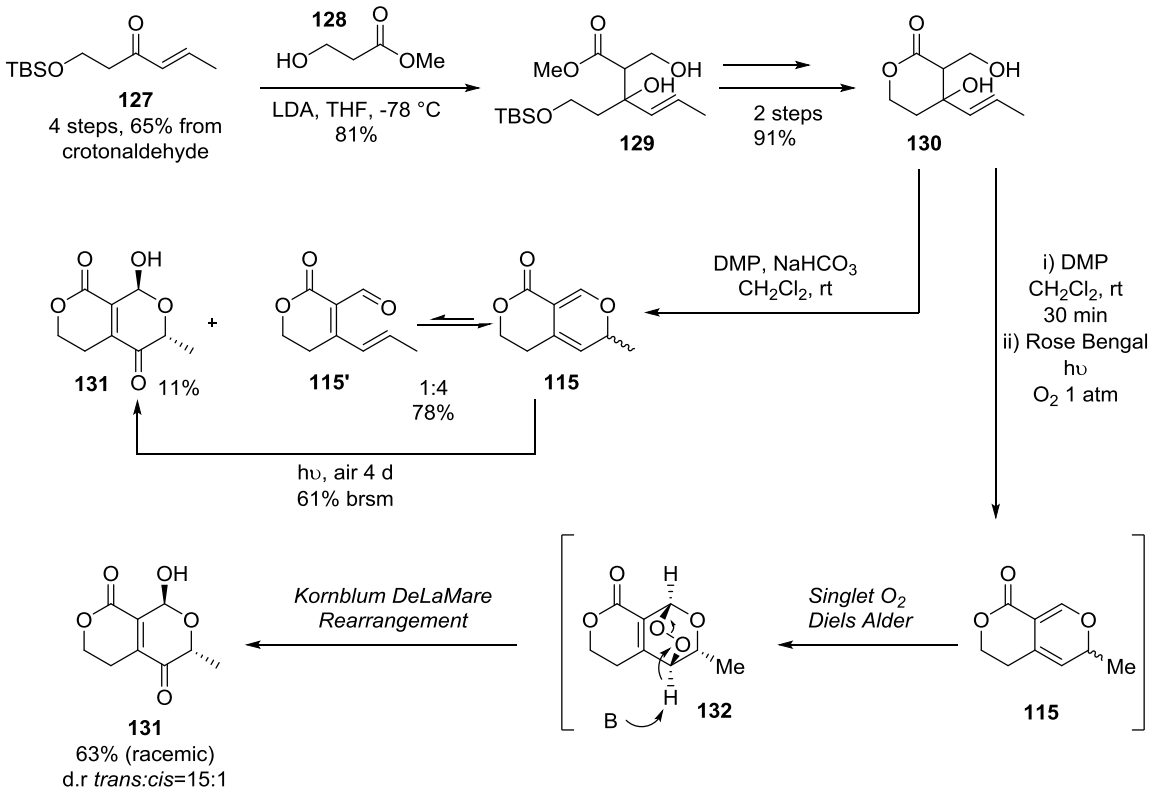

These oxidation results were extremely encouraging, as they clearly showed the ability of *2H*-pyran **115** to act as a diene in a cycloaddition event. More importantly, in accordance with previous observations on related pyrans,[12,13,65,70,74,75] compound **115** seems to impart a facial selectivity (*trans:cis* d.r 15:1), with $^1O_2$ approaching from the least hindered face of the *2H*-pyran, away from the methyl group. With this relevant precedent in hand, we decided to design our own shorter route to *2H*-pyran **115.**

2.3.2 First Synthetic Route: Cuprate Addition of Metallated Propenyl and Oxidation of Formylated Lactone

We envisioned a streamlined access to pyran **115** by a three step route from the commercially available unsaturated lactone **133** (**Scheme 2.10**). Cuprate addition of a suitable metallated propenyl species such as **134** followed by enolate trapping with a formate equivalent should provide α-formylated lactone **135**. Further oxidation of **135** could produce **115**.

Scheme 2.10 First Retrosynthetic Strategy to *2H*-pyran 115

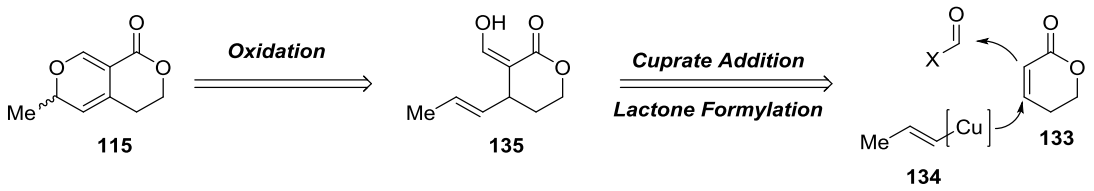

Preliminary experiments quickly revealed that this one pot process was possible but that it also may not be an ideal reaction candidate for scale-up purposes (**Scheme 2.11 (A)**). Indeed, the yields of intermediate **135** were unreproducible, and an undesired side product **136** was isolated, arising from 1,4-addition of intermediate enolate **137a** into the starting lactone **133**. Upon searching for literature conditions to minimize this side reaction, we found that tributylphosphine[113] was reported to be an effective copper ligand in the Michael addition of unsaturated lactones. Indeed, upon use of tributylphosphine in generating cuprate **134b**, no side product was observed; however, we were still plagued with other issues (**Scheme 2.11 (B)**). For instance, purification of the crude product was particularly cumbersome with a mixture of 1,4-adduct **138**, lactone **135**, and tributylphosphine

requiring separation. Intermediate **138** was also found to be volatile, which made the purification step more challenging.

Scheme 2.11 Cuprate Addition Studies to α,β-unsaturated Lactone 133

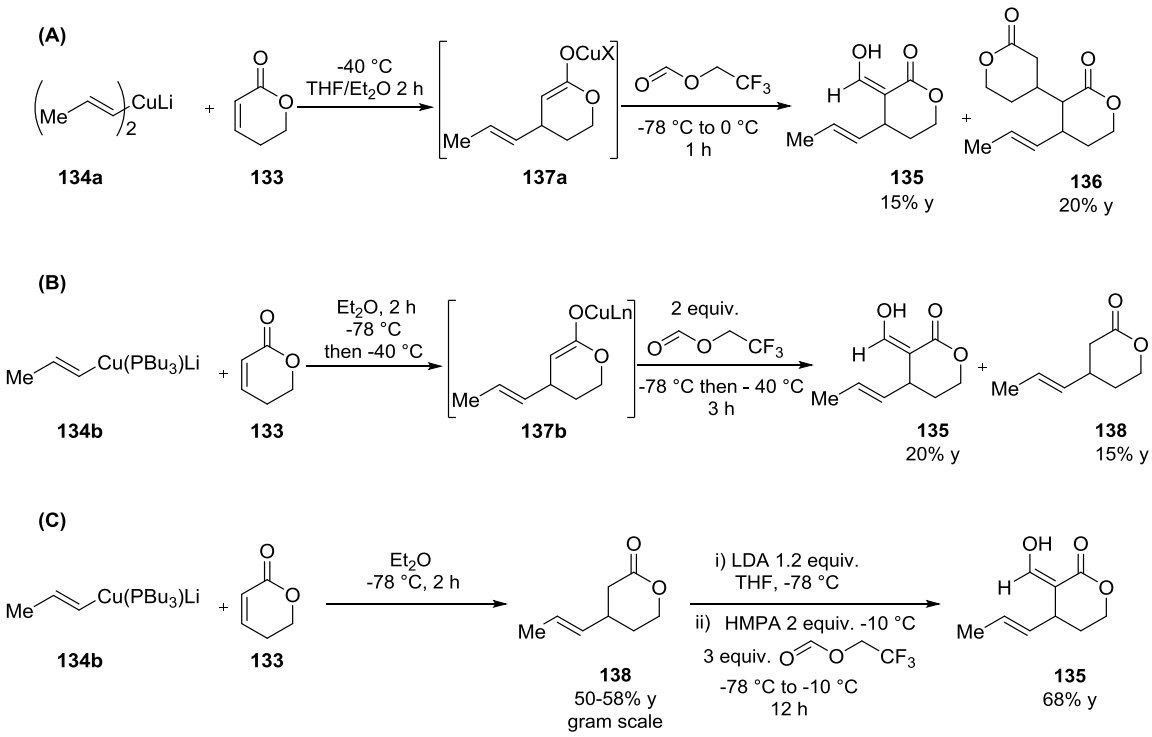

A higher yielding procedure involved a stepwise route, involving initially a conjugate addition of organocuprate **134b** to adduct **138** (**Scheme 2.11 (C)**). After careful purification and handling, the subsequent enolate formylation step was successfully conducted using LDA in THF followed by enolate quenching with 2,2,2-trifluoroethyl formate,[114,115] affording the key α-formylated lactone **135**.

Our focus next shifted to the oxidation step to convert **135** to *2H*-pyran **115**. An extensive screen was conducted featuring a wide range of oxidation methods (**Table 2.2**). Stoichiometric[116] or catalytic DDQ,[117–119] selenium oxide elimination, or Saegusa

protocols afforded the desired product in low yield, and both PIDA and DMP oxidations were unsuccessful. Oxidants known to promote *2H*-pyran formation in related epoxyquinol-containing pyrans[70,120] including Bobbitt's reagent and TEMPO/CuCl (entries 2 and 4 respectively, **Table 2.2**) failed to promote the targeted transformation. Metal-mediated reactions were equally unproductive, despite having shown great success in previous dehydrogenations of cyclic ketones,[121] in allylic C-H activation/β-hydride eliminations[122] or dehydrogenations of cyclohexenones[123] (entries 3, 5 and 6, **Table 2.2**).

Table 2.2 Oxidation Screen toward *2H*-Pyran 115[a]

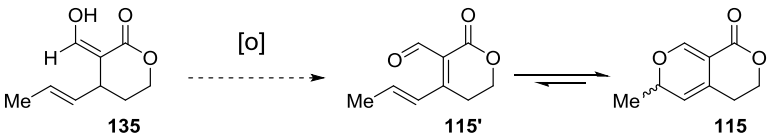

135 **115'** **115**

Entry	Representative Oxidative Conditions	Solvent	Temp., Time	Results
1	DDQ 1.5 equiv.	Dioxane/pH 7 buffer 20:1	rt, 10 min	Full conversion 10-30% isolated yield
2	Bobbit's reagent on SiO_2	CH_2Cl_2	40 °C, 4 h	No reaction
3	Rh/C or Pd/C or Pt/C 10 mol%	mesitylene	130 °C, 16 h	No reaction
4	TEMPO cat. CuCl, 1 atm O_2	Dioxane	rt, 12h	Decomposition
5	White's Catalyst 10 mol%, *p*-NO_2BzOH 10 mol% 2,6-Me_2-BQ 1 equiv.	1,2-DCE	70 °C, 12 h	No reaction
6	$Pd(TFA)_2$ 5 mol%, Diazafluorenone 5 mol% Cs_2CO_3 1 equiv., 1 atm O_2	DMSO	75 °C, 18 h	Decomposition
7	PIDA or PIFA 1.1 equiv.	CH_2Cl_2 or MeCN	35 °C, 3 h	Decomposition
8	DMP 1.1 equiv.	CH_2Cl_2	rt	Decomposition

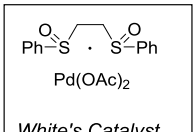

White's Catalyst

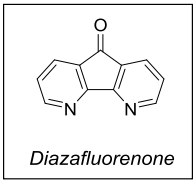

Diazafluorenone

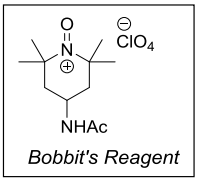

Bobbit's Reagent

a Reactions run on a 10-20 mg scale under an atmosphere of air, argon or oxygen

Of note, several conditions gave interesting results. IBX induced α-hydroxylation (**Scheme 2.12 (A)**, product **139**), enamine-based Saegusa oxidations[124,125] yielded enamine formation (**Scheme 2.12 (B)**, product **140**) or an unexpected Pd(II)-mediated oxidative 5-*exo*-trig cyclization to afford 5-6 fused lactone **141** in the presence of a sub-stoichiometric amount of diphenyl prolinol (**Scheme 2.12 (B)**). To the best of our knowledge, formation of **141** is the first example of a Wacker type oxypalladation of an α-formylated lactone. Literature precedents have demonstrated the ability of tethered alcohols and phenols to partake in such oxypalladation process, racemically[126] or enantioselectively[127,128] by using a chiral ligand such as sparteine or bisoxazoline derivatives. We believe that the prolinol acts as a ligand for Pd(II) in the present case, as control experiments without this ligand showed decomposition. It is unclear at this stage if the chiral enantiopure L-prolinol imparts asymmetric induction into this process. Further experiments such as conducting the reaction with a racemic mixture of diphenyl prolinol and comparing the reaction outcome by chiral HPLC would help assess potential for an enantioselective transformation.

Scheme 2.12 Other Oxidative Conditions of Interest

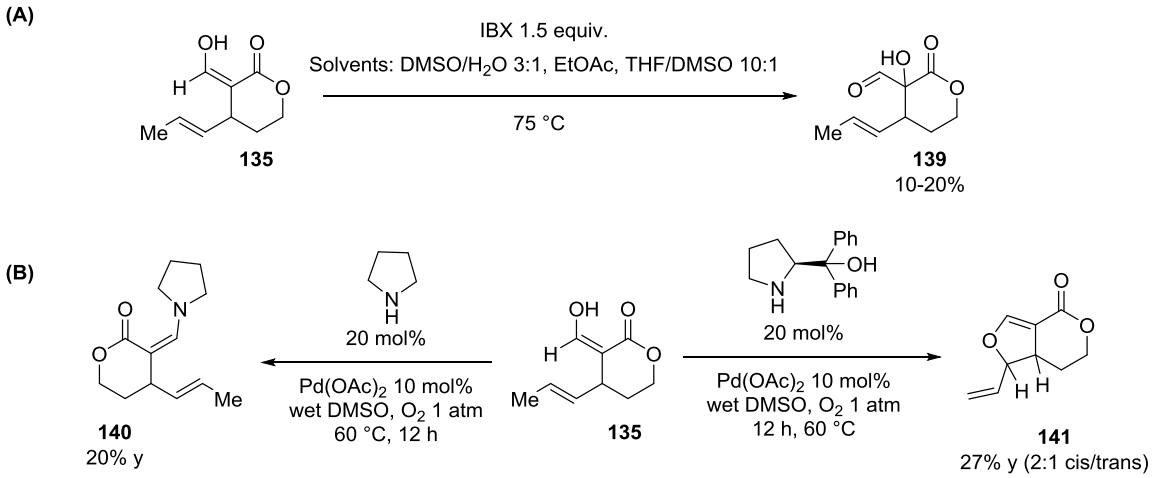

Given the unexpected difficulty to promote an effective and reproducible oxidation of α-formylated lactone **135**, an alternative synthetic route was explored, using an aldol condensation as the key step.

2.3.3 Second Synthetic Route: Use of an Allylic 1,3-Diol in an Aldol Condensation

We hypothesized that a short alternative route to the cuprate addition/formylation/oxidation sequence may arise from an intramolecular aldol condensation of enone ester **142** (**Scheme 2.13**). This oxidized building block was imagined to be derived from transesterification of diol **143** with a masked formylacetic ester **144**.

Scheme 2.13 Second Route: Retrosynthetic Analysis

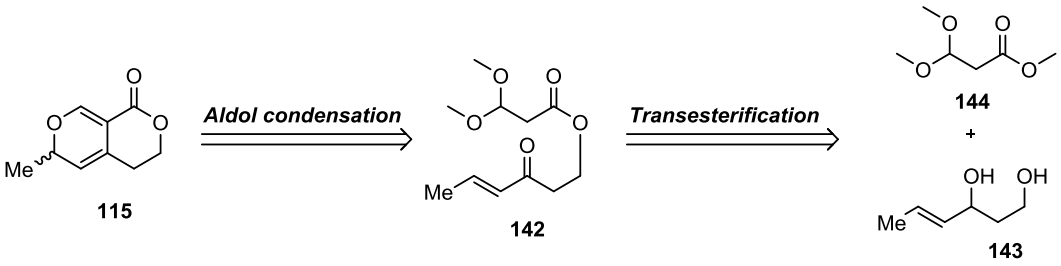

1,3-Diol **143**[111] was transesterified with the commercially available methyl 3,3-dimethoxypropionate **144** in the presence of Otera's catalyst (**A**) (**Scheme 2.14**).[129,130] The resulting coupled product **145** was then efficiently oxidized with DMP to rapidly afford the targeted enone ester **142**.

Scheme 2.14 Synthesis of β-Dimethyl Acetal Ester 142

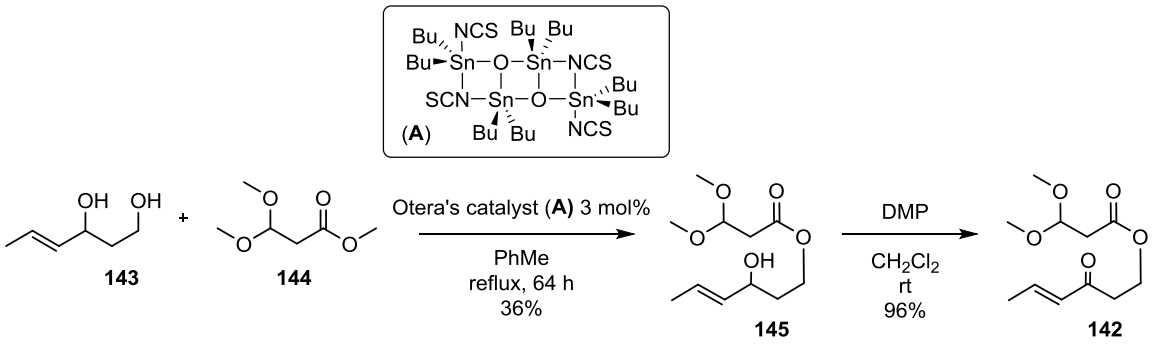

A range of methods were subsequently screened to effect the deprotection of the dimethyl acetal, followed by intramolecular aldol condensation into the enone moiety of **142**. Both Lewis and Brønsted acids (including combinations of), as well as basic conditions were tested (**Table 2.3**). La(III), Bi(III) and Er(III) metals degraded the starting material or lead to ester cleavage. The strongly coordinating Lewis acid $BF_3.OEt_2$ induced an undesired methanol elimination to form enol ether **C**. Among the acidic conditions tried, Amberlyst-15 promoted conversion to a mixture of deprotected enol ether **C** and formyl acetic ester **D**, the latter rapidly degrading upon standing. A combination of Lewis and Brønsted acids were equally uneffective, and induced decomposition of the starting material. Dual use of magnesium bromide dietherate and trimethylamine, a common soft enolization tactic[131] aimed at lowering the pKa of the α-ester hydrogen, cleanly afforded enol ether **C**. Attempts at resubjecting product **C** to several hydrolysis conditions led to degradation or the formation of the sensitive, quickly decomposing aldehyde **D**. With this extensive screening yielding unproductive pathways, a third route was pursued.

Table 2.3 Aldol Condensation Screen[a]

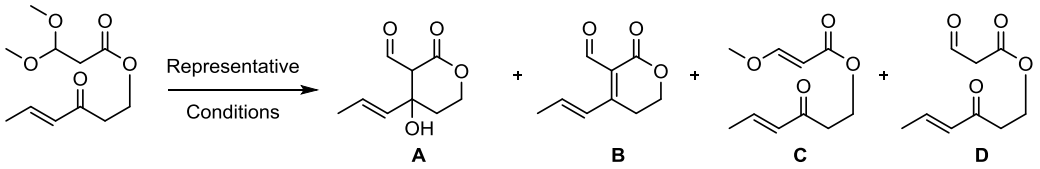

Lewis Acid	Bronsted Acid	Bronsted Base	Solvent	Temp, Time	Result
$La(OTf)_3$ 10 mol%	-	-	wet MeCN	40 °C, 16 h	SM+Degradation
Montmorillonite K-10	-	-	CH_2Cl_2	rt, 16 h	Recovered SM
$BiCl_3$ 15 mol%	-	-	wet MeCN	70 °C, 16 h	Ester Cleavage
$Er(OTf)_3$ 15 mol%	-	-	$MeNO_2$	40 °C, 16 h	Degradation
$BF_3.OEt_2$ 1 equiv.	-	-	CH_2Cl_2	-78 °C to 0 °C, 3 h	low conversion to C
$MgBr_2.OEt_2$ 1 equiv.	-	Et_3N 1 equiv.	CH_2Cl_2	0 °C, 3 h	77% (C)
-	Amberlyst 15	-	H_2O/Acetone	rt, 16 h	SM+ C+D
-	CSA 10 mol%	-	MeOH	rt, 16 h	Ester cleavage
-	$TsOH.H_2O$ 10 mol%	-	Acetone	rt, 16 h	Degradation
-	TFA excess	-	CH_2Cl_2/H_2O	40 °C, 16 h	SM+Degradation
$La(OTf)_3$ 10 mol%	Benzoic acid 1 equiv.	-	wet MeCN	60 °C, 16 h	Degradation

[a] Reactions run on a 10-20 mg scale, under air or nitrogen atmosphere. Yields refer to pure, isolated compounds.

2.3.4 Third Synthetic Route: Metal-Mediated Diyne Cyclization

Formal [2+2+2] diyne cyclizations have been successfully carried out to form *2H*-pyrans using metals such as Ni(0), Rh(I) and Ru(I) (**Chapter 1**, *Section 1.2.1).* We wished to apply a similar methodology to cyclize diynoates of general structure **146** (**Scheme 2.15**) to α-pyran **147**. It was anticipated **146** could be accessed by esterification of TMS-protected propiolate **148** with but-3-yn-1-ol **149**.

Scheme 2.15 Planned Metal Mediated Cyclization of Diynoate 146

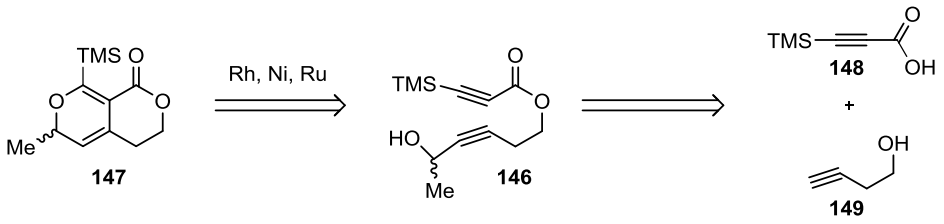

To this end, diynoate **146** was synthesized in three steps from TMS acetylene **150** (**Scheme 2.16**). Lithiation of the terminal alkyne followed by anion quenching with dry $CO_{2(g)}$[132] afforded the TMS protected ynoate **148**.[133] From **148**, esterification was effected *via in situ* acyl chloride formation,[134] followed by nucleophilic displacement with but-3-yn-1-ol **149**. Final lithiation of the resulting terminal alkyne **151** followed by addition into acetaldehyde enabled access to racemic diynoate ester **146**.

Scheme 2.16 Access to Diynoate 146

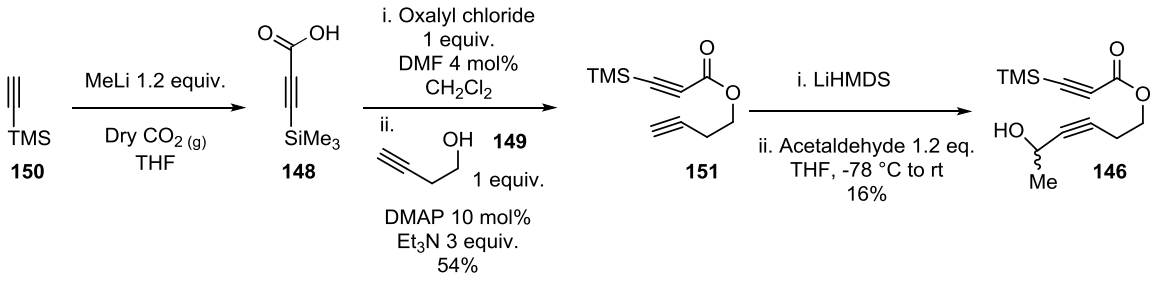

We next focused our efforts on triggering the cycloisomerization using metals such as cationic ruthenium and rhodium (**Scheme 2.17**) in several solvents.[20,25] Disappointingly, these conditions did not produce the desired cyclized framework of **147**, and we instead observed ester cleavage of **146**.

Scheme 2.17 Metal-mediated Cyclization of Diynoate 146

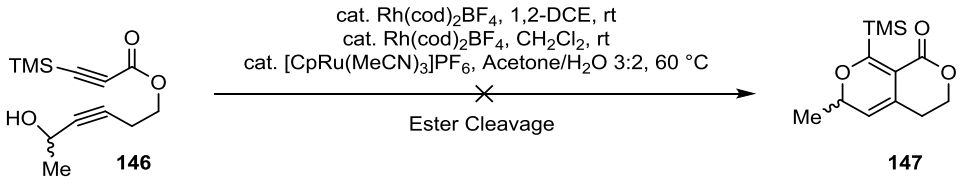

2.3.5 Fourth Approach: Saucy-Marbet Rearrangement of a Propargyl Vinyl Ether

We envisaged a potential way to alleviate ester cleavage would start by first installing the *2H*-pyran moiety followed by lactonization (**Scheme 2.18**). Literature precedents[46,135] demonstrated the formation of *2H*-pyran structures *via* Ag(I) or Au(I)-mediated Claisen rearrangement/isomerization of propargyl vinyl ethers (**Chapter 1**, *Section 1.2.3*). We hoped a similar transformation would be successful in the production of pyran **115**. Claisen rearrangement of propargyl vinyl ether **152** would yield *2H*-pyran **153**, which could be further deprotected and lactonized to pyran **115.**

Scheme 2.18 Potential Route to *2H*-Pyran 115 *via* Claisen Rearrangement/Isomerization

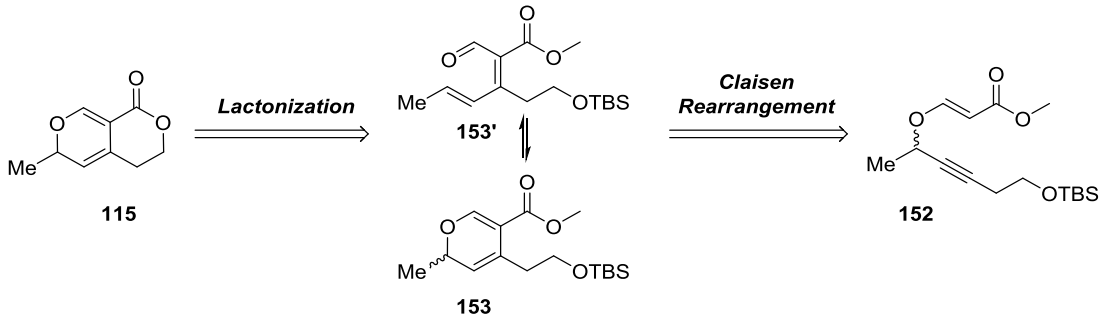

Propargyl vinyl ether **152** was thus easily assembled by lithium acetylide addition of TBS-protected but-3-yn-1-ol into acetaldehyde,[136] followed by tributylphosphine

mediated conjugate addition[137] of the resulting alcohol with methyl propiolate. At this stage, a Saucy-Marbet rearrangement was attempted. Screening a variety of Lewis acids and alkynophilic metals (**Scheme 2.19**), we discovered that AuCl most efficiently promoted the transformation to allene **154**, which upon DBU treatment isomerized to α-pyran **153**.

Scheme 2.19 Saucy-Marbet Rearrangement: Metal Screen

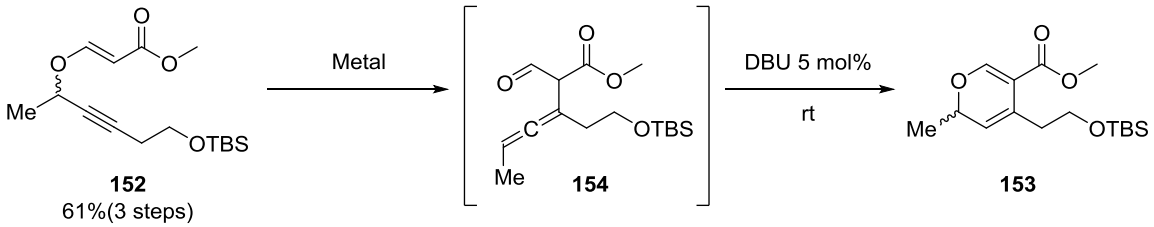

152
61%(3 steps)
from but-3-yn-1-ol

154

153

Catalyst (5 mol%)	Solvent	Temperature (°C)	Time	Results
$AgSbF_6$	CH_2Cl_2	30	4 h	No reaction
$Sc(OTf)_3$	1,2-DCE	rt	4 h	Decomposition
AuCl	CH_2Cl_2	30	2 h	75% y
$AuCl/AgSbF_6$	CH_2Cl_2	30	5 h	Low conversion
PPh_3AuCl	CH_2Cl_2	30	5 h	No reaction

By following this reaction by ^1H NMR, we observed clean conversion of propargyl vinyl ether **152** (**Figure 2.7 (A)**) under mild heating at 30 ˚C in the presence of Au(I) to allene **154**. This is marked by the downfield shift of the enol ether proton H_1 from a doublet at 7.5 ppm to a 9.6 ppm singlet signal, corresponding to an aldehyde proton (**Figure 2.7 (B)**). After adding a catalytic amount of DBU and stirring the reaction at room temperature, clean isomerization to pyran **153** was observed, evident by H_1 shifting from 9.6 ppm to a

singlet at 7.6 ppm (**Figure 2.7 (C)**), characteristic of a *2H*-pyran structure. Compound **153** was isolated upon silica gel chromatography but required storage at low temperature (-20 ˚C) to minimize degradation. In $CDCl_3$, this compound only exists as the pyran valence isomer, with no detectable formation of dienal **153'**.

Figure 2.7 Stacked NMR Plot Illustrating the Rearrangement of Propargyl Vinyl Ether 152 to Pyran 153

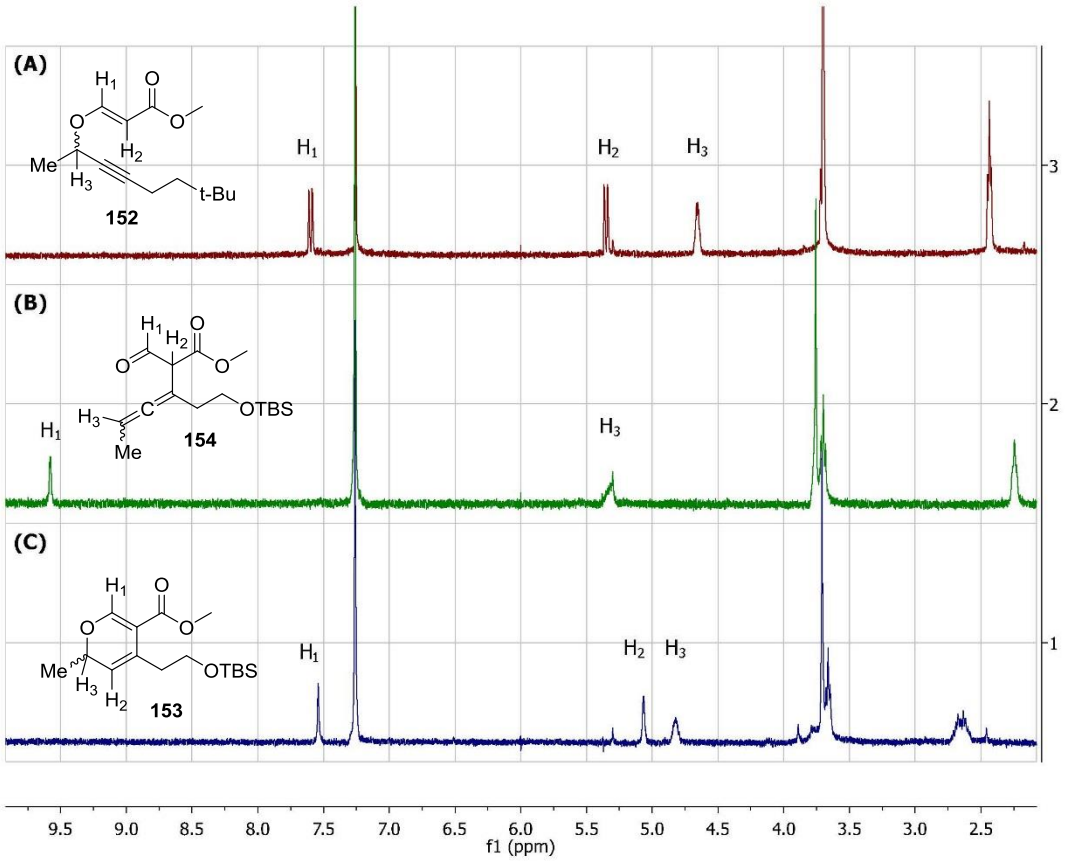

We then turned our attention to the deprotection of the silicon protected primary hydroxyl and methyl ester functionalities of **153** to induce final lactonization. Acidic conditions and fluoride sources were tested (**Scheme 2.20**) and gave low to moderate yield

of the deprotected alcohol, potentially due to the labile character of the already present pyran functionality, which has a tendency for decomposition. Attempts to lactonize the resulting deprotected alcohol **155** with DBU or under thermal heating failed and resulted in decomposition (**Scheme 2.20**).

Scheme 2.20 Attempted Deprotection/Lactonization to Pyran 115

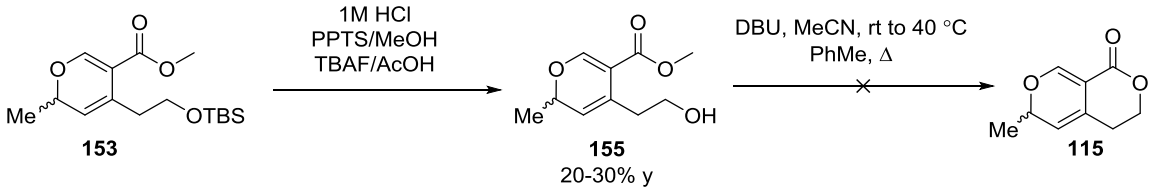

An intramolecular version of the Saucy-Marbet reaction was alternatively investigated. Transesterification of diol **156** with methyl propiolate in the presence of Otera's catalyst[129,130] yielded diynoate **157**. Tributyphosphine catalyzed etherification afforded a mixture of dimer (**158**) and trimer vinyl enol ether macrocycles. A Saucy-Marbet rearrangement was attempted on this species and gave no reaction.

Scheme 2.21 Alternative Access to Pyran 115: Intramolecular Propargyl Claisen Rearrangement

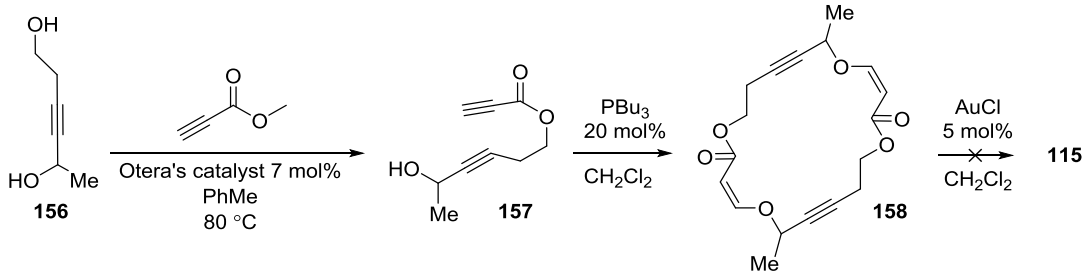

Future plans include a larger screen of lactonization conditions (acidic, basic and Lewis acid conditions) from alcohol **155** to *2H*-pyran **115**. Despite the challenges faced in

designing a shorter route to α-pyran **115**, we remained commited in exploring its potential reactivity in Diels-Alder events and other relevant transformations toward swerilactone A.

2.4 Reactivity of the Fused *2H*-Pyran Lactone in Diels-Alder Cycloadditions

The fully lactonized α-pyran **115** was synthesized according to Tan's published route (**Scheme 2.9**).[111] In our hands, the route proved scalable, in which an appreciable amount (~1g) of material was synthesized in a single batch. The ratio between the two valence isomers (**115**:**115'**) was found to vary in different solvents as determined by ^{1}H NMR analysis. In all cases, the *2H*-pyran is favored, with the highest ratio observed in deuterated methanol and chloroform (3.6:1 and 3.5:1 respectively), and reaching almost equal proportion to the dienal in DMSO-d_6 (**Table 2.3**). The latter result is in accordance with previously reported behaviors of *2H*-pyrans, where the dienal content increased in polar aprotic solvents due to dipole minimization.[5] In our case, aprotic solvents with a high dielectric constant increase the content of the dienal form **115**' (cf. $(CD_3)_2CO$, CD_3CN, DMSO-d_6).

Table 2.4 Solvent Effect on Valence Isomerism of Pyran 115

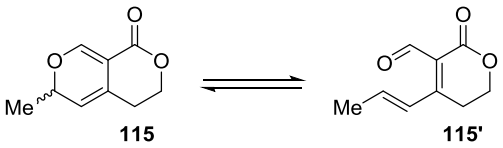

Dielectric Constant	Deuterated Solvent	*2H*-Pyran (**115**) /Dienal (**115'**)[a]
46.7	DMSO-d_6	1.2:1
37.5	CD_3CN	1.7:1
32.7	CD_3OD	3.6:1
20.6	$(CD_3)_2CO$	1.6:1
8.9	CD_2Cl_2	2.6:1
7.6	THF-d_8	1.9:1
4.8	$CDCl_3$	3.5:1
2.3	Benzene-d_6	2.1:1
2.4	Toluene-d_8	2:1

[a] Ratio of **115**/**115'** determined by integration of ^{1}H NMR spectra in each deuterated solvent at 23 °C

2.4.1 Model Ketene Study

With an ample amount of **115** at our disposal, we turned our attention to a model ketene cycloaddition study. In this regard, **115** was reacted with isobutyryl chloride in the presence of Hünig's base or triethylamine (**Scheme 2.22**).

Scheme 2.22 Ketene [4+2] Cycloaddition Model Studies

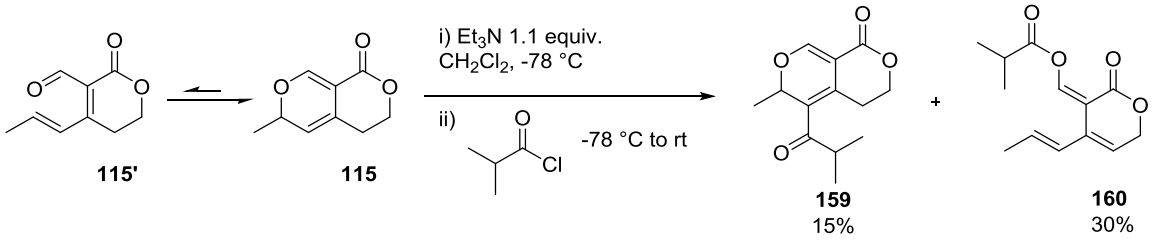

To our surprise, the acyl chloride was not deprotonated under these conditions to form a ketene. Instead, acylation of **115** to compound **159** was observed, along with the *O*-acylated product **160**. A rationale behind these results may be explained by looking closely at the equilibrium of the valence isomerism for pyran **115** (**Scheme 2.23**). In its closed form, **115** theoretically possesses one electrophilic position (shown in red) and one nucleophilic position (shown in blue), based on electron delocalization along the ring system. In its opened dienal form **115'**, two electrophilic positions coexist (shown in red). In the presence of a suitable base, the acidic δ hydrogen of **115'** can be deprotonated to form the cross-conjugated, extended enolate **161**. The latter compound is responsible for production of the *O*-acylation product **160**, a behavior reported on similar enal systems upon deprotonation with triethylamine.[138]

Scheme 2.23 Impact of Valence Isomerism on Acylation

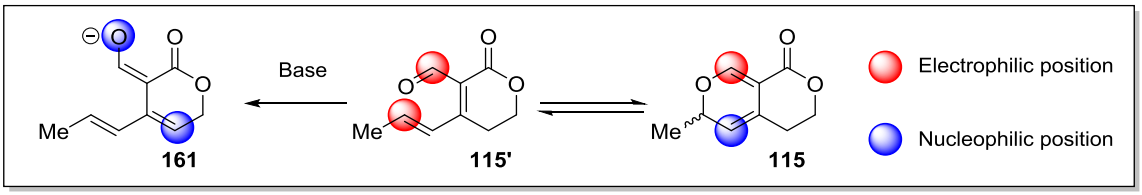

To avoid these side-reactions, slowly adding the *2H*-pyran **115** into a solution of the acyl chloride-triethylamine solution was attempted. Polymerization of the ketene was observed and **115** was recovered.

2.4.2 Reactivity in Thermal Diels-Alder Cycloadditions

Despite the reactivity issues encountered carrying out a ketene cycloaddition study with simple acyl chlorides (which would require bases strong enough to deprotonate **115'**), we tested the normal demand reactivity of **115** to gain valuable insights (**Scheme 2.24**). To this end, thermolysis of **115** in the presence of several electron poor dienophiles such as methyl vinyl ketone, *N*-benzyl maleimide, and *N*-aryl maleimide yielded the desired cycloadducts **162**, **163**, and **164**, respectively, in 30-40% yield.

Scheme 2.24 Normal Demand Diels-Alder Reactivity of α-Pyran 115

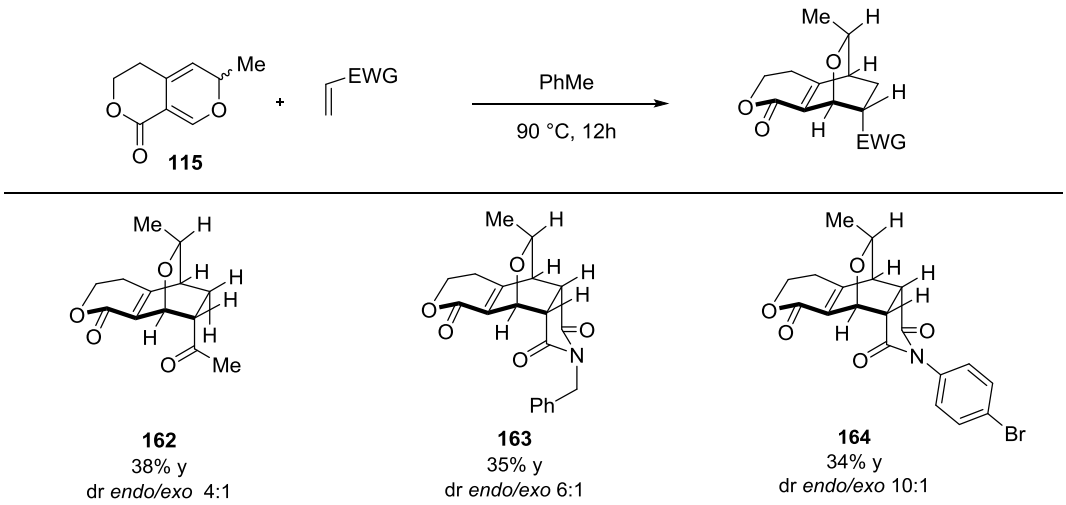

The configuration of these adducts was unambiguously assessed using 2D NMR techniques (*cf.* **Scheme 2.25** for the computed lowest energy conformer of **163** and key NOESY and HMBC correlations). As predicted by frontier molecular orbital theory, due to secondary stabilizing interactions of the electron poor dienophiles, the *endo* adducts are the major products and display the expected regioselectivity based on predicted structure polarity/orbital coefficients. Additionally, the methyl group contained in **115** impart facial

selectivity, forcing the dienophile to approach from the most accessible face, an observation made by the Tan group in their $^1O_2$ cycloaddition.[111]

Scheme 2.25 Lowest Energy Conformer of Adduct 163 (MMFF) and Key 2D NMR Correlations

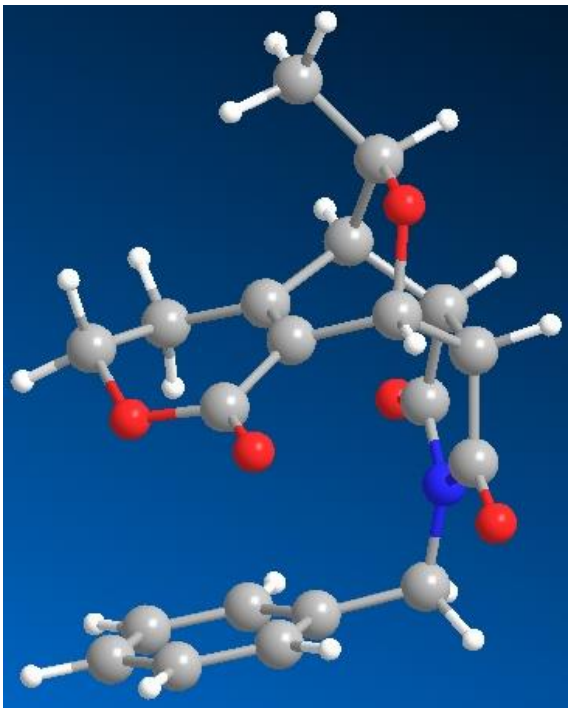

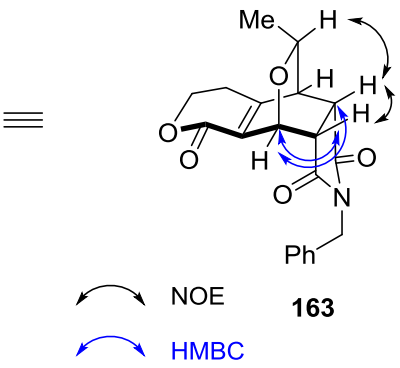

163

We observed moderate yields for these reactions, and a small quantity of **115** was recovered in each case. A test reaction was carried out to help understand if a decomposition pathway was impairing our yield or if additional side-products were formed. Heating **115** in toluene by itself did not provide *in situ* dimerization of **115**, surprisingly given the large body of literature taking advantage of *2H*-pyrans ability to self-dimerize (**Chapter 1**, *Section 1.3.1*).[12,74,139] Other literature reports demonstrated the potential of *2H*-pyrans to undergo 1,5-hydride shifts, forming acyl ketenes[140] (**Scheme 2.26 (A)**) and 1,7-hydride shifts (**Scheme 2.26 (B)**).[13]

Scheme 2.26 Reported Side Reactions of Dienals through Hydride Shifts

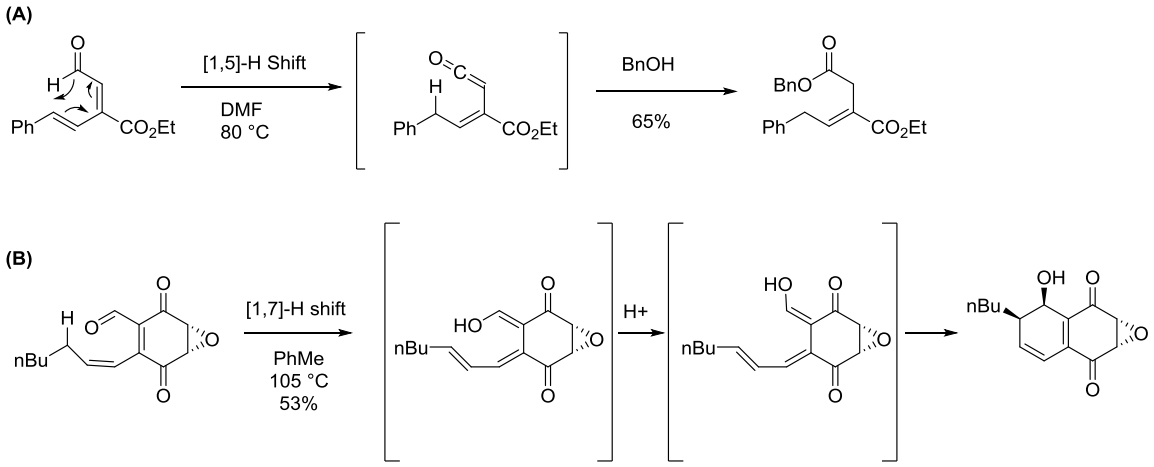

In our case, decomposition slowly occured over time, with complete decomposition observed at temperatures greater than 90 ˚C (**Scheme 2.27 (A)**). Improving the yields for this series of experiment may be possible by degassing the solvent and adding the radical quencher butylated hydroxytoluene (BHT) to minimize radical side reactions.

Of note, inverse demand cycloaddition mode was also investigated with ethyl vinyl ether, but gave rise to *2H*-pyran decomposition and a very low yield (<5%) of cycloadduct as assessed by crude ^{1}H NMR (**Scheme 2.27 (B)**). Nonetheless, as a proof-of-concept, these experiments clearly show the ability of **115** to partake in normal demand [4+2] cycloaddition and its lack of reactivity in the inverse demand mode.

Scheme 2.27 Attempted Self-Dimerization of Pyran 115 and Inverse Demand Cycloaddtion

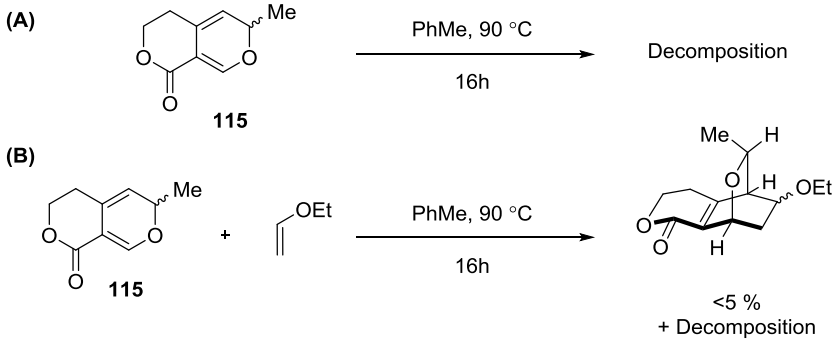

2.4.3 Radical Cation [4+2] Cycloaddition

Sorting through the literature for Diels-Alder processes, we became interested in a different Diels-Alder mode: cation radical cycloadditions of enols and their derivatives,[141,142] mediated by photocatalysts or chemical oxidants. Expanding upon Prof. Bauld's use of triarylaminium salts to promote radical cation [4+2] cycloaddition of carbodienes with alkenes,[143–145] Schmittel and coworkers investigated the reaction of ketenes with carbodienes in the presence of a one electron oxidant such as triarylamminiumyl hexafluoroantimonate.[146,147] Contrary to thermal activation, the reaction afforded [4+2] cycloadducts, avoiding the common [2+2] pathway (**Scheme 2.28 (A)**).

This strategy could also represent an amenable avenue in our proposed biomimetic approach (**Scheme 2.2**). Similarly to the well-known DeMayo cyclization,[148] 1,3 dicarbonyls and ketones in their enol tautomer form are also suitable to single electron transfer.[149,150] Flowers and coworkers conducted chemical oxidation of 1,3-dicarbonyls

and using Ce(IV) and observed a radical cation formation,[151] followed by intramolecular cyclization (**Scheme 2.28 (B)**). Silyl enol ethers can be oxidized to a radical cation and were shown to participate in radical cyclization. [152–154] Trauner utilized this strategy to elegantly assemble a precursor to (-)-guanacastepene E *via* anodic oxidation (**Scheme 2.28 (C)**).[153]

Scheme 2.28 Overview of Radical Cation Cyclization of Ketenes and Enol Derivatives

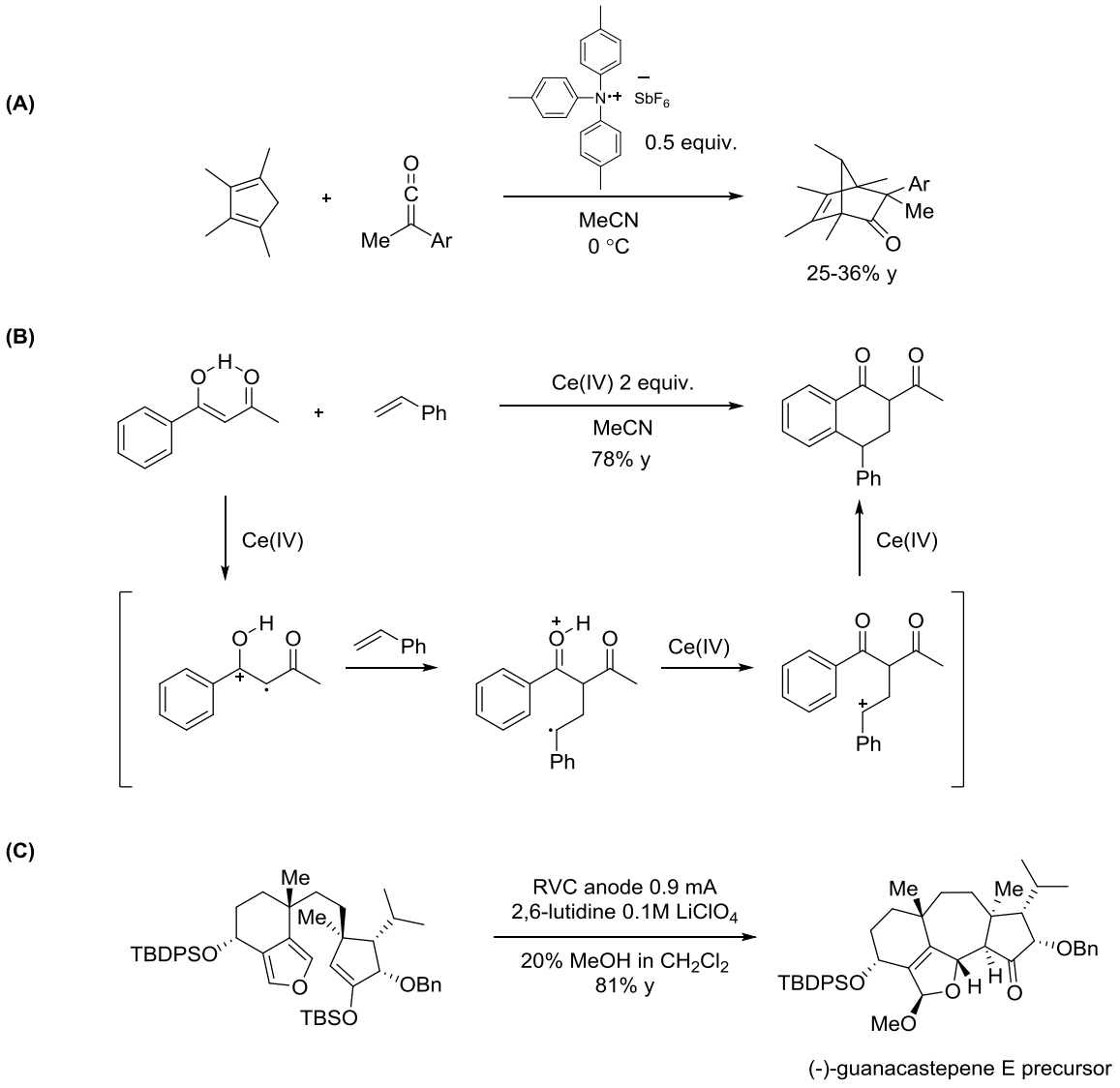

More recently, advances in photoredox catalysis[155] have inspired the Yoon group, who reported the use of ruthenium photocatalysts in the excited state to promote one electron oxidation of stilbene derivatives, in which a cation radical can participate in Diels-Alder cycloadditions with several inert dienes (**Scheme 2.29 (A)**).[156] The mechanism for

this transformation is believed to rely on a radical chain process. *Trans*-anethole **165** (E_{ox}= 1.1 V) is oxidized to a radical cation **166** $^{+\cdot}$ by the excited photocatalyst *$Ru(bpz)_3^{2+}$ (E_{ox}=1.4 V). This oxidized species further reacts with isoprene **167** to generate a stabilized radical cation cycloadduct **168**$^{+\cdot}$ Propagation of the radical chain process and formation of product **169** are induced by the oxidation of another equivalent of *trans*-anethole **165** by the oxidized cycloadduct **168**$^{+\cdot}$.[157]

Yoon and coworkers applied their methodology to the synthesis of heitzamide A, and showcased the complementary character of radical cation cycloaddition. The umpolung strategy imparted by a cation radical formation gives rise to coupling products between electronically mismatched sites. The end result is a reverse of the inherent polarity of both partners. The innate polarization of both neutral diene and dienophile predicts the formation of a regioisomer of heitzamide A in the case of a thermal [4+2] cycloaddition and is verified experimentally (**Scheme 2.29 (B)**). In contrast, using a Ru(II) photocatalyst to trigger the photosensitized electron transfer (PET), a precursor of heitzamide A is obtained in good yield (**Scheme 2.29 (C)**).

Scheme 2.29 Yoon's Radical Cation [4+2] Cycloaddition and Application to Natural Product Synthesis

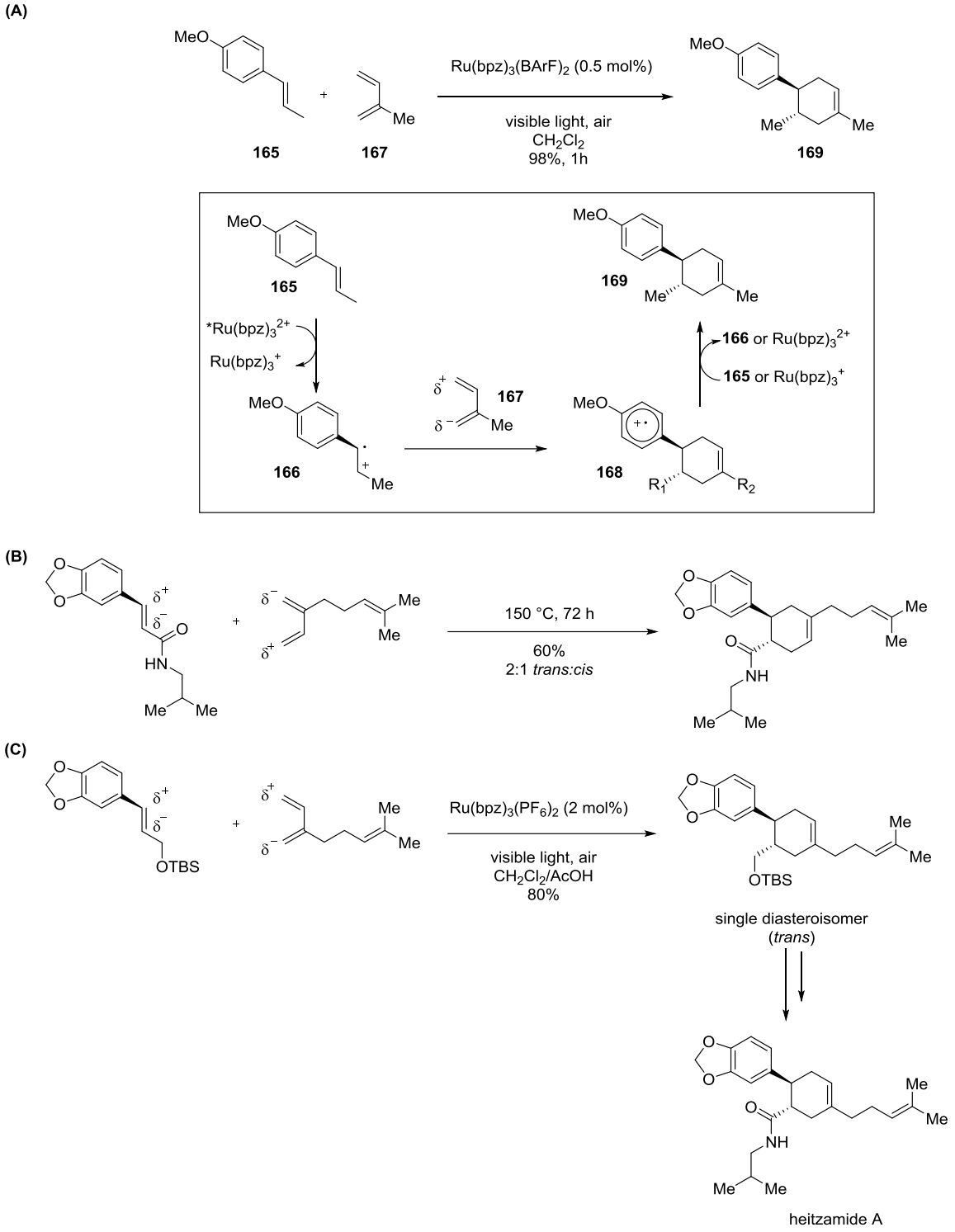

Inspired by this body of work and the possibility of **115** being a competent diene in this type of cycloaddition process, we pursued a small model study. We first targeted the reaction of ethyl vinyl ether with **115** in the presence of a Ru (II) photocatalyst $RuCl_2(bpy)_3.6H_2O$ (**Scheme 2.30 (A)**) in dry dichloromethane. In lieu of a cycloadduct, we isolated a mixture of two compounds, which were attributed to lactol **131** and endoperoxide **132** by comparison with the work of Tan and coworkers.[111] The same outcome was found upon using the pyran alone without ethyl vinyl ether in this reaction. In degassed dichloromethane, no reaction was observed in the presence of the ruthenium photocatalyst.

Scheme 2.30 Attempted Radical Cation [4+2] Cycloaddition of *2H*-Pyran 115

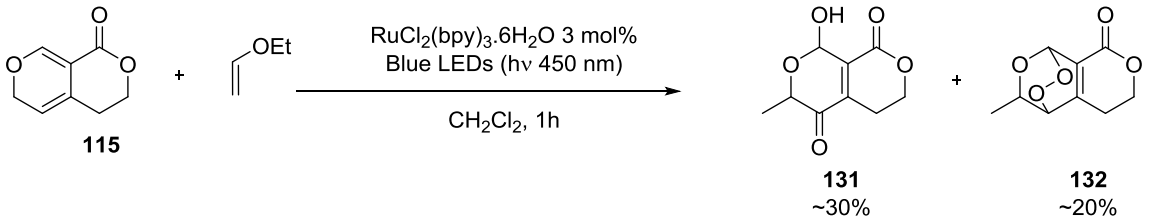

Unclear to us was the mechanism of this oxidative process. We questioned the role of the ruthenium catalyst, whether if it was serving as a photosensitizer generating singlet oxygen,[158] or if it promoted excitation of the pyran to a diradical,[159,160] further trapped by triplet oxygen. The ruthenium catalyst has a reported excited state triplet energy of 61 kcal/mol at its emission maximum (470 nm),[161] a value higher than needed to irreversibly excite O_2 to $^1O_2$ (37.5 kcal/mol). The first hypothesis was tested by introducing a catalytic amount of the singlet oxygen quencher DABCO, and, in this case, no reaction occurred (**Scheme 2.31 (A)**). The second hypothesis proved incorrect, as using the radical scavenger

BHT did not inhibit the reaction, and the previously isolated compounds were obtained (**Scheme 2.31 (B)**). In the absence of photocatalyst or light, the photooxygenation of **115** was not observed, and we recovered the starting material. From these control experiments, we believe the ruthenium catalyst only acts a photosensitizer for $^1O_2$ in this reaction.

Scheme 2.31 Photooxygenation of *2H*-Pyran 115: Mechanistic probes

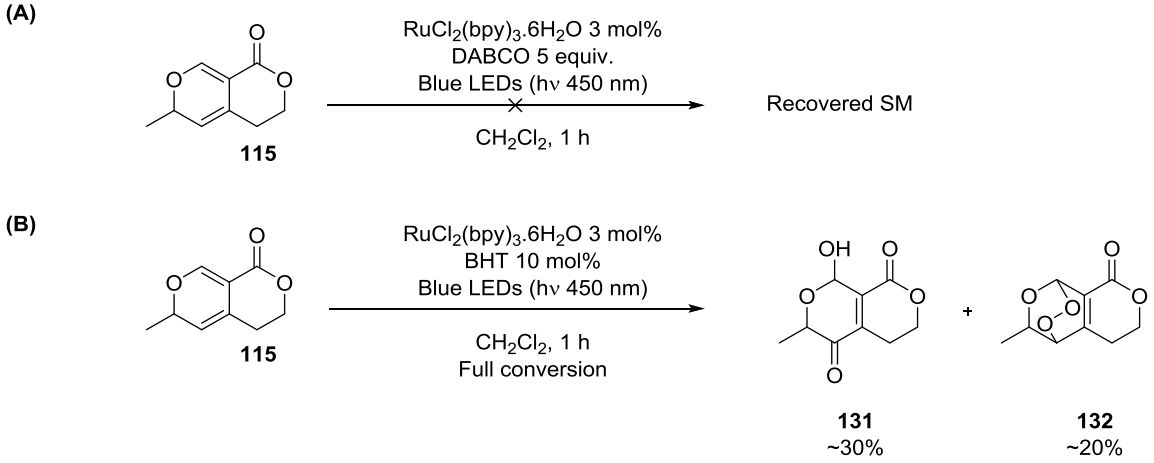

The more easily oxidizable *trans*-anethole **165** (E_{ox} =1.1 V) was chosen to validate the hypothesis of *2H*-pyran **115** participating in radical cation [4+2] event (**Scheme 2.32**). Using a catalytic amount of triphenyl pyrylium tetrafluoroborate **170** (E_{ox} = 2 V), a known promoter of photoinduced single electron transfer,[162–164] *trans*-anethole **165** (E_{ox} = 1.1 V in MeCN) reacted with **115** in a [4+2] cycloaddition, yielding adduct **171** in 20% yield. The relative configuration for this adduct (*endo*, *trans*) was deduced through 2D NMR experiments (HSQC, HMBC, NOESY) and careful analysis of the coupling constants of the cyclohexene ring. We were pleased with this result, as it may expand our options regarding the key cycloaddition event toward swerilactones A and B, outside of a normal

demand Diels-Alder reaction. For example, an electron rich, enol ether substituted lactone dienophile could be accessed and its reactivity in radical cation cycloaddition with pyran **115** may be probed.

Scheme 2.32 Radical Cation Cycloaddition of *Trans*-Anethole 163 and *2H*-Pyran 115

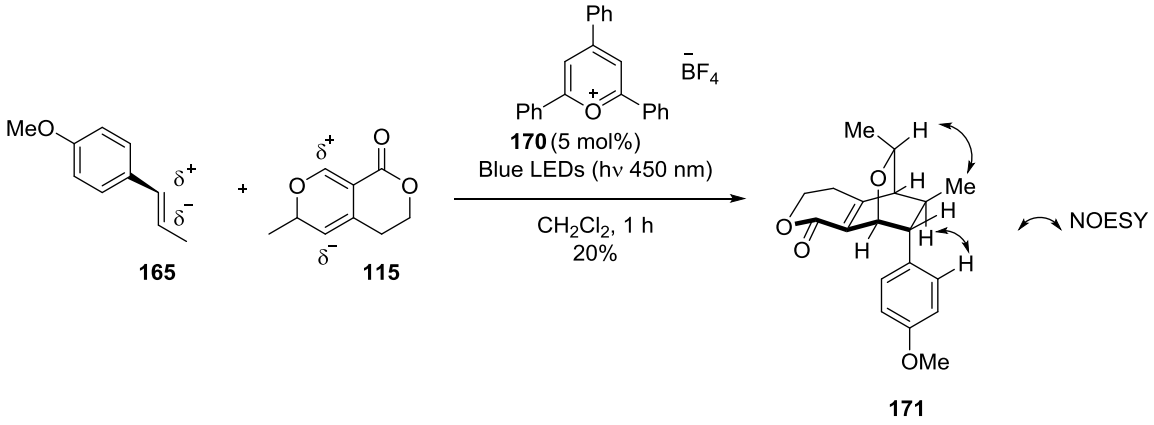

2.5 Summary and Conclusion

Throughout this chapter, we have presented our efforts aimed at the synthesis of the core of a lactonized *2H*-pyran *via* a Saucy-Marbet rearrangement, which is meant to serve as a diene in our proposed biomimetic synthesis of swerilactones A and B. Contrary to the largely documented propensity of *2H*-pyrans to self-dimerize or participate in hydride shift to form acyl ketene, our targeted pyran was found to be heat sensitive, resulting in decomposition.

We were nonetheless able to explore the preliminary reactivity of this key component in Diels-Alder cycloadditions. We have shown that thermal normal demand (**Section 2.4.2**) and radical cation [4+2] (**Section 2.4.3**) were two accessible modes of reactivities for *2H*-pyran **115**, whereas thermal inverse demand represented a largely

unproductive pathway. The following chapter will focus on accessing several lactone dienophiles, with an aim to pinpoint the best way of merging the two reaction partners.

2.6 Experimental Section

General Information: ^{1}H NMR spectra were recorded at 300, 400, or 500 MHz at ambient temperature with $CDCl_3$, CD_3OD, DMSO-d_6 or benzene-d_6 (Cambridge Isotope Laboratories, Inc.) as solvents. Data for ^{1}H NMR are reported as follows: chemical shift, integration, multiplicity (br = broad, ovrlp = overlapping, s = singlet, d = doublet, t = triplet, q = quartet, m = multiplet) and coupling constants in Hz. ^{13}C NMR spectra were recorded at 100.0, or 125 MHz at ambient temperature with the same solvents unless otherwise stated. Chemical shifts are reported in parts per million relative to the deuterated solvents. All ^{13}C NMR spectra were recorded with complete proton decoupling. Infrared spectra were recorded on a Nicolet Nexus 670 FT-IR spectrophotometer. High-resolution mass spectra were obtained in the Boston University Chemical Instrumentation Center using a Waters Q-TOF API-US mass spectrometer. Melting points were recorded on a Mel-Temp apparatus (Laboratory Devices). Analytical LC-MS was performed on a Waters Acquity UPLC (Ultra Performance Liquid Chromatography (Waters MassLynx Version 4.1) with a Binary solvent manager, SQ mass spectrometer, Water 2996 PDA (PhotoDiode Array) detector, and ELSD (Evaporative Light Scattering Detector). An Acquity UPLC BEH C_{18} 1.7 μ m column was used for analytical UPLC-MS. Optical rotations were recorded on an AUTOPOL III digital polarimeter at 589 nm, and specific rotations are given $[\alpha]_D^{20}$ (concentration in grams/100 mL solvent). SFC analysis of enantioenriched compounds was

performed on a Berger SFC (Waters) System with a diode array detector using a SFC Chiralcel®OD-H (Chiral Technologies Inc., 100 × 4.6 mm I.D., 5μm) column. Preparative HPLC was performed on a Gilson PLC2020 using a Waters SunFire™ Prep C18 OBD™ 5μm 19X50 mm column. Analytical thin layer chromatography was performed using 0.25 mm silica gel 60-F plates. Flash chromatography was performed using 200-400 mesh silica gel (Scientific Absorbents, Inc.). Yields refer to chromatographically and spectroscopically pure materials, unless otherwise stated. HPLC grade tetrahydrofuran, methylene chloride, diethyl ether, toluene, acetonitrile, and benzene were purchased from Fisher and VWR and were purified and dried by passing through a PURE SOLV® solvent purification system (Innovative Technology, Inc.). Other ACS grade solvents for chromatography were purchased from Fisher. Select photochemistry experiments were performed using a jacketed beaker covered in tape with spiralled blue LEDs strip (hν = 450 nm) on the inside walls. A flow of cold water was used to cool the beaker down upon irradiation. All other reactions were carried out in oven-dried glassware under an argon atmosphere unless otherwise noted.

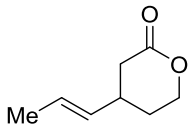

1,4-Adduct 138: In a 1L flame-dried 3 neck-flask equipped with a 60 mL addition funnel under nitrogen, ether (60 mL) was added and the reaction was cooled to -78 °C. (*E*)-1-Bromoprop-1-ene (3.5 mL, 40.7 mmol, 1.55 equiv.) (volatile) was introduced *via* syringe. A solution of 1.7 M *tert*-butyllithium in pentane (46.4 mL, 3 equiv.) was added

dropwise over 10 min. The walls of the addition funnel were rinsed with a small quantity of ether.

To a separate 200 mL flame-dried Schlenk flask under nitrogen, copper(I) iodide (7.5 g, 39.4 mmol, 1.5 equiv.) (previously dried with a heat gun under high vacuum) was added and the vessel was purged 3 times with a vacuum/nitrogen cycle. At room temperature, ether (50 mL) was introduced, followed by freshly distilled tributylphosphine (23.6 mL, 94.6 mmol, 3.6 equiv.) dropwise. An exotherm developed. The reaction mixture turned from a suspension to a clear solution after 5 minutes of vigorous stirring. After 20 min, the cuprate solution was cannulated into the addition funnel, and then added over 10 min to the vinyl lithium solution at -78 °C. The solution turned from pale yellow to a bright yellow slurry and was stirred for 1.5 h at -78 °C.

2H-Pyran-2-one, 5,6-dihydro- (2.52 mL, 26.3 mmol, 1 equiv.) was added into an addition funnel and was dissolved in dry ether (50 mL). This solution was added at -78 °C slowly over 60 minutes into the yellow cuprate solution. The walls of the addition funnel were rinsed with a small quantity of ether (5 mL). The reaction was stirred for 60 minutes at -78 °C. TLC showed complete conversion (EtOAc/Hex 3:7, $KMnO_4$ stain). The reaction mixture was quenched with saturated NH_4Cl (100 mL), extracted with ether (3 x 50 mL), and was washed with brine. The ethereal solvent was removed *in vacuo* using a rotavap with a weak pull (Note: the 1,4 adduct was found to be volatile; care was taken to keep the water bath cold with ice). The crude oil was then purified on a long height column using a gradient of Hexanes/EtOAc (100:0, 95:5, 93:7, 9:1, 88:12, 85:15, 83:17, 4:1, 7:3, 1:1, 0:100) to yield the desired after careful concentration (weak pull rotavap, cold water bath).

The 1,4-adduct was obtained as a colorless, volatile oil. A final weight was obtained by air drying the concentrated sample for 10 minutes (13.15 mmol, 1.84 g, 50%).

R_f = 0.25 (hex/EtOAc 7:3 UV, $KMnO_4$); **IR** νmax (film): 2970, 2959, 2913, 1736, 1461, 1441, 1402, 1250, 1217, 1172, 1069, 968 cm^{-1}; **^{1}H NMR** (500 MHz, $CDCl_3$) δ 5.52 (dqd, *J* = 15.5, 6.0, 1.0 Hz, 1H), 5.37 (ddq, *J* = 15.5, 6.5, 1.5 Hz, 1H), 4.43 (dt, *J* = 11.5, 4.5 Hz, 1H), 4.27 (ddd, *J* = 11.5, 10.0, 3.5 Hz, 1H), 2.68 (ddd, *J* = 17.0, 6.0, 1.5 Hz, 1H), 2.61 (m, 1H), 2.32 (dd, *J* = 17.0, 10.0 Hz, 1H), 1.95 (ddd, *J* = 13.0, 8.0, 4.5, 1.5 Hz, 1H), 1.68 (ddd, *J* = 6.5, 1.5, 1 Hz, 1H), 1.67 (m, 1H); **^{13}C NMR** (126 MHz, $CDCl_3$) δ 170.9, 132.4, 125.8, 68.3, 36.1, 34.3, 29.0, 17.8; **HR-MS**: *m/z* Calcd for $[C_8H_{12}O_2+H]^+$ 140.08, found.

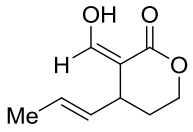

Formylated lactone 135: To a 100 mL flame-dried Schlenk flask under nitrogen was added freshly distilled *N*,*N*-diisopropylamine (0.5 mL, 3.583 mmol, 1.25 equiv) dissolved in THF (14 mL). A solution of 2.5 M of *n*-BuLi in hexanes (1.4 mL, 1.2 equiv.) was added dropwise at -78 °C, and flask was transferred to an ice bath. The reaction was stirred for 30 minutes at 0 °C.

A solution of 1,4 adduct **137** (400.7 mg, 2.8 mmol, 1 equiv.) in THF (6 mL) was then added dropwise at -78 °C over 10 minutes, followed by hexamethylphosphoramide (0.99 mL, 5.7 mmol, 2 equiv.). The flask was transferred to a chiller cooled at -10 °C for 1h. The reaction mixture was cooled back to -78 °C before 2,2,2-trifluoroethyl formate (860 μL, 8.8 mmol,

3 equiv.) was added *via* syringe. The reaction was left to warm slowly at 0 °C in a chiller overnight.

The crude mixture was quenched with ammonium chloride and aqueous HCl. Water and ether were added; the organic phase was separated and the water layer was extracted with ether (3x). The organic layer was then washed with 10% aqueous NaOH (3x). The basic aqueous layer was further reacidified at 0 °C with 2N HCl until pH 3 was reached. Extraction of the acidified aqueous layer with methylene chloride (3x) was followed by drying and concentration in *vacuo* to yield a crude oil. Purification on silica gel (ethyl acetate/hexanes (slow gradient from 5% to 30%)) afforded the desired formylated lactone as an orange oil.

R_f = 0.33 (hex/EtOAc, 7:3, UV, $KMnO_4$); **IR** νmax (film): 2963, 2919, 2857, 2764, 1656, 1604, 1476, 1417, 1372, 1340, 1272, 1226, 1124, 1068, 965, 857, 775, 720 cm^{-1}; **^{1}H NMR** (500 MHz, $CDCl_3$) δ 12.58 (d, *J* = 16.0 Hz, 1H), 7.16 (d, *J* =16.0 Hz, 1H), 5.5 (dd, *J* = 18.0, 8.0 Hz, 1H), 5.3 (dd, *J* = 18.0, 8.0 Hz, 1H), 4.35 (m, 1H), 4.25 (m, 1H), 3.15 (m, 1H), 1.95 (m, 1H), 1.75 (m, 1H), 1.73 (d, *J* = 8.0 Hz, 3H); **^{13}C NMR** (100 MHz, $CDCl_3$) δ 171.7, 165.5, 132.0, 128.3, 100.9, 66.8, 36.7, 29.2, 17.7; **HR-MS**: *m/z* Calcd for $[C_9H_{12}O_3+H]^+$ 168.08, found

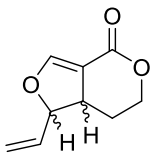

5/6 fused lactone 141: In a thick wall microwave vial, formylated lactone **135** (122.0 mg, 725.4 μmol, 1 equiv.), palladium acetate (16.3 mg, 72.5 μmol, 10 mol%), and

diphenyl-[(2*S*)-pyrrolidin-2-yl]methanol (36.8 mg, 145.1 μmol, 20 mol%) were dissolved in wet DMSO (2.7 mL). Oxygen was then bubbled through the reaction for 30 minutes using an attached balloon after which time the vial was transferred to a preheated oil bath at 70°C and stirred at this temperature for 12 h. TLC showed incomplete conversion. Direct loading of the crude on silica (EtOAc in hexanes, slow gradient 3%, 5%, 10%, 15%, 20%, 22%) yielded partial separation of the two diastereoisomers. The diastereomeric mixture was separated using prep TLC (Hex/EtOAc 88:12) to yield the two diastereomers **141a** and **141b** as colorless oils.

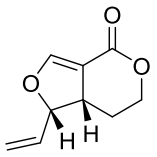

cis

Major (*cis*) 5/6 fused lactone diastereoisomer 141a:

R_f = 0.47(hex/EtOAc, 3:2 UV, $KMnO_4$); **IR** νmax (film): 2992, 2952, 2932, 2884, 2857, 1718, 1645, 1625, 1131, 1064, 835, 777 cm^{-1}; **^{1}H NMR** (500 MHz, $CDCl_3$) δ 7.36 (d, *J* = 2.0 Hz, 1H), 6.05 (ddd, *J* = 17.5, 10.5, 7.0 Hz, 1H), 5.4 (dd, *J* = 17.5, 1.0 Hz, 1H), 5.353 (dd, *J* = 10.5, 1.0 Hz, 1H), 4.86 (dd, *J* = 12.0, 7.0 Hz 1H), 4.50 (ddd, *J* = 12.0, 4.5, 2.5 Hz, 1H), 4.23 (ddd, *J* = 12.0, 12.0, 2.5 Hz, 1H), 3.14 (dddd, *J* = 12.0, 12.0, 4.5, 2.5 Hz, 1H), 2.06 (dddd, *J* = 12.0, 4.5, 2.5, 2.5 Hz, 1H), 1.85 (dddd, *J* = 12.0, 12.0, 12.0, 4.5 Hz, 1H); **^{13}C NMR** (126 MHz, $CDCl_3$) δ 162.5, 157.2, 134.5, 119.6, 108.0, 93.758, 68.8, 44.1, 27.9.; **HR-MS**: *m/z* Calcd for $[C_9H_{10}O_3+H]^+$ 167.0708, found 167.0712.

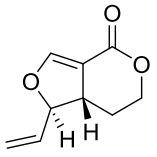

trans

Minor (trans) 5/6 fused lactone diastereoisomer 141b:

R_f = 0.41 (hex/EtOAc, 3:2 UV, $KMnO_4$); **IR** νmax (film): 2992, 2952, 2932, 2884, 2857, 1718, 1645, 1625, 1131, 1064, 835, 777 cm^{-1}; **^{1}H NMR** (500 MHz, $CDCl_3$) δ 7.38 (d, *J* = 2.5 Hz, 1H), 5.78 (ddd, *J* = 17.5, 10.5, 7.0 Hz, 1H), 5.40 (dd, *J* = 10.5, 7.0 Hz, 1H), 5.32 (dd, *J* = 17.5, 7.0 Hz, 1H), 5.30 (dd, *J* = 10.5, 1.0 Hz, 1H), 1H), 4.85 (ddd, *J* = 12.0, 5.0, 2.5 Hz, 1H), 4.23 (ddd, *J* = 12.0, 12.0, 2.5 Hz, 1H), 3.49 (dddd, *J* = 12.0, 10.5, 5.0, 2.5 Hz, 1H), 1.89 (dddd, *J* = 12.0, 5.0, 2.5, 2.5 Hz, 1H),), 1.79 (dddd, *J* = 12.0, 12.0, 12.0, 5.0 Hz, 1H); **^{13}C NMR** (126 MHz, $CDCl_3$) δ 163.3, 156.6, 131.7, 118.6, 88.5, 68.9, 41.2, 25.0.; **HR-MS**: *m/z* Calcd for $[C_9H_{10}O_3+H,]^+$ 167.0708, found 167.0714.

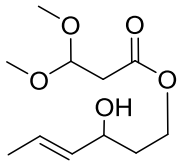

Transesterification product 145: To a flame-dried 100 mL round bottom flask mounted with a water condenser was added (*E*)-hex-4-ene-1,3-diol (947.33 mg, 1.72 mmol, 2.4 equiv.) and methyl 3,3-dimethoxypropanoate (500 mg, 3.37 mmol, 1 equiv.) dissolved in toluene (30 mL). The reaction mixture was heated at reflux (110 °C) for 48 hr. The reaction was found incomplete by TLC analysis (Hexanes/EtOAC 75:25, CAM stain). Nonetheless, the crude was concentrated *in vacuo* and was directly purified on silica gel (Hexanes/EtOAc 100:0, 9:1, 85:15, 8:2, 7:3, 6:4, 1:1, 0:100). The desired compound **145** was isolated as a clear oil (284.0 mg, 1.22 mmol, 36%). **R_f** = 0.19 (hex/EtOAc, 7:3, $KMnO_4$); **IR** νmax (film): 3487, 3470, 3441, 3405, 2971, 2940, 2917, 2833, 1737, 1452,

1380, 1313, 1257, 1169, 1117, 1056, 967, 921, 830 cm^{-1}; **^{1}H NMR** (500 MHz, $CDCl_3$) δ 5.69 (dqd, *J* = 15.0, 6.5, 1 Hz, 1H), 5.49 (d, *J* = 15.0, 7.0, 1.5 1H), 4.82 (t, *J* = 6.0 Hz, 1H), 4.30 (m, 1H), 4.15 (m, 1H), 3.36 (s, 6H), 2.65 (d, *J* = 6.0 Hz, 1H), 1.88 (d, *J* = 4.0 Hz, 1H), 1.84 (*J* = 6.5 Hz, 1H, AB system), 1.84 (*J* = 6.5 Hz, 1H, AB system), 1.69 (ddd, *J* = 6.5, 1.5, 1.0 Hz, 3H); **^{13}C NMR** (126 MHz, $CDCl_3$) δ 169.9, 133.4, 126.9, 101.16, 69.47, 61.67, 53.3 (3C), 53.3 (3C), 38.8, 36.0, 17.5.; **HR-MS**: *m/z* Calcd for $[C_{11}H_{20}O_5+Na]^+$ 255.1208, found 255.1203.

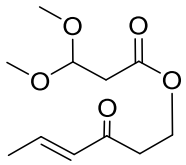

Enone 142: In a 100 mL round bottom flask under argon, transesterification product **144** (581.20 mg, 2.50 mmol. 1 equiv.) was dissolved in CH_2Cl_2 (20 mL) and water (90.1 mg, 5.0 mmol, 2 equiv). Dess Martin periodinane (1.59 g, 3.75 mmol, 1.5 equiv.) was added at room temperature. TLC after 60 minutes showed almost complete conversion. 0.2 additional equiv. of DMP were introduced. After 15 minutes, the reaction was found to be complete by TLC analysis (hexanes/EtOAc 7:3, CAM stain). Reaction was quenched with sodium bicarbonate (20 ml), saturated $Na_2S_2O_3$ (20 mL), then extracted with CH_2Cl_2 (3x40 mL), and was finally washed with brine. The organic extracts were dried over sodium sulfate, filtered, and concentrated *in vacuo*. Purification on silica gel (hexanes/EtOAc 95:5, 9:1, 4:1, 7:3, 6:4, 1:1) yielded the desired product **142** (457 mg, 1.98 mmol, 79%) as a colorless oil. **R_f** = 0.25 (hex/EtOAc, 7:3, $KMnO_4$); **IR** νmax (film): 2959, 2909, 2835, 1736, 1674, 1631, 1443, 1379, 1314, 1255, 1190, 1170, 1116, 1054, 1021,

921, 839 cm^{-1}; **^{1}H NMR** (500 MHz, $CDCl_3$) δ 6.88 (dq, *J* = 15.5, 7.0 Hz, 1H), 6.14 (dq, *J* = 15.5, 1.5 Hz, 1H), 4.80 (t, *J* = 6.0 Hz, 1H), 4.41 (t, *J* = 6.5 Hz, 2H), 3.35 (s, 6H), 2.88 (t, *J* = 6.5 Hz, 2H), 2.63 (d, *J* = 6.0 Hz, 2H), 1.92 (dd, *J* = 7.0, 1.5 Hz, 3H); **^{13}C NMR** (126 MHz, CDCl3) δ 196.7, 169.6, 143.6, 131.8, 101.1, 59.7 (2C), 53.4, 38.7, 38.2, 18.2;**HR-MS**: *m/z* Calcd for $[C_{11}H_{18}O_5+Na]^+$ 253.1052, found 253.1051.

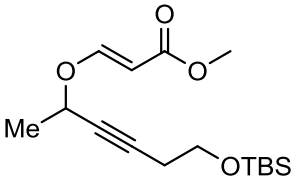

TBS-protected propargyl vinyl ether 152. Adapted from a literature procedure:[165] To a flame-dried 50 mL round bottom flask under argon, 6-[tert-butyl(dimethyl)silyl]oxyhex-3-yn-2-ol[136] (346.2 mg, 1.5 mmol, 1 equiv.) was added which was followed by addition of dry CH_2Cl_2 (12 mL). At room temperature, methyl prop-2-ynoate (127.8 mg, 1.5 mmol, 135 μL, 1 equiv.) was introduced, which was immediately followed by tributylphosphine (61.5 mg, 304.0 umol, 75 μL, 0.2 equiv.). The reaction turned red and was left stirring at room temperature for 12 h. TLC (Hex/EtOAc 85:15, $KMnO_4$) and crude ^{1}H NMR analysis showed complete conversion of the starting alcohol. The reaction was concentrated in *vacuo* and was purified on silica gel (Hex/EtOAc 98:2, 95:5, 9:1, 8:2) to yield the desired vinyl ether **152** (448 mg, 1.4 mmol, 94%) as a colorless oil. **R_f** = 0.24 (hex/EtOAc 95:5, UV, $KMnO_4$); **IR** νmax (film): 2992, 2952, 2932, 2884, 2857, 1718, 1645, 1625, 1131, 1064, 835, 777 cm^{-1}; **^{1}H NMR** (500 MHz, $CDCl_3$) δ 7.59 (d, *J* = 12.5 Hz, 1H), 5.35 (d, *J* = 12.5, 1H), 4.66 (qt, *J* = 6.5, 2 Hz, 1H), 3.71 (t, *J* = 7.0 Hz, 2H), 3.70 (s, 3H), 2.43 (td, *J* = 7.0, 2.0 Hz, 2H), 1.5 (d, *J* = 6.5 Hz, 3H), 0.89 (s, 9H), 0.07 (s, 6H); **^{13}C NMR** (100 MHz,

$CDCl_3$) δ 168.1, 160.4, 98.3, 85.2, 78.5, 67.9, 61.5, 51.0, 25.8 (3C), 23.0, 22.1, 18.3, -5.3 (2C); **HR-MS**: *m/z* Calcd for $[C_{16}H_{28}O_4Si+H]^+$ 313.1835, found 313.1834.

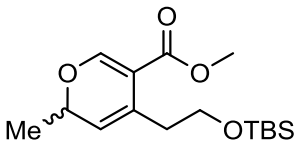

TBS-protected *2H*-pyran 153. To a 10 mL round bottom flask flame-dried under argon, methyl (*E*)-3-[5-[tert-butyl(dimethyl)silyl]oxy-1-methyl-pent-2-ynoxy]prop-2-enoate **151** (104.0 mg, 332.8 μmol, 1 equiv.) was dissolved in dry CH_2Cl_2 (2 mL). Gold (I) chloride (5.05 mg, 16.64 μmol, 5 mol%, obtained from Strem) was added, and the reaction was heated at 30 °C for 2.5 h after which time TLC analysis showed complete conversion and crude ^{1}H NMR analysis of an aliquot showed full conversion to the allene intermediate **153**.

At room temperature, DBU (2.5 mg, 16.6 μmol, 2.5 μL, 5 mol%) was added to the reaction mixture in one portion. The reaction was stirred for 3 hours, after which time ^{1}H NMR of an aliquot showed complete conversion from the allene to the *2H*-pyran. The crude product was directly concentrated and purified on silica gel (Hex/EtOAc 97:3, 95:5, 90:10) to afford the desired product **153** as a colorless oil (78 mg, 249.6 mmol, 75%). This compound was found to decompose upon storage on the benchtop overnight, but could be stored for longer periods in a -20 °C or -40 °C freezer. $\mathbf{R_f}$ = 0.35 (Hex/EtOAc 95:5, UV, $KMnO_4$); **IR** νmax (film): 3025, 2983, 2969, 2928, 2891, 2859, 1716, 1437, 1256, 1099, 835, 776 cm^{-1}; **^{1}H NMR** (500 MHz, $CDCl_3$) δ 7.44 (s, 1H), 5.06 (ddd overlap, *J* = 1.5, 1.5, 1.0 Hz, 1H), 4.82 (, *J* = 6.5, 1.0 Hz, 1H), 3.70 (s, 3H), 3.66 (t, *J* = 6.5 Hz, 2H), 2.68 (qt app, *J* = 6.5, 6.5, 7.0, 1.5 Hz , 1H, AB system), 2.61 (qt app, *J* = 6.5, 6.5, 7.0, 1.5 Hz , 1H, AB system), 1.39 (d, *J* = 6.5 Hz); **^{13}C NMR** (125 MHz, $CDCl_3$) δ 166.1, 157.1, 130.1, 118.1,

109.1, 73.3, 62.4, 51.0, 36.1, 25.9(2C), 20.6, 18.3, -5.3(3C); **HR-MS**: *m/z* Calcd for $[C_{16}H_{28}O_4Si+H]^+$ 313.1835, found 313.1835.

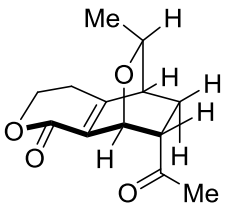

Cycloadduct 162: In a flame-dried thick wall microwave vial under nitrogen, methyl vinyl ketone (8.4 mg, 120.4 μmol, 1 equiv.) and *2H*-pyran **115** (20.0 mg, 120.4 μmol, 1 equiv.) were dissolved in anhydrous toluene (2 mL) and heated overnight at 90°C for 12 h. Concentration *in vacuo* followed by purification on silica gel (hexanes/EtOAc, 95:5, 9:1, 8:2, 3:7, 4:6, 1:1, 3:7, 0:100) yielded the cycloadduct **162** as an oil (28.3 mg, 46.6 μmol, 38%, *endo*/*exo* dr 4:1 by ^{1}H NMR,). The *endo* structure of the major product was confirmed by 2D NMR analysis (COSY, ^{13}C, HSQC, HMBC, NOESY). **R_f** = 0.08 (Hex/EtOAc 1:1, UV, $KMnO_4$); **IR** νmax (film): 2968, 2927, 2871, 1708, 1466, 1414, 1375, 1361, 1279, 1268, 1248, 1203, 1174, 1152, 1107, 1077, 1010, 968, 907 cm^{-1}; **^{1}H NMR** (500 MHz, $CDCl_3$) δ 5.21 (d, *J* = 3 Hz, 1H), 4.43 (m, 2H), 4.01 (qd, *J* = 6, 1.5 Hz, 1H), 3.34 (m, 1H), 2.70 (ddd, *J* = 14 Hz, 1H, AB system), AB system, 4.00 (m, 1H), 3.34 (m, 1H), 2.71 (qd, *J* = 18.5, 7, 5.5 Hz, 1H), 2.68 (m, 1H), 2.49(ddd, *J* = 18.5, 7, 5.5 Hz, 1H), 2.23 (s, 3H), 2.08 (ddd, *J* = 13, 5, 3 Hz, 1H), 1.72 (ddd, *J* = 13, 9, 3 Hz, 1H), 0.95 (d, *J* = 6 Hz, 1H) ; **^{13}C NMR** (125 MHz, $CDCl_3$) δ 205.5, 161.0, 158.2, 127.4, 71.7, 66.4, 65.1, 51.7, 40.9, 29.3, 27.5, 23.5, 21.6; **HR-MS**: *m/z* Calcd for $[C_{13}H_{16}O_4+H]^+$ 237.1049, found .

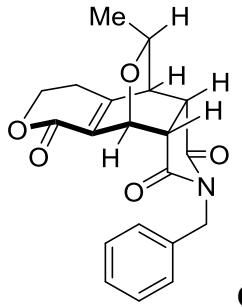

Cycloadduct 163: In a flame-dried thick wall microwave vial under nitrogen, 1-benzylpyrrole-2,5-dione (33.79 mg, 180.54 μmol, 1 equiv.) and *2H*-pyran **115** (30.00 mg, 180.54 μmol, 1 equiv.) were dissolved in anhydrous toluene (2 mL) and heated at 90 °C for 12 h. Concentration *in vacuo* followed by purification on silica gel (hexanes/EtOAc, 95:5, 9:1, 8:2, 3:7, 4:6, 1:1, 3:7, 0:100) yielded the cycloadduct **163** as an amorphous solid (22.5 mg, 63.7 μmol, 35%, *endo*/*exo* dr 6:1 by ^{1}H NMR). The *endo* structure of the major product was confirmed by 2D NMR analysis (COSY, ^{13}C, HSQC, HMBC, NOESY). $\mathbf{R_f}$ = 0.10 (Hex/EtOAc 1:1, UV, $KMnO_4$); **IR** νmax (film): 2955, 2925, 2853, 1773, 1700, 1604, 1496, 1466, 1412, 1396, 1345, 1280, 1172, 1152, 1076, 909, 733 cm^{-1}; **^{1}H NMR** (500 MHz, C_6D_6) δ 7.29 (dd, *J* = 7.5, 1.0 Hz, 2H), 7.03 (dd, *J* = 7.5, 7.5 Hz, 2H), 6.96 (dd, *J* = 7.5, 1.0 Hz, 1H), 5.45 (d, *J* = 4.5 Hz, 1H), 4.33 (d, *J* = 14 Hz, 1H, AB system), 3.99 (d, *J* = 14 Hz , 1H, AB system), 3.30 (m, 1H), 3.24 (qd, *J* = 6.5, 1.0 Hz, 1H), 2.72 (dd, *J* = 8.0, 4.5 Hz, 1H), 2.68 (m, 1H), 2.31(dd, *J* = 4.0, 1.0 Hz, 1H), 2.07 (dd, *J* = 8.0, 4.0 Hz, 1H), 1.30 (m, 2H), 0.42 (d, *J* = 6.5 Hz, 3H); **^{13}C NMR** (125 MHz, $CDCl_3$) δ 176.1, 173.8, 159.4, 154.4, 135.7, 129.2 (2C), 128.9 (2C), 128.3, 128.3, 70.0, 65.3, 64.3, 44.4, 42.5, 42.2, 40.4, 27.7, 21.0.; **HR-MS**: *m/z* Calcd for $[C_{20}H_{19}O_5N+H]^+$ 354.1263, found 354.1267.

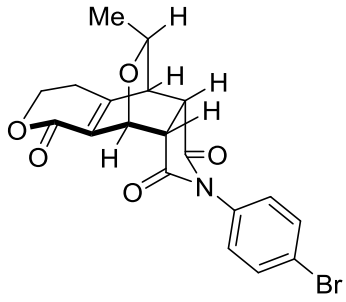

Cycloadduct 164: In a flame-dried thick wall microwave vial under nitrogen, 1-(4-bromophenyl)pyrrole-2,5-dione (62.6 mg, 248.4 μmol, 1.2 equiv.) and *2H*-pyran **115** (34.4 mg, 207.0 μmol, 1 equiv.) were dissolved in toluene (2 mL) and heated at 90 °C for 12 h. Concentration *in vacuo* followed by purification on silica gel (hexanes/EtOAc, 95:5, 9:1, 8:2, 3:7, 4:6, 1:1, 3:7, 0:100) yielded the cycloadduct **164** as an amorphous solid-oil (29.7 mg, 71 μmol, 34%, *endo*/*exo* dr 10:1 by ^{1}H NMR). The *endo* structure of the major product was confirmed by 2D NMR analysis (COSY, ^{13}C, HSQC, HMBC, NOESY). **R_f** = 0.24 (Hex/EtOAc 3:2, UV, $KMnO_4$); **IR** νmax (film): 3482, 3058, 2971, 2902, 1779, 1713, 1490, 1412, 1381, 1278,1224, 1182, 1152, 1037, 815, 774, 734 cm^{-1}; **^{1}H NMR** (500 MHz, $CDCl_3$) δ 7.56 (d, *J* = 9.0 Hz, 2H), 7.00 (d, *J* = 9.0 Hz, 2H), 5.39 (d, *J* = 4.5 Hz, 1H), 4.46 (ddd, *J* = 7.0, 5.5, 5.5 Hz , 1H, AB system), 4.27 (ddd, *J* = 7.0, 5.5, 5.5 Hz, 1H, AB system) 4.11 (qd, *J* = 6.0, 1 Hz, 1H), 3.65 (dd, *J* = 8.0, 4.5 Hz, 1H), 3.38 (dd, *J* = 8.0, 3.5 Hz, 1H) 3.36 (dd, *J* = 3.5, 1.0 Hz, 1H), 2.56 (ddd, *J* = 7.0, 5.5, 5.5 Hz, 1H), 2.53 (ddd, *J* = 7.0, 5.5, 5.5 Hz, 1H), 1.06 (d, *J* = 6.0 Hz, 3H); **^{13}C NMR** (101 MHz, $CDCl_3$) δ 175.2, 172.6, 159.6, 155.3, 132.5, 132.4 (2C), 130.1, 127.3 (2C), 122.8, 70.1, 66.2, 64.7, 44.5, 42.4, 41.1, 28.3, 21.2.; **HR-MS**: *m/z* Calcd for $[C_{20}H_{19}O_4N+H]^+$ 418.0212, found 418.0294

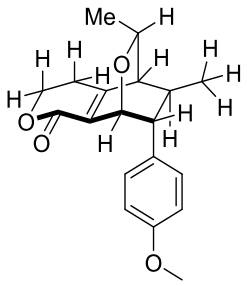

Radical Cation Cycloadduct 171: In a 10 mL Schlenk flask under nitrogen in the dark, *trans*-anethole (10.0 mg, 67.5 μmol, 10 μL, 1 equiv.), *2H*-pyran **115**[111] (33.6 mg, 202.4 umol, 3 equiv.), and 2,4,6-triphenylpyrylium tetrafluoroborate (1.3 mg, 3.5 μmol, 5 mol%) were introduced. Dry, thoroughly degassed CH_2Cl_2 (1.5 mL) (*via* freeze-pump-thaw cycle 3 times) was added and the flask was irradiated at 450 nm (Blue LEDs) in a water cooled jacketed beaker at room temperature for 12 h. TLC analysis (EtOAc/hexanes. 25:75) showed the presence of 4 new products, and complete consumption of *trans*-anethole. The crude was concentrated and carefully purified on silica gel (hex/EtOAc 9:1, 4:1, 7:3, 3:2, 1:1, 2:3, 3, 7, 0:100) to afford the desired cycloadduct (5 mg, 15.9 μmol, 23%) as a yellow oil.

R_f = 0.22 (hex/EtOAc 1:1, UV, $KMnO_4$); **IR** νmax (film): 3965, 2931, 1716, 1611, 1513, 1464, 1410, 1247, 1180, 1035, 994, 811 cm^{-1}; **^{1}H NMR** (500 MHz, $CDCl_3$) δ 6.93 (d, *J* = 9.0 Hz, 2H), 6.78 (d, *J* = 9.0 Hz, 2H), 4.73 (d, *J* = 2.0 Hz, 1H), 4.53 (m, 1H), 4.37 (q, *J* = 6.0 Hz, 1H), 3.75 (s, 3H), 2.87 (dd, *J* = 7.0, 2.0 Hz,1H), 2.83 (dt, *J* = 6.0, 18.0 Hz,1H), 2.61 (dt, *J* = 18.0, 6.0 Hz,1H), 2.42 (s app, 1H), 1.86 (qdd, *J* = 7.0, 7.0, 2.0 Hz, 1H), 1.25 (d, *J* = 7.0 Hz, 3H), 1.00 (d, *J* = 6.0 Hz, 3H); **^{13}C NMR** (125 MHz, $CDCl_3$) δ 161.3, 159.2, 158.4, 133.0, 128.6, 128.4, 114.0, 69.5, 66.3, 64.5, 55.2, 51.8, 48.3, 37.6, 27.9, 21.6, 16.7. **HR-MS**: *m/z* Calcd for $[C_{19}H_{22}O_4+H]^+$ 315.1586, found 315.1589.

Selected Spectra

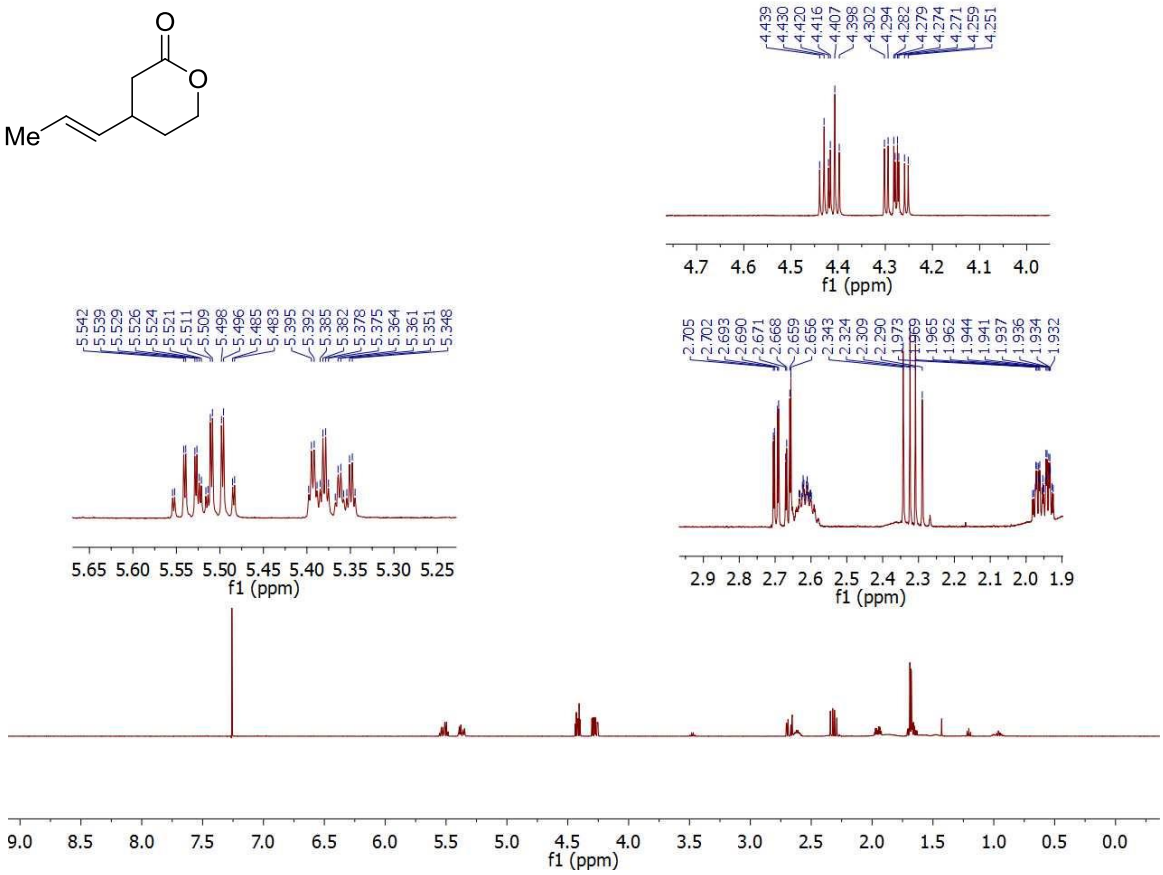

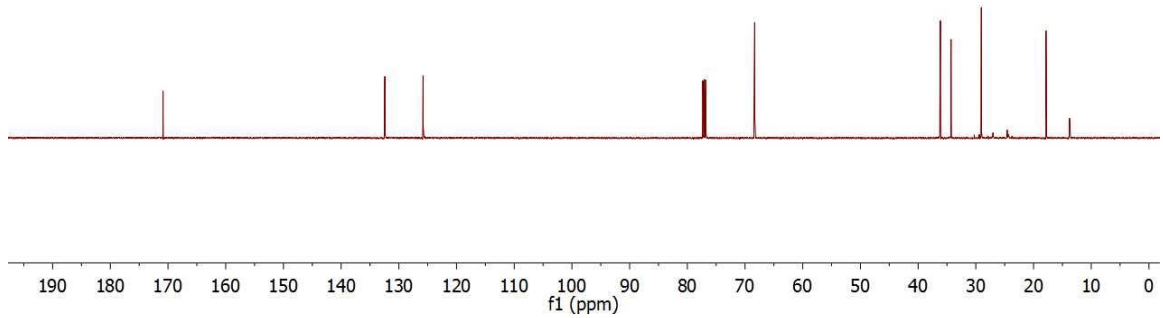

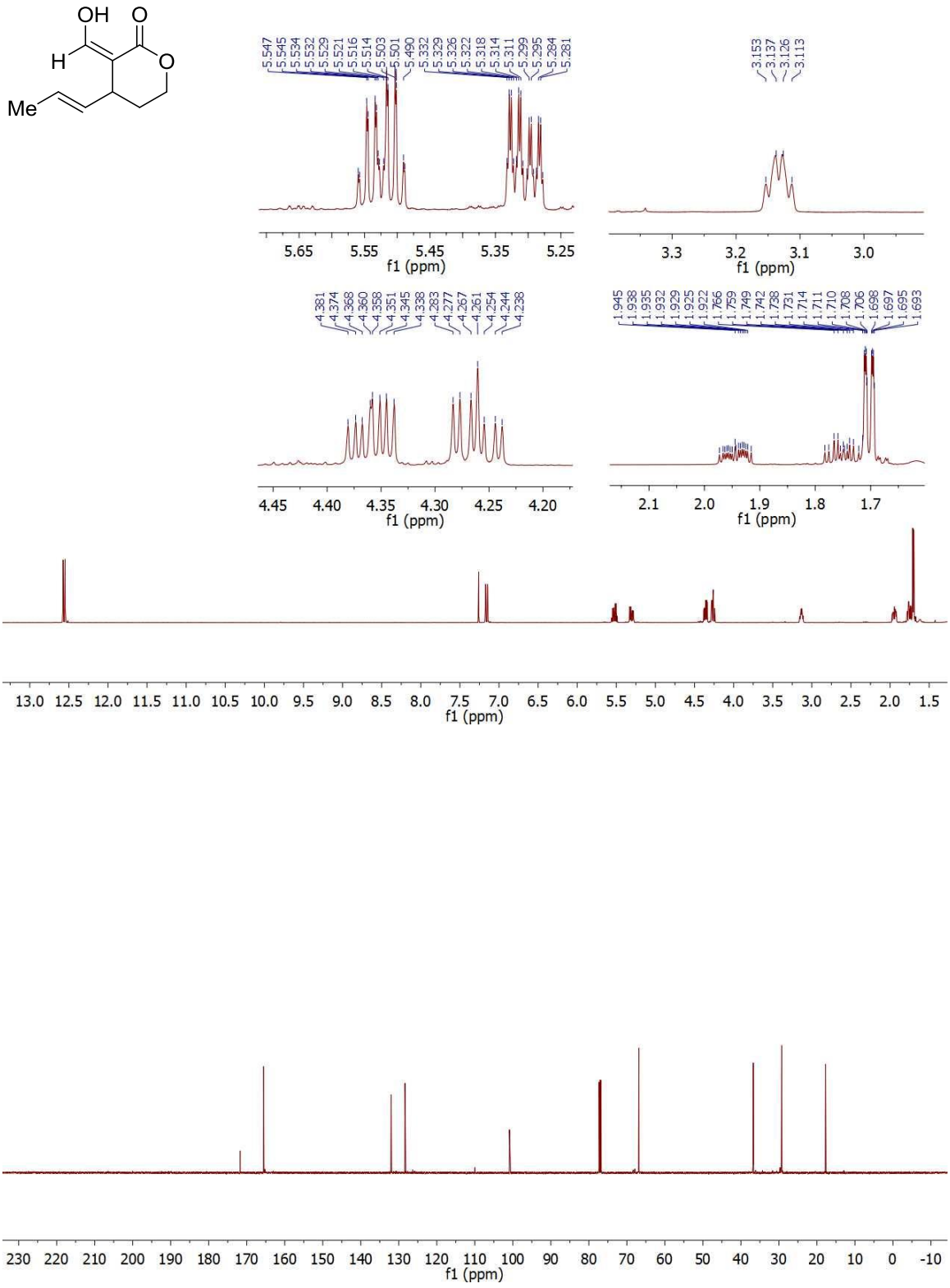
OH
O
H
O
Me
5.547
5.545
5.534
5.532
5.529
5.521
5.516
5.514
5.503
5.501
5.490
5.332
5.329
5.326
5.322
5.318
5.314
5.311
5.299
5.295
5.284
5.281
5.65
5.55
5.45
5.35
5.25
f1 (ppm)
3.153
3.137
3.126
3.113
3.3
3.2
3.1
3.0
f1 (ppm)
4.381
4.374
4.368
4.360
4.358
4.351
4.345
4.338
4.283
4.277
4.267
4.261
4.254
4.244
4.238
4.45
4.40
4.35
4.30
4.25
4.20
f1 (ppm)
1.945
1.938
1.935
1.932
1.929
1.925
1.922
1.766
1.759
1.749
1.742
1.738
1.731
1.714
1.711
1.710
1.708
1.706
1.698
1.697
1.695
1.693
2.1
2.0
1.9
1.8
1.7
f1 (ppm)
13.0 12.5 12.0 11.5 11.0 10.5 10.0 9.5 9.0 8.5 8.0 7.5 7.0 6.5 6.0 5.5 5.0 4.5 4.0 3.5 3.0 2.5 2.0 1.5
f1 (ppm)
230 220 210 200 190 180 170 160 150 140 130 120 110 100 90 80 70 60 50 40 30 20 10 0 -10
f1 (ppm)

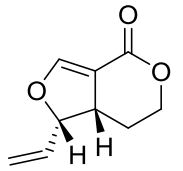
O
O
O
H
H

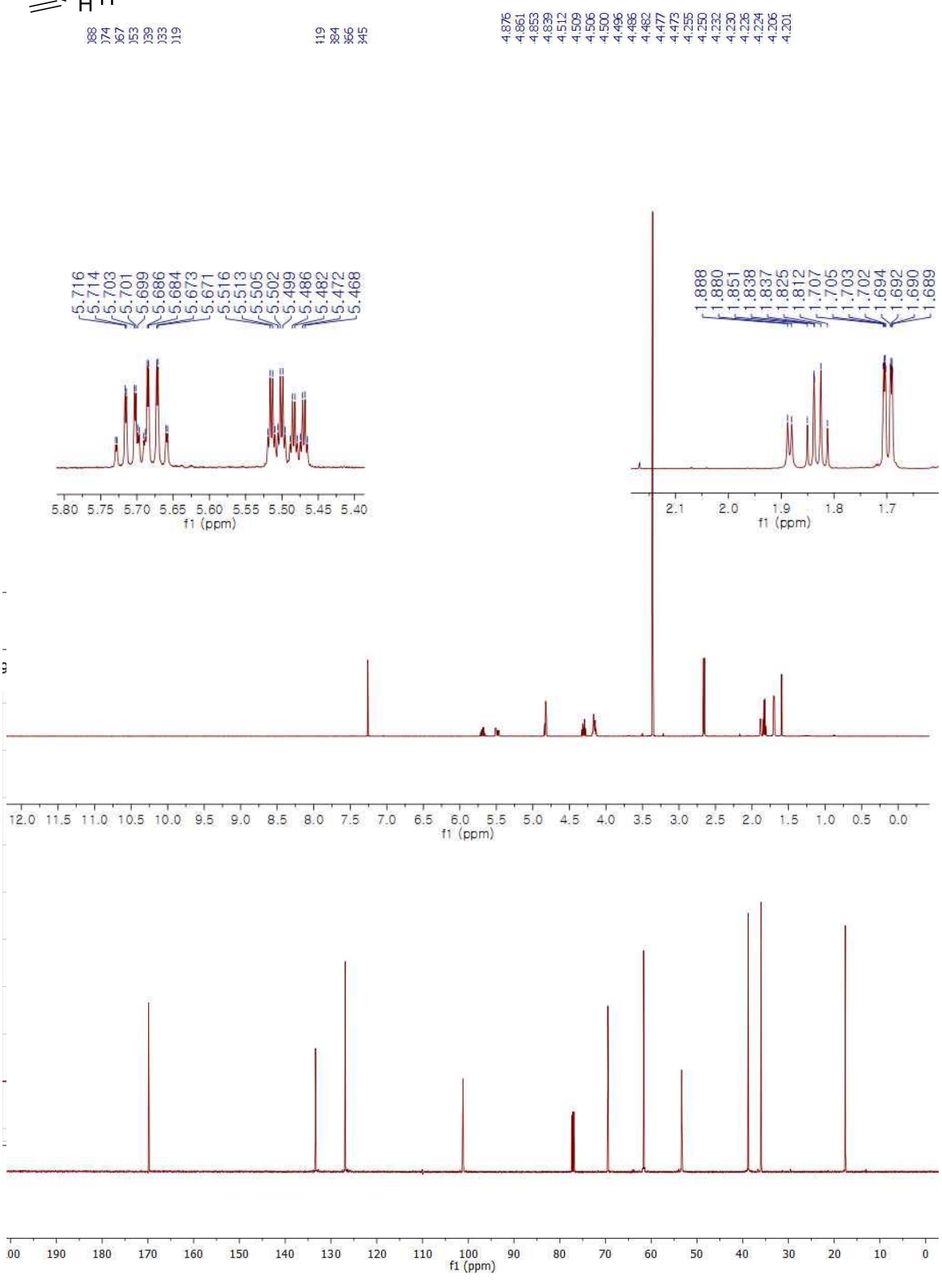
5.716
5.714
5.703
5.701
5.699
5.686
5.684
5.673
5.671
5.516
5.513
5.505
5.502
5.499
5.486
5.482
5.472
5.468
1.888
1.880
1.851
1.838
1.837
1.825
1.812
1.707
1.705
1.703
1.702
1.694
1.692
1.690
1.689
f1 (ppm)
f1 (ppm)
f1 (ppm)
f1 (ppm)

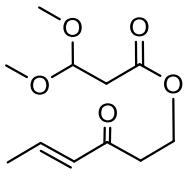

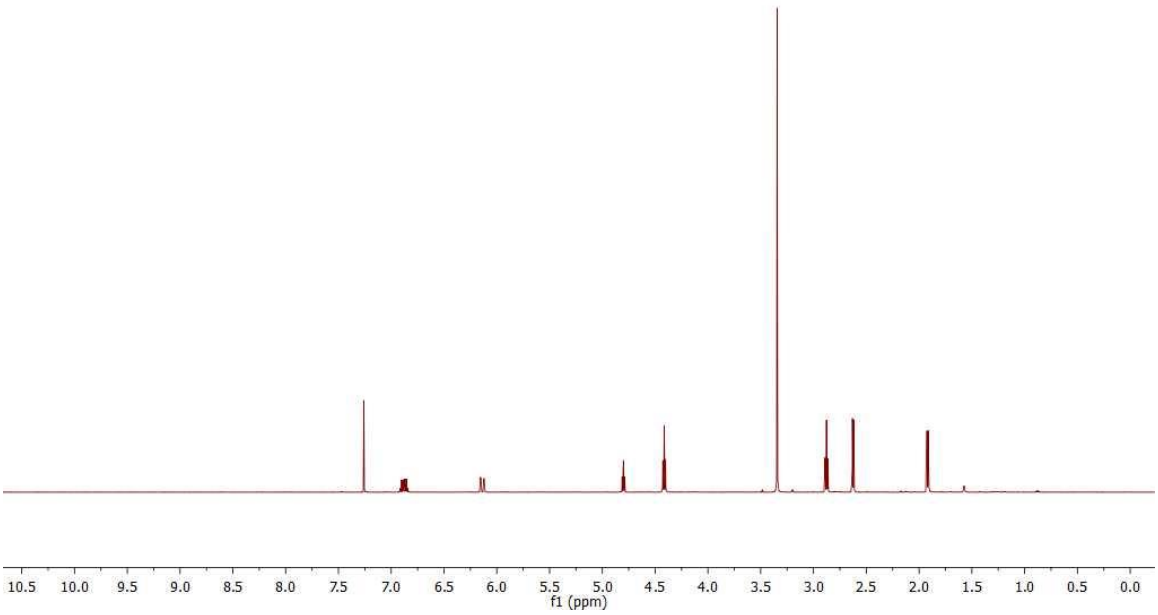
10.5 10.0 9.5 9.0 8.5 8.0 7.5 7.0 6.5 6.0 5.5 5.0 4.5 4.0 3.5 3.0 2.5 2.0 1.5 1.0 0.5 0.0
f1 (ppm)

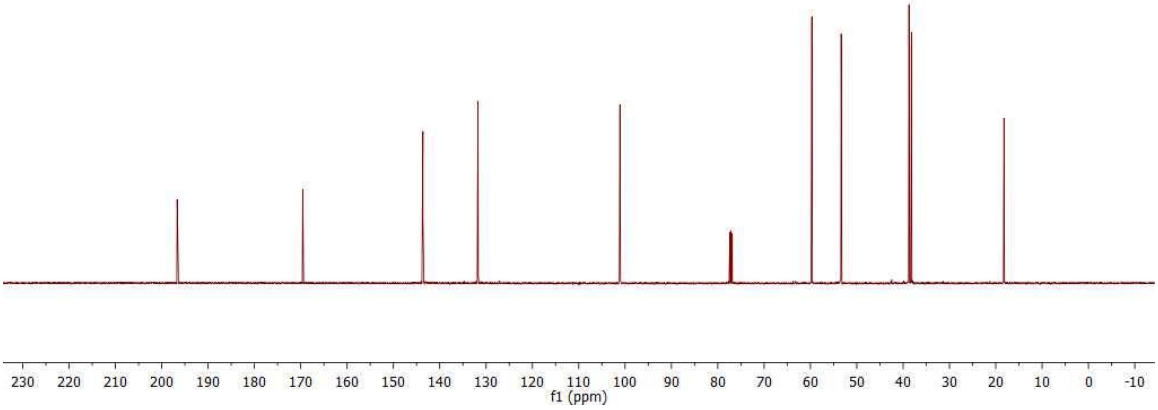
230 220 210 200 190 180 170 160 150 140 130 120 110 100 90 80 70 60 50 40 30 20 10 0 -10
f1 (ppm)

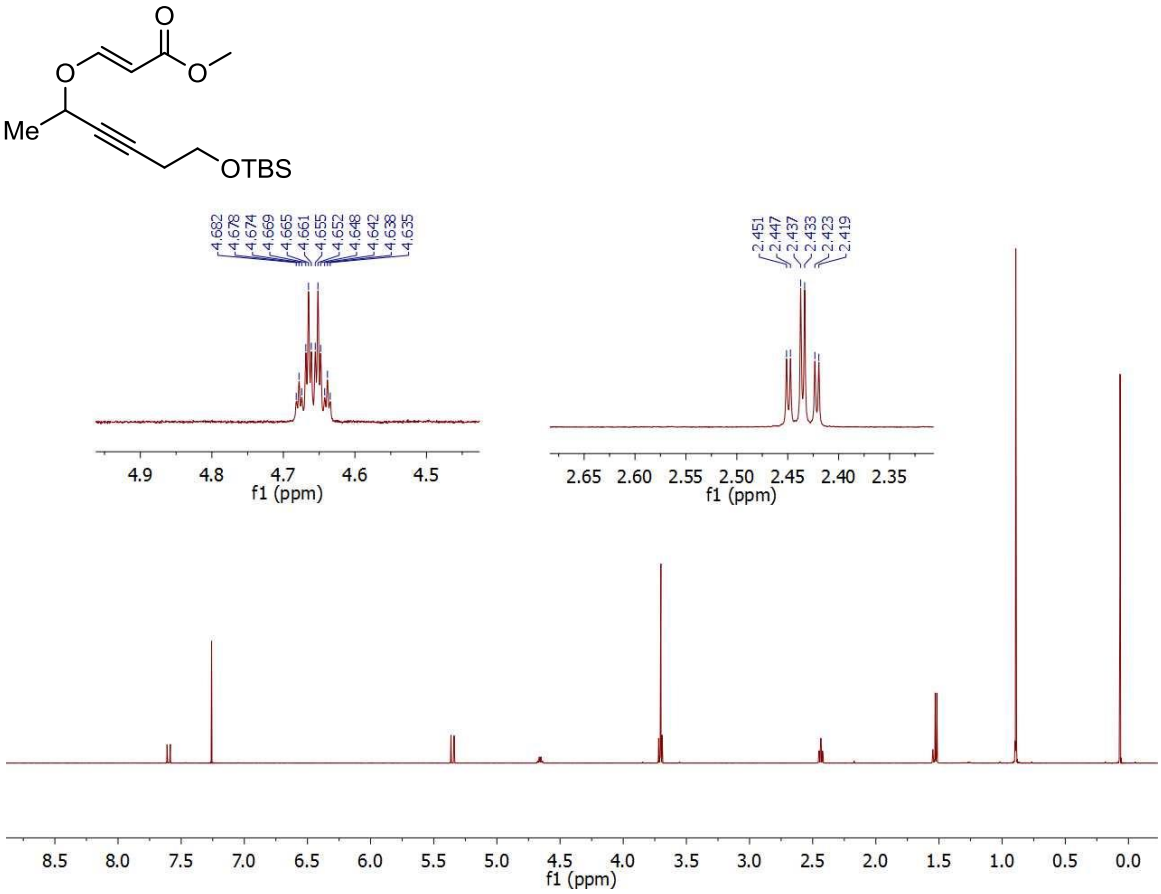
O
O
O
Me
OTBS
4.682
4.678
4.674
4.669
4.665
4.661
4.655
4.652
4.648
4.642
4.638
4.635
2.451
2.447
2.437
2.433
2.423
2.419
4.9 4.8 4.7 4.6 4.5
f1 (ppm)
2.65 2.60 2.55 2.50 2.45 2.40 2.35
f1 (ppm)
8.5 8.0 7.5 7.0 6.5 6.0 5.5 5.0 4.5 4.0 3.5 3.0 2.5 2.0 1.5 1.0 0.5 0.0
f1 (ppm)

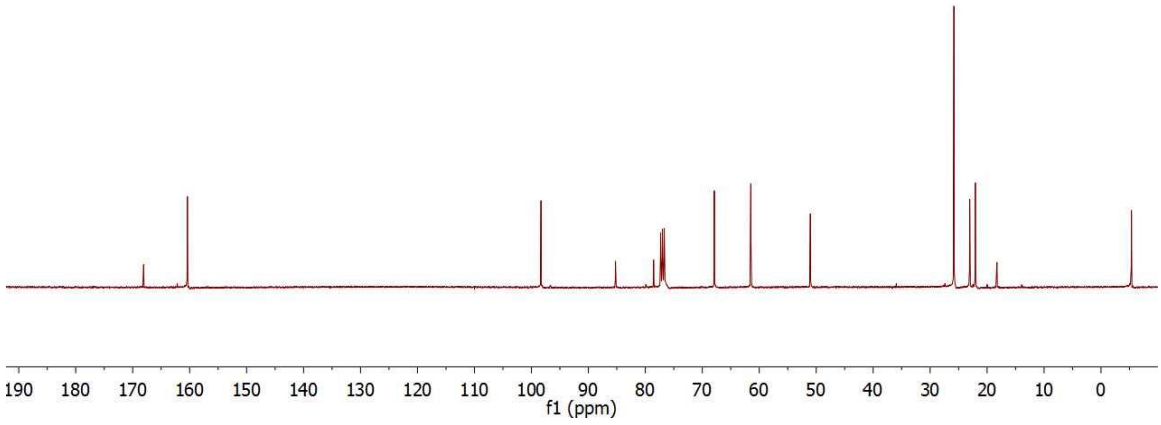
190 180 170 160 150 140 130 120 110 100 90 80 70 60 50 40 30 20 10 0
f1 (ppm)

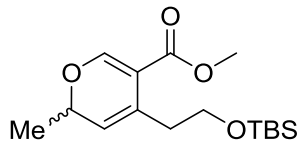
O
O
O
Me
OTBS

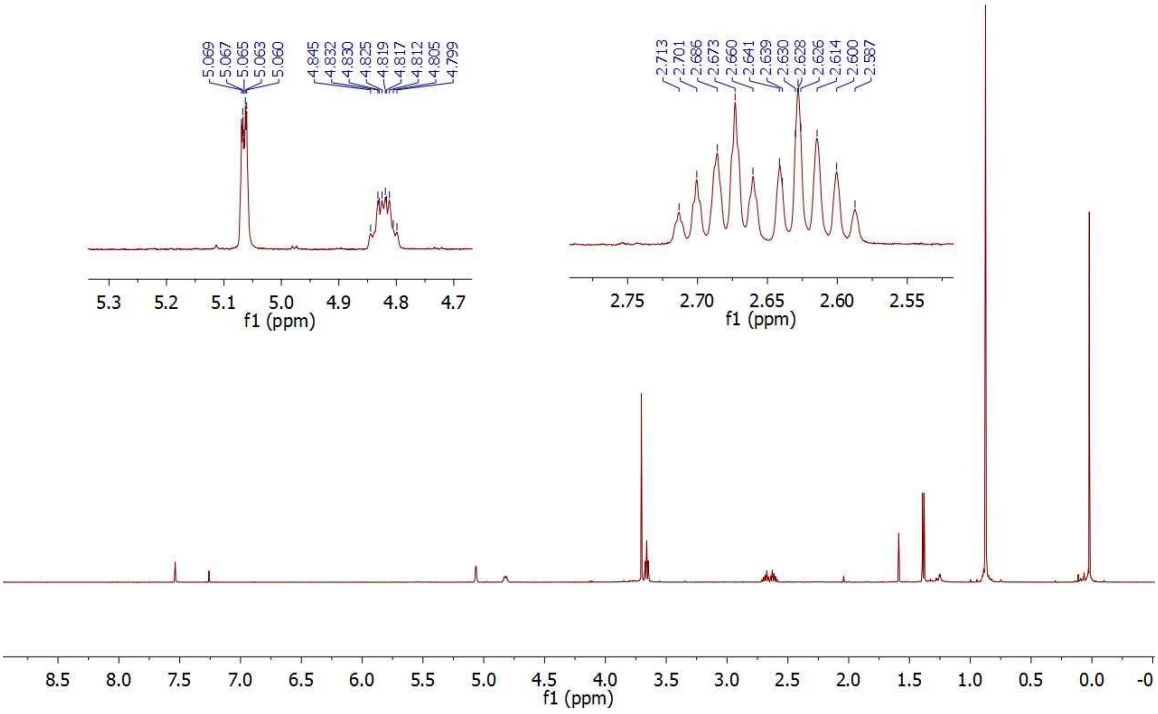
5.069
5.067
5.065
5.063
5.060
4.845
4.832
4.830
4.825
4.819
4.817
4.812
4.805
4.799
2.713
2.701
2.686
2.673
2.660
2.641
2.639
2.630
2.628
2.626
2.614
2.600
2.587
f1 (ppm)
f1 (ppm)
f1 (ppm)

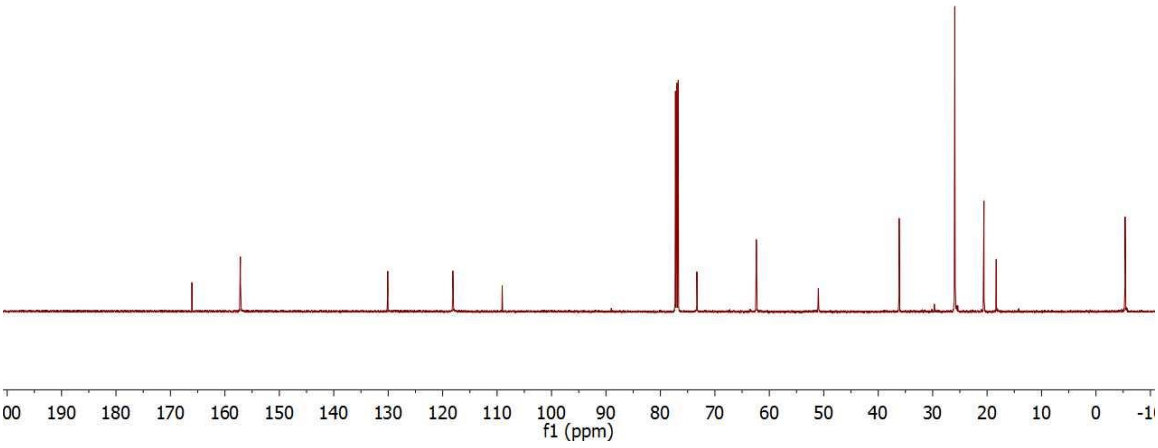
f1 (ppm)

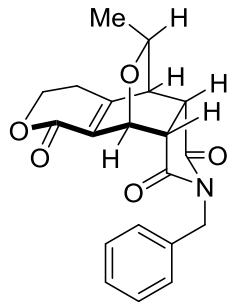
Me
H
O
H
H
H
O
O
H
O
O
N

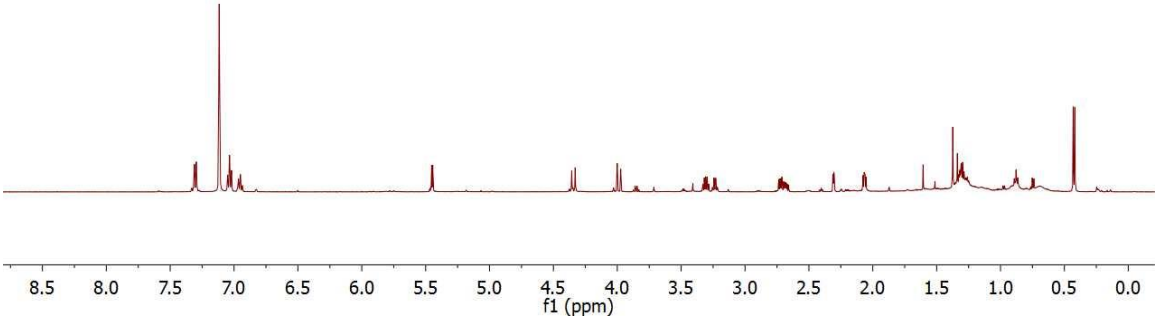
8.5 8.0 7.5 7.0 6.5 6.0 5.5 5.0 4.5 4.0 3.5 3.0 2.5 2.0 1.5 1.0 0.5 0.0
f1 (ppm)

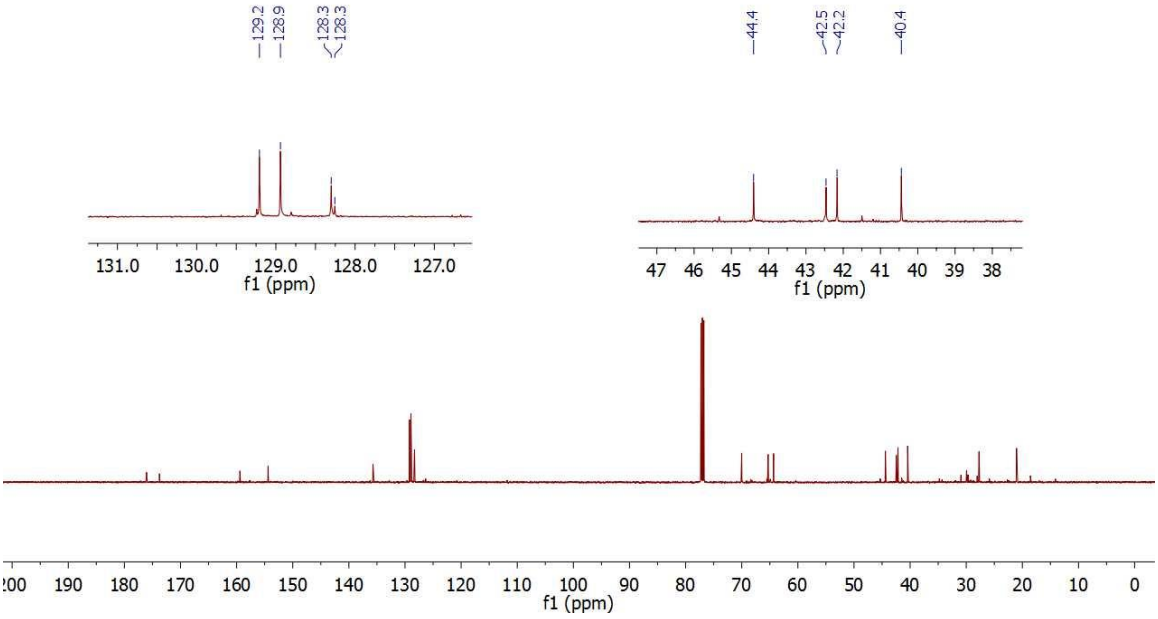
129.2
128.9
128.3
128.3
44.4
42.5
42.2
40.4
131.0 130.0 129.0 128.0 127.0
f1 (ppm)
47 46 45 44 43 42 41 40 39 38
f1 (ppm)
200 190 180 170 160 150 140 130 120 110 100 90 80 70 60 50 40 30 20 10 0
f1 (ppm)

Key NOESY Correlations for *Endo* Adduct **163**

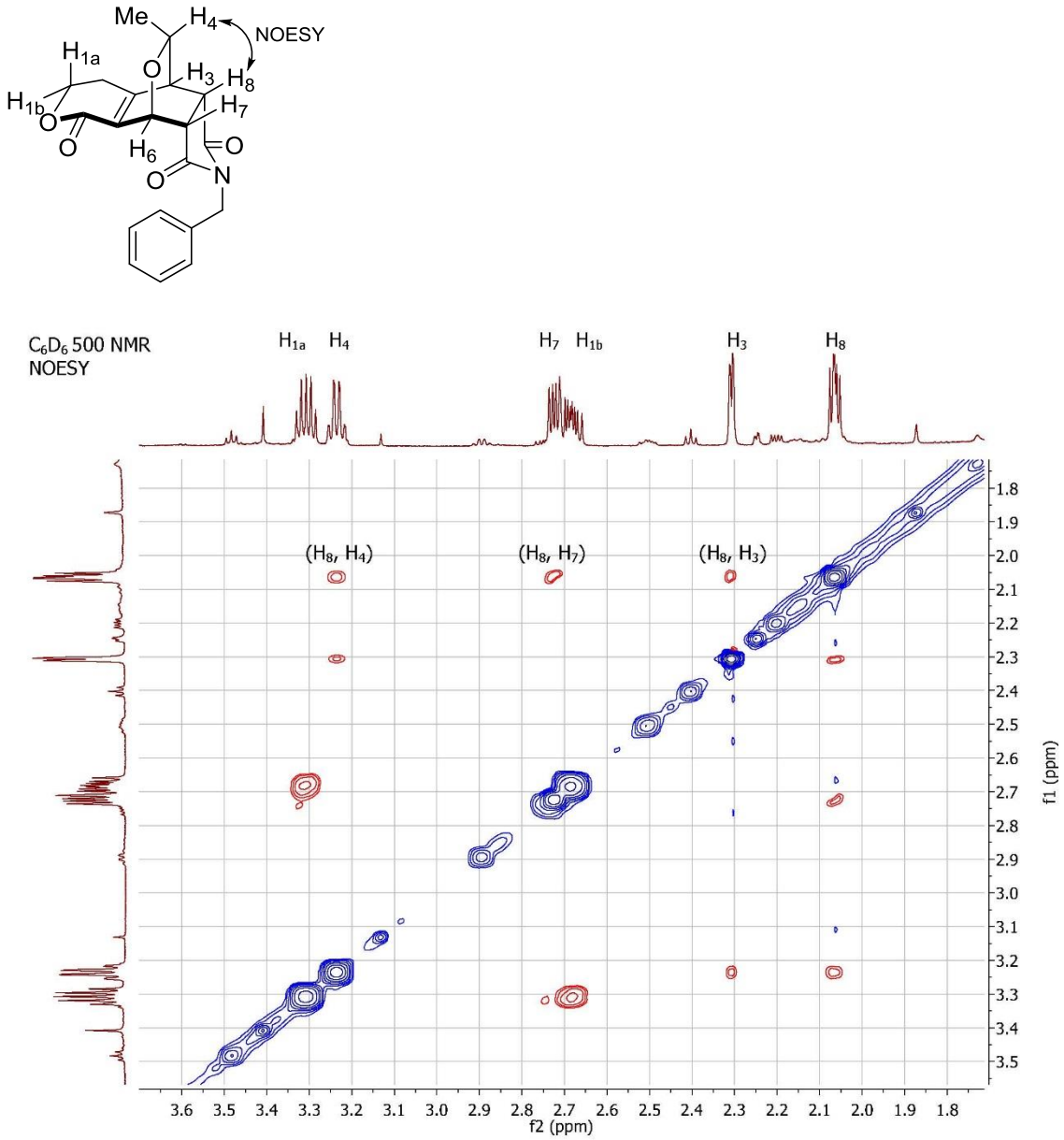

Key HMBC Correlations for *Endo* Adduct **163**

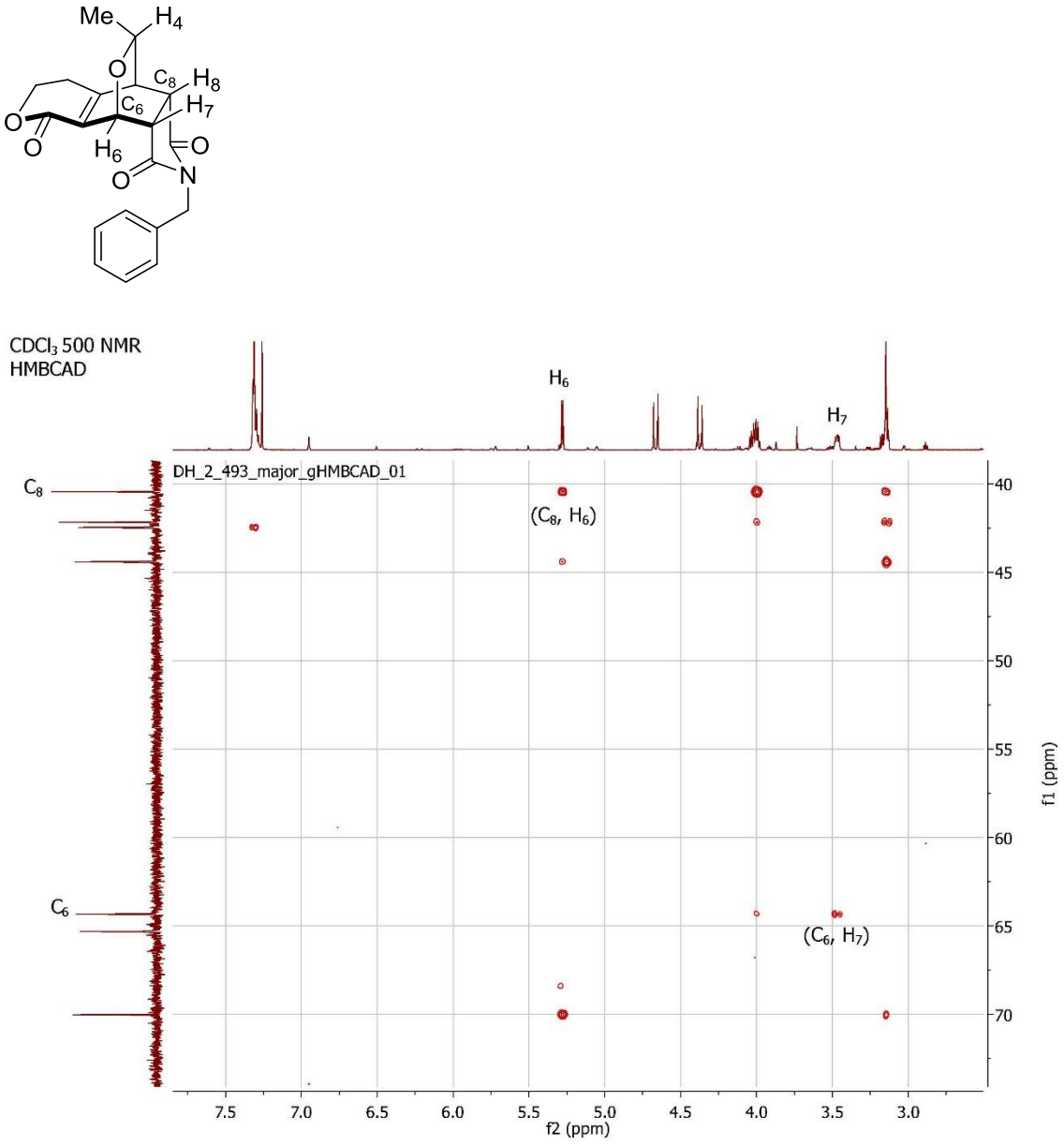

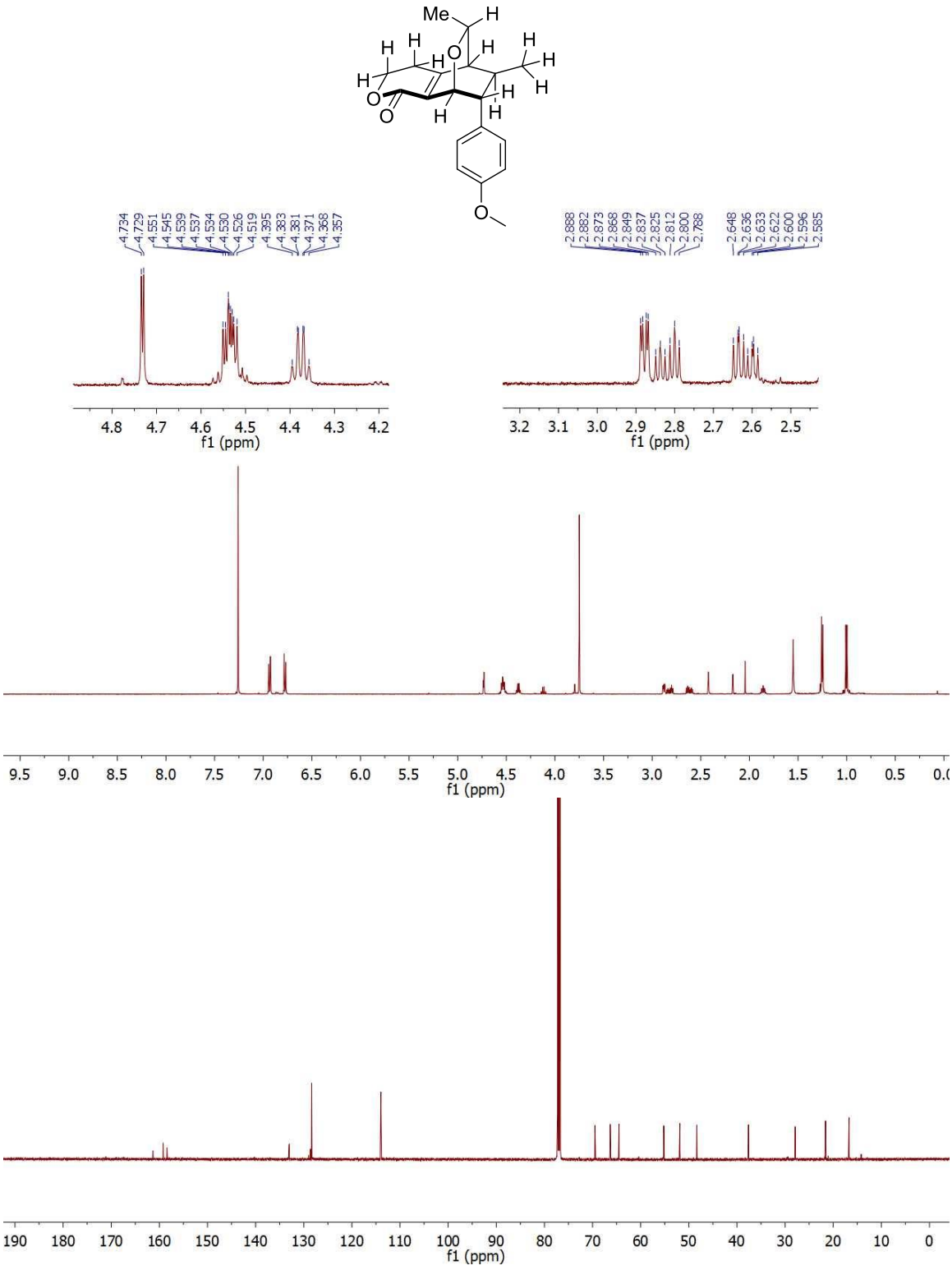
Me
H
H
H
O
H
H
H
H
H
H
O
O
H
H
H
O
4.734
4.729
4.551
4.545
4.539
4.537
4.534
4.530
4.526
4.519
4.395
4.383
4.381
4.371
4.368
4.357
2.888
2.882
2.873
2.868
2.849
2.837
2.825
2.812
2.800
2.788
2.648
2.636
2.633
2.622
2.600
2.596
2.585
4.8 4.7 4.6 4.5 4.4 4.3 4.2
f1 (ppm)
3.2 3.1 3.0 2.9 2.8 2.7 2.6 2.5
f1 (ppm)
9.5 9.0 8.5 8.0 7.5 7.0 6.5 6.0 5.5 5.0 4.5 4.0 3.5 3.0 2.5 2.0 1.5 1.0 0.5 0.0
f1 (ppm)
190 180 170 160 150 140 130 120 110 100 90 80 70 60 50 40 30 20 10 0
f1 (ppm)

Key NOESY Correlations for Cycloadduct **171**

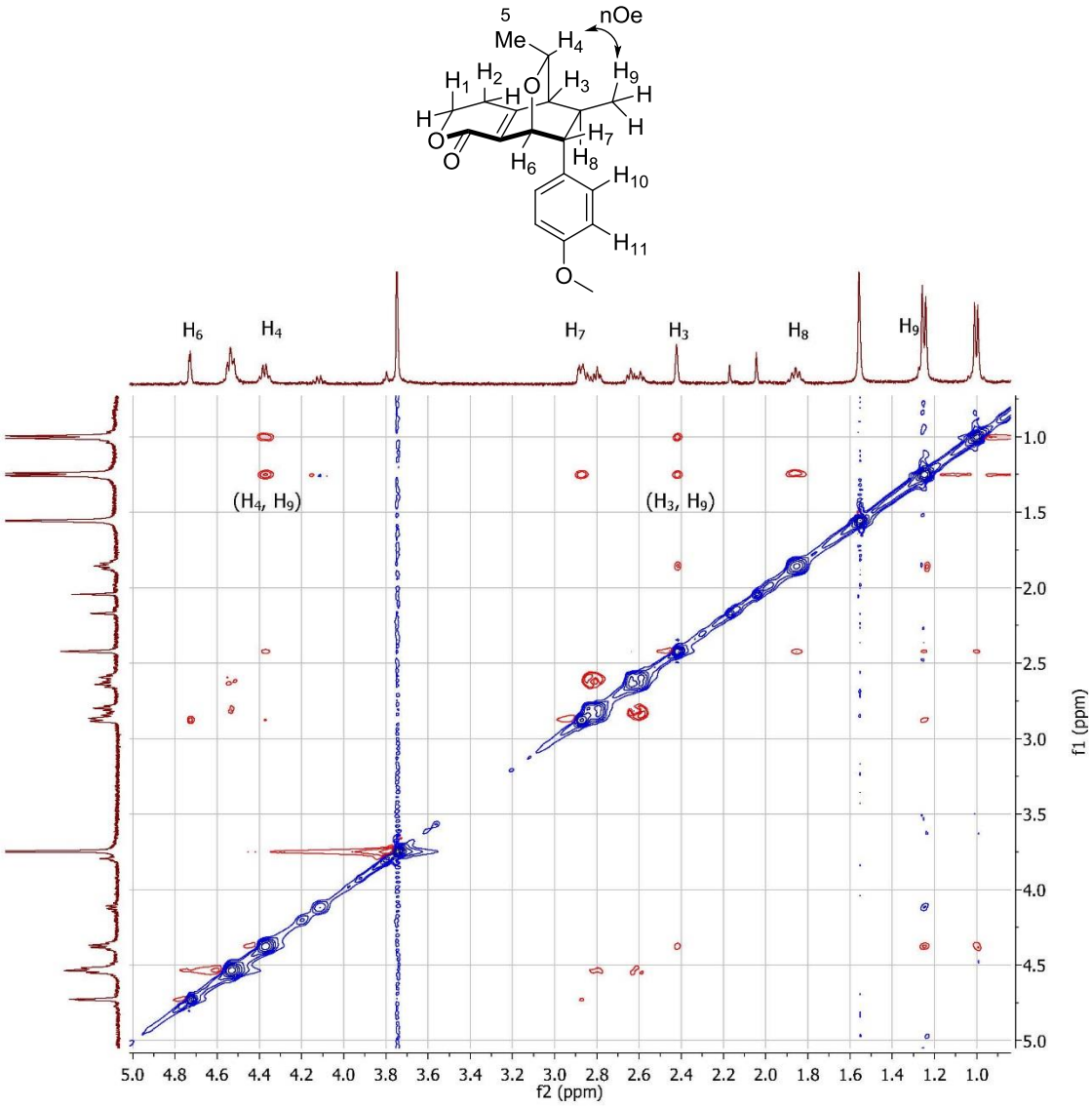

Key NOESY Correlations for Cycloadduct **171**

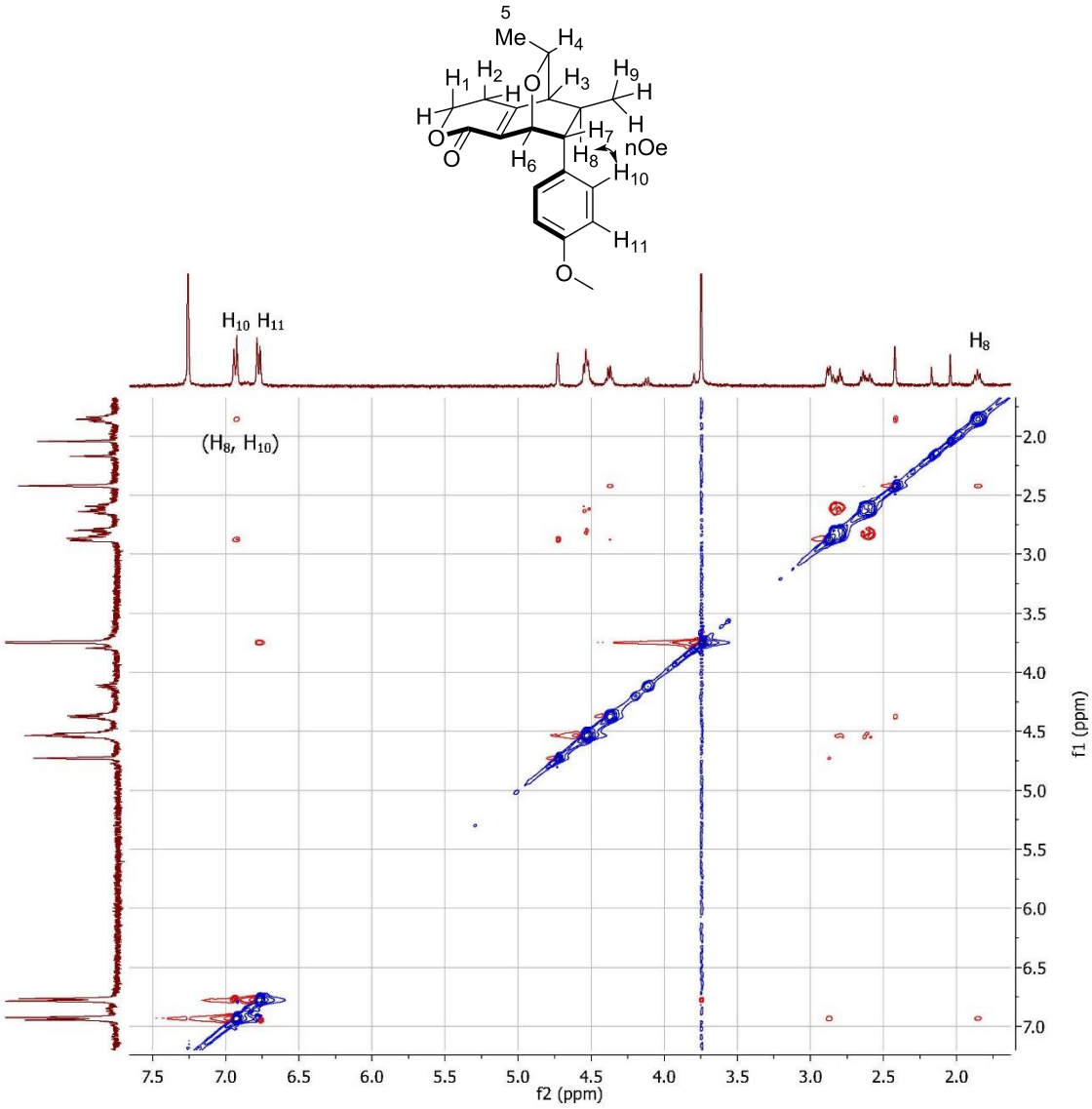

CHAPTER 3

Preparation of Substituted Lactone Dienophiles and Studies toward a Biomimetic Synthesis of Swerilactones A and B

3.1 Introduction

The reactivity of both *2H*-pyran diene **115** and the enol **114** or ketene precursor **122** at the outset of our studies was unknown, and thus, the feasibility of the [4+2] cycloaddition was an open question (**Figure 3.1** for our proposed Diels-Alder cycloaddition approaches).

Figure 3.1 Proposed Cycloadditions of Pyran 115 with Ketene and Enol Dienophiles

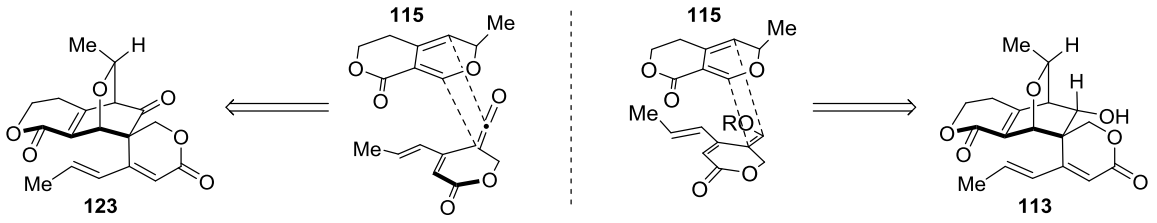

We planned to target a variety of dienophiles for the key formal Diels-Alder cycloaddition to increase our chance of finding an ideal substrate for this reaction (**Figure 3.2** for representative lactone dienophiles).

Figure 3.2 Planned Dienophilic Lactones

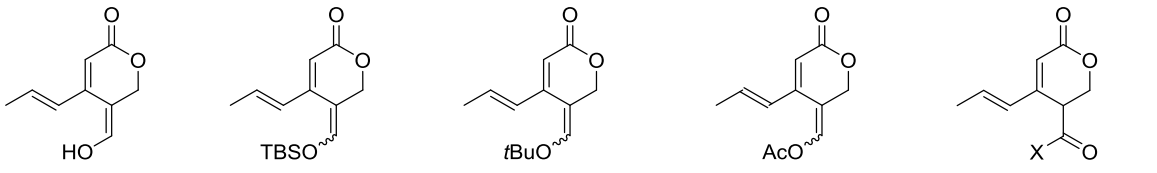

We conceived a viable synthetic pathway *en route* to several lactone-containing dienophiles with an enol or aldehyde functional group at the 4-position such as **114** or **122**, which would be derived from cross-coupling of β-halogenated sorbate **172** with α-stannylated acrylate derivatives such as **173** (**Scheme 3.1**). Diene **172** was envisioned to arise from two pathways: direct C-H halogenation of sorbic acid **174** or stepwise cross-coupling of *gem*-dibromoolefin **175** with propenyl metal reagents **176**.

Scheme 3.1 Retrosynthesis of Substituted Lactone Dienophiles: A Unified Strategy

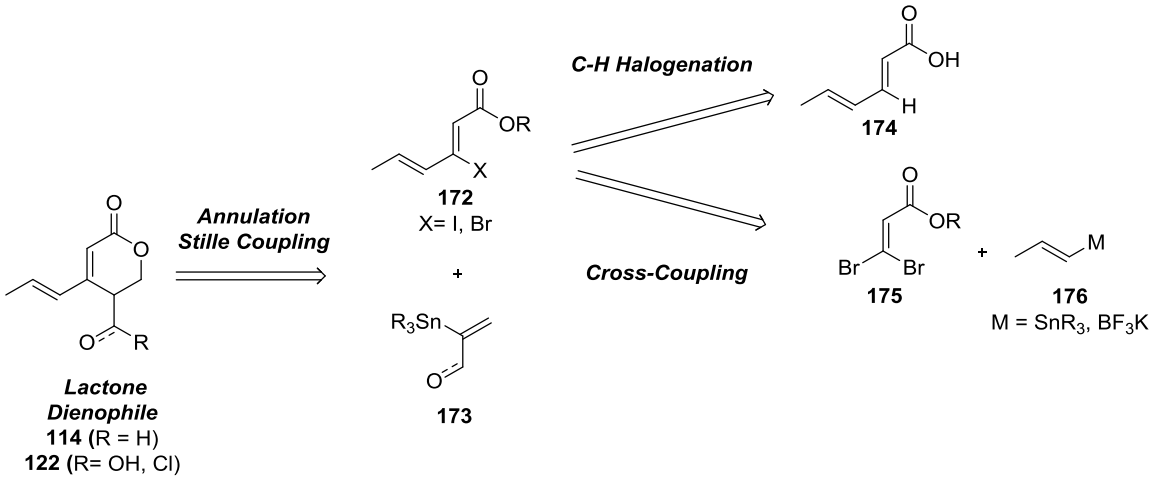

3.2 En route to Lactone Dienophiles: Synthesis of a Key β-Bromo Sorbate Derivative

3.2.1 First Synthetic Route: C-H Activation of Sorbic Acid and Derivatives

The field of C-H activation has greatly expanded over the last several years in terms of scope and application of many directing groups. A large focus of the area is centered on C-H activation of benzoate derivatives[166] and heterocyclic compounds. Prof. Yu and coworkers have pioneered efforts in the C-H halogenation of benzoates using a carboxylate

functionality as a directing group.[167,168] They demonstrated successful C-H iodination of simple benzoates in the presence of Pd(II) and iodonium acetate (**Scheme 3.2 (A)**).[169] Due to their prevalence in medicinal chemistry and synthetic versatility, aryl halides have been targeted by many research groups, and C-H halogenations have been reported using a range of directing groups and metal catalysts including Pd(II),[170–174] Rh(III),[175–179] Ru(II),[180,181] Cu(II),[171] and Co(III).[182]

In contrast, vinylic C-H activations are less precedented[183] and tend to rely on stronger amide directing groups, potentially due to an increased rotational freedom and decreased electron density of vinylic C-H bonds *versus* aryl C-H bonds. Babu and coworkers demonstrated the successful C-H arylation of acrylamides (**Scheme 3.2 (B)**).[184] The Glorius group has shown examples of C-H halogenation of vinyl amides[179] along with the C-H alkynylation of diisopropyl amide protected sorbate and cinnamates;[185] the latter efficiently proceeding in the presence of Rh(III) and excess 1-[(triisopropylsilyl)ethynyl]-1,2-benziodoxol-3(1H)-one (TIPS-EBX) (**Scheme 3.2 (C)).**

Scheme 3.2 Literature Examples of C-H activation of Benzoates and Vinylogous Amides

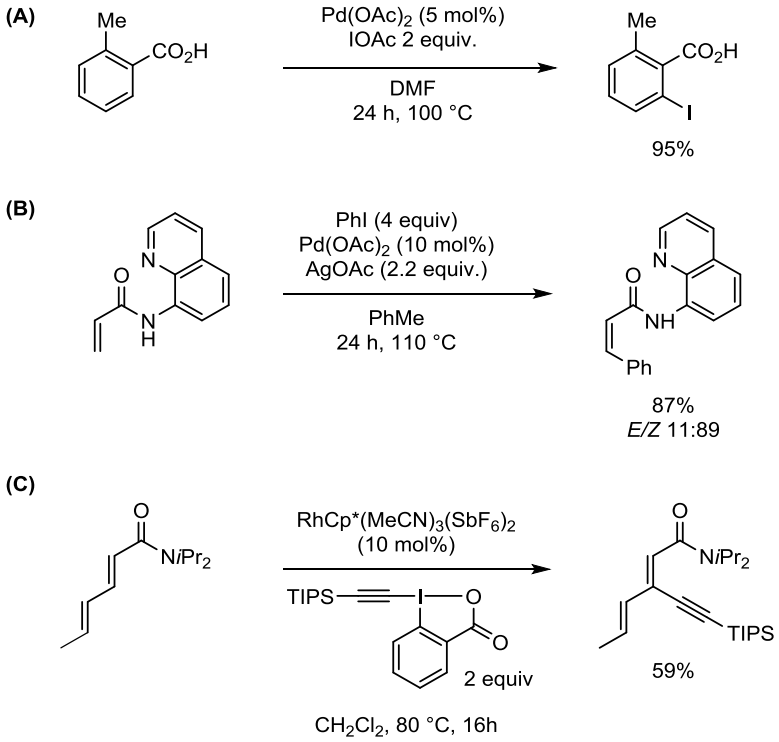

With β-C-H activation of sorbates and derivatives being fairly restricted,[185] a broad C-H activation screen (>70 conditions total) was conducted on intermediate **174** and its derivatives (representative conditions are shown in **Table 3.1**). Different directing groups were implemented, ranging from a simple carboxylic acid to the more strongly coordinating diisopropyl,[179,185] bidendate PIP ((2-pyridine-2-yl)isopropyl) and 8-aminoquinoline amides, which have been widely used in C-H activation.[186–188] A variety of metals known to induce C-H activation/halogenation were investigated (as Pd(II), Rh(III), and Ru(II)), common additives known to participate in the C-H activation (CsOAc, $NaHCO_3$, PivOH, *p*-TSA), and external oxidants ($Cu(OAc)_2$, $Na_2S_2O_8$) were evaluated.

Disappointingly, regardless of the directing group, metal, additive, halogen source or solvent used, we were unable to convert efficiently the sorbate starting material to its desired C-H halogenated product. Either extremely low conversion (**Table 3.1**, entry 1, 3 and 4), or decomposition was observed (**Table 3.1**, entry 2). In the case of an arylated directing group such as 8-aminoquinoline **174d**, the reaction suffered from iodination on the heteroaromatic ring instead of the vinylic position (**Table 3.1,** entry 5), a known side-reaction of this directing group.[189]

Table 3.1 C-H Activation Studies on Sorbic Acid and Derivatives: Representative Conditions[a]

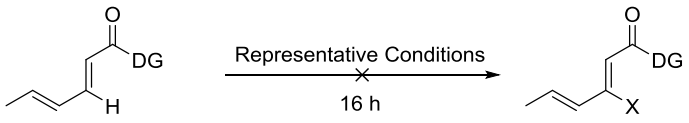

174a-d **177**

Entry	Directing Group (DG)	Metal (5 mol%)	'X^+' source 1.5 equiv.	Additives	Solvent Temp.	Results
1	OH (**174a**)	$Pd(OAc)_2$	I_2	CsOAc 1 equiv. $NaHCO_3$ 1 equiv.	DMF 120 °C	No reaction
2	OH (**174a**)	$Pd(OAc)_2$	NBS	TfOH 6 equiv. $Na_2S_2O_8$ 2 equiv.	DCE 120 °C	Decomposition
3	$NiPr_2$ (**174b**)	$[RhCp^*Cl_2]_2$	NIS	$AgSbF_6$ 10 mol% PivOH 30 mol%	DCE 120 °C	5% conversion (^{1}H NMR)
4	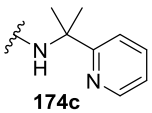 **174c**	(*p*-cymene)$RuCl_2$	NIS	$Cu(OAc)_2$ 1 equiv. KPF_6 20 mol%	*t*AmylOH 110°C	No reaction
5	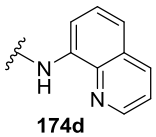 **174d**	$Pd(OAc)_2$	NIS	pTSA 50 mol%	PhMe 110 °C	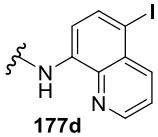 **177d** 30%

[a] Reactions run on a 10-20 mg scale under an atmosphere of air or argon. Conversion was assessed by crude ^{1}H NMR.

3.2.2 Second Synthetic Route: Stepwise Cross-Couplings of a Gem-Dibromolefin

Failed attempts at inducing a direct C-H halogenation of sorbate derivatives prompted a switch in strategy with an emphasis to examine and develop a stepwise pathway towards bromo sorbate **172** (**Scheme 3.3**). In this regard, starting from di-*tert*-butyl tartrate **178**,[190] oxidative cleavage afforded the corresponding *tert*-butyl glyoxylate as a mixture of hydrated and dehydrated forms,[191] which upon distillation over P_2O_5 dessicant was directly used in a Ramirez olefination.[192] The key *gem*-dibromoolefin **175** could be obtained on gram scale. Cross-coupling with a metallated propenyl species (**176**) was subsequently attempted.

Both Suzuki coupling of **175** with the propenyl potassium tetrafluoroborate salt of **176** and Stille coupling with stannylated **176**[193] were studied under a variety of conditions (**Scheme 3.3**). Despite reports by Molander and coworkers regarding highly stereoselective Suzuki cross-coupling of 1,1-dibromoalkenes with alkenyltrifluoroborates,[194] the Stille coupling performed far better in terms of conversion and selectivity as only minimal amounts of *(E,E)*-propenylated **172** and di-propenylated side-products were observed by ^{1}H NMR analysis (<15%, **Scheme 3.3**, entry 4 and 5). A substoichiometric amount of copper iodide was found to increase the reaction rate (**Scheme 3.3**, entry 5 *vs.* entry 4), an effect seen in other literature reports.[195] These optimized conditions proved robust and scalable, yielding gram quantities of the desired *tert*-butyl bromosorbate *(Z,E)*-**172**. Of note, similar cross-coupling screens were attempted with methyl and ethyl ester protected β-brominated sorbates, but the higher steric crowding

imparted by the *tert*-butyl ester version of **172** correlated with enhanced stereoselectivities for the cross-coupling.

Scheme 3.3 Elaboration of *tert*-butyl Bromo Sorbate 172 *via* Stepwise Cross-Couplings

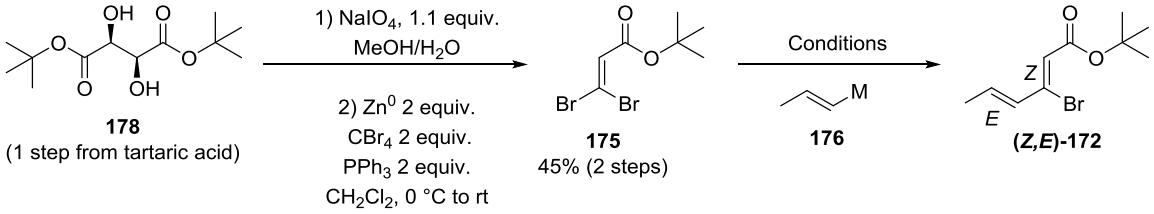

Entry	M	Catalyst	Ligand	Solvent	Additives	Temp. Time	Results
1	BF_3K (1.1 equiv.)	$Pd(PPh_3)_4$ (7 mol%)	-	$PhMe/H_2O$ (3:1)	Cs_2CO_3 (3 equiv.)	80 °C 16 h	Complete conversion (30% isomers)
2	BF_3K (1.1 equiv.)	$Pd(OAc)_2$ (5 mol%)	SPhos (10 mol%)	THF/H_2O (4:1)	K_3PO_4 (3 equiv.)	80 °C 16 h	Incomplete conversion
3	BF_3K (1.1 equiv.)	$Pd(OAc)_2$ (3 mol%)	XPhos (6 mol%)	THF/H_2O (4:1)	K_3PO_4 (3 equiv.)	80 °C 16 h	Incomplete conversion
4	$SnBu_3$ (1.1 equiv.)	Pd_2dba_3 (2.5 mol%)	$(2\text{-furyl})_3P$ (20 mol%)	PhMe	-	90 °C 16 h	Complete conversion Isomers present (<15%)
5	$SnBu_3$ (1.1 equiv.)	Pd_2dba_3 (2.5 mol%)	$(2\text{-furyl})_3P$ (20 mol%)	PhMe	CuI (0.2 equiv.)	90 °C 5 h	84% y Minor amount of isomers (<10%)

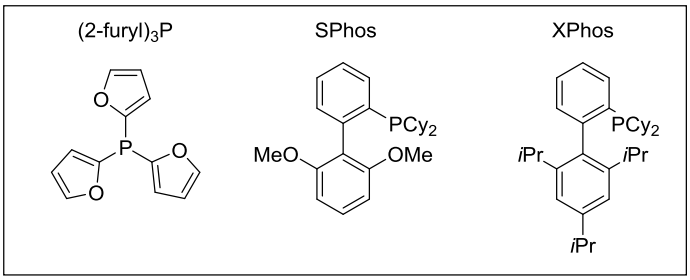

3.3 Synthesis of Ester and Enol Substituted Lactones *via* Oxa-6π Electrocyclization

3.3.1 Access to Ester Substituted Lactones Dienophiles

According to our retrosynthetic analysis involving a ketene dienophile (**Chapter 2, Scheme 2.5)**, a precursor such as carboxylic acid substituted lactone **122** is required. The key β-bromo sorbate **172** was cross-coupled with α-stannylated methyl acrylate **179**[196] in the presence of catalytic $Pd(PPh_3)_4$ and CuI (**Scheme 3.4**). The reaction was found to proceed efficiently on gram scale, generating the full carbon containing framework (*Z,E*)-**180**, with a small amount of (*E,E*) isomerization byproduct (<10%). *Tert*-butyl ester deprotection was carried out using TFA to afford a mixture of deprotected, ring-opened compound **181** along with the lactone product **182**. The open form **181** was further cyclized in moderate yield to **182**. With methyl ester substituted lactone **182** in hand, we were able to induce ester deprotection by dealkylation using excess MgI_2 [197,198] to the free carboxylate substituted lactone **122**.

Scheme 3.4 Synthesis of Carboxylic Acid-Substituted Lactone 122

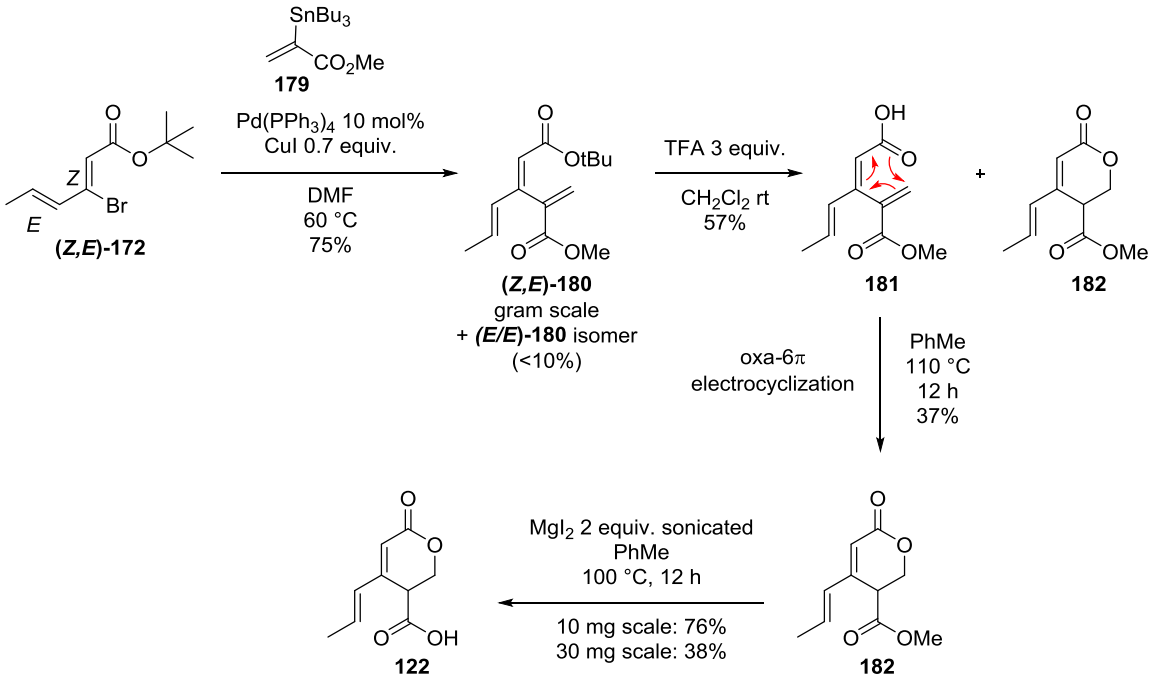

3.3.2 Access to Enol-Substituted Lactone Dienophiles

In addition to ketene precursor **122**, we remained interested in synthesizing a free enol or an enol ether substituted lactone **114**. The gram scale synthesis of sorbate **172** enabled us to further investigate Stille cross-coupling with α-stannylated alcohol **183**[196,199] (**Table 3.2**), which could potentially generate compound **184**, a substrate well suited for further oxidation and annulation to enol **114**. As expected, a prominent side reaction in this coupling under mild heating was the lactonization of compound **184** to produce lactone **185** (**Table 3.2,** entry 1 and 2). Switching from $Pd(PPh_3)_4$ to a more electrophilic and reactive source of palladium such as $[Pd(allyl)Cl]_2$ (**Table 3.2,** entry 3) did not result in improvement of the ratio of **184** to **185**. Reaction conditions reported to effect Stille

coupling of unactivated Csp^3-X bond at room temperature[200–202] (**Table 3.2**, entry 4, 5, 6) were also met with limited success. The stereochemistry of the desired allylic alcohol **184** was assigned by NOESY experiments, demonstrating retention of configuration during the cross-coupling process.

Table 3.2 Stille Coupling of Sorbate 172 with α-Stannylated Alcohol 184

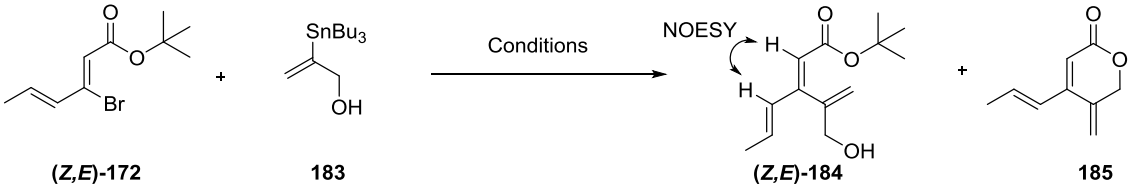

(*Z,E*)-172 183 (*Z,E*)-184 185

Entry	Catalyst Ligand	Additives	Solvent	Temp.,Time	Outcome
1	$Pd_2dba_3.CHCl_3$ 5 mol% $P(2\text{-furyl})_3$ 20 mol%	CuI 0.7 equiv.	DMF	80 °C, 16 h	**185** (62%)[a]
2	$Pd(PPh_3)_4$ 10 mol% CuI 0.7 equiv.	CuI 0.7 equiv.	DMF	60 °C, 16 h	**184** (34%),[a] **185** (44%)[a]
3	$[Pd(\pi\ allyl)Cl]_2$ 2.5 mol% PCy_3 15 mol%	-	THF	40 °C, 48 h	Incomplete conversion **184:185** (1:1)[b]
4	Pd_2dba_3 3 mol% $P(t\text{-Bu})_3$ 6 mol%	-	PhMe	rt, 20 h	Low conversion **184:185** (1:1)[b]
5	$PdCl_2$ 10 mol% $P(t\text{-Bu})_3$ 20 mol%	CuI 1 equiv. CsF 2 equiv.	DMF	rt, 16 h	Low conversion **184:185** (1:1)[b]
6	Pd_2dba_3 3 mol% $P(t\text{-Bu})_3$ 6 mol% CsF 2 equiv. 4A MS	CuI 0.7 equiv.	NMP	rt, 16 h	No reaction

[a] Isolated yield

[b] Ratio of **184:185** determined by crude ^{1}H NMR

Looking to overcome the poor selectivity in the Stille cross-coupling with stannylated alcohol **183**, we reasoned that adjusting the substitution and oxidation level of the stannylated acrylate coupling partner may provide a better outcome (**Scheme 3.5**).

First, by masking **183** as TBS-protected alcohol **186**, we obtained a TBS-protected coupling product of unknown alkene stereochemistry in good yield (**Scheme 3.5 (A)**), and

upon TBAF treatment, we isolated the isomer of alcohol (*Z,E)*- **184** (*E,E*-**184**). We presumed *E/Z* isomerization of the alkenyl bromide moiety occurred during the cross-coupling step, as *E/Z* isomerization is also a step reaction we observed in the cross-coupling of **172** with stannylated methyl acrylate **179** (**Scheme 3.4**). This hypothesis was confirmed by sequential TBS protection of (*Z,E)*-**184**, followed by TBAF desilylation. We obtained the starting (*Z,E*-**184**), without production of (*E,E*-**184**). We believe the steric repulsion imparted by the *tert*-butyl group, which worked in our favor in the selective cross-coupling to *(Z,E)*-**172**, is responsible for the observed isomerization around the vinylic C-Pd bond to **187** (**Scheme 3(B)** and **3(C)** for two potential mechanistic hypothesis). Similar to our reaction screen of stannylated alcohol **183** (**Table 3.2**), examination of reaction conditions, including several sources of Pd(0), ligands and temperature did not change the reaction outcome. Triethylsilyl (TES) and trimethylsily (TMS) protected allylic alcohols were also evaluated as reaction partners in the cross-coupling, but these protecting groups tended to be labile, falling off during the reaction, and still afforded a large amount of *E/Z* isomerization.

Scheme 3.5 Stille Coupling with Silyl Protected Alcohol 186 and Potential Isomerization Mechanisms

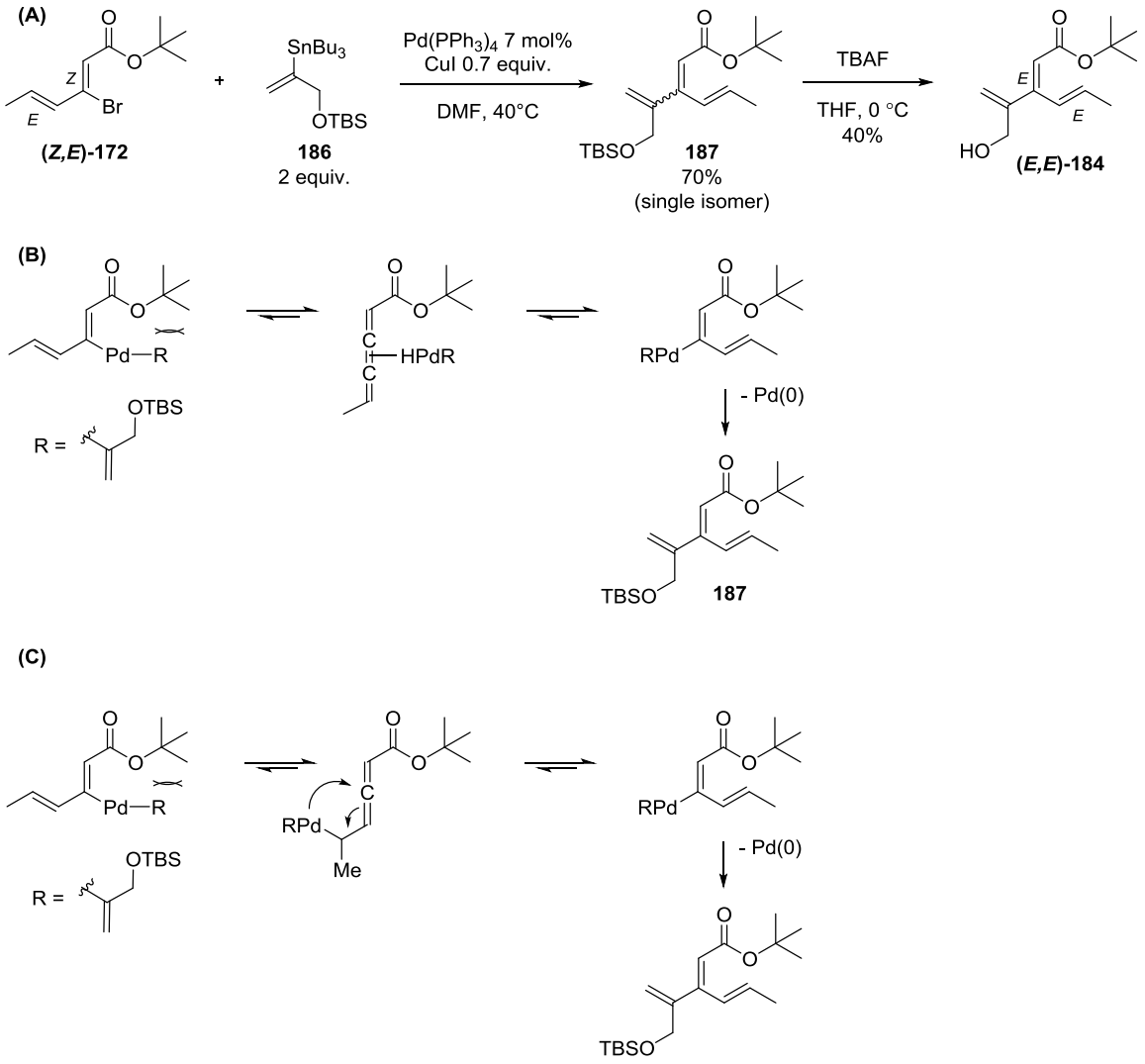

The oxidation state of the stannane partner was further adjusted to the corresponding aldehyde. Acrylate **188**[196,199] polymerized readily under the reaction conditions, yielding intermediate **189** in low yield (**Scheme 3.5 (A)**). The resolution of these issues came by employing diethyl acetal-protected aldehyde **190**. This stannane, under the usual coupling conditions, generated the retentive cross-coupling compound **191**,

along with a minor amount of isomerization side product (10%) and deprotected aldehyde coupling product **189** (5%) (**Scheme 3.5 (B)**).

Scheme 3.6 Stille Coupling with Stannylated Acrylates

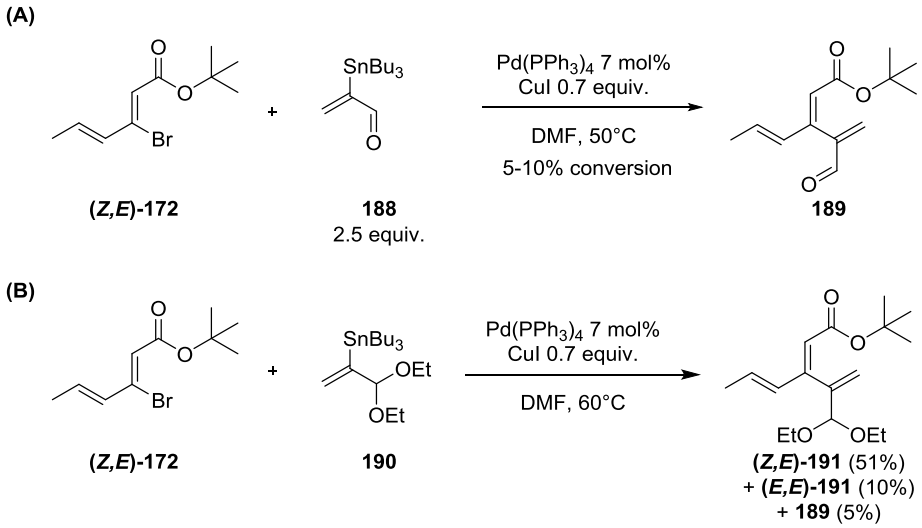

With a reliable route to protected cross-coupling product **191**, the annulation to form the six membered-ring lactone core became our next focus. Direct treatment of diethyl acetal **191** with TFA, anticipated to result in global deprotection of both the *tert*-butyl ester and the acetal, instead afforded the lactone-acetal **192** (**Scheme 3.7 (A)**). A literature report had demonstrated opening of a related hemiacetal to a regioisomeric enol form under basic conditions (**Scheme 3.7 (B)**).[203] Accordingly, we hoped that compound **192** could be similarly rearranged to the desired enol structure **114**. Several deprotection conditions were tried (acidic and basic), but all unfortunately triggered decomposition of starting material **192.**

Scheme 3.7 Attempted Synthesis of Free Enol 114 from Lactone Hemiacetal 192

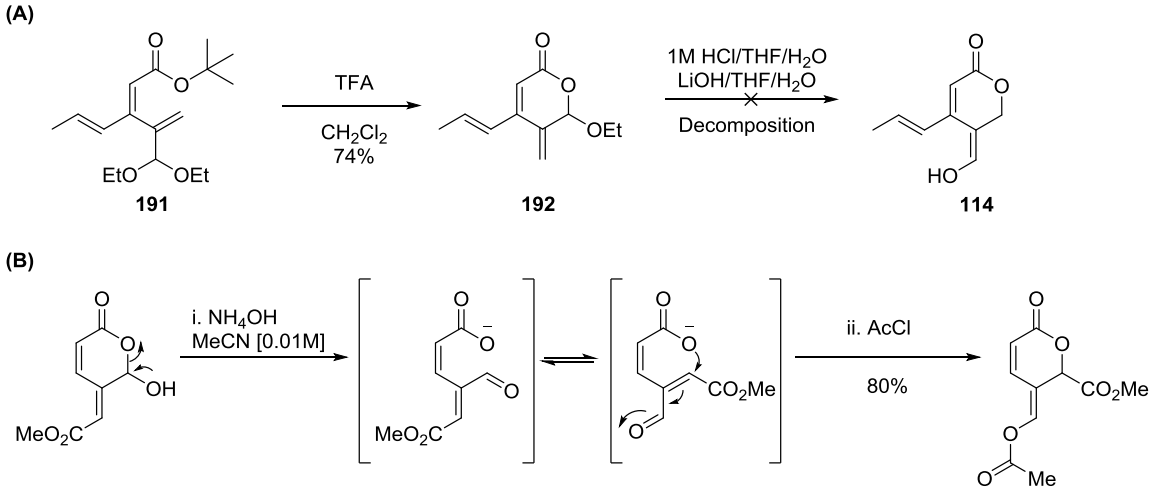

Stepwise deprotection proved more efficacious, as submission of **191** to aqueous HCl under mild heating cleanly promoted formation of acrylate **189** (**Scheme 3.8**). TFA cleavage was then evaluated, producing the non-lactonized carboxylic acid **193** in moderate yield. Surprisingly, under thermal heating or microwave irradiation, this compound did not cyclize *via* oxa-6π electrocyclization to enol **114**, and **193** was recovered. Lewis acid conditions (TMSOTf) also failed, immediately decomposing the uncyclized carboxylate **193**.

Scheme 3.8 Stepwise Deprotection Studies to Free Enol 114

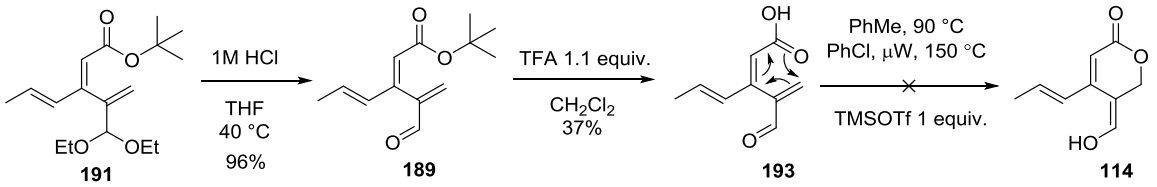

We then explored the possibility of a simultaneous *tert*-butyl deprotection/oxa-6π electrocyclization mediated by Lewis acids in order to target a substituted enol ether instead of a free, enol lactone such as **114**, which may potentially be unstable and prone to polymerization. Silyl triflates have been reported to cleave *tert*-butyl esters selectively, generating the corresponding carboxylates *via* intermediacy of a silyl ester.[204] In our case, employing 2,6-lutidine buffered TBSOTf conditions on **189**, we observed a clean conversion by TLC to afford what is likely the deprotected ester. However, upon a variety of work-up conditions (pH 7 buffer, 1N HCl, lutidine.TfOH salt precipitation) we could not isolate TBS-protected enol **114a** or the free enol **114** (**Scheme 3.9**). Switching to substoichiometric amount of TMSOTf, we were surprised to isolate the *tert*-butyl protected enol **114b** as a single isomer. However, the reaction to produce **114b** was difficult to reproduce and consequently only ^{1}H NMR data was available.

Scheme 3.9 Attempted Synthesis of Enol Ether 114 and Derivatives

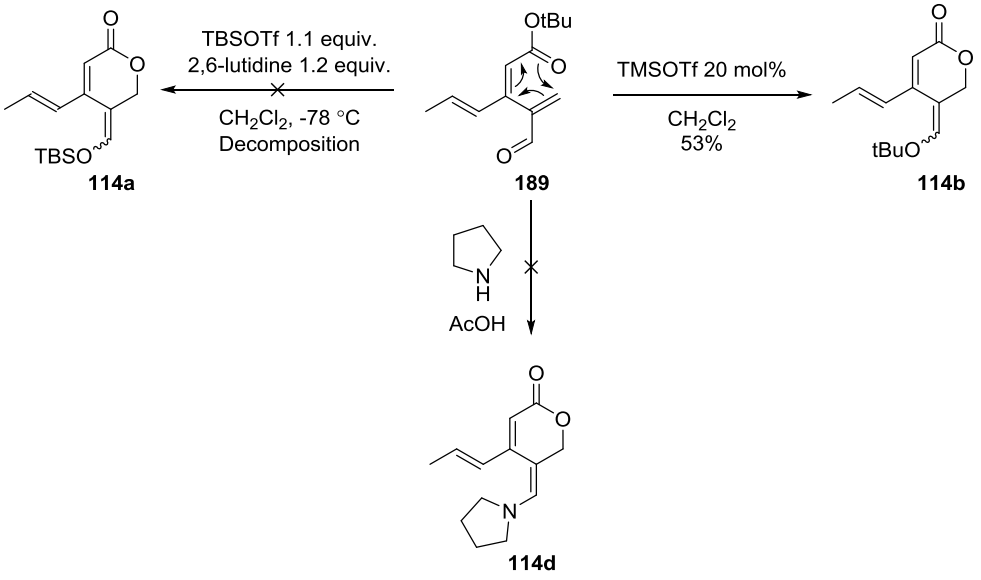

We believe this particular deprotection condition triggers a fast *tert*-butyl cation dissociation and transfer to the emerged enolate (*cf*. **Scheme 3.10** for a mechanistic rationale). Inspired by accounts reporting [2,3]-Wittig rearrangement catalyzed by secondary amines,[205] we attempted to react **189** with stoichiometric pyrrolidine, to achieve both oxa-6π electrocylization catalysis and formation of an electron-rich enamine substituted lactone. Unfortunately, this strategy proved unfruitful, and decomposition of the starting material took place.

Scheme 3.10 Mechanistic Rationale for TMSOTf Deprotection of Ester 189

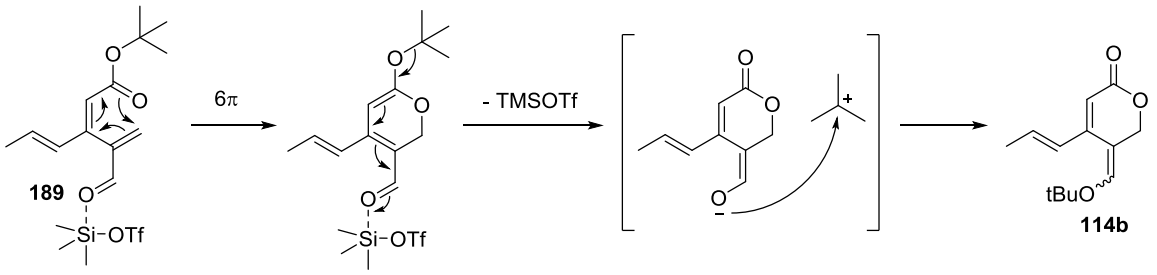

Having synthesized an electron rich enol ether substituted lactone **114b**, a remaining aim was to access an electron poor enol ether substituted lactone to react in normal demand Diels-Alder with *2H*-pyran **115**. By heating **189** in acetic anhydride with a catalytic amount of bismuth (III) triflate, we obtained acetate enol ether **114c** in good yield (**Scheme 3.11**). NOESY NMR experiments were used to assign configuration of the enol acetate, wherein the acetate group was found to reside on the same side as the propenyl side chain. Mechanistically, we propose a first acetal formation would take place in the presence of Bi(III) and acetic anhydride. Upon loss of one acetate group, an intermediate oxonium would be generated and could adopt two conformations (**Scheme 3.11**, oxonium structure

A and **B**). Considering the propenyl side-chain may adopt an out-of-plane conformation, an unfavored allylic strain may destabilize conformation **B** over **A**, which would account for the fixed geometry observed in the final product **114c**.

Scheme 3.11 Synthesis of Enol Acetate Substituted Lactone 114c: Mechanistic and Stereochemical Rationale

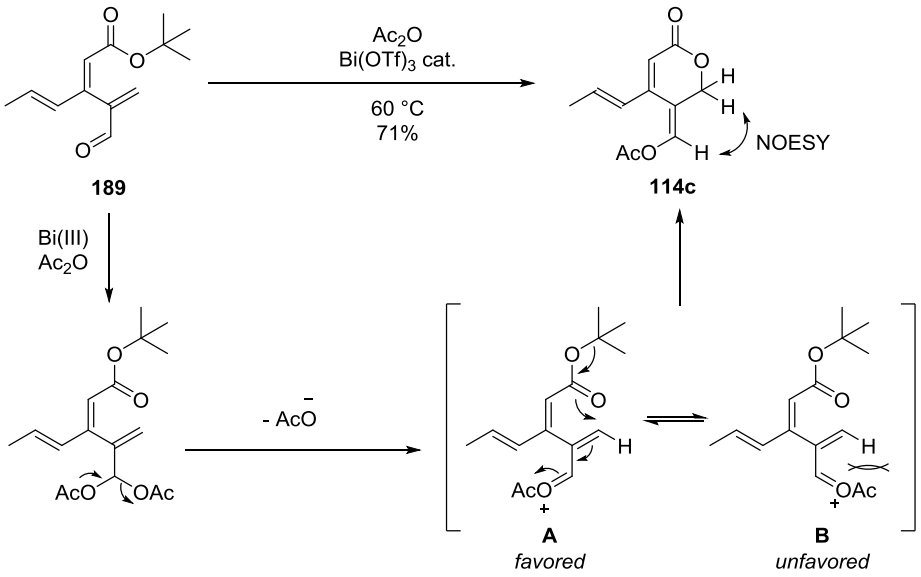

3.4 Studies toward a Biomimetic, Formal [4+2] Cycloaddition

3.4.1 Ketene/2H-Pyran Coupling Attempts

With our primary goal to access both electron rich and electron poor lactone dienophiles fulfilled, investigating the reactivity of diene **115** and ketene precursor **122** or enol ethers **114b**,**c** became a primary focus.

We suspected that activating the carboxylic acid substituted lactone **122** directly instead of going through the acyl chloride may alleviate issues encountered during our ketene model studies with pyran **115** (i.e. direct *2H*-pyran acylation,**Chapter 2**, *Section*

2.4.1, **Scheme 2.22**). First, lactone **122** was activated using Mukaiyama's reagent **194**[206,207] (**Scheme 3.12 (A)**), which is known to perform well in the activation of carboxylic acids in a range of reactions, including ketene generation.[208,209] Unfortunately, at room temperature, decomposition of both the *2H*-pyran and lactone **122** were observed.

We sought to invoke the stepwise route involving *in situ* formation of a ketene enolate from **122**, which may further react with dienal **115'** (**Chapter 2**, *Section 2.2.2*, **Scheme 2.8**). In the presence of CDI as a carboxylate activator and with a catalytic amount of NHC **195**,[105] a successful combination in stepwise annulation,[210] we were disappointed to observe decomposition of both partners **122** and **115** (**Scheme 3.12 (B)**). An identical result was obtained when attempting to generate a more reactive anhydride ester from **122** that could be deprotonated and trapped as a ketene enolate with benzotetramisole catalyst **196** [109] (**Scheme 3.12 (B)**). Of note, the lactone **122** was difficult to dissolve in solvents compatible with ketene formation (*e.g.* non nucleophilic, polar, aprotic solvents such as CH_2Cl_2, THF), minimizing the efficiency of these reactions.

Scheme 3.12 Coupling Studies between *2H*-Pyran 115 and Ketene Precursor 122

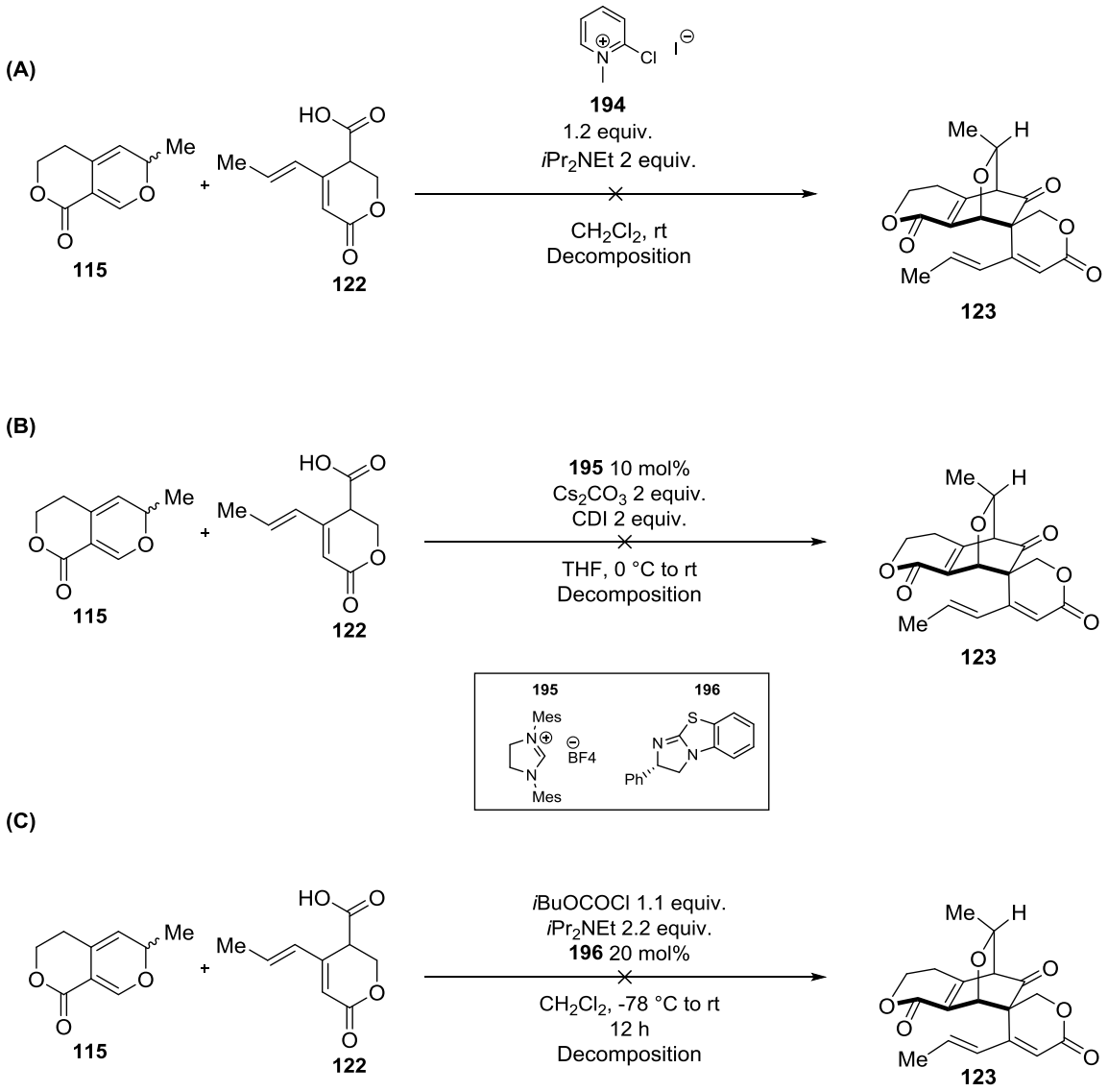

3.4.2 Enol-Substituted Lactone as Dienophile: Concerted and Stepwise Approaches to Swerilactones A and B Core

Given the challenges encountered during our proposed ketene [4+2] cycloaddition, the exploration of the biomimetic formal Diels-Alder approach with lactone dienophile **114**

and derivatives was pursued (**Chapter 2**, **Section 2.2**). In comparison with the *tert*-butyl enol ether **114b**, the synthesized enol acetate **114c** offered the greatest versatility, as it could intervene in all normal demand cycloaddition, radical cation Diels-Alder annulation, and stepwise aldol reaction toward the swerilactone A and B core.

For example, we hoped the electron-withdrawing character of the enol acetate **114c** in comparison to *tert*-butyl enol ether **114b** could be an advantage and enhance reactivity. Heating a mixture of *2H*-pyran **115** with **114c** in toluene, no cycloadduct was isolated; **114 c** was fully recovered and **115** decomposed over the course of the reaction (**Scheme 3.13(A)**) as assessed by crude ^{1}H NMR analysis. It was then envisioned to use a radical cation cyclization promoted by photocatalyst **170**, which we had shown could occur between pyran **115** as a diene and an easily oxidizable dienophile (**Chapter 2**, *Section 2.4.3*, **Scheme 2.32**). With these conditions, the recovery of enol acetate **114c** and the simultaneous degradation of **115** was observed (**Scheme 3.13(B)**). The lack of reactivity of **114c** in the generation of a radical cation may be due to its relatively lower electron density compared to other dienophiles, which may translate into a higher oxidation potential, out of the redox potential range for triphenylpyrylium tetrafluoroborate (E_{ox}= 2V). We plan to test these conditions using the more electron rich and potentially easier to oxidize *ter*t-butyl enol ether **114b.**

Scheme 3.13 Diels-Alder Cycloaddition Studies between *2H*-Pyran 115 and Enol Acetate 114c

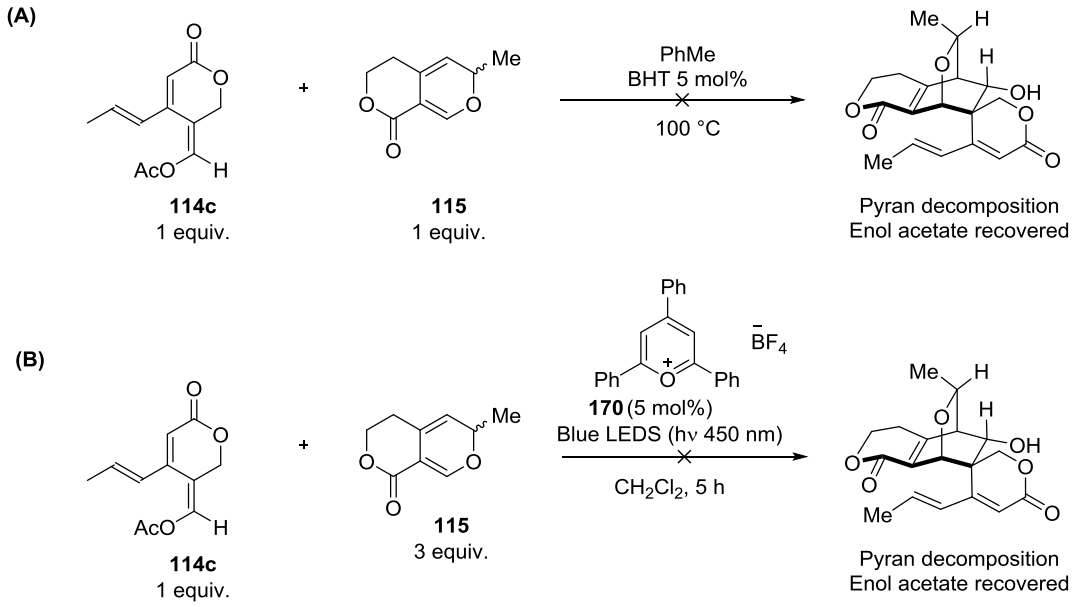

The prospect of employing enol acetate **114c** in a more controlled reactivity pattern arose from numerous reported examples addressing aldol coupling of enol acetates with aldehydes. This type of transformation was shown to proceed *via* Lewis acid catalysis[211–215] or under basic conditions,[216,217] by unmasking the enolate anion from the enol acetate and creating C-C bonds. By targeting the addition of the *in situ* formed enolate **114** from **114c** to the dienal **115'**, we may access an aldol reaction to adduct **121**' as a first key C-C forming step *en route* to the swerilactone A and B core (**Scheme 3.14)**. This strategy would overlap with the proposed biosynthesis for swerilactones A and related natural products (**Chapter 2**, *Section 2.1.2*, **Scheme 2.1**).

The mild Lewis acid $Sc(OTf)_3$ was introduced in catalytic amount to a mixture of **114c** and **115:115'** (**Scheme 3.14 (A)**). In this case, we recovered starting enol acetate **114c** without detecting the desired product. We switched to basic conditions, adding K_2CO_3 in

excess to a mixture of **114c** and **155'** in methanol, warming the temperature from 0 $^{\circ}$C to 40 $^{\circ}$C in order to increase the conversion of **114c.** The unexpected acetal containing lactone structure **197** was generated as the major product (**Scheme 3.14 (B)**). Efforts to reproduce the synthesis of **197** were met with limited success and consequently this compound could only be characterized by ^{1}H NMR.

Scheme 3.14 Stepwise Coupling Studies between Dienal 115' and Enol Acetate 114c

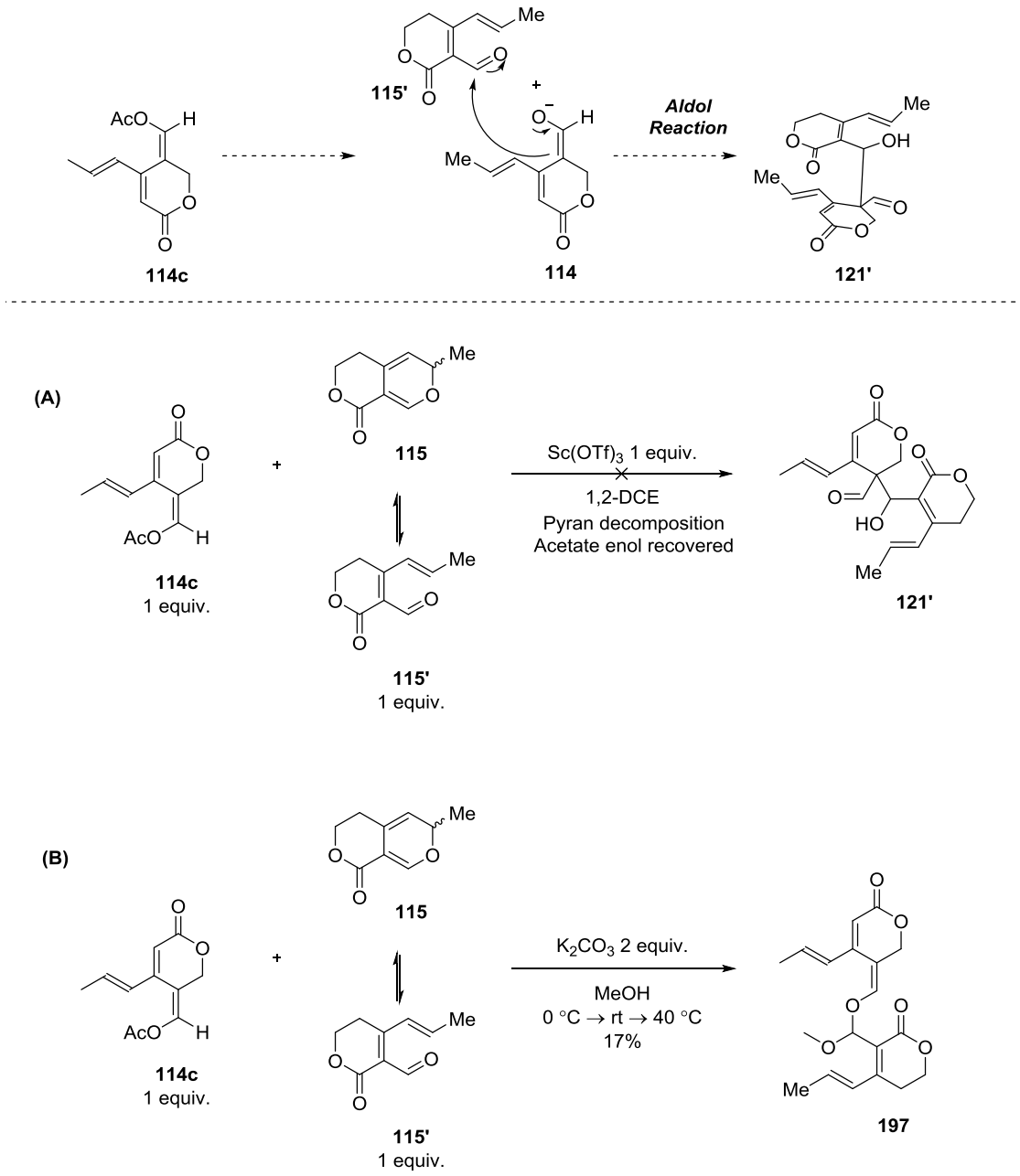

Two mechanistic rationales for the formation of this product are outlined in **Scheme 3.15**. We postulate the *in situ* generated methoxide adds to the aldehyde moiety of **115'**,

creating hemiacetal anion **198** (**Scheme 3.15(A)**). This intermediate could further add into the conjugated system of **114c**, and upon E1/CB elimination of the acetate group from structure **199**, acetal product **197** would emerge. Alternatively, in the presence of potassium methoxide, *in situ* deprotection of **114c** to **114'** could be induced (**Scheme 3.15(B)**). This enolate may react in an aldol fashion with **115'**, generating a hydroxyl anion **197'**, which upon hydroxide elimination and methoxide addition would generate lactone acetal **197**.

Formation of this unwanted side-product may be avoided by conducting the aldol reaction with a stronger base in non-nucleophilic, aprotic solvents such as THF or CH_2Cl_2. It nonetheless constitutes a proof of concept that dienal **115'** can undergo nucleophilic attack into its aldehyde moiety.

Scheme 3.15 Mechanistic Proposals toward Acetal 197

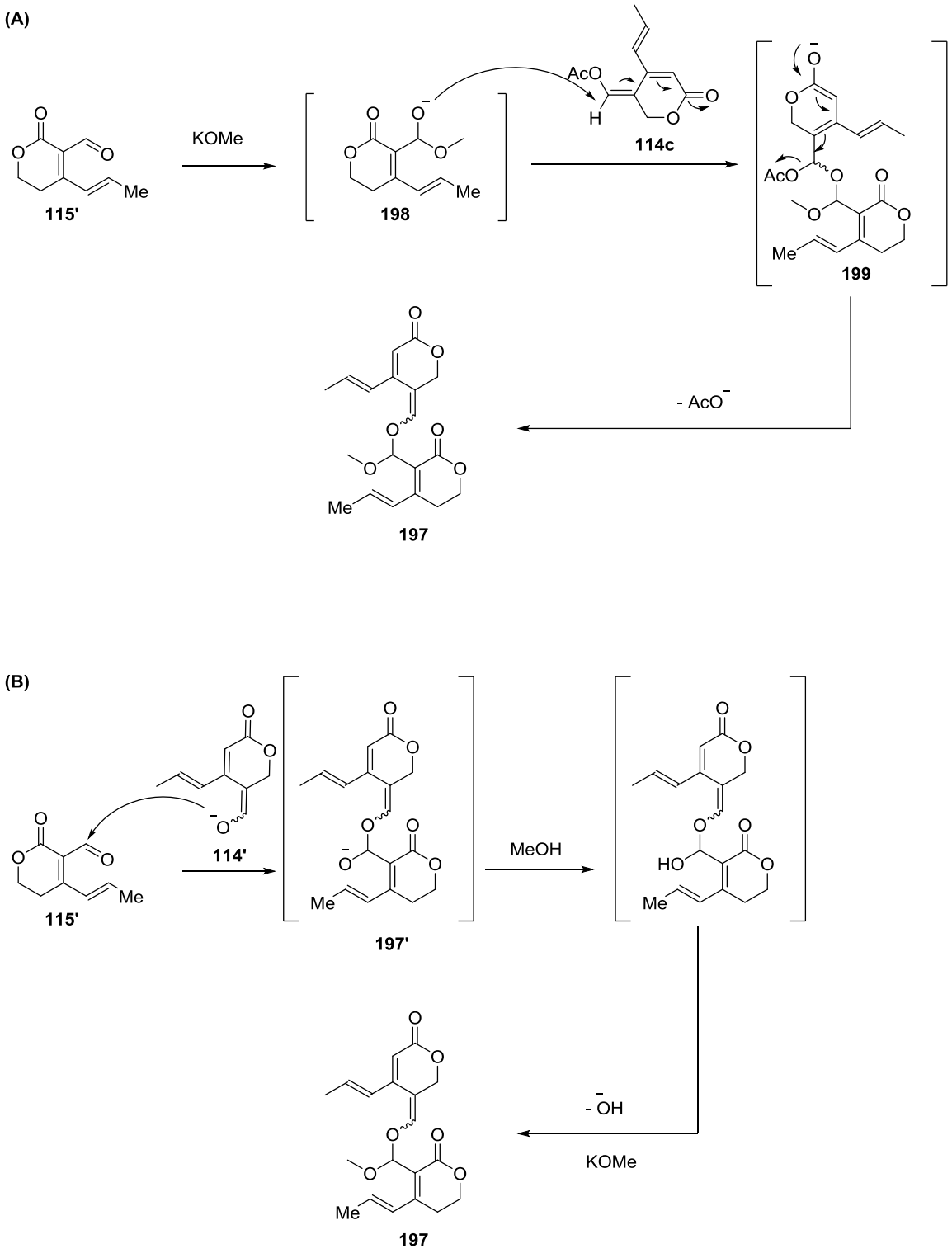

3.4.3 Proposal toward the Synthesis of Swerilactone A and B Core Structures

With the syntheses of two key building blocks **115** and **114b/114c** achieved, we propose to test their coupling through different pathways. Probing the feasibility of the aldol pathway between **115**' and **114c** would first require investigating the nucleophilic addition of a simple enolate, for example with the enolate derived from ethyl acetate. In the case this step was successful and produced an aldol adduct, we plan on testing the reactivity of the aldol pathway with **114c** by employing basic or Lewis acid conditions (**Scheme 3.16**). The feasibility of this step, which forms the sterically congested aldol product **121'** remains an open question. Literature precedents regarding the formation of stereogenic centers *via* aldol reaction are focused on Mukayama Aldol with reactive silyl enol ethers[218–220] and enamine-based transformations using organocatalysis.[221–223] If the aldol adduct **121'** is produced, perhaps the process could be made stereoselective by employing a combination of chiral ligands and Lewis acid metals. This intermediate **121'** may be deprotonated and trigger a series of C-C bond forming steps (as we initially outlined in **Chapter 2**, *Section 2.2.1*, **Scheme 2.4)**, *via* oxa-Michael addition and final vinylogous Aldol reaction.

Scheme 3.16 Proposed Route toward Swerilactone A and B Core via Aldol Reaction of 114c and 115'

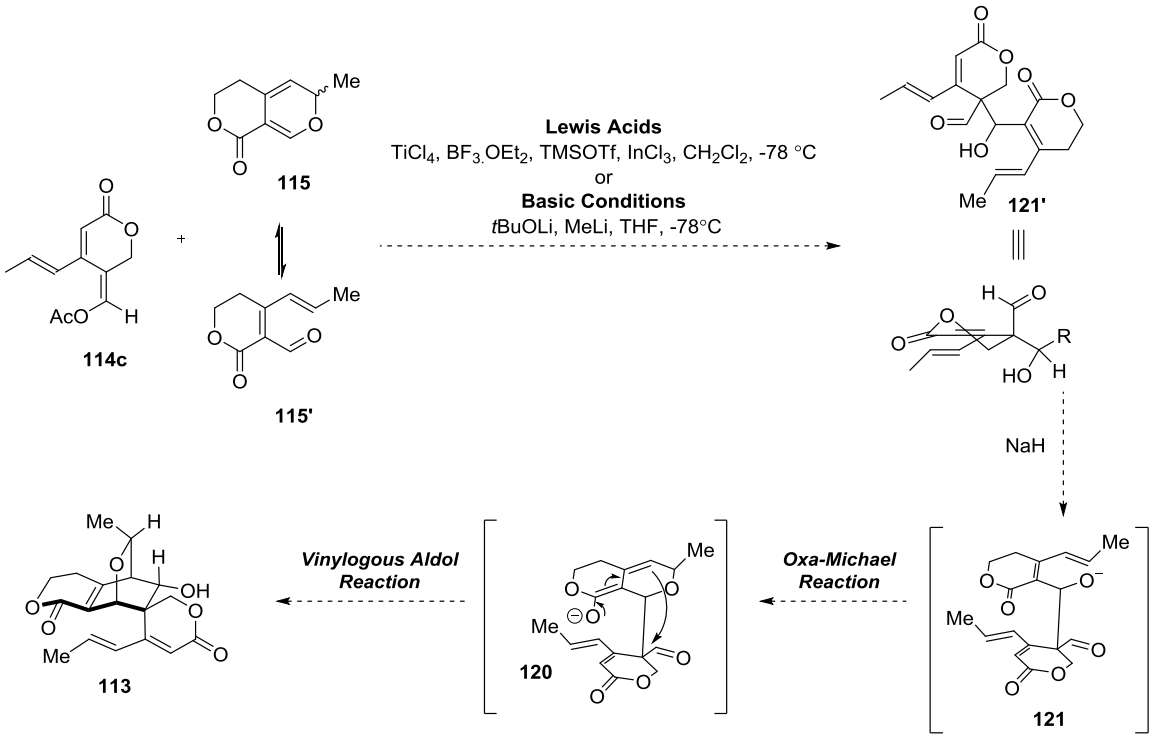

Alternatively, we propose the exploration of the radical cation cycloaddition pathway from *tert*-butyl enol ether **114b** with triphenylpyrylium tetrafluoroborate **170** or with stronger chemical oxidants such as CAN or $Mn(OAc)_3$ (**Scheme 3.17**). Use of enal substrates **194** and **195** (**Scheme 3.8**) in related experiments may also be possible.

Scheme 3.17 Proposed Route toward Swerilactone A Core: Radical Cation Cycloaddition of 114b and 115

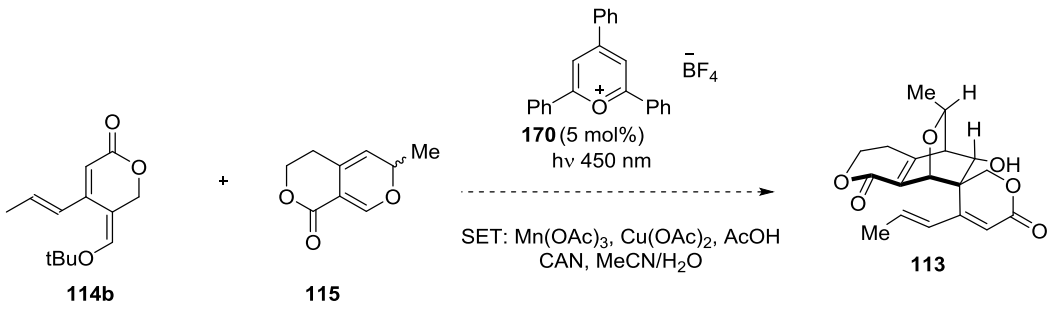

3.5 Proposal toward the Synthesis of Related Swerilactone Natural Products

During the course of our studies in this family of natural products, we remained interested in targeting other members, such as (+)-swerileduginin A (**100**). We hypothesized this compound could arise from a biomimetic cascade between two molecules of gentiogenal (**200**) in their iminium and enamine form (see **Scheme 3.18** for a proposed forward startegy and potential catalysts). Enamine-iminium cascades have been applied in many elegant biomimetic approaches to natural products[224–227] and we envisioned a similar concept could be applied toward (+)-swerileduginin A (**100**).

Scheme 3.18 Proposal toward (+)-Swerileduginin *via* Enamine/Iminium Cascade

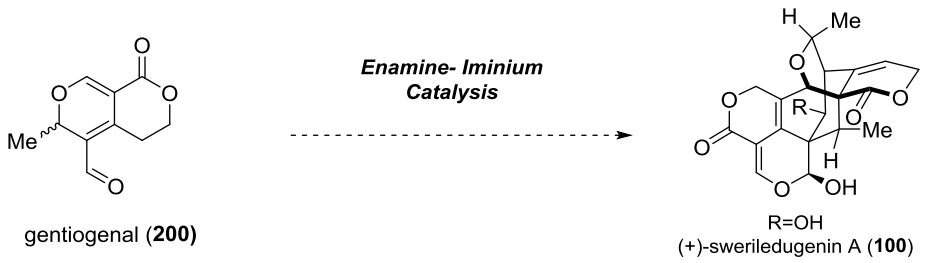

Mechanistically, we hoped the *in situ* generation of enamine **200a** and iminium **200b** (**Scheme 3.19**) would trigger a vinylogous Michael addition to C-C linked pseudo-dimer **201**. This intermediate could undergo retro oxa-6π to yield oxatriene **202**., which may be suited for a vinylogous Michael addition, affording the iminium-containing ring

system **203**. Iminium-enamine equilibration may then occur, forming **204**. Upon hydrolysis to intermediate **205**, an aldol reaction could generate **206**. Further hydrolysis to **207** followed by isomerization of the enal system and intramolecular nucleophilic attack would afford the lactol-containing (+)- swerileugenin (**100**).

Scheme 3.19 Enamine/Iminium Cascade: Mechanistic Proposal

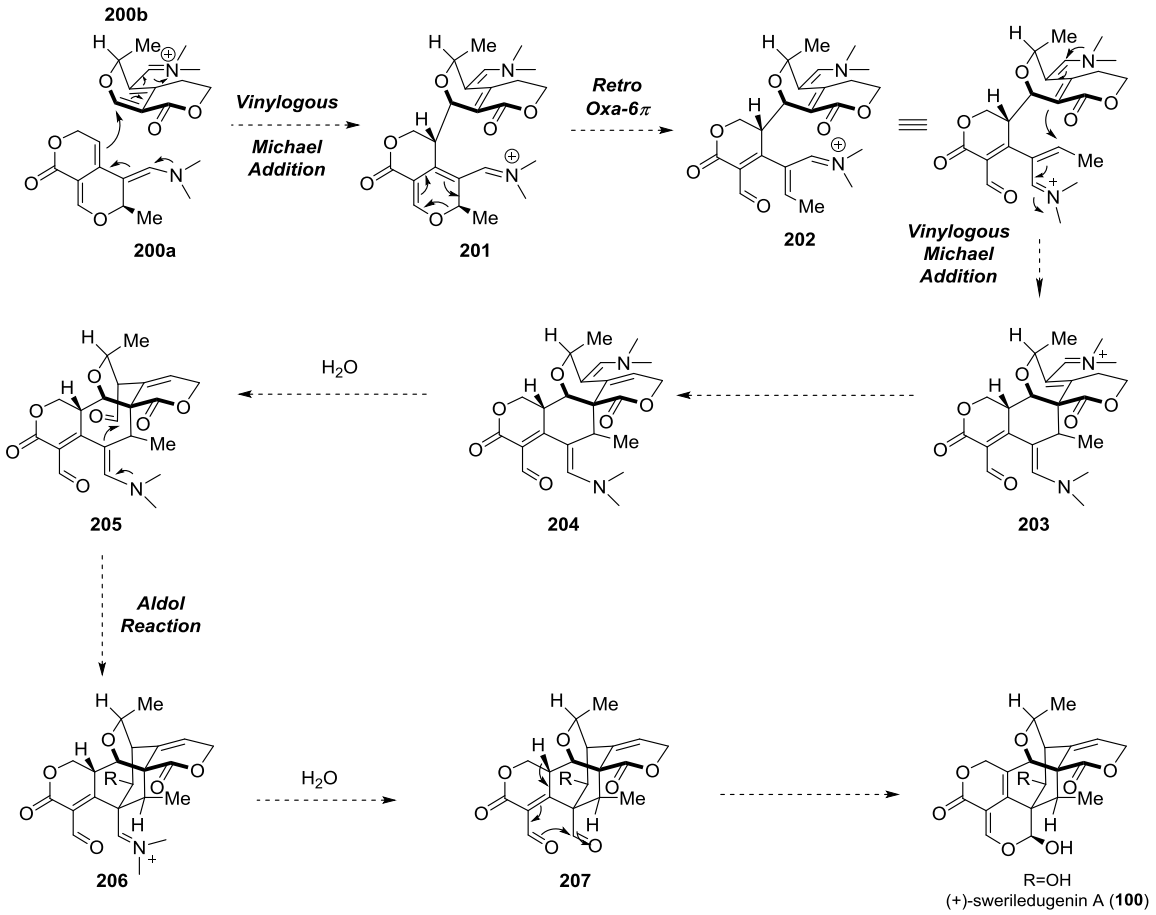

In that regard, we have conducted preliminary studies targeting gentiogenal (**200**). In collaboration with Tim Harig (REU program, undergraduate student), we showed that

the commercially available compound gentiopicrin (**208**) could undergo glycosidic cleavage to the *O*-methyl protected gentiopicrin aglycon **209** (**Scheme 3.20 (A)**). This protected compound was then found to rearrange to gentiogenal (**200**) with a combination of MgI_2 and TFA, in low yield, thereby mimicking the known biosynthetic transformation of gentiopicrin (**208**) by the enzyme β-glucosidase to gentiogenal (**200**).[228,229] We have considered a mechanistic rationale for this transformation to include dual activation of the terminal alkene with TFA and of the lactone moiety with MgI_2 (**Scheme 3.20 (B)**). Protonation of pyran **209** could trigger acetal opening to oxonium **210**. Upon loss of methanol, intermediate **211** may tautomerize to its enol form, which is poised for an ene reaction that would generate dienal **200'**. Oxa-6π electrocyclization would follow, affording the desired gentiogenal (**200**).

Scheme 3.20 Elaboration of Gentiogenal (200): Dual Lewis and Brønsted Acid Activation of Gentiopicroside (207)

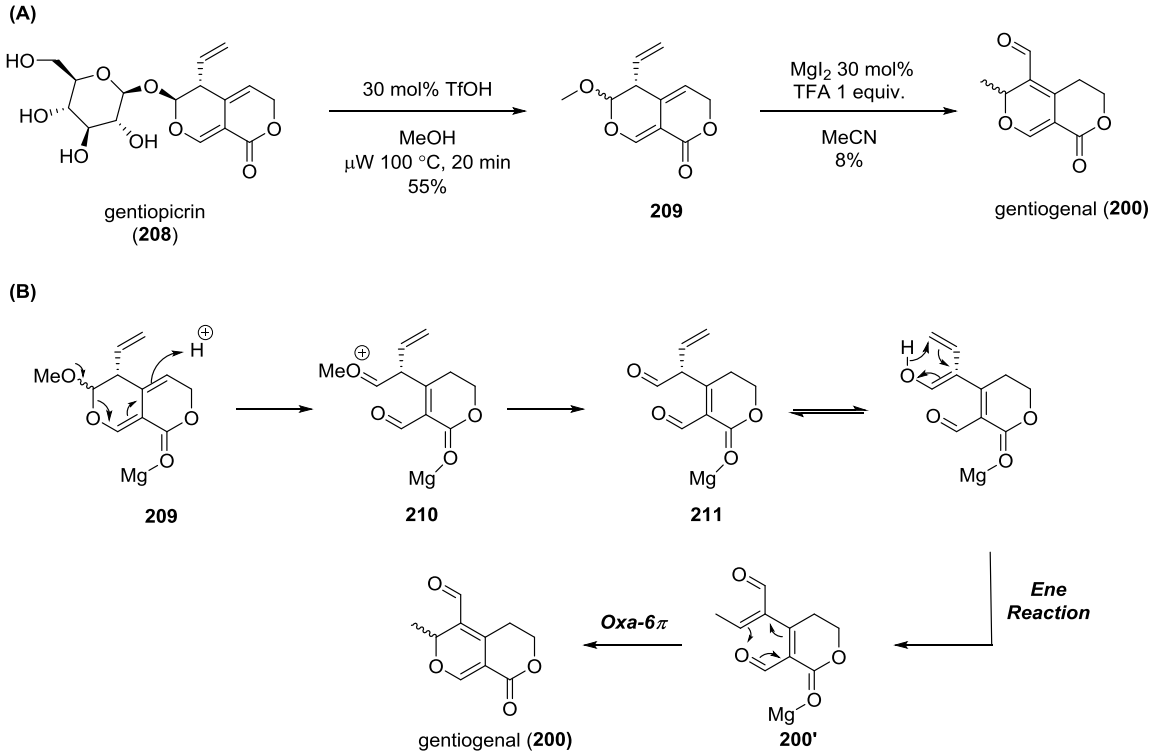

This route enabled a low-yielding synthesis of gentiogenal, and would not be practical for larger scale access. We have alternatively attempted to formylate the *2H*-pyran substrate **115**. Under typical formylation conditions, such as Vilsmeier-Haack, or by chlorinating or brominating **115**, a strategy that could have paved the way for Pd(0)-mediated carbonylation, we were unable to produce the desired gentiogenal natural product (**200**) (**Scheme 3.21**). The attempt to leverage the observed nucleophilicity of **115** at its γ-position (**Chapter 2**, *Section 2.4.1*, **Scheme 2.22**) with 2,2,2-trifluoroethyl formate in the presence of acetic acid was equally unproductive.

Scheme 3.21 Attempted Formylation Experiments of 115

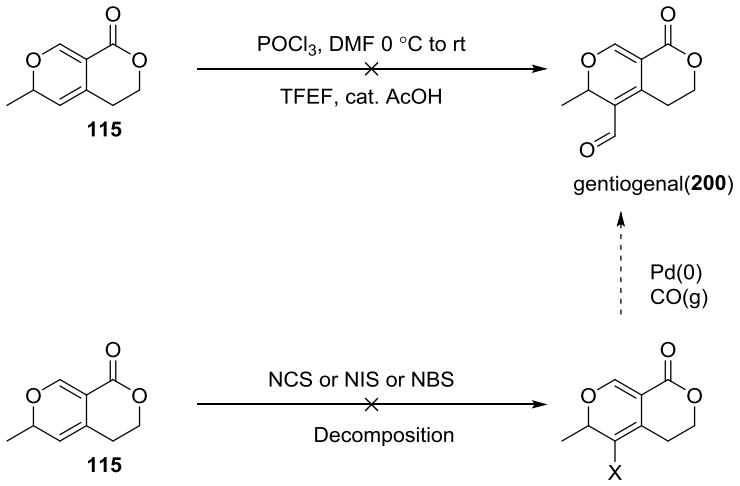

We propose to investigate alternative formylation conditions to effect the formation of gentiogenal (**200**). A Rieche formylation[230] promoted with $TiCl_4$ and dichloromethyl methyl ether could be attempted, although competing chelation to pyran **115** and opening to its dienal may be an unproductive reaction pathway. In addition, ethyl orthoformate might potentially serve as a masked formylating agent in this transformation. Once gentiogenal is obtained, its reactivity in enamine-iminium catalysis would be assessed.

3.6 Conclusion

Throughout this work, we have presented our efforts to access the core structure of swerilactone A (**98**) and B (**99**) biomimetically *via* a formal Diels-Alder cycloaddition. We have successfully completed the synthesis of a sensitive acyclic precursor to the *2H*-pyran diene **115** through Saucy-Marbet rearrangement of propargyl vinyl ether **152**. We have

further investigated the reactivity of compound **115** in several cycloadditions, and have shown thermal normal demand and radical cation Diels-Alder cycloadditions were productive modes of reactivity, whereas inverse demand cycloaddition was unfruitful.

Several enol ether substituted lactones **114b** and **114c** meant to participate as electron-rich dienophiles were subsequently synthesized *via* stepwise cross-couplings of a β-brominated sorbate derivative, and final lactonization was undertaken by Lewis acid catalyzed oxa-6π electrocyclization, a seldomly applied strategy to construct six-membered ring lactones. The successful synthesis of both *2H*-pyran diene **115** and enol ether lactone dienophiles **114b-c** enabled further studies toward their coupling. We targeted several pathways to assemble these two fragments, from normal demand to radical cation cycloaddition to stepwise aldol coupling. Even though we have not been able to bring these compounds together in a desired fashion thus far, we believe this work constitutes an advancement in understanding *2H*-pyran reactivities, outside of their known [4+2] dimerization, and that our proposed routes could ultimately yield the core structure of swerilactones A and B.

Finally, we have synthesized key intermediates such as gentiogenal toward the synthesis of the congener (+)-swerileduginin A (**100**). We believe the proposed enamine-iminium cascade has significant potential and if successful would generate interesting polycyclic structures.

3.7 Experimental Section

General Information: ^{1}H NMR spectra were recorded at 300, 400, or 500 MHz at ambient temperature with $CDCl_3$, CD_3OD, DMSO-d_6 or benzene-d_6 (Cambridge Isotope Laboratories, Inc.) as solvents. Data for ^{1}H NMR are reported as follows: chemical shift, integration, multiplicity (br = broad, ovrlp = overlapping, s = singlet, d = doublet, t = triplet, q = quartet, m = multiplet) and coupling constants in Hz. ^{13}C NMR spectra were recorded at 100.0, or 125 MHz at ambient temperature with the same solvents unless otherwise stated. Chemical shifts are reported in parts per million relative to the deuterated solvents. All ^{13}C NMR spectra were recorded with complete proton decoupling. Infrared spectra were recorded on a Nicolet Nexus 670 FT-IR spectrophotometer. High-resolution mass spectra were obtained in the Boston University Chemical Instrumentation Center using a Waters Q-TOF API-US mass spectrometer. Melting points were recorded on a Mel-Temp apparatus (Laboratory Devices). Analytical LC-MS was performed on a Waters Acquity UPLC (Ultra Performance Liquid Chromatography (Waters MassLynx Version 4.1) with a Binary solvent manager, SQ mass spectrometer, Water 2996 PDA (PhotoDiode Array) detector, and ELSD (Evaporative Light Scattering Detector). An Acquity UPLC BEH C_{18} 1.7 μm column was used for analytical UPLC-MS. Optical rotations were recorded on an AUTOPOL III digital polarimeter at 589 nm, and specific rotations are given $[\alpha]_D^{20}$ (concentration in grams/100 mL solvent). SFC analysis of enantioenriched compounds was performed on a Berger SFC (Waters) System with a diode array detector using a SFC Chiralcel®OD-H (Chiral Technologies Inc., 100 × 4.6 mm I.D., 5μm) column. Preparative HPLC was performed on a Gilson PLC2020 using a Waters SunFire™ Prep C18 OBD™

5μm 19X50 mm column. Analytical thin layer chromatography was performed using 0.25 mm silica gel 60-F plates. Flash chromatography was performed using 200-400 mesh silica gel (Scientific Absorbents, Inc.). Yields refer to chromatographically and spectroscopically pure materials, unless otherwise stated. HPLC grade tetrahydrofuran, methylene chloride, diethyl ether, toluene, acetonitrile, and benzene were purchased from Fisher and VWR and were purified and dried by passing through a PURE SOLV® solvent purification system (Innovative Technology, Inc.). Other ACS grade solvents for chromatography were purchased from Fisher. Select photochemistry experiments were performed using a jacketed beaker covered in tape with spiralled blue LEDs strip ($h\nu$ = 450 nm) on the inside walls. A flow of cold water was used to cool the beaker down upon irradiation. All other reactions were carried out in oven-dried glassware under an argon atmosphere unless otherwise noted.

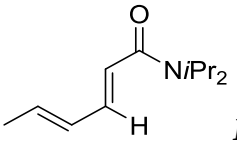

***N,N*-diisopropyl sorbate amide 174b:** prepared according to literature procedure.[185]

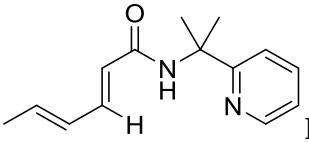

PIP sorbate amide 174c: To a flame-dried 250 mL round bottom flask, sorbic acid (from Aldrich) (653.9 mg, 5.8 mmol, 1.1 equiv.) was dissolved in anhydrous CH_2Cl_2 (20.00 mL). DMF (581.2 mg, 8.0 mmol, 618 μL, 1.5 equiv.) was added and at 0 °C, oxalyl chloride (706.55 mg, 5.57 mmol, 477.40 μL, 1.05 equiv.) was introduced dropwise. After stirring at room temperature for 4 hours, a solution of PIP amine (722.0 mg, 5.3 mmol, 1 equiv.) and triethylamine (590.1 mg, 5.8 mmol, 808 μL, 1.1 equiv.) in CH_2Cl_2 (20.00 mL) was added dropwise at 0°C.

Reaction was left to warm up overnight at room temperature, and then quenched with sat. $NaHCO_3$ solution. The aqueous phase was extracted 3 times with CH_2Cl_2, dried over sodium sulfate, concentrated *in vacuo* to yield a dark oil. Purification on silica gel (gradient of EtOAc in hexanes 5%, 10%, 15%, 20%, 30%) afforded the desired product as an off-white solid. $\mathbf{R_f}$ =0.12 (Hexanes/EtOAc 75:35, UV, $KMnO_4$); **Mp** 110-111 ˚C; **IR** νmax (film):3313, 3058, 2978, 2933, 1660, 1539, 1432, 1346, 1258, 1150, 997, 787 cm^{-1}; **^{1}H NMR** (400 MHz, $CDCl_3$) δ 8.51 (m, 1H), 7.76 (br s, 1H), 7.71 (td, *J* = 7.6, 1.6 Hz, 1H), 7.41 (d, *J* = 8.4 Hz, 1H), 7.19 (m, 1H), 7.16 (m, 1H), 6.18 (m, 1H), 6.06 (m, 1H), 5.9 (d, *J* = 14.8 Hz, 1H), 1.82 (d, *J* = 6.4 Hz, 3H), 1.79 (s, 6H); **^{13}C NMR** (101 MHz, $CDCl_3$) δ

165.5, 164.6, 147.6, 140.2, 137.0, 136.8, 129.8, 123.2, 121.8, 119.5, 56.5, 27.6, 18.4; **HR-MS**: *m/z* Calcd for $[C_{14}H_{18}ON_2+H]^+$ 231.1497, found .

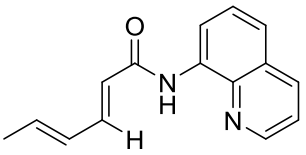

8-Aminoquinoline sorbate amide 174d: To a flame-dried 100 mL round bottom flask: sorbic acid (from Aldrich) (1.0 g, 9.1 mmol, 1.1 equiv.) was dissolved in CH_2Cl_2 (20 mL). DMF (912.5 mg, 12.5 mmol, 971 µL, 1.5 equiv.) was introduced and at 0 °C, oxalyl chloride (1.11 g, 8.7 mmol, 749 µL, 1.05 equiv.) was added dropwise.

After stirring at room temperature for 4 hours, a solution of quinolin-8-amine (1.20 g, 8.3 mmol, 1 equiv.) and triethylamine (926.1 mg, 9.2 mmol, 1.3 mL, 1.2 equiv.) in CH_2Cl_2 (20 mL) was added dropwise at 0 °C.

Reaction was left to warm up overnight at room temperature, and then quenched with sat. $NaHCO_3$ solution. The aqueous phase was extracted 3 times with CH_2Cl_2, dried over sodium sulfate, concentrated *in vacuo* to yield a dark oil.

Purification on silica gel (gradient of EtOAc in hexanes, 3%, 5%, 8%, 10%) yielded the desired as an off-white solid. $\mathbf{R_f}$ =0.24 (Hexanes/EtOAc 99:1, UV, $KMnO_4$); **Mp** 113-115 ˚C; **IR** νmax (film):3348, 1677, 1640, 1527, 1486, 1425, 1385, 1337, 1141, 997 cm^{-1}; **^{1}H NMR** (500 MHz, $CDCl_3$) δ 9.86 (s, 1H), 8.87 (dd, *J* = 7.6, 1.4 Hz, 1H), 8.17 (dd, *J* = 8.3, 1.7 Hz, 1H), 7.56 (t, *J* = 7.9 Hz, 1H), 7.50 (dd, *J* = 8.2, 1.4 Hz, 1H), 7.46 (dd, *J* = 8.3, 4.2 Hz, 1H), 7.40 (dd, *J* = 14.9, 10.6 Hz, 1H), 6.32-6.25 (m, 1H), 6.20 (m, 1H), 6.15 (m, 1H),

1.89 (d, *J* = 6.2 Hz, 3H), 1.79 (s, 6H); **^{13}C NMR** (101 MHz, $CDCl_3$) δ 164.6, 148.0, 142.3, 138.5, 138.4, 136.3, 134.7, 129.8, 127.9, 127.5, 122.4, 121.5, 121.4, 116.6, 18.6; **HR-MS**: *m/z* Calcd for $[C_{15}H_{14}ON_2+H]^+$ 239.1184, found 239.1184.

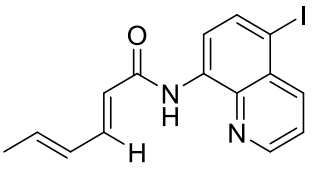

C_5-iodination product 177d: In a thick-wall microwave vial equipped with a stir bar under air: 8-aminoquinoline sorbate amide **174d** (10 mg, 42.0 μmol, 1 equiv.) was introduced, followed by $Pd(OAc)_2$ (0.47 mg, 2.10 μmol, 5 mol%), NIS (11.33 mg, 50.4 μmol, 1.2 equiv.), *p*-TSA.H_2O (3.99 mg, 21 μmol, 50 mol%). Dry toluene (600 μL) was added and the reaction was heated at 110 °C for 12 h. TLC (hexanes/EtOAc 7:3, UV+$KMnO_4$) showed incomplete conversion to an upper spot. The crude mixture was concentrated *in vacuo* and purified on silica gel (Hex/EtOAc 9:1 85:15, 4:1, 7:3) to afford the desired as a yellow solid (4.7 mg, 12.91 umol, 30%). **R_f** =0.45 (hexanes/EtOAc 9:1, UV, $KMnO_4$); **Mp** 136-137 ˚C; **IR** νmax (film):3340, 2959, 2924, 2869, 1679, 1516, 1473, 1380, 1356, 1315, 1260, 1136, 980 cm^{-1}; **^{1}H NMR** (500 MHz, $CDCl_3$) δ 9.86 (br s, 1H) 8.75 (dd, *J* = 4.4, 1.6 Hz, 1H), 8.59 (d, *J* = 8.0 Hz, 1H), 8.35 (dd, *J* = 8.8, 2.0 Hz, 1H), 8.06 (d, *J* = 8.4 Hz, 1H), 7.52 (dd, *J* = 8.8, 4.0 Hz, 1H), 7.36 (dd, *J* = 14.8, 10.4 Hz, 1H), 6.22 (m, 1H), 6.19 (m, 1H), 6.11 (d, *J* = 14.8 Hz, 1H), 1.89 (d, *J* = 6.0 Hz, 3H); **^{13}C NMR** (101 MHz, $CDCl_3$) δ 164.6, 148.6, 142.7, 140.7, 139.0 (2C overlap), 138.3, 135.5, 129.7, 129.5, 123, 122, 118.0, 89.0, 18.7; **HR-MS**: *m/z* Calcd for $[C_{15}H_{13}OIN_2+H]^+$ 365.0151, found 365.0146.

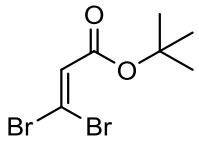

***Tert*-butyl 3,3-dibromoacrylate 175.**

Preparation of pure, dehydrated tert-butyl glyoxylate:

Di-*tert*-butyl tartrate was synthesized according to reported literature procedures.[190,231]

The *tert*-butyl glyoxylate was synthesized using a modified literature procedure.[190]

Di-*tert*-butyl tartrate (11.30 g, 43.1 mmol, 1 equiv.)[190] was dissolved in methanol (220 mL). Using an addition funnel, a solution of sodium metaperiodate (11.06 g, 51.7 mmol, 1.2 equiv.) in water (80 mL) was added at 0 °C dropwise. After 3 hours, TLC showed complete conversion (hexanes/ethyl acetate 7/3, $KMnO_4$).

Et_2O (200 mL) and H_2O (100 mL) were added, the phases were separated and the water phase was extracted once with Et_2O (100mL). The combined organic layers were dried over Na_2SO_4 and filtered. Concentration under cold conditions gave a crude mixture, still containing methanol, which is dried a second time using sodium sulfate, concentrated *in vacuo* with a room temperature water bath. It was then redissolved in ether (200 mL) transferred to a separatory funnel, and washed with a minimal amount of water (2x20 mL) to pull the remaining methanol out of the organic phase. The ether layer was dried again, concentrated under cold water bath to give a yellow crude oil. After concentration in a 100 mL flask, the aldehyde was transferred in a Kugelrohr receiving flask, which was put under high vacuum at room temperature for 20 minutes, then cooled to -78 °C. 3 spatula portions of P_2O_5 were added at -78°C to control the exothermic dehydration reaction. The crude

mixture was then distilled under high vacuum using a Kugelrohr distillation apparatus (120 °C, 50 rpm) to yield a clear oil, kept cold at -78 °C.

Preparation of the gem-dibromoolefin 169 from tert-butyl glyoxylate

To a flame-dried two-neck 1L flask equipped with a 125 mL addition funnel:

carbon tetrabromide (57.08 g, 172.1 mmol, 2 equiv.) and zinc (0) (11.26 g, 172.1 mmol, 2 equiv.) were added, the apparatus was purged with a vaccum/nitrogen cycle 3 times. before adding dry CH_2Cl_2 (300 mL). Triphenylphosphine (45.15 g, 172.1 mmol, 2 equiv.) was added into the addition funnel, and dissolved with CH_2Cl_2 (180 mL).

At 0 °C, the homogenous solution of phosphine was added over 45 minutes. The reaction was stirred at room temperature for 20 minutes, turning yellow upon triphenylphosphine addition, and red-orange by the end of the addition.

The aldehyde, kept at -78°C in its receiving flask from the distillation, was diluted with portions of dry CH_2Cl_2, transferred *via* cannula to the addition funnel, rinsed several times (total volume of CH_2Cl_2 300 mL). This cold solution of aldehyde was then added over 30 minutes at 0°C into the reaction flask. The reaction was left to warm up to room temperature and stirred for 48 h.

Hexanes was added to precipitate the phosphine oxide and the crude was filtered over celite, rinsing thoroughly the reddish slurp with hexanes, then ethyl acetate. Purification on silica gel (Hexanes/EtOAc 100:0, 99:1, 98:2) afforded the desired product as a yellow oil $\mathbf{R_f}$ =0.1 (Hexanes/EtOAc 99.5:0.5, UV, $KMnO_4$); **IR** νmax (film):3053, 2978, 2930, 1721, 1591, 1477, 1453, 1368, 1301, 1136, 972, 866, 849, 822, 756, 690 cm^{-1}; **^{1}H NMR** (400 MHz, $CDCl_3$) δ 6.8 (s, 1H), 1.5 (s, 9H); **^{13}C NMR** (126 MHz, $CDCl_3$) δ 162.1, 129.6,

104.7, 82.2, 28.1; **HR-MS**: *m/z* Calcd for $[C_7H_{10}O_2Br_2+H]^+$ 284.9126, found no ionization for this compound.

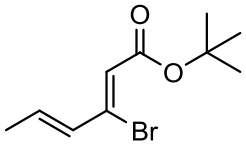

***T*ert-butyl bromosorbate 172:** In a flame-dried, 500 mL 3-neck round bottom flask under nitrogen, Pd_2dba_3 (250.7 mg, 273.9 μmol, 3 mol%), P(2-Furyl)$_3$ (423.8 mg, 1.8 mmol, 20 mol%) and CuI (347.7 mg, 1.83 mmol, 20 mol%) were added, and flask was purged 3 times with a vacuum/nitrogen cycle.

In a separate flame-dried 250 mL round bottom flask, *tert*-butyl 3,3-dibromoacrylate **175** (2.61 g, 9.1 mmol, 1 equiv.) and tributyl-[(*E*)-prop-1-enyl]stannane[193] (3.33 g, 10.0 mmol, 1.1 equiv.) were introduced under argon. Rigorously degassed (*via* freeze-pump-thaw cycle 3 times) toluene (100 mL) was added under argon and the resulting diluted solution of starting materials were transferred to the main round bottom flask *via* cannula.

The reaction was moved to an oil bath and heated at 90 °C for 4.5 hours, after which time a ^{1}H NMR crude aliquot of the reaction showed complete conversion of the *gem*-dibromo olefin starting material (starting material and product have identical Rf in EtOAc/Hexanes eluent system). The crude reaction was quenched with 15% aqueous KF solution, extracted with EtOAc 3 times, washed with brine, dried over Na_2SO_4, and concentrated *in vacuo*. Purification on silica gel doped with 15% w/w solid KF (hexanes/EtOAc 100:0, 99:1, 98:2) afforded the desired product as a yellow oil (1.90 g, 7.69 mmol, .84%).

R_f =0.1 (Hexanes/EtOAc 99.5:0.5, UV, $KMnO_4$); **IR** νmax (film):2977, 2933, 1719, 1476, 1451, 1391, 1367, 1257, 1144, 952, 853 cm^{-1}; **^{1}H NMR** (500 MHz, $CDCl_3$) δ 6.52 (dq, *J* = 14.0, 7.0 Hz 1H), 6.21 (s, 1H), 6.11 (dq, *J* = 14.0, 2.0 Hz 1H), 1.91 (dd, *J* = 7.0, 2.0 Hz 1H), 1.51 (s, 9H); **^{13}C NMR** (126 MHz, $CDCl_3$) δ 164.1, 138.4, 134.0, 130.6, 120.9, 81.1, 28.2 (3C), 18.0; **HR-MS**: *m/z* Calcd for $[C_{10}H_{15}O_2Br+H]^+$ 247.0334, found no ionization for this compound.

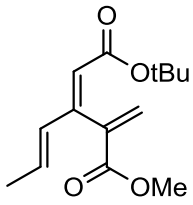

Coupling product 180: In a flame-dried 250 mL Schlenk flask under nitrogen: *tert*-butyl bromosorbate **172** (1.53 g, 6.19 mmol, 1 equiv.), methyl 2-tributylstannylprop-2-enoate **179**[196] (5.11 g, 13.62 mmol, 2.2 equiv.), palladium tetrakis (715.42 mg, 619.11 umol, 10 mol%) and copper iodide (884.32 mg, 4.64 mmol, 0.75 equiv., previously dried under high vacuum with a heatgun) were dissolved in dry, degassed (freeze-pump-thaw cycle, 3x) DMF (70.00 mL). The flask was heated at 60 °C for 3h. Reaction was assessed complete by crude ^{1}H NMR of an aliquot. 10% aqueous KF solution was added (50 mL) and the crude was diluted with ethyl acetate. The aqueous layer was extracted with EtOAc (50 mL x2), and the combined organic layers were washed with water (50 mL) to pull out most of the DMF. The organic layer was dried over sodium sulfate, concentrated *in vacuo* and dry loaded on silica gel (hexanes/EtOAc 99.5:0.5, 99:1, 98:2, 97:3, 96:4, 95:5, 9:1, 85:15, 8:2, 7:3) to afford the desired as a viscous yellow oil. **R_f** = 0.18 (Hexanes/EtOAc 95:5, UV, $KMnO_4$); **IR** νmax (film): 2978, 2952, 2854, 1727,

1705, 1638, 1589, 1437, 1392, 1366, 1291, 1237, 1138, 1040, 987, 965, 934, 877, 814 cm^{-1}; **^{1}H NMR** (500 MHz, $CDCl_3$) δ 6.51 (d, *J* = 1.4 Hz, 1H), 6.22 (d, *J* = 14.0 Hz, 1H), 5.97 (dq, *J* = 14.0, 6.5 Hz, 1H), 5.72 (s, 1H), 5.51 (d, *J* = 1.4 Hz, 1H), 3.74 (s, 2H), 1.82 (d, *J* = 6.5 Hz, 3H); **^{13}C NMR** (126 MHz, $CDCl_3$) δ 165.8, 165.5, 148.7, 137.5, 134.8, 132.8, 127.2, 120.7, 80.4, 52.0, 28.0 (3C), 18.5; **HR-MS**: *m/z* Calcd for $[C_{14}H_{20}O_4+Na]^+$ 275.1259, found 275.1259.

TFA deprotection of coupling product 180: In a 100 mL round bottom flask, acrylate **180** (1.20 g, 4.76 mmol, 1 equiv.) was dissolved in CH_2Cl_2 (45.00 mL). At room temperature, trifluoroacetic acid (recent bottle, 1.63 g, 14.28 mmol, 1.09 mL, 3 equiv.) was added, and after 5 hours, TLC showed complete conversion (hexanes/EtOAc 3:7). The crude mixture was concentrated *in vacuo*, and TFA was azeotroped with toluene (3x) under vacuum. Crude ^{1}H NMR showed complete conversion to a mixture of the opened carboxylic acid and closed lactone form. Purification on silica gel (hexanes/EtOAc 9:1, 8:2, 7:3, 6:4, 1:1) afforded carboxylate **181** (228 mg, 1.16 mmol, 24%, upper spot, Rf = 071, Hexanes/EtOAc 75:25, UV, $KMnO_4$) and lactone **182** (313.0 mg, 1.6 mmol, 33%, lower spot) as yellow oils. Compound **181** (228 mg, 1.16 mmol, 1 equiv.) was further thermalized in toluene (20 mL) for 16 h. Concentration of the crude mixture *in vacuo* followed by silica gel purification (hexanes/EtOAc 9:1, 8:2, 7:3, 6:4, 1:1) afforded the lactonized product **182** (85 mg, 0.43 mmol, 37%).

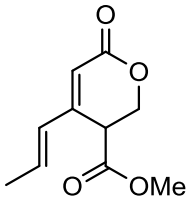

Lactone 182: R_f =0.11 (Hexanes/EtOAc 75:25, UV, $KMnO_4$); **IR** νmax (film): 2954, 2919, 2853, 1726, 1644, 1605, 1440, 1378, 1306, 1255, 1220, 1089, 970, 873, 808 cm^{-1}; **^{1}H NMR** (500 MHz, $CDCl_3$) δ 6.29 – 6.15 (m, 2H), 5.93 – 5.89 (m, 1H), 4.75 (dd, *J* = 11.5, 1.5 Hz, 1H), 4.45 (dd, *J* = 11.5, 4.2 Hz, 1H), 3.75 (s, 3H), 3.50 (dd, *J* = 4.2, 1.5 Hz, 1H), 1.91 (d, *J* = 6.0 Hz, 3H); **^{13}C NMR** (126 MHz, $CDCl_3$) δ 169.4, 164.2, 149.8, 136.1, 129.5, 116.8, 67.9, 53.1, 40.4, 18.9 ; **HR-MS**: *m/z* Calcd for $[C_{10}H_{12}O_4+H]^+$ 197.0814, found 197.0815.

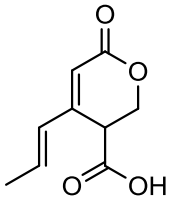

Carboxylic acid substituted lactone 122: In a flame-dried thick wall microwave vial under argon, lactone **182** (33.5 mg, 170.7 μmol, 1 equiv.) was introduced. In the glove box, magnesium iodide (95.0 mg, 341.5 μmol, 2 equiv., new bottle kept inside the glovebox and covered in aluminum foil) was transferred into the vial. Dry toluene (1.5 mL) was added, before an argon balloon was bubbled through the vial while sonicating the mixture simultaneously for 30 minutes, to ensure proper degassing and activation of the magnesium surface. The vial was then sealed and heated at 110 °C overnight, in the dark. TLC showed disappearance of starting material and base line spot (CH_2Cl_2/MeOH 95:5). The crude is quenched with 1M HCl, extracted with CH_2Cl_2 (3x), dried and concentrated

in vacuo. Crude ^{1}H NMR showed complete conversion to the carboxylic acid. Purification on silica gel with first EtOAc/Hexanes (1:1 then 100:0), and then a gradient of MeOH in CH_2Cl_2 (from 5% to 20%) afforded the polar desired compound as a yellow viscous gum (12.0 mg, 65.9 μmol, 37%). **R_f** =0.1 (CH_2Cl_2/MeOH 95;5, UV, $KMnO_4$); **IR** νmax (film): 3427, 2930, 2856, 2252, 1696, 1641, 1593, 1411, 1381, 1282, 1244, 118, 1087, 966, 911, 869 cm^{-1}; **^{1}H NMR** (500 MHz, $CDCl_3$) δ 6.26-6.24 (m, 2H), 5.93 (s, 1H), 4.80 (d, *J* = 11.5 Hz, 1H), 4.47 (dd, J = 11.5, 4.0 Hz, 1H), 3.53 (d, J = 4.0 Hz, 1H), 1.93 (d, *J* = 5.0 Hz, 3H); **^{13}C NMR** (126 MHz, $CDCl_3$) δ 166.6, 157.4, 154.6, 136.9, 129.9, 114.5, 69.9, 42.6, 18.9; **HR-MS**: *m/z* Calcd for $[C_9H_{10}O_4+H]^+$ 183.0579, found 183.0582.

Cross-coupling of stannylated alcohol 183 and bromo sorbate 172: In a flame-dried microwave vial under argon: palladium tetrakis (21.04 mg, 18.21 μmol, 10 mol%) was introduced inside the glovebox followed by *tert*-butyl bromosorbate **172** (45.00 mg, 182.09 μmol, 1 equiv.) and stannane **183**[196] (126.41 mg, 364.18 μmol, 2 equiv.). Flask was purged with argon, before copper iodide (previously dried under high vacuum with a heat gun, 26.01 mg, 136.57 μmol) was added. Dry DMF (2.00 mL) was transferd *via* syringe and the whole mixture was degassed by bubbling argon through for 15 minutes. The reaction was stirred at 40 °C overnight under argon, after which time TLC showed complete conversion (hexanes/EtOAc 85:15, UV, $KMnO_4$). The crude was quenched with 15% KF aqueous solution, extracted with EtOAc (2x), dried over sodium sulfate, filtered and concentrated *in vacuo*. Purification on a mixture of 15% w/w ground KF on SiO_2 (gradient of hexanes/EtOAc 98:2, 95:5, 90:10, 88:12, 86:14, 85:15) enabled isolation of the desired

alcohol **184** (14.00 mg, 62.42 μmol, 34%) and the undesired lactonization product **185** (12.00 mg, 79.9 μmol, 43%) as yellow oils.

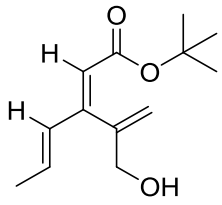

Alcohol coupling product 184: R_f =0.28 (Hexanes/EtOAc 4:1, UV, $KMnO_4$); **IR** νmax (film):3431, 2977, 2931, 2857, 1692, 1592, 1452, 1367, 1293, 1247, 1137, 1053, 966 cm^{-1}; **^{1}H NMR** (400 MHz, $CDCl_3$) δ 6.01 (app d, *J* = 15.6 Hz, 1H), 5.99 (dq, *J* = 15.6, 6.4 Hz, 1H), 5.69 (s, 1H), 5.37 (d, *J* = 1.2 Hz, 1H), 4.88 (d, *J* = 1.2 Hz, 1H), 4.20 (d, *J* = 5.6 Hz, 2H), 3.47 (t, *J* = 5.6 Hz, 1H), 1.81 (dd, *J* = 6.4, 0.8 Hz, 3H), 1.45 (s, 9H); **^{13}C NMR** (101 MHz, $CDCl_3$) δ 153.3, 145.6, 135.3, 132.1, 120, 114.6, 80.9, 66.7, 28.1 (3C), 18.5; **HR-MS**: $[M+H]^+$ calculated for $[C_{13}H_{20}O_3+H]^+$ 225.1491, found 225.1509.

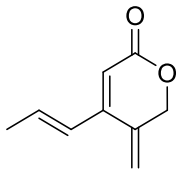

Lactonized coupling product 185: R_f =0.24 (Hexanes/EtOAc 4:1, UV, $KMnO_4$); **IR** νmax (film): 3436, 2974, 2931, 2876, 1706, 1648, 1578, 1395, 1291, 1221, 1054, 966, 933, 872 cm^{-1}; **^{1}H NMR** (500 MHz, $CDCl_3$) δ 6.37 (dq, *J* = 15.6, 6.7 Hz, 1H), 6.17 (ddd, *J* = 15.6, 1.5, 0.9 Hz, 1H), 5.94 (d, *J* = 0.9 Hz, 1H), 5.58 (dd, *J* = 1.0, 2.0 Hz, 1H), 5.45 (dd, *J* = 1.0, 3.0 Hz, 1H), 4.85 (m, 2H), 1.92 (dd, *J* = 6.7, 1.5 Hz, 1H); **^{13}C NMR**

(126 MHz, $CDCl_3$) δ 164.9, 150.1, 136.3, 135.6, 125.2, 117.62, 113.3, 70.9, 19.0; **HR-MS**: $[M+H]^+$ calculated for $[C_9H_{10}O_2+H]^+$ 151.0759, found 151.0753.

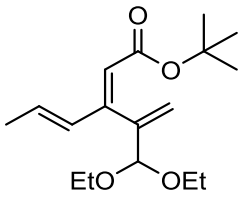

Diethyl acetal protected coupling product 191: In a 50 mL Schlenk flask under nitrogen, palladium tetrakis (79.49 mg, 68.79 μmol, 10 mol%) was introduced in the glove box, followed by copper iodide (98.26 mg, 515.92 μmol, 0.75 equiv.) (previously dried under high vacuum with a heat gun), *tert*-butyl bromosorbate **172** (170.00 mg, 687.90 μmol, 1 equiv.) and stannane **190**[196] (557.47 mg, 1.38 mmol, 2 equiv.). Dry, distilled DMF (8.00 mL) was degassed *via* freeze-pump-thaw cycle (3x), and then cannulated to the Schlenk flask containing the catalysts and substrates. The flask was transferred to an oil bath heated at 60 °C, and stirred 12 hours. Crude ^{1}H NMR of an aliquot showed complete conversion. Reaction was quenched with 15% KF aqueous solution, extracted with EtOAc (2x), dried over sodium sulfate, filtered and concentrated *in vacuo*. Purification on a mixture of 15% w/w ground KF on SiO_2 (hexanes/EtOAc 99:1, 98:2, 95:5, 92:8, 90:10, 88:12, 86:14, 85:15) yielded the desired as a yellow oil (103.50 mg, 350 μmol, 50%). $\mathbf{R_f}$ =0.30 (Hexanes/EtOAc 95:5, UV, $KMnO_4$); **IR** νmax (film): 2975, 2929, 1708, 1588, 1448, 1367, 1290, 1135, 1061, 966, 870 cm^{-1}; **^{1}H NMR** (400 MHz, $CDCl_3$) δ 6.10-6.13 (m, 2H), 5.67 (d, *J* = 1.0 Hz, 1H), 5.61 (s, 1H), 5.05 (s, 1H), 4.98 (d, *J* = 1.0 Hz, 1H), 3.70 (q, *J* = 7.0 Hz, 2H), 3.53 (q, *J* = 7.0 Hz, 2H), 1.81 (d, *J* = 7.5 Hz, 3H), 1.44 (s, 9H), 1.18 (t, *J* = 7.0 Hz, 6H).; **^{13}C NMR** (126 MHz, $CDCl_3$) δ 165.5, 152.9, 142.9, 135.2,

133.3, 118.8, 115.0, 79.9, 79.7, 62.7 (2C), 28.14 (3C), 18.5, 15.1 (2C); **HR-MS**: $[M+H]^+$ calculated for $[C_{17}H_{28}O_4+H]^+$ 297.2066, found no ionization for this compound.

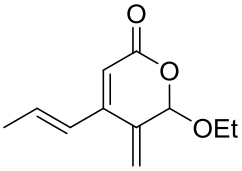

Acetal lactone 192: In a 10 ml round bottom flask, diethyl acetal product **191** (15.10 mg, 50.94 μmol, 1 equiv.) was dissolved in CH_2Cl_2 (1 mL). At 0°C, trifluoroacetic acid (11.6 mg, 102 μmol, 2 equiv.) was introduced *via* syringe. The reaction immediately turned yellow. TLC (hex/EtOAc) shows complete conversion. The reaction was directly concentrated *in vacuo*, and reconcentrated with toluene (2x) to azeotrope TFA. Crude was purified on silica gel (Hexanes/EtOAc 9:1, 8:2, 7:3, 6:4) to isolate desired as a clear oil (7.4 mg, 38.10 μmol, 74%). $\mathbf{R_f}$ = 0.22 (Hexanes/EtOAc 85:15, UV, $KMnO_4$); **IR** νmax (film): 2978, 2930, 1716, 1648, 1581, 1443, 1395, 1225, 1103, 973, 872, 618 cm^{-1}; **^{1}H NMR** (500 MHz, $CDCl_3$) δ 6.39 (dq, *J* = 15.5, 6.5 Hz, 1H), 6.19 39 (d, *J* = 15.5 Hz, 1H), 5.94 (s, 1H), 5.70 (s, 1H), 5.64 (s, 1H), 5.63 (s, 1H), 4.00 (dq, *J* = 9.5, 7.0 Hz, 1H), 3.71 (dq, *J* = 9.5, 7.0 Hz, 1H), 1.91 (dd, *J* = 6.5, 1.7 Hz, 3H), 1.25 (t, *J* = 7.0 Hz, 3H).; **^{13}C NMR** (126 MHz, $CDCl_3$) δ 163.7, 148.0, 136.6, 136.3, 125.7, 120.0, 112.8, 101.8, 64.9, 19.0, 15.0; **HR-MS**: $[M+H]^+$ calculated for $[C_{11}H_{14}O_3+H]^+$ 195.1021, found 195.1030.

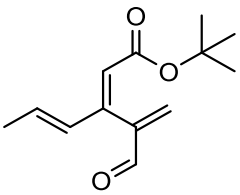

Acrylate 193: In a 50 mL round bottom flask, diethyl acetal **191** (383.30 mg, 1.29 mmol, 1 equiv.) was dissolved in THF (10.00 mL). At room temperature,

HCl (1 M, 1.94 mL, 1.5 equiv.) was added, and reaction was heated at 40 °C. After 3 hours TLC (hex/EtOAc 9:1) showed complete conversion to a lower spot. The reaction was quenched with water, extracted with EtOAc (3x), dried over Na_2SO_4 and concentrated *in vacuo.* The yellow crude oil was purified on silica gel (Hex/EtOAc, 99:1, 98:2, 96:4 plateau, 95:5, 9:1, 8:2) to afford the desired compound as a yellow oil (172 mg, 774 μmol, 60%). **R_f** = 0.39 (Hexanes/EtOAc 9:1, UV, $KMnO_4$); **IR** νmax (film): 2976, 2921, 2853, 1705, 1638, 1589, 1456, 1368, 1290, 1260, 1120, 1140, 964, 873 cm^{-1}; **^{1}H NMR** (400 MHz, $CDCl_3$) δ 9.59 (s, 1H), 6.32 (d, *J* = 0.8 Hz, 1H),), 6.23 (d, *J* = 15.5 Hz, 1H), 6.14 (d, *J* = 0.8 Hz, 1H), 5.85 (dq, *J* = 15.5, 8.5 Hz, 1H), 5.80 (s, 1H), 1.80 (dq, *J* = 8.5, 1.5 Hz, 3H), 1.41 (s, 9H); **^{13}C NMR** (126 MHz, $CDCl_3$) δ 191.2, 165.2, 146.7, 135.0, 133.1, 132.4, 121.1, 110.0, 80.5, 28.1 (3C), 18.5; **HR-MS**: $[M+H]^+$ calculated for $[C_{13}H_{18}O_3+H]^+$ 283.1334, found 283.1346.

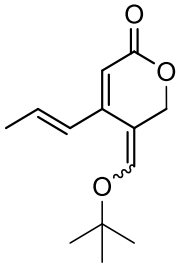

***Tert*-butyl enol 114b:** In a flamed dried 10 mL Schlenk flask under argon: acrylate **189** (20.0 mg, 90 μmol, 1 equiv.) was dissolved in CH_2Cl_2 (1.5 mL). The reaction was cooled down to -78 °C. After 5 minutes, trimethylsilyl triflate (new bottle, freshly distilled using a Hickman apparatus under high vacuum at room temperature) (4.00 mg, 18.00 μmol, 3.26 μL, 0.2 equiv.) was added at -78 °C. Upon addition of TMSOTf, the reaction turned immediately yellow. TLC (Hex/EtOAc 8:2) after 15 minutes shows

incomplete conversion. Reaction was transferred to an ice bath, and stirred 15 minutes at 0 °C. TLC (Hex/EtOAc 6:4) after 15 minutes indicated complete conversion. The reaction was quenched with aqueous saturated NH_4Cl, extracted with CH_2Cl_2 (15 mLx2), dried and concentrated *in vacuo.* Crude ^{1}H NMR showed clean conversion to *tert*-butyl enol ether cyclized product **114b** as a single enol ether isomer (stereochemistry not assigned) (crude yield 10.6 mg, 47.7 μmol, 53%)**.** This compound degrades upon silica gel purification, thus it is better used as is. Efforts to reproduce the synthesis of **114b** were met with limited success and consequently this compound could only be characterized by ^{1}H NMR. $\mathbf{R_f}$ = 0.10 (Hexanes/EtOAc 4:1, UV, $KMnO_4$); **^{1}H NMR** (400 MHz, $CDCl_3$) δ 6.88 (d, J = 1.5 Hz, 1H), 6.37 – 6.23 (m, 1H), 6.08 (dq, J = 19.5, 1.5 Hz, 1H), 5.66 (s, 1H), 4.98 (m, 2H), 1.90 (dd, J = 6.5, 1.5 Hz, 3H) 1.36 (s, 9H).

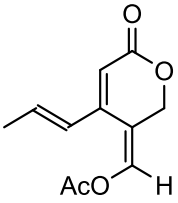

Enol acetate 114c: In a flame-dried thick wall microwave vial under argon: *tert*-butyl bromosorbate **172** (37.0 mg, 166.5 μmol, 1 equiv.) was dissolved in acetic anhydride (2 mL). Bismuth triflate (5.5 mg, 8.3 μmol, 5 mol%) was then added. The reaction turned immediately dark orange and was heated at 60 °C. After 2 h, full conversion by TLC (Hex/EtOAc 95:5, eluted twice to see separation of starting material from product) was observed. The reaction was diluted with EtOAc and water, transferred to a separatory funnel and the organic phase was collected. The aqueous phase was extracted once with EtOAc. Washing of the organic phase with aqueous $NaHCO_3$ (2x) removed most of the

acetic acid. Drying and concentration of the organic phase afforded a crude oil that solidified to needles upon standing. Purification on SiO_2 (hex/EtOAc 99:1, 98:2, 96:4, 95:5, 9:1, 8;2, 7;3, 1;1, 4:6, 0:100) yielded a major compound as an off-white solid (12.00 mg, 57.6 μmol, 71%). **R_f** =0.37 (Hexanes/EtOAc 3:2, UV, $KMnO_4$); **Mp** 118-119 ˚C; **IR** νmax (film):3091, 2957, 2936, 2919, 2867, 1704, 1629, 1391, 1360, 1225. 1024, 897 cm^{-1}; **^{1}H NMR** (400 MHz, $CDCl_3$) δ 7.50 (ap s, 1H), 6.47 (dq overlap, *J* = 15.5, 6.5 Hz, 1H), 6.33 (s, 1H), 6.25 (ap d, *J* = 15.5 Hz, 1H), 4.83 (s, 2H), 2.08 (s, 3H), 1.94 (dd, *J* = 6.5, 1.5 Hz, 3H); **^{13}C NMR** (100 MHz, $CDCl_3$) δ 170.4, 161.9, 152.5, 151.4, 136.8, 124.2, 113.6, 109.2, 59.5, 20.8, 19.1; **HR-MS**: $[M+H]^+$ calculated for $[C_{13}H_{18}O_3+H]^+$ 209.0814, found 209.0816.

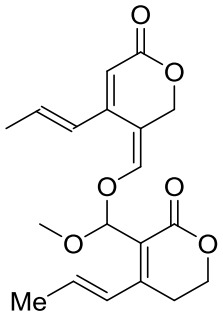

Acetal lactone 197: In a thick wall microwave vial under argon, enol acetate **114c** (12.0 mg, 57.6 μmol, 1 equiv.) and *2H*-pyran **115** (11.5 mg, 69.2 μmol, 2 equiv.) were dissolved in MeOH (700 μL). At 0 °C, potassium carbonate (9.6 mg, 69.2 μmol, 1 equiv.) was introduced at once. Reaction turned from a white slurry to yellow immediately. The reaction was left to stir at room temperature for 30 minutes, after which time TLC (hex/EtOAc 6:4, UV, $KMnO_4$) showed minor conversion.

One more equivalent of potassium carbonate was added. Reaction was heated at 40 °C for 1 hour. It was quenched with ammonium chloride, diluted with CH_2Cl_2 and extracted (2x) with CH_2Cl_2. After concentration, crude ^{1}H NMR showed cleavage of the acetate, and the presence of a few products. Silica gel purification (9:1, 8:2, 7:2, 6:4, 1:1) afforded the acetal lactone **197** as a clear oil (3.4 mg, 9.8 μmol, 17%). Efforts to reproduce the synthesis of **197** were met with limited success and consequently this compound could only be characterized by ^{1}H NMR. $\mathbf{R_f}$ =0.15 (Hexanes/EtOAc 3:2, UV, $KMnO_4$); **^{1}H NMR** (500 MHz, $CDCl_3$) δ 7.39 (s, 1H), 6.48 (dq, *J* = 15, 6.5 Hz, 1H), 6.33 (dq, *J* = 15.5, 1.0 Hz, 1H), 6.33 (m, 1H), 6.22 (s, 1H), 6.22 (m, 1H), 5.78 (s, 1H), 4.40 (t, *J* = 6.0 Hz, 2H), 4.15 (s, 2H), 3.36 (s, 3H), 2.57-2.52 (m, 2H), 1.94 (dd, *J* = 6.5, 1.5 Hz, 3H), 1.90 (d, *J* = 5 Hz, 3H).

Selected Spectra

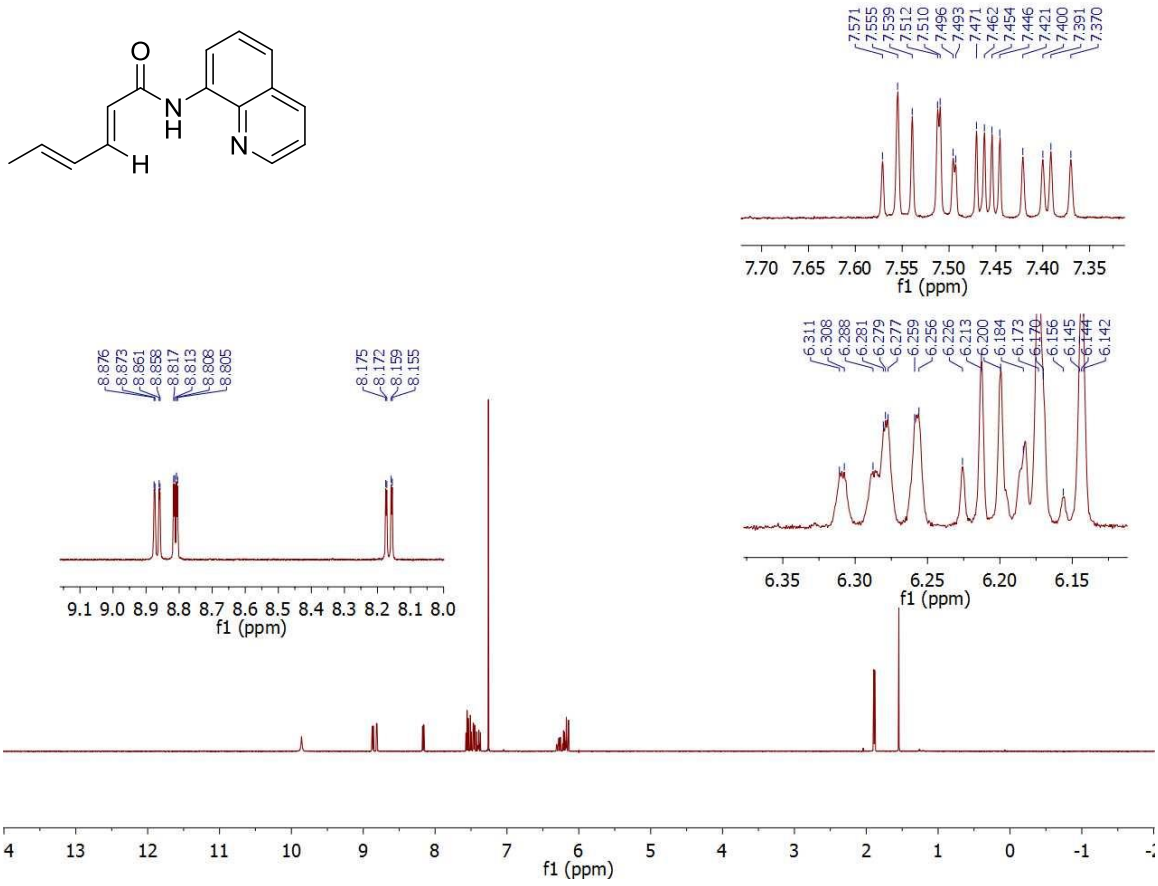

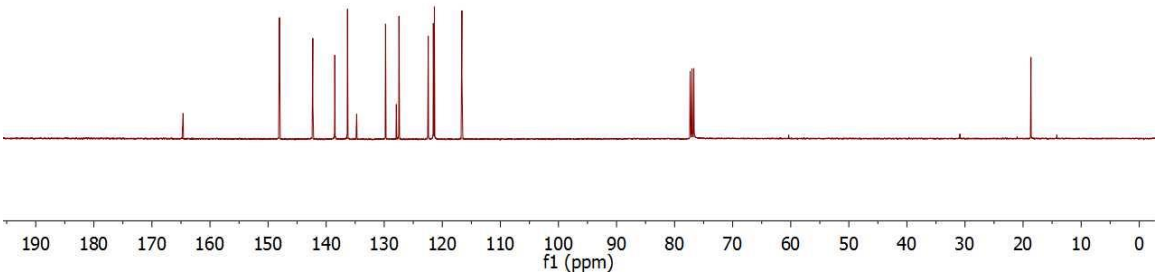

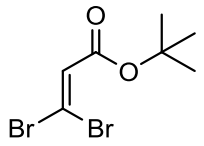
O
O
Br
Br

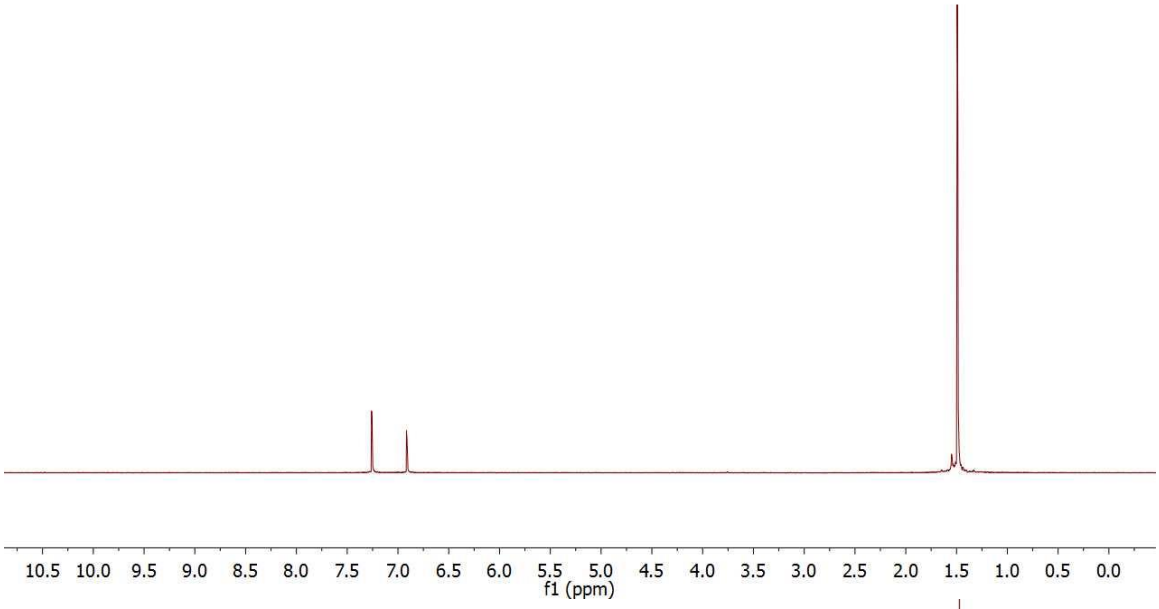
10.5 10.0 9.5 9.0 8.5 8.0 7.5 7.0 6.5 6.0 5.5 5.0 4.5 4.0 3.5 3.0 2.5 2.0 1.5 1.0 0.5 0.0
f1 (ppm)

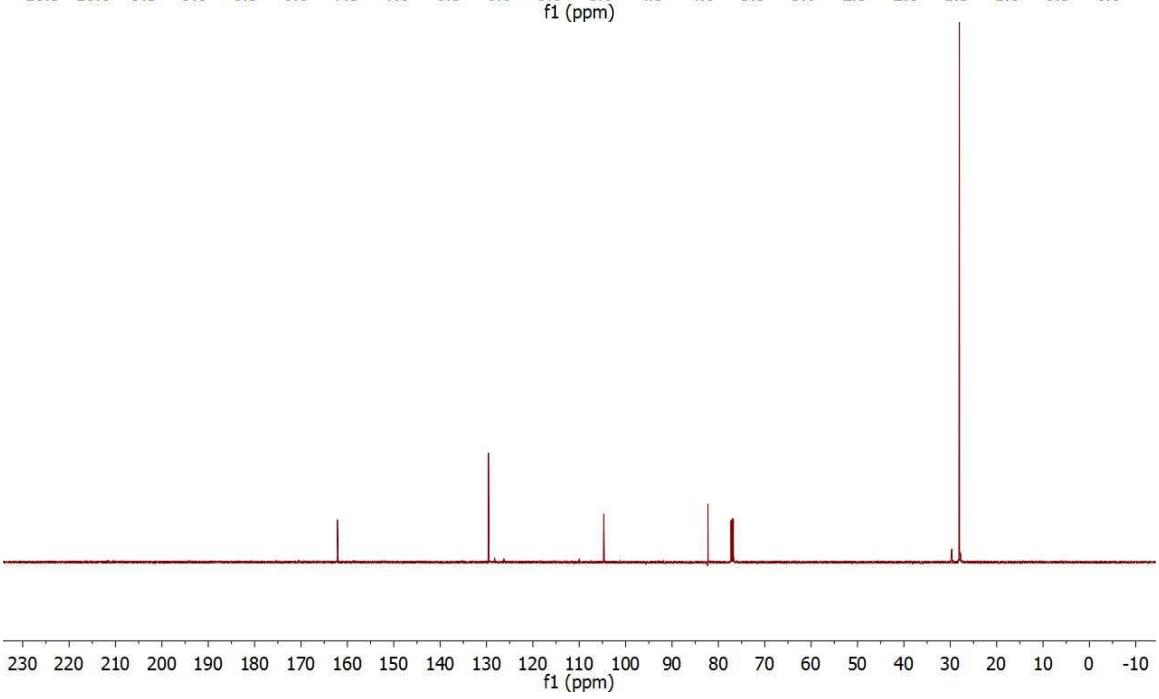
230 220 210 200 190 180 170 160 150 140 130 120 110 100 90 80 70 60 50 40 30 20 10 0 -10
f1 (ppm)

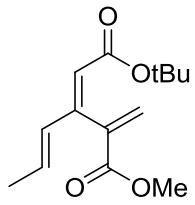
O
OtBu
O
OMe

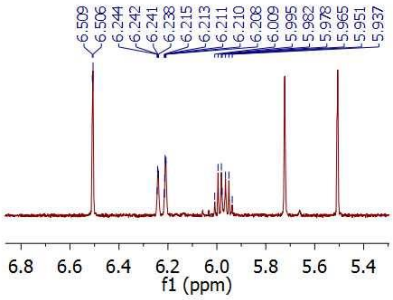
6.509
6.506
6.244
6.242
6.241
6.238
6.215
6.213
6.211
6.210
6.208
6.009
5.995
5.982
5.978
5.965
5.951
5.937
6.8 6.6 6.4 6.2 6.0 5.8 5.6 5.4
f1 (ppm)

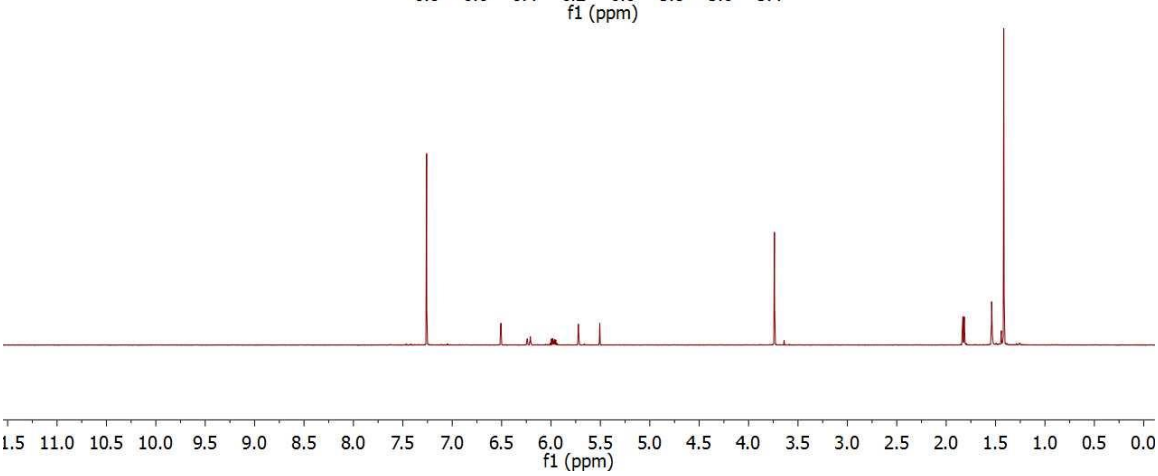
1.5 11.0 10.5 10.0 9.5 9.0 8.5 8.0 7.5 7.0 6.5 6.0 5.5 5.0 4.5 4.0 3.5 3.0 2.5 2.0 1.5 1.0 0.5 0.0
f1 (ppm)

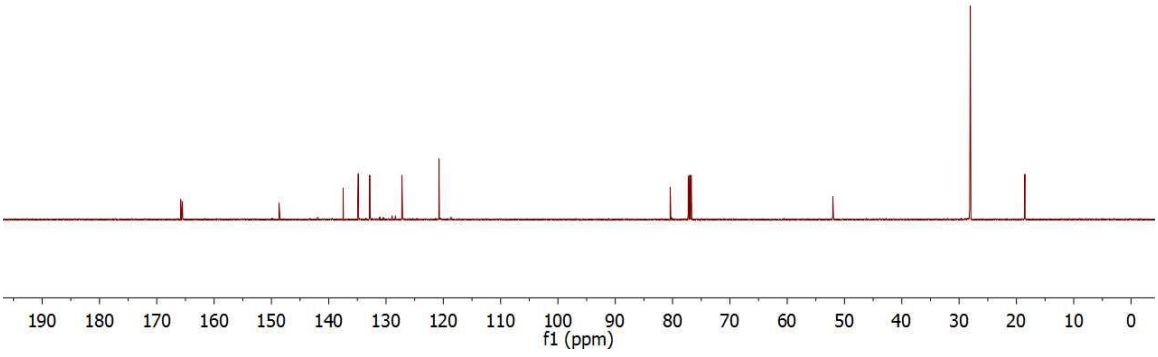
190 180 170 160 150 140 130 120 110 100 90 80 70 60 50 40 30 20 10 0
f1 (ppm)

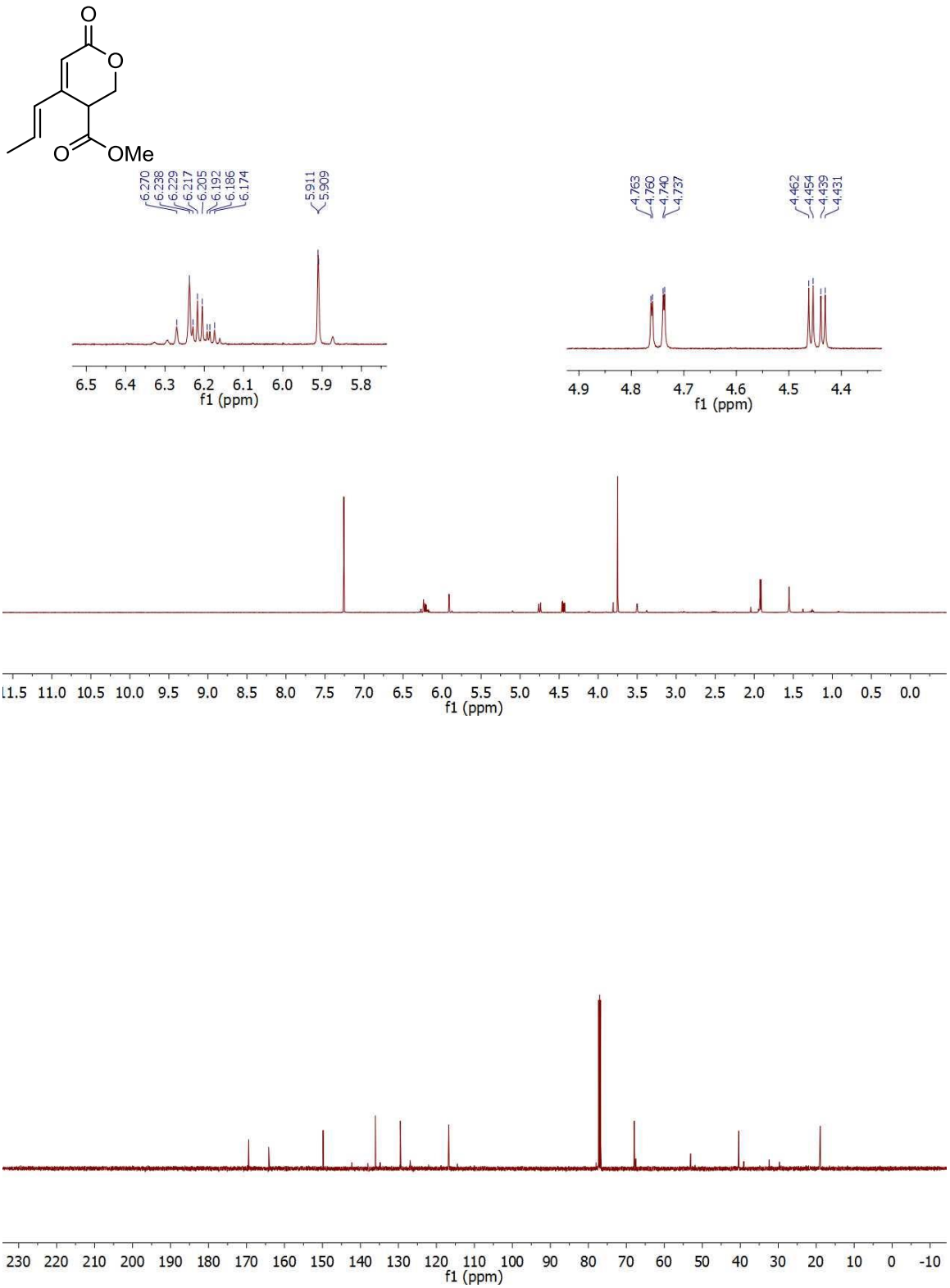
O
O
O
OMe
6.270
6.238
6.229
6.217
6.205
6.192
6.186
6.174
5.911
5.909
4.763
4.760
4.740
4.737
4.462
4.454
4.439
4.431
6.5 6.4 6.3 6.2 6.1 6.0 5.9 5.8
f1 (ppm)
4.9 4.8 4.7 4.6 4.5 4.4
f1 (ppm)
11.5 11.0 10.5 10.0 9.5 9.0 8.5 8.0 7.5 7.0 6.5 6.0 5.5 5.0 4.5 4.0 3.5 3.0 2.5 2.0 1.5 1.0 0.5 0.0
f1 (ppm)
230 220 210 200 190 180 170 160 150 140 130 120 110 100 90 80 70 60 50 40 30 20 10 0 -10
f1 (ppm)

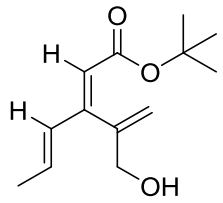
O
H
O
H
OH

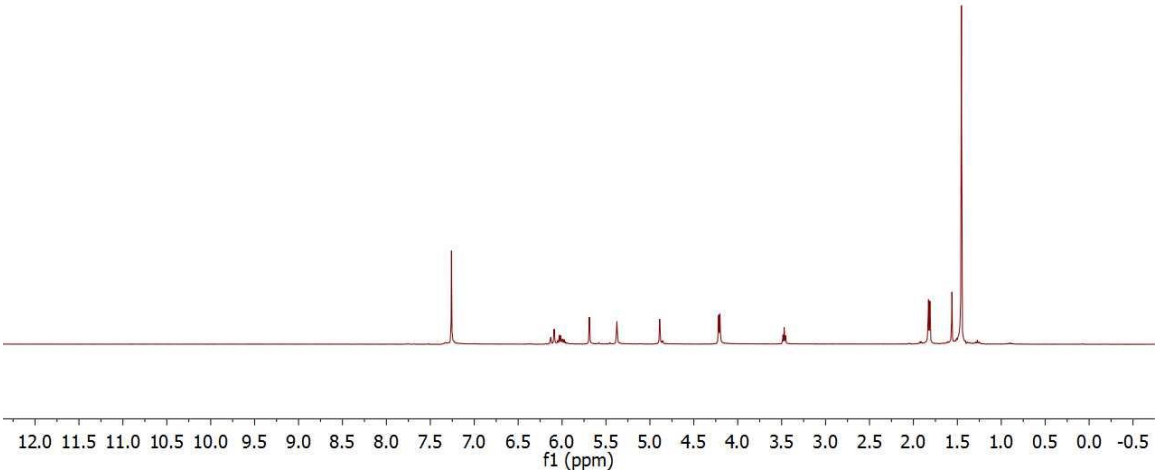
12.0 11.5 11.0 10.5 10.0 9.5 9.0 8.5 8.0 7.5 7.0 6.5 6.0 5.5 5.0 4.5 4.0 3.5 3.0 2.5 2.0 1.5 1.0 0.5 0.0 -0.5
f1 (ppm)

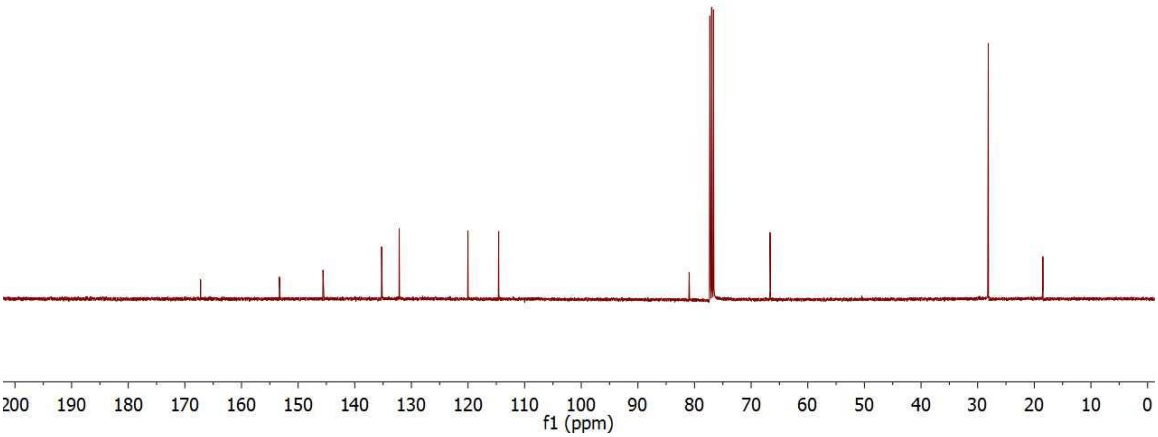
200 190 180 170 160 150 140 130 120 110 100 90 80 70 60 50 40 30 20 10 0
f1 (ppm)

Key NOESY Correlations for Alcohol Coupling Product 184

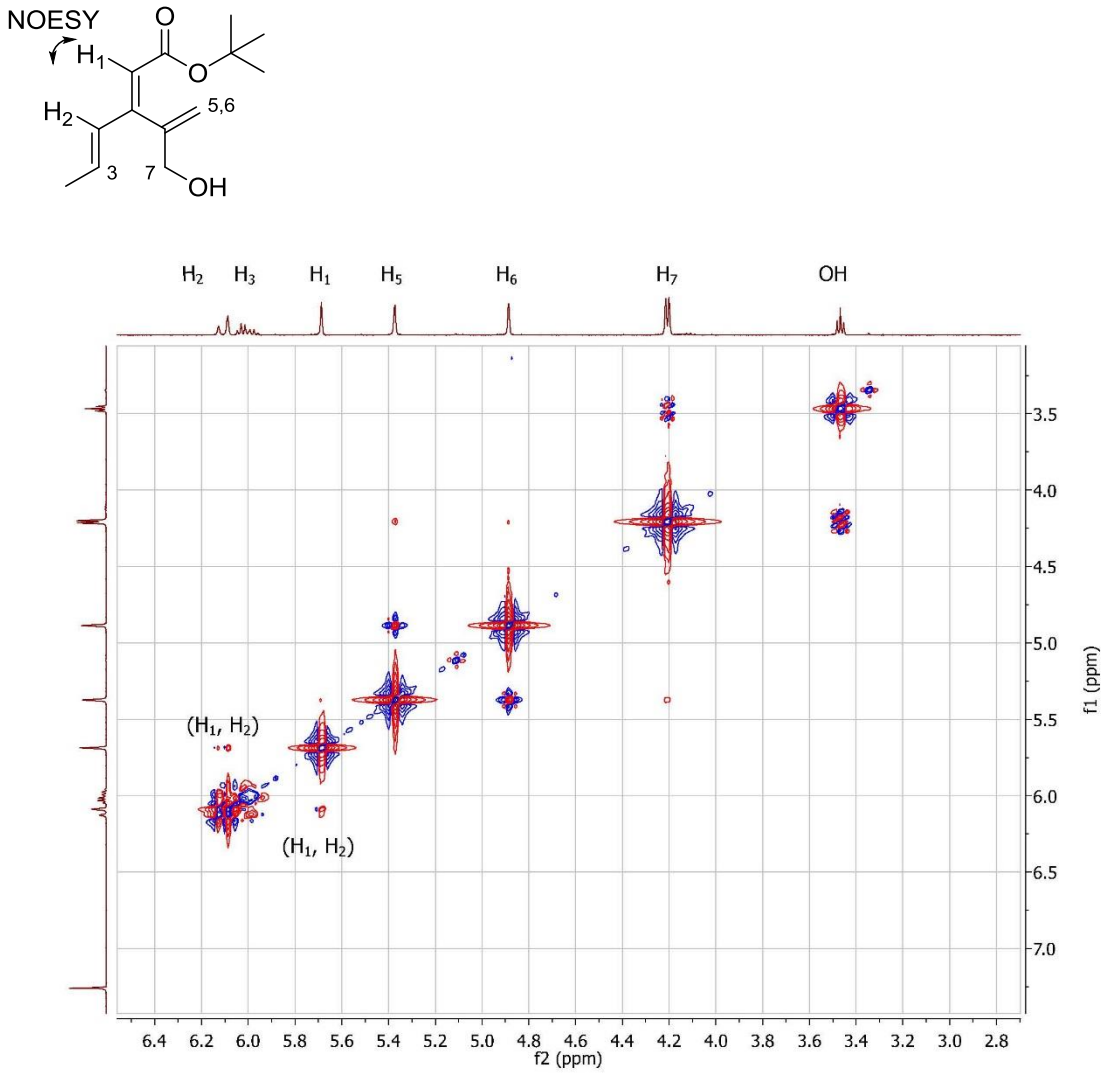

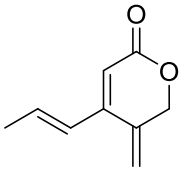
O
O

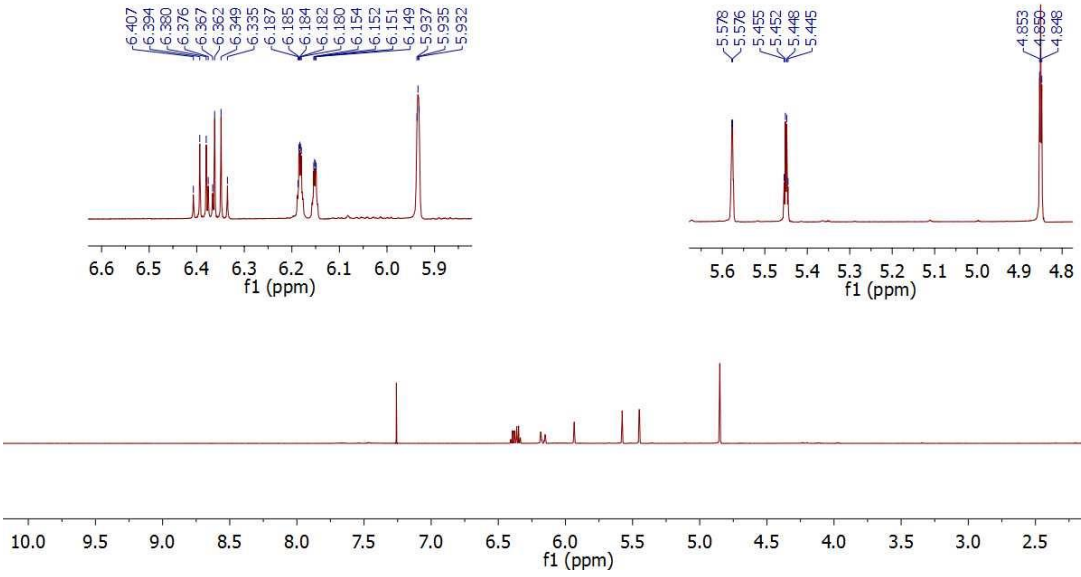
6.407
6.394
6.380
6.376
6.367
6.362
6.349
6.335
6.187
6.185
6.184
6.182
6.180
6.154
6.152
6.151
6.149
5.937
5.935
5.932
5.578
5.576
5.455
5.452
5.448
5.445
4.853
4.850
4.848
6.6 6.5 6.4 6.3 6.2 6.1 6.0 5.9
f1 (ppm)
5.6 5.5 5.4 5.3 5.2 5.1 5.0 4.9 4.8
f1 (ppm)
10.0 9.5 9.0 8.5 8.0 7.5 7.0 6.5 6.0 5.5 5.0 4.5 4.0 3.5 3.0 2.5 2.0
f1 (ppm)

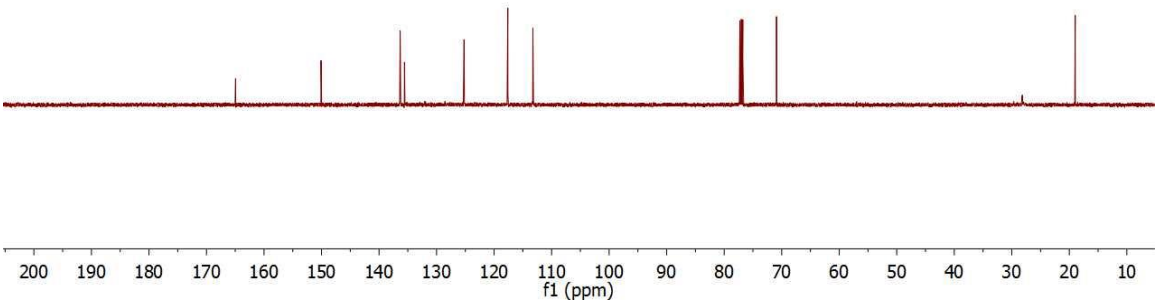
200 190 180 170 160 150 140 130 120 110 100 90 80 70 60 50 40 30 20 10
f1 (ppm)

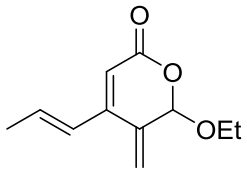
O
O
OEt

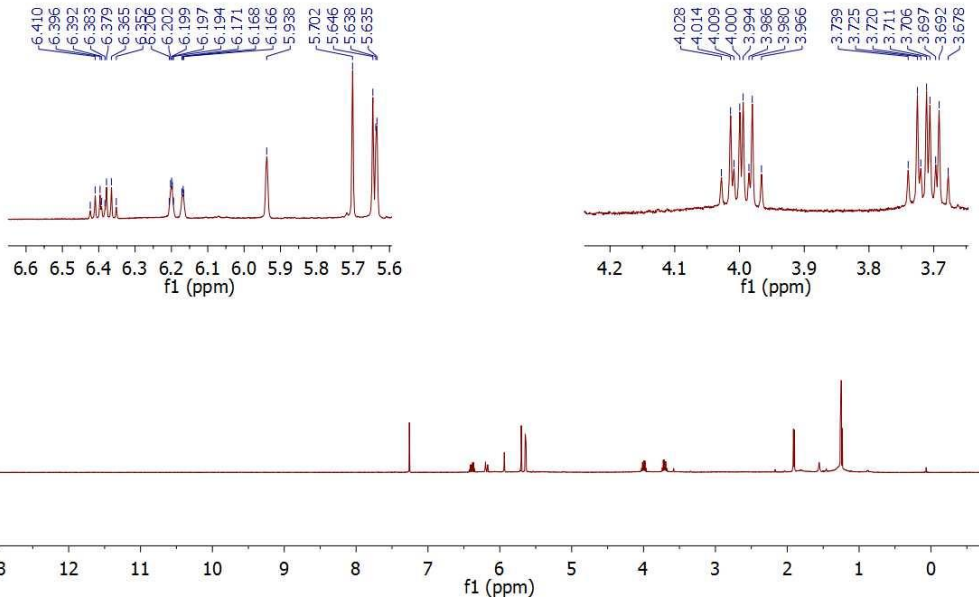
6.410
6.396
6.392
6.383
6.379
6.365
6.352
6.336
6.202
6.199
6.197
6.194
6.171
6.168
6.166
5.938
5.702
5.646
5.638
5.635
6.6 6.5 6.4 6.3 6.2 6.1 6.0 5.9 5.8 5.7 5.6
f1 (ppm)
4.028
4.014
4.009
4.000
3.994
3.986
3.980
3.966
3.739
3.725
3.720
3.711
3.706
3.697
3.692
3.678
4.2 4.1 4.0 3.9 3.8 3.7
f1 (ppm)

4 13 12 11 10 9 8 7 6 5 4 3 2 1 0 -1
f1 (ppm)

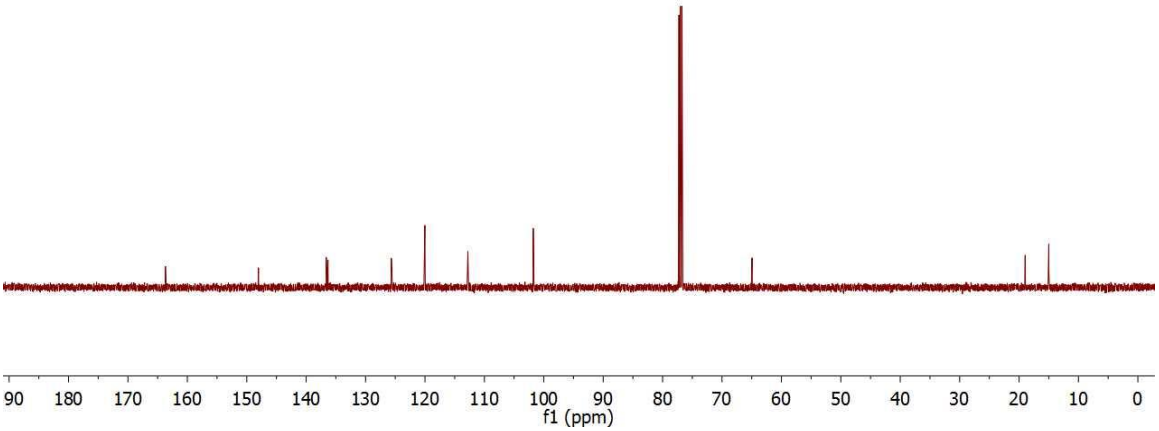
90 180 170 160 150 140 130 120 110 100 90 80 70 60 50 40 30 20 10 0
f1 (ppm)

Key NOESY Correlations for Acetal Lactone 192

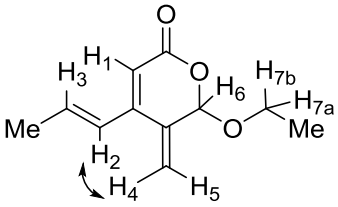

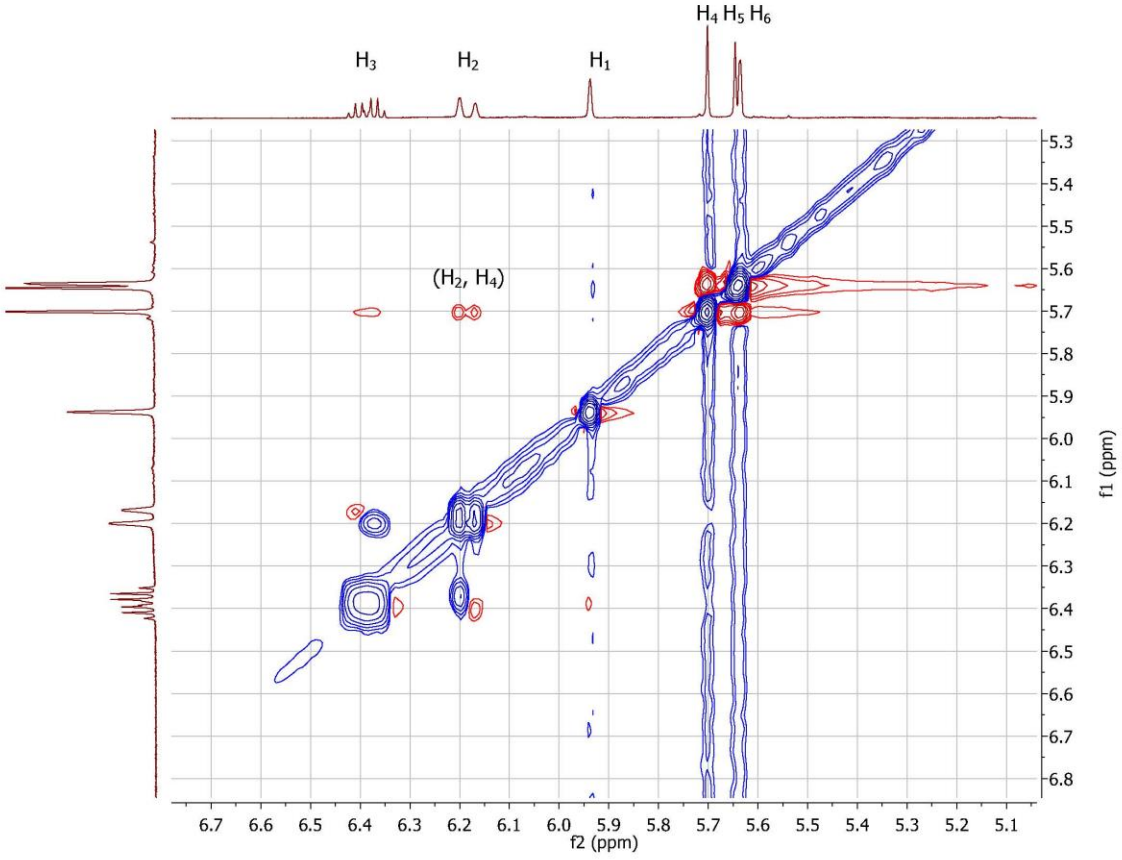

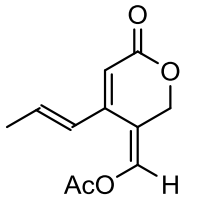
O
O
AcO
H

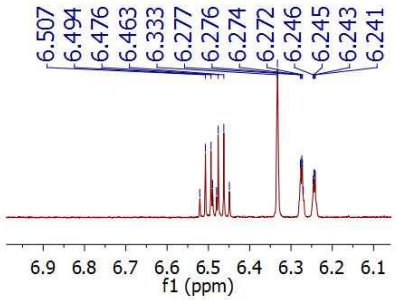
6.507
6.494
6.476
6.463
6.333
6.277
6.276
6.274
6.272
6.246
6.245
6.243
6.241
6.9 6.8 6.7 6.6 6.5 6.4 6.3 6.2 6.1
f1 (ppm)

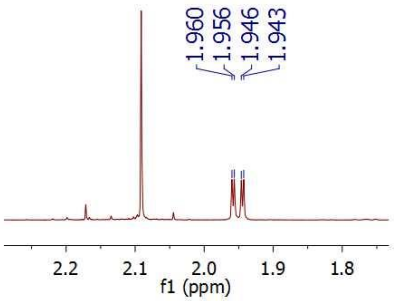
1.960
1.956
1.946
1.943
2.2 2.1 2.0 1.9 1.8
f1 (ppm)

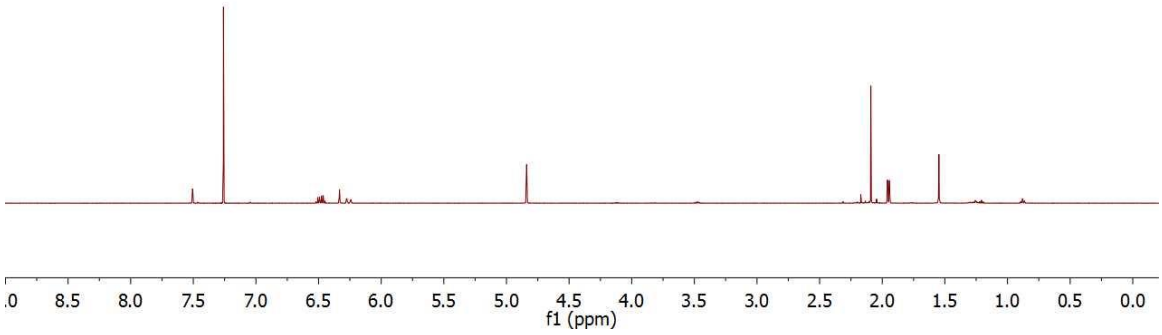
8.5 8.0 7.5 7.0 6.5 6.0 5.5 5.0 4.5 4.0 3.5 3.0 2.5 2.0 1.5 1.0 0.5 0.0
f1 (ppm)

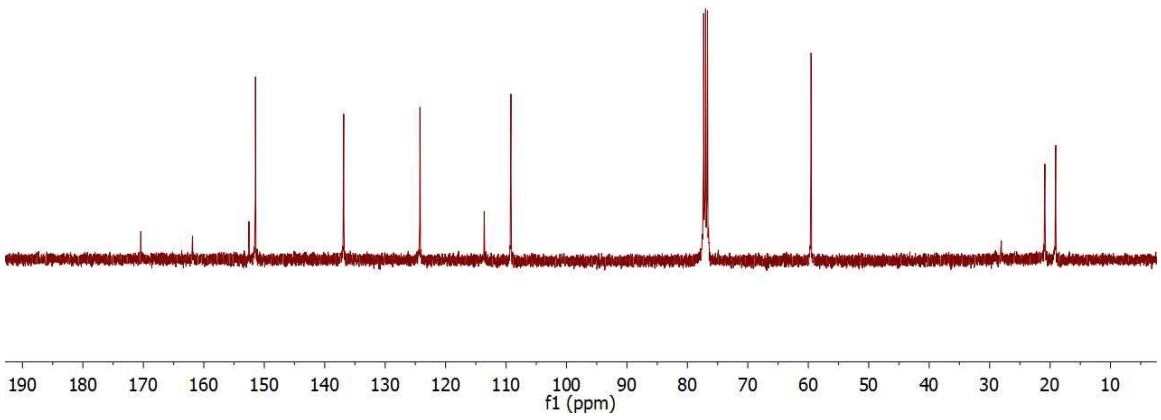
190 180 170 160 150 140 130 120 110 100 90 80 70 60 50 40 30 20 10
f1 (ppm)

Key NOESY Correlations for Enol Acetate **114c**

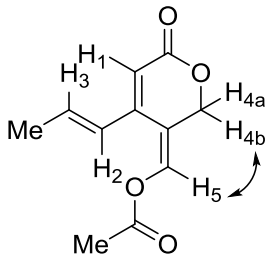

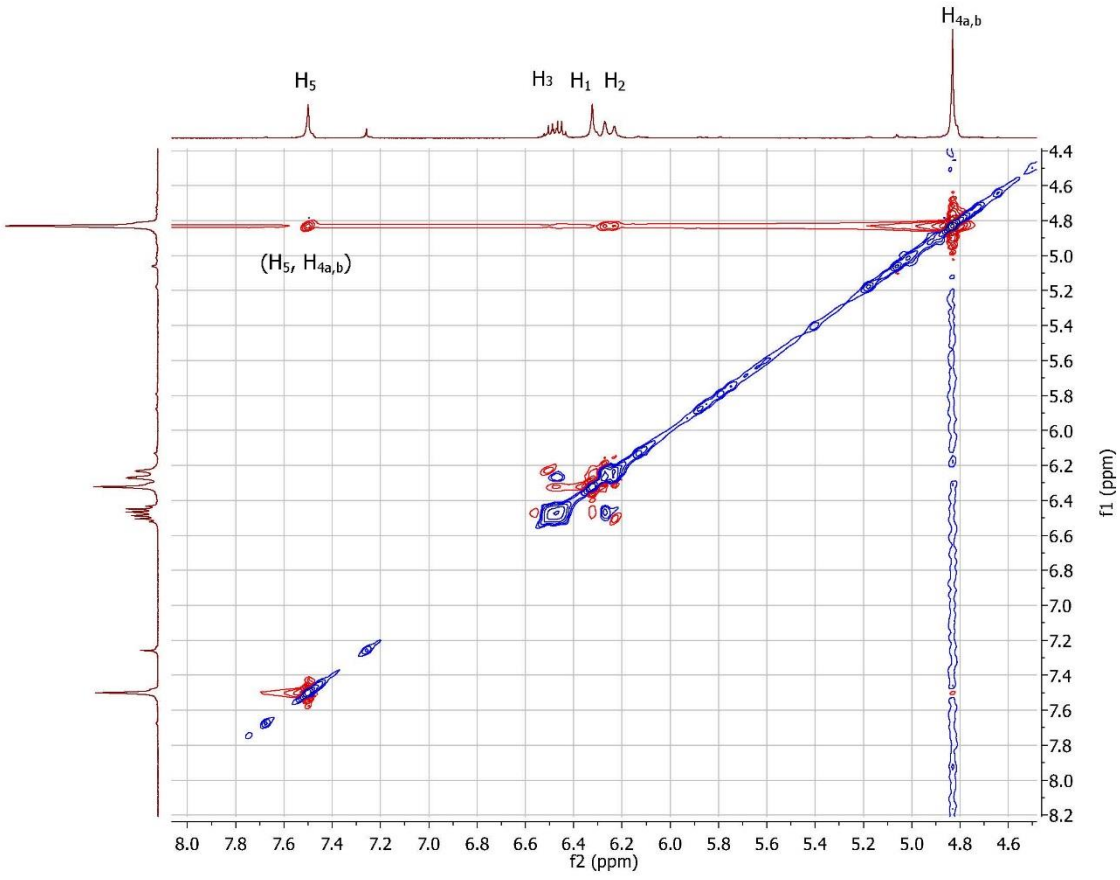

.

LIST OF JOURNAL ABBREVIATIONS

Acc. Chem. Res.	Account of Chemical Research
Acta Crystallogr.	Acta Crystallographica
Adv. Synth. Catal.	Advanced Synthesis & Catalysis
Angew. Chem. Int. Ed.	Angewandte Chemie International Edition
Aust. J. Chem.	Australian Journal of Chemistry
Biomed. Chromatogr.	Biomedical Chromatography
Beilstein J. Org. Chem..	Beilstein Journal of Organic Chemistry
Bull. Chem. Soc. Jpn.	Bulletin of the Chemical Society of Japan
Can. J. Chem.	Canadian Journal of Chemistry
Chem. Ber.	Chemische Berichte
Chem. Comm.	Chemical Communications
Chem. Eur. J.	Chemistry - A European Journal
Chem. Heterocycl. Compd.	Chemistry of Heterocyclic Compounds
Chem. Lett.	Chemistry Letters
Chem. Pharm. Bull.	Chemical and Pharmaceutical Bulletin
Chem. Rev.	Chemical Reviews
Chem. Sci.	Chemical Science
Chemistry	Chemistry
Chinese Chem. Lett.	Chinese Chemical Letters
Dalton Trans.	Dalton Transactions
Eur. J. Org. Chem.	European Journal of Organic Chemistry

Helv. Chim. Acta	Helvetica Chimica Acta
J. Am. Chem. Soc.	Journal of the American Chemical Society
J. Antibiot.	Journal of Antibiotics
J. Chem. Soc., Chem. Commun.	Journal of the Chemical Society, Chemical Communications
J. Chem. Soc., Perkin Trans. 1	Journal of the Chemical Society, Perkin Transactions 1
J. Nat. Prod.	Journal of Natural Products
J. Org. Chem.	Journal of Organic Chemistry
Molecules	Molecules
Nature	Nature
Org. Lett.	Organic Letters
Phytochemistry	Phytochemistry
Proc. Natl. Aca. Sci. USA	Proceedings of the National Academy of Sciences USA
Russ. Chem. Bull.	Russian Chemical Bulletin
Russ. J. Org. Chem.	Russian Journal of Organic Chemistry
Synlett	Synlett
Synthesis	Synthesis
Tetrahedron	Tetrahedron
Tetrahedron Lett.	Tetrahedron Letters

BIBLIOGRAPHY

(1) Büchi, G.; Yang, N. C. *J. Am. Chem. Soc.* **1957**, *79*, 2318–2323.

(2) Marvell, E. N.; Caple, G.; Gosink, T. A.; Zimmer, G. *J. Am. Chem. Soc.* **1966**, *88*, 619–620.

(3) Marvell, E. N.; Gosink, T. A.; Churchley, P.; Li, T. H. *J. Org. Chem.* **1972**, *37*, 2989–2992.

(4) Marvell, E. N.; Chadwick, T.; Caple, G.; Gosink, T. A.; Zimmer, G. *J. Org. Chem.* **1972**, *37*, 2992–2997.

(5) Krasnaya, Z. A. *Chem. Heterocycl. Compd.* **1999**, *35*, 1255–1271.

(6) Lillya, C. P.; Kluge, A. F. *J. Org. Chem.* **1971**, *36*, 1977–1988.

(7) Gosink, T. A. *J. Org. Chem.* **1974**, *39*, 1942–1944.

(8) Adams, R. D.; Chen, L. *J. Am. Chem. Soc.* **1994**, *116*, 4467–4468.

(9) Moorhof, C. M. *Synthesis* **1997**, 685–690.

(10) Lee, P. S.; Zhang, X.; Houk, K. N. *J. Am. Chem. Soc.* **2003**, *125*, 5072–5079.

(11) Spellmeyer, D. C.; H, K. N. *J. Org. Chem.* **1996**, *60*, 7134–7141.

(12) Li, C.; Porco, J. A. J. *J. Org. Chem.* **2005**, *70*, 6053–6065.

(13) Li, C.; Johnson, R. P.; Porco, J. A. *J. Am. Chem. Soc.* **2003**, *125*, 5095–5106.

(14) Natali, M.; Aakeröy, C.; Desper, J.; Giordani, S. *Dalton Trans.* **2010**, *39*, 8269–8277.

(15) Malerich, J. P.; Maimone, T. J.; Elliott, G. I.; Trauner, D. *J. Am. Chem. Soc.* **2005**, *127*, 6276–6283.

(16) Tsuda, T.; Kiyoi, T.; Miyane, T.; Saegusa, T. *J. Am. Chem. Soc.* **1988**, *110*, 8570–8572.

(17) Harvey, D. F.; Johnson, B. M.; Ung, C. S.; Vollhardt, P. C. *Synlett* **1989**, *1*, 15–18.

(18) Tekavec, T. N.; Louie, J. *J. Org. Chem.* **2008**, *73*, 2641–2648.

(19) Tekevac, T. N.; Louie, J. *Org. Lett.* **2005**, *7*, 4037–4039.

(20) Trost, B. M.; Rudd, M. T.; Costa, M. G.; Lee, P. I.; Pomerantz, A. E. *Org. Lett.* **2004**, *6*, 4235–4238.

(21) Trost, B. M.; Rudd, M. T. *J. Am. Chem. Soc.* **2002**, *124*, 4178–4179.

(22) Rauser, M.; Schroeder, S.; Niggemann, M. *Chem. - A Eur. J.* **2015**, *21*, 15929–15933.

(23) Tanaka, K.; Otake, Y.; Wada, A.; Noguchi, K. *Org. Lett.* **2007**, *9*, 2203–2206.

(24) Miyauchi, Y.; Kobayashi, M.; Tanaka, K. *Angew. Chem. Int. Ed.* **2011**, *50*, 10922–10926.

(25) Tsuchikama, K.; Yoshinami, Y.; Shibata, T. *Synlett* **2007**, 1395–1398.

(26) Hsung, R. P.; Shen, H. C.; Douglas, C. J.; Morgan, C. D.; Degen, S. J.; Yao, L. J. *J. Org. Chem.* **1999**, *64*, 690–691.

(27) McLaughlin, M. J.; Shen, H. C.; Hsung, R. P. *Tetrahedron Lett.* **2001**, *42*, 609–613.

(28) Shen, H. C.; Wang, J.; Cole, K. P.; Mclaughlin, M. J.; Morgan, C. D.; Douglas, C. J.; Hsung, R. P.; Coverdale, H. A.; Gerasyuto, A. I.; Hahn, J. M.; Liu, J.; Sklenicka, H. M.; Wei, L.; Zehnder, L. R.; Zificsak, C. A. *J. Org. Chem.* **2003**, *68*, 1729–1735.

(29) Cravotto, G.; Nano, G. M.; Tagliapietra, S.; Giuria, V. *Synthesis* **2001**, 49–51.

(30) Riveira, M. J.; Quiroga, G. N.; Mata, E. G.; Gandon, V.; Mischne, M. P. *J. Org. Chem.* **2015**, *80*, 6515–6519.

(31) Cossy, J.; Rakotoarisoa, H.; Kahn, P.; Desmurs, J.-R. *Tetrahedron Lett.* **1998**, *39*, 9671–9674.

(32) Kurdyumov, A. V.; Lin, N.; Hsung, R. P.; Gullickson, G. C.; Cole, K. P.; Sydorenko, N.; Swidorski, J. J. *Org. Lett.* **2006**, *8*, 191–193.

(33) Hubert, C.; Moreau, J.; Batany, J.; Duboc, A.; Hurvois, J. P.; Renaud, J. L. *Adv. Synth. Catal.* **2008**, *350*, 40–42.

(34) Hu, J.; Dong, W.; Wu, X.; Tong, X. *Org. Lett.* **2012**, *14*, 5530–5533.

(35) Ikawa, M.; Stahmann, M. A.; Link, K. P. *J. Am. Chem. Soc.* **1944**, *66*, 902–906.

(36) Salomon, R. G.; Burns, J. R.; Dominic, W. J. *J. Org. Chem.* **1976**, *41*, 2918–2920.

(37) Jonassohn, M.; Sterner, O.; Anke, H. *Tetrahedron* **1996**, *52*, 1473–1478.

(38) Hsung, R. P.; Kurdyumov, A. V.; Sydorenko, N. *Eur. J. Org. Chem.* **2005**, 23–44.

(39) Carlone, A.; Marigo, M.; North, C.; Landa, A.; Jørgensen, K. A. *Chem. Commun.* **2006**, No. 47, 4928.

(40) Krasnaya, Z. A.; Bogdanov, V. S.; Burova, S. A.; Smirnova, Y. V. *Russ. Chem. Bull.* **1995**, *44*, 2118–2123.

(41) Tejedor, D.; López-Tosco, S.; Méndez-Abt, G.; Cotos, L.; García-Tellado, F. *Acc. Chem. Res.* **2016**, *49*, 703–713.

(42) Vidhani, D. V.; Krafft, M. E.; Alabugin, I. V. *J. Org. Chem.* **2014**, *79*, 352–364.

(43) Vidhani, D. V.; Krafft, M. E.; Alabugin, I. V. *Org. Lett.* **2013**, *15*, 4462–4465.

(44) Motika, S. E.; Wang, Q.; Ye, X.; Shi, X. *Org. Lett.* **2015**, *17*, 290–293.

(45) Xiong, Y.; Schaus, S. E.; Porco, J. A. *Org. Lett.* **2013**, *15*, 1962–1965.

(46) Menz, H.; Kirsch, S. F. *Org. Lett.* **2006**, *8*, 4795–4797.

(47) Harschneck, T.; Kirsch, S. F. *J. Org. Chem.* **2011**, *76*, 2145–2156.

(48) Sherry, B. D.; Maus, L.; Laforteza, B. N.; Toste, F. D. *J. Am. Chem. Soc.* **2006**, *128*, 8132–8133.

(49) Tambar, U. K.; Kano, T.; Stoltz, B. M. *Org. Lett.* **2005**, *7*, 2413–2416.

(50) Tambar, U. K.; Kano, T.; Zepernick, J. F.; Stoltz, B. M. *J. Org. Chem.* **2006**, *71*, 8357–8364.

(51) Tambar, U. K.; Kano, T.; Zepernick, J. F.; Stoltz, B. M. *Tetrahedron Lett.* **2007**, *48*, 345–350.

(52) Jacob, S. D.; Brooks, J. L.; Frontier, A. J. *J. Org. Chem.* **2014**, *79*, 10296–10302.

(53) Pujanauski, B. G.; Bhanu Prasad, B. A.; Sarpong, R. *J. Am. Chem. Soc.* **2006**, *128*, 6786–6787.

(54) Rautenstrauch, V. *J. Org. Chem.* **1984**, *49*, 950–952.

(55) Shi, X.; Gorin, D. J.; Toste, F. D. *J. Am. Chem. Soc.* **2005**, *127*, 5802–5803.

(56) Xie, P.; Yang, J.; Zheng, J.; Huang, Y. *Eur. J. Org. Chem.* **2014**, *2014*, 1189–

1194.

(57) Beaudry, C. M.; Malerich, J. P.; Trauner, D. *Chem. Rev.* **2005**, *105*, 4757–4778.

(58) Pancharoen, O.; Picker, K.; Reutrakul, V.; Taylor, W. C.; Tuntiwachwuttikul, P. *Aust. J. Chem.* **1987**, *40*, 455–459.

(59) Kashiwada, Y.; Yamazaki, K.; Ikeshiro, Y.; Yamagishi, T.; Fujioka, T.; Mihashi, K.; Mizuki, K.; Cosentino, L. M.; Fowke, K.; Morris-Natschke, S. L.; Lee, K.-H. *Tetrahedron* **2001**, *57*, 1559–1563.

(60) Kurdyumov, A. V.; Hsung, R. P.; Ihlen, K.; Wang, J. *Org. Lett.* **2003**, *5*, 3935–3938.

(61) Kang, Y.; Mei, Y.; Du, Y.; Jin, Z. *Org. Lett.* **2003**, *5*, 4481–4484.

(62) Lu, Y.-H.; Lin, C.-N.; Ko, H.-H.; Yang, S.-Z.; Tsao, L.-T.; Wang, J.-P. *Helv. Chim. Acta* **2003**, *86*, 2566–2572.

(63) Ko, H.-H.; Lin, C.-N.; Yang, S.-Z. *Helv. Chim. Acta* **2000**, *83*, 3000–3005.

(64) Lee, J. C.; Strobel, G. A.; Lobkovsky, E.; Clardy, J. *J. Org. Chem.* **1996**, *61*, 3232–3233.

(65) Li, C.; Lobkovsky, E.; Porco, J. A. J. *J. Am. Chem. Soc.* **2000**, *122*, 10484–10485.

(66) Shoji, M.; Imai, H.; Mukaida, M.; Sakai, K.; Kakeya, H.; Osada, H.; Hayashi, Y. *J. Antibiot.* **2002**, *55*, 829–831.

(67) Kakeya, H.; Onose, R.; Koshino, H.; Yoshida, A.; Kobayashi, K.; Kageyama, S.; Osada, H. *J. Am. Chem. Soc.* **2002**, *124*, 3496–3497.

(68) Shoji, M.; Yamaguchi, J.; Kakeya, H.; Osada, H.; Hayashi, Y. *Angew. Chem. Int. Ed.* **2002**, *41*, 3192–3194.

(69) Shoji, M.; Imai, H.; Shiina, I.; Kakeya, H.; Osada, H.; Hayashi, Y. *J. Org. Chem.* **2004**, *69*, 1548–1556.

(70) Li, C.; Bardhan, S.; Pace, E. a; Liang, M.-C.; Gilmore, T. D.; Porco, J. A. J. *Org. Lett.* **2002**, *4*, 3267–3270.

(71) Joshi, K. C.; Singh, P.; Taneja, S.; Cox, P. J.; Allan Howie, R.; Thomson, R. H. *Tetrahedron* **1982**, *38*, 2703–2708.

(72) Cannon, J. R.; Joshi, K. R.; McDonald, I. A.; Retallack, R. W.; Sierakowski, A. F.; Wong, L. C. H. *Tetrahedron Lett.* **1975**, *16*, 2795–2798.

(73) Ahmed, A. A.; Jakupovic, J.; Bohlmann, F.; Regaila, H. A.; Ahmed, A. M. *Phytochemistry* **1990**, *29*, 2211–2215.

(74) Shoji, M.; Imai, H.; Mukaida, M.; Sakai, K.; Kakeya, H.; Osada, H.; Hayashi, Y. *J. Org. Chem.* **2005**, *70*, 79–91.

(75) Li, C.; Porco, J. A. J. *J. Am. Chem. Soc.* **2004**, *126*, 1310–1311.

(76) Semmelhack, M. F.; Schmid, C. R.; Cortes, D. A.; Chou, C. S. *J. Am. Chem. Soc.* **1984**, *106*, 3374–3376.

(77) Onegi, B.; Kraft, C.; Köhler, I.; Freund, M.; Jenett-Siems, K.; Siems, K.; Beyer, G.; Melzig, M. F.; Bienzle, U.; Eich, E. *Phytochemistry* **2002**, *60*, 39–44.

(78) Weiss, C. R.; Moideen, S. V. K.; Simon, L. C.; Houghton, P. J. *J. Nat. Prod.* **2000**, *63*, 1306–1309.

(79) Malerich, J. P.; Trauner, D. *J. Am. Chem. Soc.* **2003**, *125*, 9554–9555.

(80) Jpn. Kokai Tokyo Koho. JP 82-28080, 1982.

(81) Paduraru, M. P.; Wilson, P. D. *Org. Lett.* **2003**, *5*, 4911–4913.

(82) Geng, C. A.; Zhang, X. M.; Shen, Y.; Zuo, A. X.; Liu, J. F.; Ma, Y. B.; Luo, J.; Zhou, J.; Jiang, Z. Y.; Chen, J. J. *Org. Lett.* **2009**, *11*, 4120–4123.

(83) Geng, C. A.; Zhang, X. M.; Shen, Y.; Zuo, A. X.; Liu, J. F.; Ma, Y. B.; Luo, J.; Zhou, J.; Jiang, Z. Y.; Chen, J. J. *Org. Lett.* **2009**, *11*, 4838–4841.

(84) Geng, C.-A.; Zhang, X.-M.; Ma, Y.-B.; Jiang, Z.-Y.; Luo, J.; Zhou, J.; Wang, H.-L.; Chen, J.-J. *Tetrahedron Lett.* **2010**, *51*, 2483–2485.

(85) Geng, C.-A.; Wang, L.-J.; Zhang, X.-M.; Ma, Y.-B.; Huang, X.-Y.; Luo, J.; Guo, R.-H.; Zhou, J.; Shen, Y.; Zuo, A.-X.; Jiang, Z.-Y.; Chen, J.-J. *Chem. - A Eur. J.* **2011**, *17*, 3893–3903.

(86) Geng, C.-A.; Zhang, X.-M.; Ma, Y.-B.; Luo, J.; Chen, J.-J. *J. Nat. Prod.* **2011**, *74*, 1822–1825.

(87) Geng, C. A.; Chen, X. L.; Zhou, N. J.; Chen, H.; Ma, Y. B.; Huang, X. Y.; Zhang, X. M.; Chen, J. J. *Org. Lett.* **2014**, *16*, 370–373.

(88) Geng, C.-A.; Chen, X.-L.; Huang, X.-Y.; Ma, Y.-B.; He, K.; Zhou, N.-J.; Cao, T.-W.; Zhang, X.-M.; Chen, J.-J. *Tetrahedron Lett.* **2015**, *56*, 2163–2166.

(89) Kim, K. H.; Kim, N. D.; Seong, B.-L. *Molecules* **2010**, *15*, 5878–5908.

(90) Takagi, R.; Nerio, T.; Miwa, Y.; Matsumura, S.; Ohkata, K. *Tetrahedron Lett.* **2004**, *45*, 7401–7405.

(91) Bell, M.; Frisch, K.; Jørgensen, K. A. *J. Org. Chem.* **2006**, *71*, 5407–5410.

(92) Jiang, X.; Shi, X.; Wang, S.; Sun, T.; Cao, Y.; Wang, R. *Angew. Chem. Int. Ed.* **2012**, *51*, 2084–2087.

(93) Maeda, K.; Terada, T.; Iwamoto, T.; Kurahashi, T.; Matsubara, S. *Org. Lett.* **2015**, *17*, 5284–5287.

(94) Jiang, X.; Wang, R. *Chem. Rev.* **2013**, *113*, 5515–5546.

(95) Klas, K.; Tsukamoto, S.; Sherman, D. H.; Williams, R. M. *J. Org. Chem.* **2015**, *80*, 11672–11685.

(96) Kim, H. J.; Ruszczycky, M. W.; Choi, S.; Liu, Y.; Liu, H. *Nature* **2011**, *473*, 109–112.

(97) Ose, T.; Watanabe, K.; Mie, T.; Honma, M.; Watanabe, H.; Yao, M.; Oikawa, H.; Tanaka, I. *Nature* **2003**, *422*, 185–189.

(98) Ose, T.; Watanabe, K.; Yao, M.; Honma, M.; Oikawa, H.; Tanaka, I. *Acta Crystallogr.* **2004**, *D60*, 1187–1197.

(99) Ruch, C.; Guimara, W.; Udier-blagovic, M.; Jorgensen, W. L. *J. Am. Chem. Soc.* **2005**, *127*, 3577–3588.

(100) Huisgen, R.; Otto, P. *Chem. Ber.* **1969**, *102*, 3475–3485.

(101) Mayr, H.; Heigl, U. W. *J. Chem. Soc., Chem. Commun.* **1987**, 1804–1805.

(102) Paull, D. H.; Weatherwax, A.; Lectka, T. *Tetrahedron* **2009**, *65*, 6771–6803.

(103) Alden-Danforth, E.; Scerba, M. T.; Lectka, T. *Org. Lett.* **2008**, *10*, 4951–4953.

(104) Wolfer, J.; Bekele, T.; Abraham, C. J.; Dogo-Isonagie, C.; Lectka, T. *Angew. Chem. Int. Ed.* **2006**, *45*, 7398–7400.

(105) Douglas, J.; Churchill, G.; Smith, A. D. *Synthesis* **2012**, *44*, 2295–2309.

(106) Kaeobamrung, J.; Kozlowski, M. C.; Bode, J. W. *Proc. Natl. Acad. Sci. U.S.A* **2010**, *107*, 20661–20665.

(107) Zhao, X.; Ruhl, K. E.; Rovis, T. *Angew. Chem. Int. Ed.* **2012**, *51*, 12330–12333.

(108) Simal, C.; Lebl, T.; Slawin, A. M. Z.; Smith, A. D. *Angew. Chem. Int. Ed.* **2012**, *51*, 3653–3657.

(109) Morrill, L. C.; Smith, A. D. *Chem. Soc. Rev.* **2014**, *43*, 6214–6226.

(110) Bekele, T.; Shah, M. H.; Wolfer, J.; Abraham, C. J.; Weatherwax, A.; Lectka, T. *J. Am. Chem. Soc.* **2006**, *128*, 1810–1811.

(111) Tan, H.; Chen, X.; Liu, Z.; Wang, D. Z. *Tetrahedron* **2012**, *68*, 3952–3955.

(112) Kornblum, N.; DeLaMare, H. E. *J. Am. Chem. Soc.* **1951**, *73*, 880–881.

(113) Bennabi, S.; Narkunan, K.; Rousset, L.; Bouchu, D.; Ciufolini, M. A. *Tetrahedron Lett.* **2000**, *41*, 8873–8876.

(114) Zayia, G. H. *Org. Lett.* **1999**, *1*, 989–991.

(115) Hill, D. R.; Hsiao, C.-N.; Kurukulasuriya, R.; Wittenberger, S. J. *Org. Lett.* **2002**, *4*, 111–113.

(116) Meyer, W. L.; Brannon, M. J.; Burgos, C. G.; Goodwin, T. E.; Howard, R. W. *J. Org. Chem.* **1985**, *50*, 438–447.

(117) Alagiri, K.; Devadig, P.; Prabhu, K. R. *Chem. - A Eur. J.* **2012**, *18*, 5160–5164.

(118) Liu, L.; Floreancig, P. E.; Pennsyl, V. *Org. Lett.* **2010**, *12*, 17–20.

(119) Sharma, G. V. M.; Lavanya, B.; Mahalingam, A. K.; Krishna, P. R. *Tetrahedron Lett.* **2000**, *41*, 10323–10326.

(120) Kleinke, A. S.; Li, C.; Rabasso, N.; Porco, J. A. J. *Org. Lett.* **2006**, *8*, 2847–2850.

(121) Dong, S.; Qin, T.; Hamel, E.; Beutler, J. A.; Porco, J. A. *J. Am. Chem. Soc.* **2012**, *134*, 19782–19787.

(122) Stang, E. M.; White, M. C. *J. Am. Chem. Soc.* **2011**, *133*, 14892–14895.

(123) Diao, T. N.; Wadzinski, T. J.; Stahl, S. S. *Chem. Sci.* **2012**, *3*, 887–891.

(124) Zhu, J.; Liu, J.; Ma, R.; Xie, H.; Li, J.; Jiang, H.; Wang, W. *Adv. Synth. Catal.* **2009**, *351*, 1229–1232.

(125) Liu, J.; Zhu, J.; Jiang, H.; Wang, W.; Li, J. *Chem. Commun.* **2010**, *46*, 415–417.

(126) Worayuthakarn, R.; Boonya-udtayan, S.; Ruchirawat, S.; Thasana, N. *Eur. J. Org. Chem.* **2014**, *2014*, 2496–2507.

(127) Trend, R. M.; Ramtohul, Y. K.; Stoltz, B. M. *J. Am. Chem. Soc.* **2005**, *127*, 17778–17788.

(128) Wang, F.; Zhang, Y. J.; Yang, G.; Zhang, W. *Tetrahedron Lett.* **2007**, *48*, 4179–4182.

(129) Otera, J.; Danoh, N.; Nozaki, H. *J. Org. Chem.* **1991**, *56*, 5307–5311.

(130) Otera, J. *Chem. Rev.* **1993**, *93*, 1449–1470.

(131) Blanchette, M. A.; Choy, W.; Davis, J. T.; Essenfeld, A. P.; Masamune, S.; Roush, W. R.; Sakai, T. *Tetrahedron Lett.* **1984**, *25*, 2183–2186.

(132) Kendall, J.; McDonald, R.; Ferguson, M. J.; Tykwinski, R. R. *Org. Lett.* **2008**, *10*, 2163–2166.

(133) Foster, R. W.; Tame, C. J.; Hailes, H. C.; Sheppard, T. D. *Adv. Synth. Catal.* **2013**, *355*, 2353–2360.

(134) Medvedeva, A. S.; Andreev, M. V; Safronova, L. P.; Afonin, A. V. *Russ. J. Org. Chem.* **2005**, *41*, 1463–1466.

(135) Kotikalapudi, R.; Kumara Swamy, K. C. *Tetrahedron* **2013**, *69*, 8002–8012.

(136) Ondrusek, B. A.; Park, J. K.; McQuade, D. T. *Synlett* **2014**, *25*, 239–242.

(137) Inanaga, J.; Baba, Y.; Hanamoto, T. *Chem. Lett.* **1993**, 241–244.

(138) Fehr, C.; Magpantay, I.; Vuagnoux, M.; Dupau, P. *Chemistry* **2011**, *17*, 1257–1260.

(139) Mehta, G.; Islam, K. *Tetrahedron Lett.* **2004**, *45*, 3611–3615.

(140) Sakaguchi, T.; Okuno, Y.; Tsutsumi, Y.; Tsuchikawa, H.; Katsumura, S. *Org. Lett.* **2011**, *13*, 4292–4295.

(141) Jiao, J.; Zhang, Y.; Devery, J. J.; Xu, L.; Deng, J.; Flowers, R. A. *J. Org. Chem.* **2007**, *72*, 5486–5492.

(142) Ischay, M. A.; Yoon, T. P. *Eur. J. Org. Chem.* **2012**, No. 18, 3359–3372.

(143) Bellville, D. J.; Wirth, D. W.; Bauld, N. L. *J. Am. Chem. Soc.* **1981**, *103*, 718–720.

(144) Bauld, N. L.; Bellville, D. J.; Harirchian, B.; Lorenz, K. T.; Pabon, R. A.; Reynolds, D. W.; Wirth, D. D.; Chiou, H. S.; Marsh, B. K. *Acc. Chem. Res.* **1987**, *20*, 371–378.

(145) Bauld, N. L.; Yang, J. *Org. Lett.* **1999**, *1*, 773–774.

(146) Schmittel, M.; Von Seggern, H. *Angew. Chem. Int. Ed.* **1991**, *30*, 999–1001.

(147) Schmittel, M.; Seggern, H. Von. *J. Am. Chem. Soc.* **1993**, *115*, 2165–2177.

(148) Mayo, P. De; Takeshita, H. *Can. J. Chem.* **1963**, *41*, 440–449.

(149) Schmittel, M.; Baumann, U. *Angew. Chem. Int. Ed.* **1990**, *29*, 541–543.

(150) Schmittel, M.; Abufarag, A.; Luche, O.; Levis, M. *Angew. Chem. Int. Ed.* **1990**, *29*, 1144–1146.

(151) Casey, B. M.; Eakin, C. A.; Jiao, J.; Sadasivam, D. V.; Flowers, R. A. *Tetrahedron* **2009**, *65*, 10762–10768.

(152) Rathore, R.; Kochi, J. K. *J. Org. Chem.* **1996**, *61*, 627–639.

(153) Miller, A. K.; Hughes, C. C.; Kennedy-Smith, J. J.; Gradl, S. N.; Trauner, D. *J. Am. Chem. Soc.* **2006**, *128*, 17057–17062.

(154) Bunte, J. O.; Heilmann, E. K.; Hein, B.; Mattay, J. *Eur. J. Org. Chem.* **2004**, *7*, 3535–3550.

(155) Macmillan, D. W. C.; Rankic, D. A.; Prier, C. K. *Chem. Rev.* **2014**, *113*, 5322–5363.

(156) Lin, S.; Ischay, M. A.; Fry, C. G.; Yoon, T. P. *J. Am. Chem. Soc.* **2011**, *133*, 19350–19353.

(157) Cismesia, M. A.; Yoon, T. P. *Chem. Sci.* **2015**, *6*, 5426–5434.

(158) Ensley, H. E.; Carr, R. V. C.; Martin, R. S.; Pierce, T. E. *J. Am. Chem. Soc.* **1980**, *102*, 2836–2838.

(159) Snider, B. B.; Shi, Z. *J. Am. Chem. Soc.* **1992**, *114*, 1790–1800.

(160) Najjar, F.; André-Barrès, C.; Lauricella, R.; Gorrichon, L.; Tuccio, B. *Tetrahedron Lett.* **2005**, *46*, 2117–2119.

(161) Lu, Z.; Yoon, T. P. *Angew. Chem. Int. Ed.* **2012**, *51*, 10329–10332.

(162) Gieseler, A.; Steckhan, E. *J. Org. Chem.* **1991**, *56*, 1405–1411.

(163) Riener, M.; Nicewicz, D. A. *Chem. Sci.* **2013**, *4*, 1–10.

(164) Gesmundo, N. J.; Nicewicz, D. A. *Beilstein J. Org. Chem.* **2014**, *10*, 1272–1281.

(165) Inanaga, J.; Baba, Y.; Hanamoto, T. *Chem. Lett.* **1993**, *22*, 241–244.

(166) Engle, K. M.; Mei, T. S.; Wasa, M.; Yu, J. Q. *Acc. Chem. Res.* **2012**, *45*, 788–802.

(167) Engle, K. M.; Mei, T.-S.; Wasa, M.; Yu, J.-Q. *Acc. Chem. Res.* **2012**, *45*, 788–802.

(168) Engle, K. M.; Yu, J.-Q. *J. Org. Chem.* **2013**, *78*, 8927–8955.

(169) Mei, T.-S.; Giri, R.; Maugel, N.; Yu, J.-Q. *Angew. Chem. Int. Ed.* **2008**, *47*, 5215–5219.

(170) Bedford, R. B.; Haddow, M. F.; Mitchell, C. J.; Webster, R. L. *Angew. Chem. Int. Ed.* **2011**, *50*, 5524–5527.

(171) Yang, L.; Lu, Z.; Stahl, S. S. *Chem. Commun.* **2009**, No. 42, 6460–6462.

(172) Wang, X.-C.; Hu, Y.; Bonacorsi, S.; Hong, Y.; Burrell, R.; Yu, J.-Q. *J. Am. Chem. Soc.* **2013**, *135*, 10326–10329.

(173) John, A.; Nicholas, K. M. *J. Org. Chem.* **2012**, *77*, 5600–5605.

(174) Chu, L.; Wang, X.-C.; Moore, C. E.; Rheingold, A. L.; Yu, J.-Q. *J. Am. Chem. Soc.* **2013**, *135*, 16344–16347.

(175) Schröder, N.; Wencel-Delord, J.; Glorius, F. *J. Am. Chem. Soc.* **2012**, *134*, 8298–8301.

(176) Hwang, H.; Kim, J.; Jeong, J.; Chang, S. *J. Am. Chem. Soc.* **2014**, *136*, 10770–10776.

(177) Qian, G.; Hong, X.; Liu, B.; Mao, H.; Xu, B. *Org. Lett.* **2014**, *16*, 5294–5297.

(178) Schröder, N.; Lied, F.; Glorius, F. *J. Am. Chem. Soc.* **2015**, *137*, 1448–1451.

(179) Kuhl, N.; Schr, N.; Glorius, F. *Org. Lett.* **2013**, *15*, 3860–3863.

(180) Wang, L.; Ackermann, L. *Chem. Commun.* **2014**, *50*, 1083–1085.

(181) Teskey, C. J.; Lui, A. Y. W.; Greaney, M. F. *Angew. Chem. Int. Ed.* **2015**, *54*, 11677–11680.

(182) Yu, D.-G.; Gensch, T.; de Azambuja, F.; Vásquez-Céspedes, S.; Glorius, F. *J. Am. Chem. Soc.* **2014**, *136*, 17722–17725.

(183) Ackermann, L.; Pospech, J.; Graczyk, K.; Rauch, K. *Org. Lett.* **2012**, *14*, 930–933.

(184) Parella, R.; Babu, S. A. *J. Org. Chem.* **2015**, *80*, 12379–12396.

(185) Collins, K. D.; Lied, F.; Glorius, F. *Chem. Commun.* **2014**, *50*, 4459–4461.

(186) Chen, F.-J.; Zhao, S.; Hu, F.; Chen, K.; Zhang, Q.; Zhang, S.-Q.; Shi, B.-F. *Chem. Sci.* **2013**, *4*, 4187.

(187) Li, X.; Liu, Y. H.; Gu, W. J.; Li, B.; Chen, F. J.; Shi, B. F. *Org. Lett.* **2014**, *16*, 3904–3907.

(188) Li, B.; Liu, B.; Shi, B.-F. *Chem. Commun.* **2015**, *51*, 5093.

(189) Khan, B.; Kant, R.; Koley, D. *Adv. Synth. Catal.* **2016**.

(190) Våbenø, J.; Brisander, M.; Lejon, T.; Luthman, K. *J. Org. Chem.* **2002**, *67*, 9186–9191.

(191) Meester, W. J. N.; Maarseveen, J. H. van; Schoemaker, H. E.; Hiemstra, H.; Rutjes, F. P. J. T. *Eur. J. Org. Chem.* **2003**, *2003*, 2519–2529.

(192) Habrant, D.; Rauhala, V.; Koskinen, A. M. P. *Chem. Soc. Rev.* **2010**, *39*, 2007–2017.

(193) Shi, Y.; Peterson, S. M.; Haberaecker, W. W. I.; Blum, S. A. *J. Am. Chem. Soc.* **2008**, *130*, 2168–2169.

(194) Molander, G. A.; Yokoyama, Y. *J. Org. Chem.* **2006**, *71*, 2493–2498.

(195) Espinet, P.; Echavarren, A. M. *Angew. Chem. Int. Ed.* **2004**, *43*, 4704–4734.

(196) Nielsen, T. E.; Quement, S. Le; Juhl, M.; Tanner, D. *Tetrahedron* **2005**, *61*, 8013–8024.

(197) Lepage, O.; Kattnig, E.; Fürstner, A. *J. Am. Chem. Soc.* **2004**, *126*, 15970–15971.

(198) Qi, C.; Qin, T.; Suzuki, D.; Porco, J. A. *J. Am. Chem. Soc.* **2014**, *136*, 3374–3377.

(199) Bishop, L. M.; Roberson, R. E.; Bergman, R. G.; Trauner, D. *Synthesis* **2010**, 2233–2244.

(200) Fu, G. C. *Acc. Chem. Res.* **2008**, *41*, 1555–1564.

(201) Littke, A. F.; Fu, G. C. *Angew. Chem. Int. Ed.* **1999**, *38*, 2411–2413.

(202) Littke, A. F.; Schwarz, L.; Fu, G. C. *J. Am. Chem. Soc.* **2002**, *124*, 6343–6348.

(203) Jaroszewski, J. W.; Ettlinger, M. G. *J. Org. Chem.* **1989**, *54*, 1506–1518.

(204) Smith, A. B.; Dong, S.; Brenneman, J. B.; Fox, R. J. *J. Am. Chem. Soc.* **2009**, *131*, 12109–12111.

(205) McNally, A.; Evans, B.; Gaunt, M. J. *Angew. Chem. Int. Ed.* **2006**, *45*, 2116–2119.

(206) Mukaiyama, T.; Usui, M.; Shimada, E.; Saigo, K. *Chem. Lett.* **1975**, *4*, 1045–1048.

(207) Mukaiyama, T. *Angew. Chem. Int. Ed.* **1979**, *18*, 707–721.

(208) Novosjolova, I. *Synlett* **2013**, *24*, 135–136.

(209) Funk, R. L.; Abelman, M. M.; Jellison, K. M. *Synlett* **1989**, *1989*, 36–37.

(210) Lee, A.; Younai, A.; Price, C. K.; Izquierdo, J.; Mishra, R. K.; Scheidt, K. A. *J. Am. Chem. Soc.* **2014**, *136*, 10589–10592.

(211) Nishimoto, Y.; Onishi, Y.; Yasuda, M.; Baba, A. *Angew. Chem. Int. Ed.* **2009**, *48*, 9131–9134.

(212) Onishi, Y.; Nishimoto, Y.; Yasuda, M.; Baba, A. *Org. Lett.* **2011**, *13*, 2762–2765.

(213) Saigo, K.; Izawa, T.; Mukaiyama, T. *Chem. Lett.* **1974**, 323–326.

(214) Yanagisawa, A.; Matsumoto, Y.; Asakawa, K.; Yamamoto, H. *Tetrahedron* **2002**, *58*, 8331–8339.

(215) Yanagisawa, M.; Shimamura, T.; Iida, D.; Matsuo, J.; Mukaiyama, T. *Chem. Pharm. Bull.* **2000**, *48*, 1838–1840.

(216) Duhamel, P.; Cahard, D.; Poirier, J. *J. Chem. Soc. Perkin Trans. 1* **1993**, 2509–2511.

(217) Mahata, P. K.; Barun, O.; Ila, H.; Junjappa, H. *Synlett* **2000**, *2000*, 1345–1347.

(218) Takehira, S.; Masui, Y.; Onaka, M. *Chem. Lett.* **2014**, *43*, 498–500.

(219) Nagao, H.; Yamane, Y.; Mukaiyama, T. *Chem. Lett.* **2007**, *36*, 8–9.

(220) Ichibakase, T.; Orito, Y.; Nakajima, M. *Tetrahedron Lett.* **2008**, *49*, 4427–4429.

(221) Mase, N.; Tanaka, F.; Barbas, C. F. *Org. Lett.* **2003**, *5*, 4369–4372.

(222) Li, J.; Fu, N.; Li, X.; Luo, S.; Cheng, J.-P. *J. Org. Chem.* **2010**, *75*, 4501–4507.

(223) Markert, M.; Scheffler, U.; Mahrwald, R. *J. Am. Chem. Soc.* **2009**, *131*, 16642–16643.

(224) Ondrus, A. E.; Movassaghi, M. *Tetrahedron* **2006**, *62*, 5287–5297.

(225) Jansen, D. J.; Shenvi, R. A. *J. Am. Chem. Soc.* **2013**, *135*, 1209–1212.

(226) Hong, B.-C.; Wu, M.-F.; Tseng, H.-C.; Liao, J.-H. *Org. Lett.* **2006**, *8*, 2217–2220.

(227) Sherwood, T. C.; Trotta, A. H.; Snyder, S. A. *J. Am. Chem. Soc.* **2014**, *136*, 9743–9753.

(228) Zeng, W.; Han, H.; Tao, Y.; Yang, L.; Wang, Z.; Chen, K. *Biomed. Chromatogr.* **2013**, *27*, 1129–1136.

(229) Wang, C. L.; Liu, J. L.; Liu, Z. L.; Li, X. S.; Cao, X. Y. *Chinese Chem. Lett.* **2009**, *20*, 150–152.

(230) Rieche, A.; Gross, H.; Höft, E. *Chem. Ber.* **1960**, *93*, 88–94.

(231) Andersson, I.; Elofsson, M. *Master Thesis* **2005**, Umea University.

CURRICULUM VITAE

DIANE A. HAMANN

Boston University, Department of Chemistry, 24 Cummington Street, Boston 02215, MA

EDUCATION AND TRAINING

Ph.D. Candidate in Organic Chemistry 2010-2016

Boston University, Chemistry Department, Boston, MA

Advisor: Prof. John A. Porco, Jr.

Project 1: Synthetic Studies toward Epidithiodiketopiperazine Natural Products

Project 2: Studies toward the Total Synthesis of Swerilactone Natural Products

Master of Science MSc in Chemistry and Chemical Engineering 2010

Lyon School of Chemistry, Physics and Electronics, University Claude-Bernard Lyon I, Lyon, France

RESEARCH AND PROFESSIONAL EXPERIENCE

Boston University, Chemistry Department, Boston, MA 2010-2016

- Successfully synthesized a disulfide reagent promoting a selective tetrasulfenylation of electron-deficient diketopiperazines *via* a radical mechanism

- Synthesized several enantiopure, epoxide containing 1,3-*bis* electrophiles as intermediates for *C*-*C* and *C*-*N* bond formation en route to epidithiodiketopiperazines
- Synthesized a lactone fused *2H*-pyran precursor and studied its unexplored Diels-Alder behavior en route to swerilactone natural products
- Established novel synthetic routes to several decorated lactones to act as potential dienophile in a biomimetic [4+2] cycloaddition

The Broad Institute, Chemical Biology Platform, Cambridge, MA 2009-2010

Research Associate Intern, Diversity-Oriented Synthesis

Advisors: Dr. Lisa Marcaurelle, Dr. Jean-Charles Marie

- Contributed to the library production of 4000 compounds based on a tricyclic scaffold using an SNAr reaction
- Executed both solution phase (scale up to 200 g) and solid-phase synthesis for library development
- Presented project updates in group meetings and a final department-wide presentation
- Publication (Team Project): *J. Org. Chem.* 2013, *78*, 5160−5171.

Institute of Chemistry and Biochemistry, Organic Chemistry Laboratory May 2009

Organic Chemistry 2-Glycochemistry, University Claude Bernard Lyon I, Lyon, France

Advisor: Dr. Sebastien Vidal

- Multistep synthesis of a glycogen phosphorylase inhibitor towards the treatment of diabetes

Bayer CropScience Summer 2008

Research Center Residue Operator and Consumer Safety Dept., Lyon, France

- Prepared wheat samples for LCMS analysis, managed samples logistics for a mycotoxin level study in European wheat crops

TEACHING AND MENTORING EXPERIENCE

Teaching Assistant in General Chemistry CH101/102 (4 semesters) 2010-2011

Boston University, Boston, MA

- Supervised 20 students per lab sections, 3 times/week, graded lab reports and exams, held office hours

NSF-REU Undergraduate Student Mentor July-August 2014

Boston University, Boston, MA

- Mentored a senior undergraduate international student from Germany on a synthesis project
- Taught the student experimental techniques and how to run hypothesis-based reactions, SciFinder and dedicated softwares usage to achieve the project goals

HONORS, AWARDS AND AFFILIATIONS

American Chemical Society, Member 2014-Present

Vertex Conference Support Award August 2014

Association for Women in Science, Massachusetts Chapter, Member 2015-Present

PUBLICATIONS

Gerard, B.; Lee, M. D.; Dandapani, S.; Duvall, J. R.; Fitzgerald, M. E.; Kesavan, S.; Lowe, J. T.; Marié, J.-C.; Pandya, B. A.; Suh, B.-C.; Welzel, M.; Dombrowski, M.; **Hamann, D.;** Lemercier, B.; Murillo, T.; Akella, L. B.; Foley, M. A.; Marcaurelle, L. A. **Synthesis of Stereochemically and Skeletally Diverse Fused Ring Systems from Functionalized C-Glycosides.** *J. Org. Chem.* **2013**, *78*, 5160−5171.

Hamann, D. A; Porco, J. A. Jr. **Synthetic Studies toward the Syntheses of Swerilatones A and B**. *Manuscript in preparation.*

PRESENTATIONS

Hamann, D. A.; Porco, J. A. Jr Studies towards the Total Syntheses of the Swerilactones and Related Natural Products. 249th ACS National Meeting, Boston, MA, August 16-20, 2015.

Hamann, D. A.; Porco, J. A. Jr. Studies towards the Total Syntheses of Swerilactones A and B.

- Annual Boston Women in Chemistry Symposium, October 4th, 2014, Harvard Chemistry Department, Cambridge, MA (Poster). Boston University 14th Annual Symposium 2013 (poster presentation)
- Boston Symposium on Organic and Bioorganic Chemistry, October, 8th 2014, Merck Boston Auditorium, Boston, MA (poster presentation).
- 248th ACS National Meeting, San Francisco, CA, August 10-24, 2015 (oral presentation).

Hamann, D. A.; Porco, J. A. Jr. Studies toward Synthesis of Epidithiodiketopiperazines-A Cyclic Sulfate Strategy. Boston University 14th Annual Symposium 2013 (poster presentation)

LEADERSHIP AND VOLUNTEERING EXPERIENCE

Seminar Coordinator Officer 2013-2015

Boston University Women in Chemistry (BUWIC) Association

- Invited and hosted two high profile women faculty speakers, organized their seminar and day schedule
- Contacted industry speakers for career track lunches, head hunters for professional development evening seminars, organized a panel event on

alternative careers for scientists in collaboration with the BU Science and Engineering Business Group

SKILLS

Languages

- French Native Language
- English Full Proficiency TOEFL iBT Score 107/120

Technical Proficiency

- Softwares/Programs: Chemdraw, Spartan, Word, Power Point, Excel
- Organic chemistry/small molecules synthesis, 2D NMR, LCMS, GC-MS, microwave reactors, UV-Vis spectroscopy, purification, Schlenk and glove-box anhydrous techniques, solvent purification systems
- Beta tested and contributed to the purchase of a new electronic notebook (Scilligence ELN). Served as lab notebook administrator four years

REFERENCES

Prof. John A. Porco, Jr.

Professor of Chemistry

Department of Chemistry and Center for Molecular Discovery (BU-CMD)

Boston University, 590 Commonwealth Avenue, Boston, MA 02215

614-353-2493

porco@bu.edu

Dr. Lisa Marcaurelle

Senior Director, Chemistry

Warp Drive Bio, Inc.

400 Technology Square

Cambridge, MA 02139

(617)-588-3418